2-HYDROXYBENZOATE ANALOGUE MEDIATED APOPTOSIS IN HUMAN HT-1080 FIBROSARCOMA CELLS

A THESIS SUBMITTED FOR THE DEGREE OF DOCTOR OF PHILOSOPHY

BY

Mohammed AlKarrawi

MPhil, 1993; BSc, 1986

CARDIFF SCHOOL OF BIOSCIENCES
UNIVERSITY OF WALES CARDIFF
MARCH 2005

UMI Number: U584860

UMI U584860

AKNOWLEDGMENT

SUMMARY

The antitumour activities of 18 benzoic acid and 2-hydroxybenzoic acid analogues were investigated in HT-1080 fibrosarcoma cell line. Several approaches were used to identify the most effective apoptotic agents capable of inhibiting cell population expansion of HT-1080 cells mostly at a concentration of 0.4mM. Techniques used in this study included: cell viability assays (MTT, direct count and time-lapse tracking images), morphology (DAPI, haematoxylin-eosin, methyl green-pyronin y, and SEM), immunocytochemistry (Annexin V, caspase-3) and pharmacology (2-hydroxybenzoate uptake). The results indicated that most of these compounds showed antiproliferative activities at specific concentrations (range 0.025-8mM), with an incubation time of 2-180 hours. It is evident that zinc 2-hydroxybenzoate was the most effective antiproliferative agent at 0.3 and 0.4mM. Other analogues, mainly calcium, also showed antiproliferative activities but at higher concentrations (up to 8mM).

The growth inhibitory effect on HT-1080 cells population after treatment with either calcium or zinc 2-hydroxybenzoates was identified as the occurrence of apoptosis. This was confirmed by the morphological techniques as well as by immunoassay including annexin V and caspase-3, measured by flow cytometry. Although strong evidence has been presented here for apoptosis, the genetic mechanism remains uncertain. Neither the expression of the six proteins p53, p21, Bax, Bcl-2, histones and TNF-α, nor the cell cycle analysis was able to fully elucidate the mechanism of action of calcium and zinc 2-hydroxybenzoate on HT-1080 cells. Nonetheless, calcium and zinc 2-hydroxybenzoate-induced apoptosis clearly involved caspase-3 through Bax and p53/p21, respectively, and displayed the properties of potentially therapeutic compounds.

Table of Contents

Chapter One

General Introduction

CHAPTER ONE

General Introduction

1.1 Introduction

It has been found that certain natural products are good sources for new chemotherapeutic agents (Stellman, 1995; Chung *et al.*, 2001). Many more natural and synthetic biologically active compounds are being investigated as potential anticancer agents. Among these are the benzoic acid analogues, including salicylates. These have been shown to exert anticancer activities, particularly against colorectal cancer cells (Hector *et al.*, 2001). The role of 2-hydroxybenzoates (salicylates) in cancer has been largely based on epidemiological studies which showed that the regular use of aspirin could reduce the risk of developing colorectal cancer by 40–50 % (Ruschoff *et al.*, 1998; Stark *et al.*, 2001). The data were obtained by comparing people who regularly take aspirin with matched controls. Although many studies have been published on the effects of 2-acetylbenzoic acid, very few appear to have exploited its precursor, 2-hydroxybenzoic acid and its metal ion benzoates. The current work aims to screen and assess the anticancer activities of a total of 18 compounds, including benzoic acid, 2-hydroxybenzoic acid, 2-acetylbenzoaic acid (aspirin) and their corresponding lithium (Li), potassium (K), magnesium (Mg), calcium (Ca) and zinc (Zn) benzoate, 2-hydroxybenzoate, and 2-acetylbenzoate salts, respectively. The goal was to study the effect of a range of benzoate concentrations on HT-1080 cells viability and proliferation, their morphological characteristics, and changes in molecular biology.

1.2 Cell Death by Apoptosis

Most living cells undergo recurring cycles of cell growth and division under strictly controlled conditions. This fundamentally occurs in 4 phases (G1, S, G2 and M; see Chapter 4). In a healthy living system, cell population

growth is precisely balanced with apoptosis to maintain homeostasis of the living system. Apoptosis is a genetically controlled programmed cell death that forms part of the normal development of multicellular organisms. It serves two functions: remodelling of tissues during embryogenesis and elimination of damaged cells (Roger, 2000). It is functionally defined as an equal and opposite force to mitosis (Bowen *et al.*, 1997). Integration of proliferation and death is essential for normal developing tissues. Apoptosis usually involves single isolated cells rather than a confluent portion of a tissue (Roger, 2000). It occurs in two stages; a commitment to cell death and an execution phase characterised by morphological changes in cell structure (Wong *et al.*, 1999).

In cancer cells, the level of mitosis is elevated, compared to the level of apoptosis due mainly to defective cell cycle checkpoints (see Chapter 4). Therefore, several natural and synthetic molecules have been investigated to readjust the kinetic relationship between proliferation and cell death.

Beside apoptosis, living cells may also die by necrosis, or massive accidental cell death. Necrotic cell death can result from diseases, acute toxins or lethal external force. This type of death is characterised by an increase in plasma membrane permeability, resulting in cellular oedema, and eventually leads to osmotic lysis of the cell and spilling of the cellular contents, instigating an inflammatory response (Mitton, 2000). Therefore, inducing apoptosis is a therapeutic possibility. Many studies have elucidated the characteristic features of apoptosis, both morphological and molecular, employing different techniques (see Chapters 3 and 4). The metabolic machinery necessary for the completion of apoptosis already exists in the cell. The signal transduction required to activate the pre-existing death machinery often entails novel protein synthesis. It is generally understood that there are 3 types of gene product involved in apoptosis. The first type includes gene products that generate the death-activating signal transduction process in healthy cells during physiological cell death. These products can result in either cell proliferation or apoptosis, depending on the differentiation status of the cell. An example

is the transformating growth factor-beta (TGF-β), which is a cell type-specific type-I gene that can stimulate cell proliferation in mesenchymal cells, but causes apoptosis in certain epithelial cells (La Monica *et al.*, 2003). The second kind of apoptotic gene product establishes the sensitivity of the cell to the activation of apoptosis in response to damage. This includes *p53* and *Bcl-2*. The expression of p53 increases the sensitivity of the cells to apoptosis, and Bcl-2 reduces this sensitivity (Adams and Cory, 1998). The third type of gene product makes up the actual machinery of apoptosis e.g. the caspases.

The major machinery for the execution of apoptosis is a family of serine proteases called caspases (see Chapter 4). They are initially synthesised as procaspases, and are activated by cleavage at an aspartic acid residue. Once a caspase is activated, it cleaves other procaspases, resulting in an amplifying proteolytic cascade. Certain caspases, when activated, can cleave other proteins in the cell, such as nuclear lamins and the proteins that hold DNA-degrading enzymes in an inactive form. The caspase cascade is destructive, self-amplifying and irreversible. Adaptor proteins initiate activation of procaspases; they aggregate specific initiator procaspases together to form a complex. Initator procaspases have a small amount of protease activity, and when they are brought together, they can cleave each other, initiating their reciprocal activation. Once the caspase on the top of the cascade is triggered, it will begin cleaving downstream procaspases (Thornberry and Lazebnik, 1998).

Caspase activation can also be triggered extracellularly by the activation of death receptors. Cytotoxic killer lymphocytes, for instance, trigger apoptosis by producing a Fas ligand protein that binds to the Fas cell surface receptor. The Fas proteins can employ intracellular adaptor proteins, which bind to and aggregate procaspase-8 molecules. Procaspase-8 molecules subsequently cleave and activate each other and other downstream procaspases. When cells are under great stress, they may commit suicide by producing both Fas ligand and the Fas protein (Wajant, 2002)

Apoptosis can also be triggered by inducing mitochondria to release cytochrome c (an electron carrier) into the cytosol. Cytochrome c binds, activates and aggregates protein Apaf-1 which then binds and aggregates procaspase-9 molecules, triggering the caspase cascade (Green and Reed, 1998). The Bcl-2 family of proteins help regulate the activation of procaspases. Bcl-2 and Bcl-X inhibit apoptosis by preventing the release of cytochrome c from the mitochondria. Some members of the Bcl-2 family, however, promote apoptosis, for instance Bad functions by binding and inactivating the death inhibitor members of the Bcl-2 family. Bax and Bak stimulate the release of cytochrome c. If genes encoding Bax and Bak are inactivated, cells become extremely resistant to apoptotic agents. Other apoptotic-inducing members of the Bcl-2 family such as Bid activate Bax and Bak (Wei et al., 2001). The inhibitors of apoptosis (IAP), a family of intercellular apoptotic regulators, inhibit apoptosis in two ways. They can bind to procaspases and prevent their activation, or they bind to caspases to directly inhibit their activity. When mitochondria release cytochrome c to activate Apaf-1, they also release proteins that block IAP, assisting the induction of apoptosis.

Extracellular signals may also promote or inhibit apoptosis, by regulating the activity of the Bcl-2 and IAP families (Nicholson and Thornberry, 2003).

1.3 Cancer

It is generally accepted that cancer is a complex disease evolving from permanent damage, mainly to cells' DNA. Humans have 22 pairs of chromosomes plus the sex chromosomes (XX in the female, XY in the male). Each human has about 6 billion base pairs of DNA capable of encoding about 30,000-40,000 different proteins (Pennisi, 2001; Wu and Morris, 2001) that undergo different types of interactions and subsequent modifications. Although cells have the mechanism to correct any defective molecular interactions, it is becoming increasingly apparent that aberrant

4

cells have the same complexity of interactions as normal cells. Cancer is a complex disease arising from *normal* cells whose nature is permanently altered, forming a malignant neoplasm, such as carcinoma, sarcoma or others. The main problem in cancer cells is the regulation of the cell cycle which directs mitosis and/or apoptosis.

Disruption of restriction point control in the cell cycle is a common biological feature in human cancer. Cancer cells are characterised by their unregulated proliferation, their lower requirements for growth factors, and their negative response to signals. Alterations in cyclins and *CKI* genes are important for the genesis of certain cancers (Roger, 2000). A number of hereditary syndromes exist, in which DNA repair is defective. *Ataxia telangiectasia* syndrome is one of these disorders, which results from the failure of G1/M checkpoint delay (Dennis, 1998). Many tumours are formed because the rate of cell division exceeds that of cell death.

Two well-known types of primary genes that regulate apoptosis and cell division, that could be responsible for cancer include proto-oncogenes (e.g. *Bcl-2*) and tumour suppressor genes (e.g. *p53*) (Harrington 1994; Daniel, 2002). *Bcl-2* blocks apoptosis in tumours and therefore allows the propagation of abnormal cells. Overexpression of *Bcl-2* has been reported in a number of human tumours, e.g. adenocarcinoma of the prostate, squamous carcinoma of the lung, and nasopharyngeal carcinoma (Sherbet and Lakshmi, 1997). The two genes that are most frequently altered in cancers are *p53* and *Rb* genes. Mutations in the *p53* gene are found in 50% of human cancers, which are in the form of deletion, rearrangement, and base substitution mutations (Spence and Johnston, 2001). Some sporadic cancers such as bladder and breast cancer are the result of mutation in the *Rb* gene (Bowen, 1999).

Cancers can be treated in several ways: surgery, radiotherapy, chemotherapy, or combined treatments. The objective of any treatment is to control proliferation (cytostatic effect) and to kill cancer cells (cytotoxic effect). Apoptosis is an important factor in determining the response to

treatment and a major determinant of size of tumours, with individual cells being eliminated in about three hours (Roger, 2000).

1.4 Biological Activity of 2-Hydroxybenzoate Analogues

Naturally occurring monoaromatic compounds, such as 2-acetylbenzoic acid (aspirin) and 2-hydroxybenzoic acid (salicylic acid), have significant biological activities such as anti-oxidative and anti-inflammatory properties. Since early civilisation, many plants containing monoaromatic constituents were used as a remedy for different ailments. Different parts of the willow tree, for example, were exploited by Sumerians, Babylonians, Egyptians, and Greeks, and later, in the middle of the previous millennium, Europeans explored the active ingredient responsible for the remedy for relieving pain and controlling inflammation (Mahdi *et al.*, 2004). The active compound appeared to be salicin which hydrolyses and oxidises to give 2-hydroxybenzoic acid, the precursor of the common drug known as aspirin (Mahdi *et al.*, 2004).

Inflammation is closely associated with carcinogenesis, therefore it might be expected that substances with anti-inflammatory properties would exert anti-tumour activity (Zhou *et al.*, 2001). Many tumours, especially gastric carcinomas, contain high levels of prostaglandin, which promote cellular proliferation, tumour growth and angiogenesis (the formation of new blood vessels).

It has been illustrated that 2-acetylbenzoic acid and other non-steroidal anti-inflammatory drugs (NSAIDs) can restore proper function to cell death pathways in some types of tumours (Kim, 2001). NSAIDs have been shown to inhibit cell proliferation and induce apoptosis in a number of cell lines *in vitro*, and are therefore anticipated to have a potential role in the treatment and prevention of carcinogenesis (Zhou *et al.*, 2001).

The effects of 2-acetylbenzoate analogues on the population growth of cancer cells in culture have been actively studied, and they have been shown to interfere with cell proliferation (Marra and Liao, 2001). 2-

Acetylbenzoic acid has been shown to inhibit proliferation of human colorectal cancer cells by inhibiting cell population growth, DNA synthesis and protein synthesis (Marra and Liao, 2001). 2-Acetylbenzoic acid has also been shown to induce cell cycle arrest in the G_0/G_1 phase, thus blocking progression from G_1 to S phase (Marra and Liao, 2001; Sharma *et al.*, 2001).

2-Acetylbenzoic acid and other NSAIDs have been shown to induce apoptosis in many cancer cell lines, exhibited by the externalisation of phosphatidyl serine and nuclear chromatin condensation, a characteristic of typical apoptosis, in colorectal cancer cells (Stark *et al.*, 2001).

There is general consensus in the literature about the anti-tumour activity of NSAIDs, arising from their inhibition of prostaglandin synthesis. Prostaglandins are signalling molecules and are responsible for regulating a number of cellular functions, including gene expression, growth and differentiation (Towndrow *et al.*, 2000). The enzyme cyclooxygenase (Cox) is involved in the synthesis of prostaglandins, and there is strong evidence to suggest that prostaglandins and Cox play an important role in a number of malignancies (Munkarah *et al.*, 2002). Two isoforms of Cox exist, Cox-1 and Cox-2. The latter is found in some cancers and its expression is linked to tumour promotion (Husain *et al.*, 2001). Overexpression of Cox-2 leads to elevated levels of prostaglandins, which promote cellular proliferation, tumour growth and angiogenesis, events that contribute to the emergence of the neoplastic phenotype (Husain *et al.*, 2001; Munkarah *et al.*, 2002). High levels of Cox-2 may also have the ability to confer programmed cell death-resistance to some cancer cells by turning on genes that promote cell survival (Kim, 2001).

Thus NSAIDs exert their anti-carcinogenic properties by Cox-2 inhibition and subsequent inhibition of prostaglandin formation, which may result in the induction of apoptosis and/or inhibition of cellular proliferation (Husain *et al.*, 2001). However, NSAIDs have shown chemoprevenitive properties in cell lines that do not express either Cox-1 or Cox-2. Also, 2-

acetylbenzoic acid induced the same anti-tumour effect on cancer cells as that of aspirin, despite being a poor inhibitor of Cox-2. These findings suggest that Cox is not the only target for NSAIDs (Stark *et al.*, 2001).

The nuclear factor-kappa beta (NF-kβ) signalling pathway required for anti-tumour activity has been identified as a target for the activity of NSAIDs (Stark *et al.*, 2001). NF-kβ is a transcription factor crucial for the expression of many genes that regulate proliferation, immunity, inflammatory response and cellular adhesion, as well as playing an essential role in apoptotic cell death (Sharma *et al.*, 2001; Stark *et al.*, 2001). NF-kβ normally exists in the inactive state, bound in the cytoplasm by the inhibitor protein IkB (Stark *et al.*, 2001). Upon stimulation of the cell by a number of cytokines, oxidative stress, or pathogens, IkB is phosphorylated and degraded to release NF-kβ, which is subsequently translocated to the nucleus, where it binds to regulatory elements within the promoter region of target genes (Sharma *et al.*, 2001; Stark *et al.*, 2001). Activation of NF-kβ has been shown to inhibit apoptosis, and dysregulation of the NF-kβ pathway, resulting in abnormally high NF-kβ activity, has been observed in cancer cell lines (Stark *et al.*, 2001). NF-kβ is known to regulate several growth regulatory genes, including *p53* and *Cox-2*, and therefore is a strong potential target for the anti-tumour effects of NSAIDs (Stark *et al.*, 2001). Both aspirin and salicylate have been shown to interfere with NF-kβ activation by inhibiting the IkB kinase complex, and it has been shown that aspirin can induce apoptosis in cancer cell lines (Sharma *et al.*, 2001). Inhibition of NF-kβ activation may down-regulate genes involved in the promotion and progression of the carcinogenic process by restoring the sensitivity of cells to apoptotic stimuli (Sharma *et al.*, 2001).

The anti-oxidant properties of naturally occurring benzoate compounds are thought to have anti-tumour promoting effects. Numerous epidemiological studies have shown an inverse relationship between the dietary intake of antioxidants (found in fruit, vegetables and cereals) and the incidence of

certain cancers. The anti-oxidant (free radical scavenging) activity is thought to provide the protective mechanism (Rice-Evans *et al.*, 1997). Free radicals, a highly reactive chemical species, have been found to be involved in the initiation and promotion of carcinogenesis. Free radicals can act as inhibitors and/or promoters, cause DNA damage, activate procarcinogens and alter the normal cellular antioxidant defence system (Dizdaroglu *et al.*, 2002). Anti-oxidants act as free radical scavengers and have been shown to be anti-carcinogens, functioning as inhibitors at both the initiation and promotion/transformation stages of the carcinogenic process by offering cells protection against oxidative damage (Sun *et al.*, 1989; Thornberry and Lazebnik, 1998; Salvi *et al.*, 2001). Various antioxidant enzymes, such as manganese superoxide dismutase, zinc superoxide dismutase, catalase, glutathaione peroxidase and glutathione reductase, have shown lower levels of activity in tumour cells compared with normal cells. Other enzymes, such as glutathione S-transferase 7-7, glucose-6-phosphate dehydrogenase have shown increased levels of activity in tumour cells (Sun, 1990).

1.5 Biological Activity of Metal Ions

A number of different metal ions exist within cells, including calcium, magnesium, potassium and zinc. These play an important role in both the functional and structural aspects of cellular molecules. They are often incorporated in various forms in proteins to perform specialised functions (Luchinat, 2003). These ions can form ionic bonds with almost any molecule in the cell, for example DNA, RNA, and any other protein or molecule with a negative charge, such as oxygen or nitrogen. The folded structure of proteins is stabilised by non-covalent interactions between the different parts of the polypeptide chain, and is important for obtaining the correct conformation and specificity of an active site. The biological activity of a protein depends on its active site, a cleft or crevice on the surface responsible for binding the substrate and initiating catalysis. Some

9

enzymes only function in the presence of a specific cofactor, such as Mg^{2+}, Ca^{+2} or Zn^{2+}, which are required for the activity of certain conjugated enzymes. Intracellular calcium, for example, plays a critical role in cell survival and cell death: apoptosis or necrosis (Schanne *et al.*, 1979; Nicotera and Orrenius, 1998; Choi, 1988). The distinction between these two types of death pathways depends on the calcium ion concentration. The increase of calcium ion by 4 times damages the signalling and mitochondrial function, as well as plasma membrane, giving the morphological signs of necrosis (Choi, 1988; Dawson, 1994; Hyrc, 1997; Yu et al., 2001). In contrast, an early physiological elevation of calcium ion may not *per se* induce cellular damage, but rather it may serve as a component of a signalling cascade culminating in triggering apoptosis (Yu *et al.*, 2001).

Furthermore, magnesium and zinc ions are also known to exert a variety of other biological functions. An increase in the levels of intracellular free magnesium ion is characteristic of the early stages of apoptosis, and accumulating evidence suggests a role for magnesium in cell cycle regulation, proliferation, differentiation and apoptosis (Hartwig, 2001). In particular, magnesium is an essential cofactor in almost all enzymatic systems involved in DNA processing, including the removal of damaged DNA, and acts as an intracellular regulator of the cell cycle and apoptosis (Hartwig, 2001). Zinc also has a diverse role in many physiological systems, and has been shown to be an important regulator of apoptosis (Truong-Tran *et al.*, 2001).

The majority of evidence suggests that zinc is a physiological suppressor of apoptosis, although when present in high concentrations which exceed the capacity of homeostatic control, zinc may trigger programmed cell death in a number of mammalian cell lines (Beyersmann and Haase, 2001). Very high concentrations of zinc have also been shown to induce necrotic cell death (Troung-Tran *et al.*, 2001). It has been reported that relatively high concentrations of zinc (200-500 μM) can induce necrosis in human prostate carcinoma cells, and in other studies, zinc has been

shown to induce both necrosis and apoptosis (Hamatake *et al.,* 2000). The mechanisms of how zinc may induce apoptosis are not yet well understood, and there are many other aspects of zinc functions that require further elucidation (Beyersmann and Haase, 2001).

1.6 Benzoates Significance and Structure

Benzoic acid, 2-hydroxybenzoic acid and 2-acetylbenzoic acid (Figure 1.1) belong to the monoaromatic acid group of compounds found naturally in plants. They play a significant role in the plant's defence system (Matthews, 1991; Ryals *et al.,* 1996; Shirano *et al.,* 2002). 2-hydroxybenzoic acid, for example, plays a vital role in plant responses to pathogens and stress (Raskin, 1992; Hammond-Kosack and Jones, 1996; Ryals *et al.,* 1996; Durner *et al.,* 1997; Wildermuth *et al.,* 2001). Furthermore, these compounds (commonly, 2-acetylbenzoic acid) also exert important pharmacological characteristics as effective agents in the treatment of pain, fever, rheumatic disease and cardiovascular problems, and as a therapeutic agent against cancer (Levesque and Lafont, 2000), as well as being an anti-microbial agent (Amborabé *et al.,* 2002; Shabir, 2004).

The simplest example is benzoic acid, which is widely used as a preservative in food, cosmetic and pharmaceutical products (FDA, 1973; Amborabé *et al.,* 2002; Shabir, 2004) with low toxicity (LD50: 1700 mg/kg; LC50 rat > 26,000mg/L/Hr; MSDS, 2003). Other examples are the hydroxylated monoaromatic acids, or the phenolic acids such as salicylic acid, chemically known as 2-hydroxybenzoic acid, and its acetylated analogue, or aspirin, chemically known as 2-acetylbenzoic acid.

11

Benzoic Acid   2-Hydroxybenzoic Acid   2-Acetylbenzoic Acid
    (Salicylic Acid)   (Aspirin)
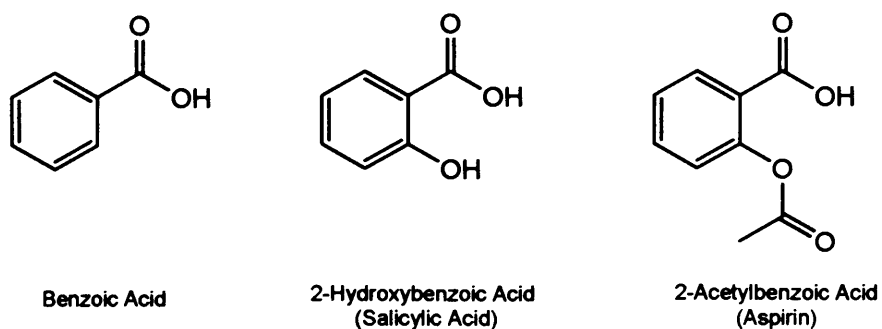
Figure 1.1 Chemical structures of benzoate analogues.
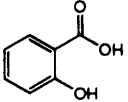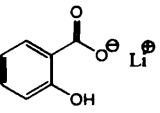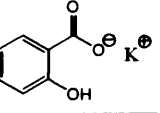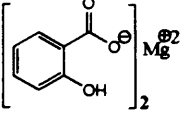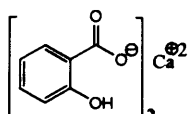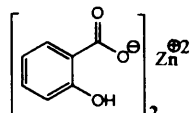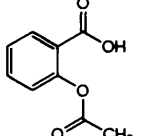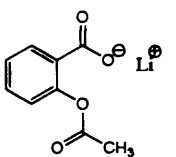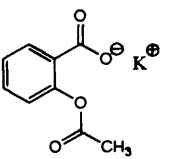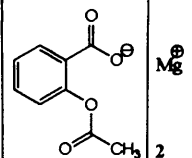
In this work 18 analogues of benzoic acid were tested and screened for anticancer activities. Table 1.1 shows the names, structures, abbreviations, and the molecular weights of these compounds which are used in this study.

Table 1.1 Chemical characteristics of benzoate analogues.

Name	Abbreviation	Structure	Molecular Weight
Benzoic Acid	BA		121
Lithium Benzoate	BnLi		127
Potassium Benzoate	BnK		159
Magnesium Benzoate	BnMg		264
Calcium Benzoate	BnCa		280
Zinc Benzoate	BnZn		305

Continued

12
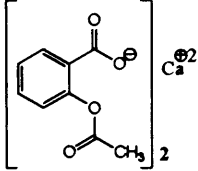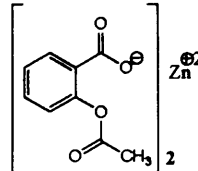
Table 1.1 Continued

Name	Abbreviation	Structure	Molecular Weight
2-Hydroxybenzoic acid	2HBA		138
Lithium 2-Hydroxybenzoate	2HBnLi		144
Potassium 2-Hydroxybenzoate	2HBnK		176
Magnesium 2-Hydroxybenzoate	2HBnMg		298
Calcium 2-Hydroxybenzoate	2HBnCa		314
Zinc 2-Hydroxy benzoate	2HBnZn		339
2-Acetylbenzoic acid	2AcBA		180
Lithium 2-Acetylbenzoate	2AcBnLi		186
Potassium 2-Acetylbenzoate	2AcBnK		218
Magnesium 2-Acetylbenzoate	2AcBnMg		382

Continued

13

Table 1.1 Continued

Name	Abbreviation	Structure	Molecular Weight
Calcium 2-Acetylbenzoate	2AcBnCa		398
Zinc 2-Acetylbenzoate	2AcBnZn		423

1.7 Aims, Objectives and Approach of this Study

The current study not only aims to elucidate the cytotoxic effect of 18 benzoate analogues on HT-1080 fibrosarcoma cell line, but also to determine their effects on the morphological and molecular constitution of the cell at mostly 0.4mM, based on the preliminary experiments. The specific objectives can be summarised as follows:

1   To investigate cell viability. Three techniques are used to measure cell viability. First, MTT cytotoxicity assay to quantify dose and time-dependent treatment; second, direct count of cells using a haemocytometer, and third, time-lapse tracing of images of growing HT-1080 cells.

2   To investigate the changes in cell morphology. The light/fluorescence and scanning electron microscope are used to evaluate the changes in cell morphology (membrane, nucleus, and cytoplasm) resulting from benzoate treatments. Four staining techniques are used; haematoxylin-eosin, methylgreen-pyronin y, observed by light microscope; and DAPI and Annexin V, observed by fluorescence microscope.

14

3 To investigate cell cycle analysis. The treated/untreated HT-1080 cell cycle is evaluated by time-lapse tracking images to measure the duration and percentages of mitotic cells, as well as measuring the cell cycle duration. Cell cycle phases are also investigated by flow cytometry after staining with propidium iodide.

4 To investigate molecular changes. Flow cytometric analyses of Annexin V and caspase-3 are conducted in this study to evaluate their distribution and define the method of cell death (apoptosis or necrosis). Furthermore, the expressions of six proteins are also investigated, using Western blotting. These comprise p21, p53, Bax, Bcl-2, histones, and TNF-α.

Chapter Two

Effect of Benzoate and 2-Hydroxybenzoate Analogues on the HT-1080 Cell Line: Cell Population Growth and Cell Viability

CHAPTER TWO

Effect of Benzoate and 2-Hydroxybenzoate Analogues on the HT-1080 Cell Line: Cell Population Growth and Cell Viability

2.1 Introduction

Many natural and synthetic biologically active compounds are being investigated as potential anticancer agents. Several have been found to exhibit therapeutic and pharmacological advantages. 2-hydroxybenzoate, 2-acetylbenzoate (aspirin), taxol and others are among these therapeutic agents (Ackerknecht, 1973; Sumner, 2000; Dewick, 2002). This Chapter focuses on the assessment of the cytotoxic effects of 18 benzoate and 2-hydroxybenzoate analogues (see chapter 1) on HT-1080 cell viability and proliferation at different concentrations and incubation periods.

In order to investigate the cytotoxic effects of these compounds, the 3-(4, 5-dimethylthiazolyl-2)-2, 5-diphenyltetrazolium bromide (MTT) assay for cell viability and proliferation was used. Other techniques to screen the cytotoxic activities of these compounds were also applied, using direct counts and capture-image time-lapse microscopy.

2.2 Cell Viability and Proliferation

All living cells are commonly propagated by cell division, during which cells replicate their molecular contents and divide into two at the right time. This process is tightly regulated and coordinated by several genes to ensure that cell proliferation occurs precisely and successfully. The whole process of cell division is organised and governed by the cell cycle (see Chapter 4), which is divided into four distinct phases (i.e. G1, S, G2, M) (see Chapter 4). Various physiological and environmental factors may alter the way in which healthy or abnormal cells divide. It is advantageous that the cell cycle of abnormal cells, like cancer cells, is altered to slow or stop its proliferation. This process forms part of the physiological response to chemotherapeutic drugs. Cancer cells undergoing the cell cycle attempt to

repair chemotherapy-induced DNA damage, and then may undergo apoptosis. In this respect, the investigation of new chemical compounds or candidates is an essential process in drug discovery. One approach for evaluating a drug candidate is to study its effects on cell population growth and cell viability. The measurements of these parameters are important for assessing the activity of chemicals and other materials in many fields, such as medicine, the pharmaceutical industry and agriculture. Therefore, a great deal of effort has been made to establish methods to evaluate these parameters quantitatively.

Many assays are commonly used to measure cell proliferation and cell death, and these assays form the *in vitro* screening process. This offers the potential to screen a large number of chemical compounds in a reasonable time-scale. For example, measurement of proliferation by counting cells under the microscope using a haemocytometer is the simplest method which is commonly used to study cell viability and proliferation in cell populations. Incorporation of trypan blue helps identify the viable cells (unstained) from non-viable cells (blue-stained). Furthermore, cell proliferation can also be monitored using time-lapse microscopy, where cell population growth can be tracked by video image (Feeney *et al.*, 2003).

Although these methods are efficient for assessing viable cell numbers, they are however time-consuming and are impractical when many samples have to be analysed. Therefore, a concerted effort has been made to establish methods that are able to assess a large number of samples. The 3-(4, 5-dimethylthiazolyl-2)-2, 5-diphenyltetrazolium bromide (MTT) colourimetric assay, first developed by Mosmann in 1983, is a reliable and simple assay to measure cell viability, proliferation, or cytotoxicity colorimetrically. It is an assay that is suitable for high throughput screening of candidate drugs since it is carried out entirely in 96-well microtiter plates (Cole, 1986). Thus, drug concentration, time of exposure to drug, length of assay, and cell density can be varied and tested at the same time. As a consequence, this method is used

extensively by many researchers to study *in vitro* chemosensitivity in various cancer cell lines and to quantify cell proliferation and cell toxicity (Cole, 1986; Carmichael *et al.*, 1987; 1988; Twentyman and Luscombe, 1987; Pieters *et al.*, 1989; Twentyman *et al.*, 1989; Huveneers-Oorsprong *et al.*, 1997; Kudo *et al.*, 2003).

The MTT assay measures the cellular metabolic activity of viable cells colorimetrically. The tetrazolium bromide salt, MTT, is a yellow dye which can be metabolised by viable cells, in part by the action of dehydrogenase enzymes, into a water-insoluble dark blue formazan by reductive cleavage of the tetrazolium ring (Mosmann, 1983). Figure 2.1 shows the biochemical pathway of the reduction process of MTT to formazan. The cellular reactions involved in MTT reduction are not completely understood, but the mitochondrial succinate dehydrogenase system seems to be primarily involved (Mosmann, 1983; Slater, 1963). The resultant formazan can be dissolved and quantified by measuring the absorbance of the solution at 570nm. The resultant absorbance value reflects the number of living cells. Both replicates and multi-well spectrophotometer are used to facilitate measuring a large number of samples and provide a rapid measurement of cell viability. One disadvantage in the use of MTT is that the resulting coloured formazan product is insoluble, precluding direct spectrophotometric absorbance measurements without first dissolving the crystals (Liu *et al.*, 2004). Nonetheless, several tetrazolium salts analogues such as 2,3-bis(2-methoxy-4-nitro-5-sulfophenyl)-5-[(phenylamino)carbonyl]-2H-tetrazolium hydroxide (XTT) (Scudiero *et al.*, 1988; Roehm *et al.*, 1991), and 3-(4,5-dimethylthiazol-2-yl)-5-(3-carboxymethoxyphenyl)-2-(4-sulfophenyl)-2H-tetrazolium, inner salt (MTS) (Cory, 1991) have been developed and become commercially available. The advantage of these three dyes is that viable cells convert them into a water-soluble formazan. Thus, a metabolic assay with any of these compounds requires one step less (i.e. solubilisation of formazan) than an assay with straightforward MTT.
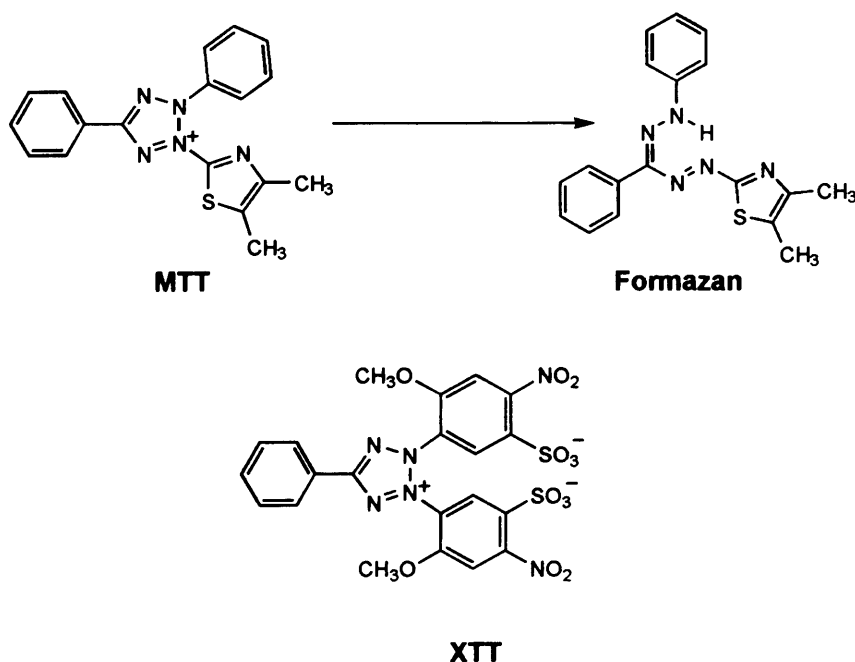
Figure 2.1 Structure of MTT and XTT, also showing biochemical reduction of MTT.

2.3 Cell Proliferation Responses to Benzoate Analogues

The biological activity of molecules in modulating cell proliferation is an important determinant of chemopreventive activity. Experimental data suggest that 2-hydroxybenzoates retard cell population growth of various cancer cell lines *in vitro* (Shiff *et al.*, 1996; Marra, 2000; Brooks *et al.*, 2003) and *in vivo* (Moorghen *et al.*, 1988). Table 2.1 lists, for example, the effect of 2-acetylbenzoic acid on the proliferation and population growth of different cell lines at different concentrations and incubation times.

Furthermore, 2-acetylsalicylic acid induced a pronounced concentration-dependent reduction in the proliferation rate of HT-29 cells (Qiao *et al.*,). For example, at 0.4mM, 2-acetylbenzoic acid reduced cell proliferation by 1.5-fold compared to controls following incubation for 96 hours. At higher concentrations (1 and 1.5mM), the reduction in cell proliferation was also apparent at 48, 72 and 96 hours (Shiff *et al.*, 1996). Sodium 2-acetylbenzoate (Na$^+$ 2-acetylbenzoate) also significantly inhibited the cellular proliferation of human pancreatic cancer cell lines (BxPC3 and

19

Panc-1) in a dose-dependent manner (Perugini *et al.,* 2000). Goel *et al,.* (2003) found similar effects with 2-acetybenzoic acid on the population growth of three different human colon cancer cells (HCT116, HCT116+chr3 and SW480), but at different rates. At 72 hours, incubation with 2-acetylbenzoic acid (acetylsalicylic acid or aspirin) treatment, the proliferation rate of HCT116+chr3 cells was significantly less than inhibition of HCT116 cells at 0.1mM (14.3% versus 40.7%) and 2.5mM (27.2% versus 47.9%). All other published investigations have concluded that the inhibitor effects of 2-hydroxybenzoate analogues, particularly 2-acetylbenzoic acid (or aspirin), on cell population growth and cell proliferation were concentration- and time-dependent (Qiao *et al.,* 1998; Zhu *et al.,* 1999; Zhou *et al.,* 2001; Kim *et al.,* 2003).

Table 2.1 Effect of 2-acetylbenzoic acid on Cell Proliferation and Cell Population Growth.

Concentration (mM)	Cell line	Max incubation time (Hour)	% of Growth inhibition*	Reference
1-3	HeLa TG	--	18-55	Kim *et al.,* 2003
0.1-10	AGS	72	21-47	Zhu *et al.,* 1999
0.4-3	HT-29	73	70-75	Qiao *et a.l,* 1998
1	AGS and MKN-28	60	37-40	Zhou *et al.,* 2001

* Cells population Growth inhibition at highest incubation time, relative to control

These results have encouraged the revival of interest in the clinical and pharmacological effects of 2-acetylbenzoate in terms of cancer treatment (Funkhouser and Sharp, 1995; Wong *et al.,* 1999; Smith *et al.,* 2000; Hector *et al.,* 2001; Claudia, 2003). This is particularly true for colon cancer with the potential for the use of 2-acetylbenzoates and other nonsteroidal antiinflammatory drugs (NSAIDs) as chemopreventive molecules.

Generally, the biological activity of a natural and synthetic compound is defined by a classic dose-response relationship, where the response is either therapeutic or toxic. The difference between the therapeutic and toxic effect of a chemical is dose-dependent. Most chemicals are therapeutic over a narrow range of doses, and are toxic at higher doses (Wedge and Camper, 2000). This concept is not new and can be traced back to Parcelsus in 1541, as he stated: *All substances are poisons; there is none which is not a poison* (quoted by Wedge and Camper, 2000).

2.4 Materials and Methods
2.4.1 Materials
2.4.1.1 General

T-flasks (25, 75 cm^2), well plates (6, 12, 24, 96-well), pipettes, obtained from Coster, Cambridge, MA, USA.

2.4.1.2 Chemicals

2-Aceylbenzoic acid (2AcBA) (aspirin), benzoic acid (BA), 2-hydroxybenzoic acid (2HBA), staurosporine, triton X-100 (Sigma, UK). Lithium, potassium, magnesium, calcium and zinc salts of benzoate, 2-hydroxybenzoate and 2-acetylbenzoate were available in the laboratory, designed and prepared by Dr. J. Mahdi.

Sodium pyruvate, ascorbic acid, 3-(4,5-dimethylthiazol-2yl)-2,5-diphenyltetrazolium bromide (MTT), and trypan blue were obtained from Sigma, UK. DMEM medium, L-glutamine, D-glucose, foetal calf-serum (FCS), gentimycin solution, Hepes buffer, and trypsin were obtained from Gibco, UK.

2.4.1.3 Cell Line

The human fibrosarcoma cell line HT-1080 was available in our laboratory at passage 9. Originally cells were kindly obtained from Dr. Steve Luckman, Biomedical Section, Cardiff University. These cells are characterised as adherent fibroblast sarcoma cells that grow in a monolayer (see Paragraph 5.2).

2.4.2 Methods

2.4.2.1 General

The handling of the human cancer cell line was performed in an enclosed sterile class II laminar flow hood. The laminar flow work surface was sterilised and kept free of contamination through the spraying of 70% industrial methylated spirits (IMS) and Virusolve anti- microbial agent before and after use. An aseptic technique was employed during all work with human cell cultures to avoid microbial contamination.

The optimal cell population growth media for HT-1080 human cell line culture was prepared from 500ml DMEM (Gibco, UK), 10% (v/v) foetal calf serum (Gibco, UK), gentimycin solution 1ml/100ml media (Gibco, UK), 1% (v/v) L-glutamine (Gibco, UK), 0.1% (v/v) Hepes buffer (1M), 0.1% (v/v) sodium pyruvate (100mM), and 0.1% (w/v) ascorbic acid (Sigma, UK). The medium was stored at 4°C and was used within three weeks of being made up.

2.4.2.2 Cells and *in vitro* Culture Conditions

HT-1080 cells were cultured in optimal DMEM medium to about 80% confluence in T-flask (25 or 75 cm^2) under a humidified atmosphere of 95% air and 5% CO_2 at 37°C. Splitting of cells was carried out by removing the medium, cells were trypsinised for 3-5 minutes to detach the adherent cells, and these were subjected to microscopic examination. The detached cells were then transfered into a 50ml centrifuge tube and

centrifuged at 120g for 4 minutes (Supermax Lorius centrifuge, U.K.). Supernatant was decanted and the cell pellet was resuspended in 10ml of warm (37°C) medium, gently resuspended, and cell number/ml was counted. The cell suspension was sub-divided into T-75 flasks by 1.8-2.5x10^6/flask, which already contained 13ml of media. The cells were then incubated in the appropriate standard conditions.

In the current work, the liquid nitrogen frozen-HT-1080 cell sample was thawed and cultured in 3 x T-75 flasks in an optimised DMEM and under standard growth conditions. After cells reached about 70% confluence, they were gently detached by trypsinisation and centrifuged, before being transferred into sterile 34 Nunc tubes, each holding approximately 1x10^6 cells in 1ml of DMEM medium containing dimethylsulfoxide (DMSO) to a 5% final concentration, which was quickly added, mixed and frozen at -70°C for 8 hours or overnight, before being transferred into a liquid nitrogen storage. The liquid nitrogen frozen HT-1080 cell samples were used in this work.

The following procedure was used in the culturing of HT-1080 cells. The medium was first decanted from the T-75 culturing flask before adding the trypsin (5ml) to detach cells and transfer them into another vessel(s). The T-75, containing cell line HT-1080 and trypsin, was incubated for 3-5 minutes. After this time, the T-75 was gently tapped to assist in the dissociation of cells. Dissociation of at least 90-95 % of cells was required (this was ensured by observing cells in the light and under the light microscope). The buffer (and cells) were aspirated into a tube suitable for centrifuging, with a 10ml pipette, and centrifuged at 1800 rpm for 4-5 minutes. The supernatant was decanted carefully, so as not to lose the pellet. The pellet was gently resuspended in 10ml of optimal DMEM medium. Finally, cells were counted using a haemocytometer.

The number of cells in the four chambers of the haemocytometer were counted and averaged. The number of cells present in 1ml of cell

suspension was then calculated, and the total cell number determined, according to the total volume of fluid from which the sample was derived.

2.4.2.3 HT-1080 Cells population Growth Curve

HT-1080 cells (4×10^4 cells/T-25 flask) were seeded in 5ml full medium. The flasks were set up in triplicate for 13 days and incubated at standard conditions. The cells were harvested each day at the same time by detaching the cells with 3ml trypsin, then immediately 3ml medium was added and the cells were transferred into a centrifuge tube. The flask was washed out with 3ml PBS, and this was added to the centrifuge tube before centrifuging at 1000g for 4 minutes. The cells were resuspended in 10ml PBS and were counted using a haemocytometer every 24 hours for 13 days. Throughout the experiment, the medium was changed with 5ml of fresh medium every three days, ensuring an adequate supply of nutrients was maintained at all times. Three flasks were counted every day with the aid of a haemocytometer for the 13-day period.

The population growth curve of HT-1080 was measured with and without the incorporation of the benzoic/benzoate compounds. Cells were seeded in a T-25 flask in the optimal growth medium and under standard growth conditions at an initial cell density (4×10^4 cells/T-25 flask), unless otherwise stated in each figure legend in the results section. For the first 5 days, HT-1080 cells were cultured without the benzoic/benzoate compounds, where cell number was measured by the haemocytometer method, as described above. The population growth curves were continued but with the incorporation of benzoate compounds at a range of concentrations and experimental conditions, as stated in the legends. Cells were again counted by haemocytometer but every 12 hours for the first 3 days.

Note that in all the experiments in Chapters 2-4, HT-1080 cells were cultured to the exponential phase (3-4 days post the initial cell seeding) specified by the population growth curve experiment above before any

24

drug treatment, unless otherwise specified. This was to ensure the consistency of any effect induced by the 2-hydroxybenzoate analogues.

2.4.2.4 Preparation of Benzoate Solutions

Concentrated stock solutions of each compound were prepared by dissolving a known mass of the compound in a certain volume of deionised water. For example, the concentration of a stock solution of 36mg 2-acetylsalicylic acid in 10ml deionised water can be calculated as follows:

$$\text{Number of Moles} = \frac{\text{Mass}}{\text{Molecular Weight}} = \frac{0.036g}{180}$$

$$= 2.0 \times 10^{-4} \text{ mole}$$

Concentration of 2-acetylsalicylic acid in 10ml is 2.0×10^{-2} M, or equivalent to 20,000mM.

The stock solution was diluted to certain concentrations in the optimal DMEM medium, according to the following equation:

Concentration of stock solution x required volume = new concentration x required volume

Or

$$C1 \times V1 = C2 \times V2$$

Thus, by adding 40µl of 2-acetylbenzoic acid solution to 1960µl of the optimal DMEM medium this would equal the maximum drug concentration (typically 0.4mM) to be tested. 40µl stock drug volume was selected due to its insignificant volume, which should result in negligible dilution effects on the DMEM. Compounds that proved difficult to dissolve in water, like 2-acetylbenzoic acid, were heated in a water bath at 50°C overnight.

After the addition of 40μl of stock drug solution to 1960μl of DMEM medium, the final concentration of the drug solution in the medium will be 0.4mM. A serial dilution of each drug was performed to the required concentration.

To ensure equality between DMEM/drug solutions and DMEM/deionised water solutions, 40μl of deionised water was also added to 2000μl of DMEM medium for the control sample.

2.4.2.5 MTT Assay Procedure

A 96-well plate (Costar, Cambridge, MA, U.S.A) was seeded with HT-1080 cells at a density of 2×10^4 cells/ml equating to 20,000 cells/well.

After that, each plate was examined under the light microscope to ensure equal distribution and density of cells within each well. Plates were left overnight in the incubator at standard culture conditions so that the cells would settle and attach to the bottom of the wells. Cells were allowed to proliferate for another 2 days before the plate was removed from the incubator and placed into a laminar flow class II fume hood, and then the medium was replaced with fresh medium containing the compound(s).

For each 96-well plate, 1.0ml of pre-warmed MTT reagent (5mg/ml stock solution in PBS, filter sterilised through a 0.22μM filter) was mixed thoroughly with 10ml of pre-warmed free FCS DMEM in a universal bottle. As a negative control, 4-8 wells were lysed by addition of Triton X-100 to a final concentration of 0.1% (1μl of 10% stock in PBS) immediately prior to addition of MTT reagent.

The old medium was aspirated from all wells and replaced with 110μl of the MTT medium mixture, which was homogenised by gentle pipetting in and out. Plates were then incubated at standard conditions for 1 hour.

After the incubation period, the plate was examined under the light microscope to determine the progress of the MTT reaction.

Viable cells contained insoluble formazan salt which could be clearly observed under the microscope. Cells treated with Triton X-100 or staurosporine showed no formazan salt. However, cells treated with staurosporine exhibited the typical morphological features of apoptosis, whereas cells treated with Triton X-100 did not. Cells treated with drugs presented varying amounts of formazan depending on the cytotoxic effect of the drug.

The absorbance of formazan in the 96-well plate was then measured by a Labsystems Multiskan MS Version 3.0 (Helsinki, Finland) at 575nm.

2.4.2.6 Time-Lapse Microscopy

HT-1080 cells were seeded and cultured in the optimal DMEM medium with an initial cell density of 1×10^3 cells per well in standard plastic 12-well plates. The plates were incubated at standard culture conditions for 3 days in an optimal DMEM medium prior to treatments. HT-1080 cell populations were treated with calcium or zinc 2-hydroxybenzate compounds at a range of different concentrations as indicated in the legends. The plates were then incubated for 22 hours on the stage of a Zeiss Axiovert 100 microscope (Zeiss, Welwyn Garden City, UK) fitted with a temperature-regulating incubator system and CO_2 supply (Solent Scientific, Portsmouth, UK). The camera, stage (xy) and focus (z) were PC computer controlled using AQM 200 software (Kinetic Imaging, Wirral, UK). Tiff-format Images (512x512 pixels) were played back for analysis as movies using the AQM 2000 software. The motorised xy microscope stage was from Prior Scientific (UK), and the phase transmission images (x10 objective lens) were captured every 5 minutes over 22 hours (264 frames per field), using an Orca I ER charge-coupled device camera (Hammamatsu, Welwyn Garden City, UK). The image sequences taken by the time-lapse microscope were viewed and analysed manually by counting the start and the end numbers of cells every one hour, using Lucida Analyse- 6 software (Kinetic Imaging, Wirral, UK).

2.4.2.7 Statistical Analysis

Cell viability assays were conducted using three replicates, unless otherwise indicated in each figure legend. The resulting average was used to calculate mean ±SE. To determine the effect of drug treatment, data were calculated as percentage of control and expressed as means ±SE. One-Way Analysis of Variance statistical analysis was performed using the Minitab statistical program. A value of $p < 0.05$–0.001 was considered significant.

2.5 Results

2.5.1 Determination of population Growth Curve of HT-1080 by Total Cell Count

The standard growth curve for cell line HT-1080 was used to determine the population growth characteristics of the cells in the culture, and cell counts were performed, using a haemocytometer. Figure 2.2 shows the growth curve characteristics for HT-1080 cell line. The first 4 days of culturing represent the lag phase of population growth. The cells enter the exponential phase from about 4 days post-seeding, and between this time and about 8 days post-seeding the cumulative cell number in the culture vessel can be seen to increase linearly with time.

After the exponential phase, the cell population growth rate declines, occasionally reaching a plateau level where there is not net population growth of cells in the culture. This phase represents a point where the cell density in the culture limits either the available area or volume for growth or becomes limiting in respect to nutrient supply. Generally, observing the culture vessel indicated that HT-1080 reached about 40-50% confluence after about 4 days of seeding. However, this period changes according to the seeded cell density. In the current work, the exponential phase was taken as a reference to treat cells with various benzoate and 2-hydroxybenzoate compounds.

450.0
400.0
350.0
300.0
250.0
200.0
150.0
100.0
50.0
0.0

Number of Cells (x 10⁴)

1 2 3 4 5 6 7 8 9 10 11 12 13

Incubation Time (Day)

Figure 2.2 Ppopulation growth profile characteristic for human fibrosarcoma HT-1080 cell line seeded into a culture vessel. Cells were cultured at initial seeding density of 4×10^4 in 3xT-25 flasks in optimal DMEM growth medium under standard conditions. Cell numbers counted by haemocytometer at 1-day interval for 13 days. Medium was changed every 3 days. Data represent mean ±SE of three replicates.

2.5.2 Cell Viability by MTT Assay

The effect of a total of 18 benzoic acid analogues, including the 2-hydroxybenzoic, 2-acetylbenzoic acids and their lithium, potassium, magnesium, calcium and zinc analogues, on the viability of HT-1080 cell line was assessed by a standard MTT assay. Staurosporine was used in each experiment as an internal cytotoxic standard drug. Cell viabilities were calculated relative to the control experiment with no drug incorporation in the HT-1080 cells culture. Results were expressed in percentages.

2.5.2.1 Response of HT-1080 to Benzoic and 2-Hydroxybenzoic Acids Analogues

The MTT cell proliferation assay for HT-1080s cell was conducted to study the effects of three monoaromatic acids, namely benzoic acid, 2-hydroxybenzoic acid and 2-acetylbenzoic acid (or Aspirin). Results of these experiments indicated that no antiproliferative properties were exerted by the incorporation of most of these acids at the following concentrations (0.025, 0.05, 0.1, 0.2, 0.4mM), and following incubation for

Figure 2.2 Ppopulation growth profile characteristic for human fibrosarcoma HT-1080 cell line seeded into a culture vessel. Cells were cultured at initial seeding density of 4×10^4 in 3xT-25 flasks in optimal DMEM growth medium under standard conditions. Cell numbers counted by haemocytometer at 1-day interval for 13 days. Medium was changed every 3 days. Data represent mean ±SE of three replicates.

2.5.2 Cell Viability by MTT Assay

The effect of a total of 18 benzoic acid analogues, including the 2-hydroxybenzoic, 2-acetylbenzoic acids and their lithium, potassium, magnesium, calcium and zinc analogues, on the viability of HT-1080 cell line was assessed by a standard MTT assay. Staurosporine was used in each experiment as an internal cytotoxic standard drug. Cell viabilities were calculated relative to the control experiment with no drug incorporation in the HT-1080 cells culture. Results were expressed in percentages.

2.5.2.1 Response of HT-1080 to Benzoic and 2-Hydroxybenzoic Acids Analogues

The MTT cell proliferation assay for HT-1080s cell was conducted to study the effects of three monoaromatic acids, namely benzoic acid, 2-hydroxybenzoic acid and 2-acetylbenzoic acid (or Aspirin). Results of these experiments indicated that no antiproliferative properties were exerted by the incorporation of most of these acids at the following concentrations (0.025, 0.05, 0.1, 0.2, 0.4mM), and following incubation for

12, 24, 48 and 72 hours. Figure 2.3 shows the most effective acids when cells were incubated for 24 hours or 72 hours at 0.4mM. 2-hydroxybenzoic acid at 0.4mM, following 48 hours' incubation, showed the highest decrease (21.7%) in cell viability compared to the control, while staurosporine decreased cell viability by about 80% at 1.0μM concentration compared to the control. It must be noted that the cell viability of HT-1080 was slightly higher at 72 hours' incubation (83.3%) compared to 48 hours incubation (78.3%) at the same drug concentration (Figure 2.3). The percentage cell death is partly an inverse function of the amount of cell division going on in the cultures.

The responses of cells to different concentrations and incubation periods generally were inconsistent with the increase of both concentrations and incubation periods. In other words, the cell viability did not gradually decrease as the drug concentration or the incubation period increased. The cytotoxic responses of the rest of the compounds which show proliferative responses are presented in Appendix A. Figure 2.4, for example, indicates that HT-1080 cell viability increased by about 10-17% compared to control upon incorporation of the 2-acetoxybenzoic acid.

The same pattern was also observed with both benzoic acid and 2-hydroxybenzoic acid treatments (Appendix A). Generally, the cytotoxic effect of these compounds may be a specifically concentration and/or incubation dependent (see results for all drugs in Appendix A).

100
89.6   83.3   78.3
80

Cell Viability (%)
60

40
20.13
20

0
BA-0.4mM/72H   2HBA-   2HBA-   Stauros
                0.4mM/72H 0.4mM/48H 0.001mM/72H
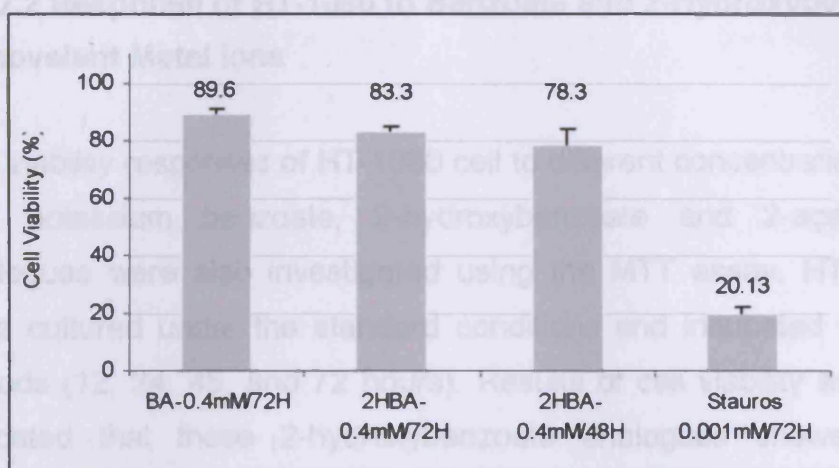
Figure 2.3 Concentration- and time-dependent effects of benzoic and 2-hydroxybenzoic acids as well as staurosporine on viability of HT-1080 cell line grown in 96-well plate for different periods and drug concentrations (Cell seeding density = 2 x10^4 cells/well, 100μl of optimal DMEM medium, population growth under standard growth conditions). Data represent mean ± SE of three replicates. Cell viability was measured by MTT assay.

48 Hours   2-AcBA/0.025mM   2-AcBA/0.4mM

120.0

100.0

Cell Viability (%)
80.0

60.0

40.0

20.0

0.0
2-AcBA 0.025 2-AcBA 0.050 2-AcBA 0.100 2-AcBA 0.200 2-AcBA 0.400   12 24 48 72   12 24 48 72

Incubation Period (Hours)
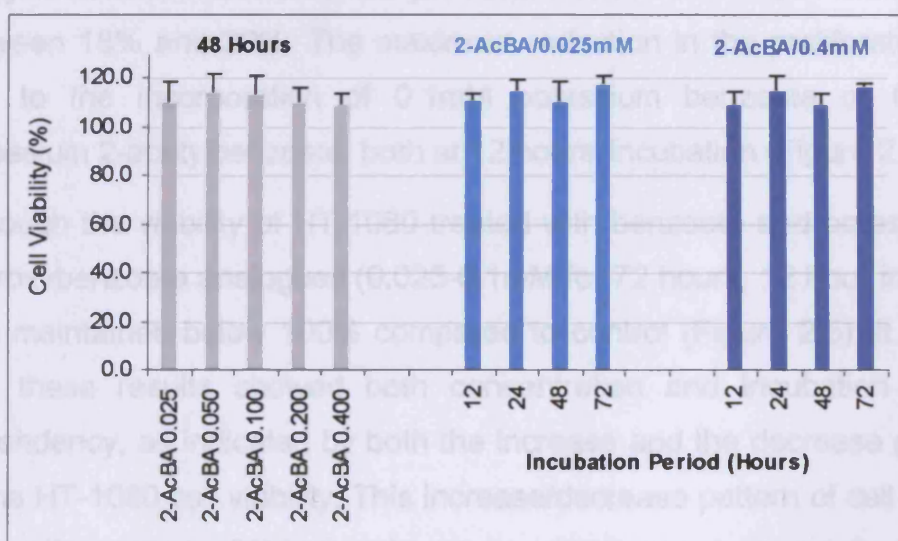
Figure 2.4 Concentration- and time-dependent effects of 2-acetylbenzoic acids on viability of HT-1080 cell line grown in 96-well plate for different periods and drug concentrations (Cell seeding density in = 2 x10^4 cells/well, 100μl of optimal DMEM medium, growth under standard growth conditions). Data represent mean ±SE of three replicates. Cell viability measured by MTT assay.

2.5.2.2 Response of HT-1080 to Benzoate and 2-Hydroxybenzoate Monovelant Metal Ions

The viability responses of HT-1080 cell to different concentration of lithium and potassium benzoate, 2-hydroxybenzoate and 2-acetylbenzoate analogues were also investigated using the MTT assay. HT-1080 cells were cultured under the standard conditions and incubated for different periods (12, 24, 48, and 72 hours). Results of cell viability assay clearly indicated that these 2-hydroxybenzoate analogues showed different cytotoxic activities to HT-1080 cells depending on the counter ion (i.e. Li^+ or K^+) present in the benzoate molecule. Generally, all potassium salts showed anti-proliferative effect at 0.025, 0.05 and 0.1mM concentrations, and at 12, 24, 48, and 72 hours' incubation periods (Figures 2.5). 12 hours after treatment with potassium benzoate, 2-hydroxybenzoate or 2-acetylbenzoate, inhibition of the proliferation rate of HT-1080 cells ranged between 18% and 30%. The maximum reduction in the proliferation was due to the incorporation of 0.1mM potassium benzoate or 0.05mM potassium 2-acetylbenzoate, both at 12 hours' incubation (Figure 2.5).

Although the viability of HT-1080 treated with benzoate and potassium 2-hydroxybenzoate analogues (0.025-0.1mM for 72 hours, 12 hour intervals) was maintained below 100% compared to control (Figure 2.5), it is clear that these results showed both concentration and incubation period-dependency, as indicated by both the increase and the decrease patterns of the HT-1080 cell viability. This increase/decrease pattern of cell viability during the course of the experiment may be more pronounced when the other concentrations (0.2 and 0.4mM) of potassium analogues are included (see Appendix A).
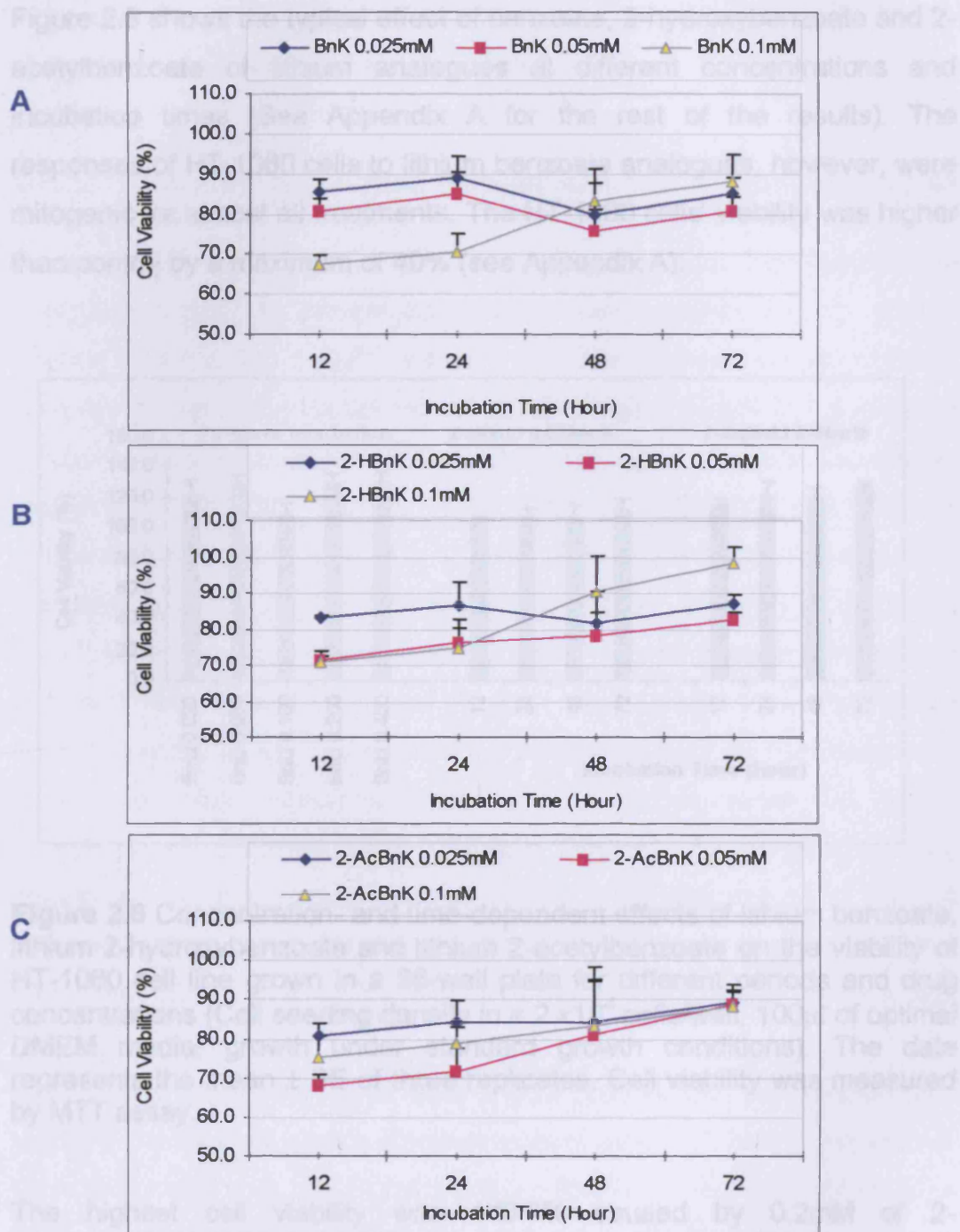
Figure 2.5 Concentration- and time-dependent effects of (A) potassium benzoate, (B) potassium 2-hydroxybenzoate, and (C) potassium 2-acetylbenzoate on viability of HT-1080 cell line grown in 96-well plate for different periods and drug concentrations (Cell seeding density in = 2 x10^4 cells/well, 100μl of optimal DMEM medium, under standard growth conditions). Data represent mean ± SE of three replicates. Cell viability measured by MTT assay.

Figure 2.6 shows the typical effect of benzoate, 2-hydroxybenzoate and 2-acetylbenzoate of lithium analogues at different concentrations and incubation times (See Appendix A for the rest of the results). The responses of HT-1080 cells to lithium benzoate analogues, however, were mitogenic for almost all treatments. The HT-1080 cells' viability was higher than control by a maximum of 40% (see Appendix A).
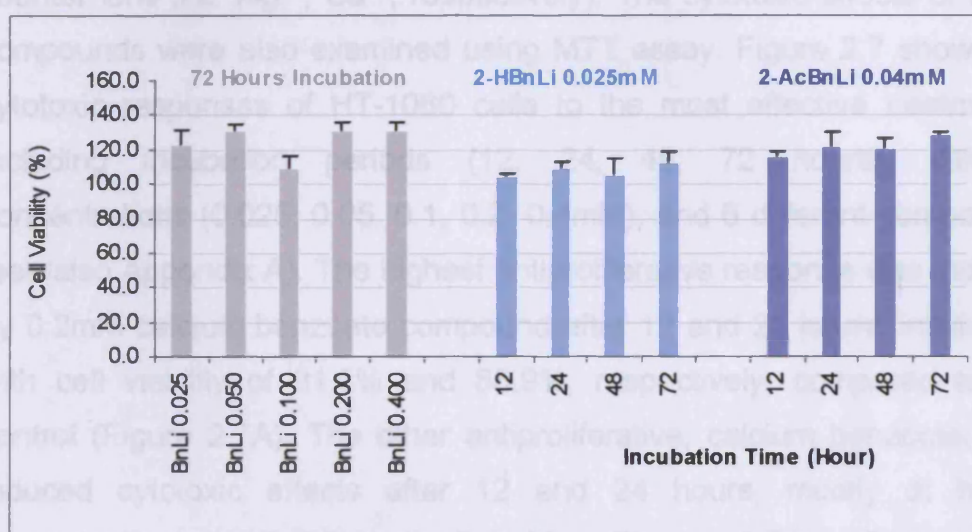
Figure 2.6 Concentration- and time-dependent effects of lithium benzoate, lithium 2-hydroxybenzoate and lithium 2-acetylbenzoate on the viability of HT-1080 cell line grown in a 96-well plate for different periods and drug concentrations (Cell seeding density in = 2 x10^4 cells/well, 100µl of optimal DMEM media, growth under standard growth conditions). The data represents the mean ± SE of three replicates. Cell viability was measured by MTT assay.

The highest cell viability was 140.7% caused by 0.2mM of 2-acetylbenzoate lithium salt when cells were treated for 72 hours (see Appendix A). It is generally accepted that the HT-1080 cell viability responses were positively related to the incubation periods in each lithium salt (see Appendix A). It is worth noting that there is a gradual increase in cell viability due to the incorporation of lithium 2-hydroxybenzoate at 0.025mM or lithium 2-acetylbenzoate at 0.4mM, but this is not significant ($p < 0.5$) (Figure 2.6). The three lithium 2-hydroxybenzoate analogues

increased the proliferation of HT-1080 cells by a maximum of 31.7% (0.2mM Li benzoate) compared to the control.

2.5.2.3 Response of HT-1080 to Benzoate and 2-Hydroxybenzoate Divalent Metal Ions

Divalent salts of benzoate, 2-hydroxybenzoate and 2-acetylbenzoate (salicylates) refer to compounds that contain magnesium or calcium counter ions (i.e. Mg^{+2}, Ca^{+2}, respectively). The cytotoxic effects of these compounds were also examined using MTT assay. Figure 2.7 shows the cytotoxic responses of HT-1080 cells to the most effective treatments, including incubation periods (12, 24, 48, 72 hours), different concentrations (0.025, 0.05, 0.1, 0.2, 0.4mM), and 6 different compounds (see also Appendix A). The highest antiproliferative response was induced by 0.2mM calcium benzoate compound after 12 and 24 hours' incubation with cell viability of 81.1% and 85.9%, respectively, compared to the control (Figure 2.7A). The other antiproliferative, calcium benzoate, also induced cytotoxic effects after 12 and 24 hours, mostly at higher concentrations (0.2mM and 0.4mM) (Figure 2.7A). Furthermore, magnesium benzoate compound induced its antiproliferative effect after 24 hours at 0.025mM and 0.05mM concentration, whereas no antiproliferative effects were induced by concentration of the higher magnesium benzoate analogue (Figure 2.7A).

Figure 2.7B shows that 0.05 and 0.4mM magnesium 2-acetylbenzoate induced the highest antiproliferative effects after 12 hours' incubation. Results showed that the highest antiproliferative effect was induced by 0.05mM and 0.4mM magnesium 2-acetylbenzoate after 12 hours' incubation: cell viabilities were 87.8% and 88.3%, respectively. Nonetheless, the other treatments (0.025, 0.05mM BnMg, 0.025, 0.05mM 2HBnMg and 0.025mM 2-AcBnMg) also induced cytotoxic effects of between 7 and 10% (Figure 2.7B), but were not significantly ($P< 0.05$) different from each other (Figure 2.7B).

Cell Viability (%) (y-axis: 0.0–160.0)

24 Hours Incubation Time — BnMg 0.025: 94.4, BnMg 0.050: 95.4, BnMg 0.100, BnMg 0.200, BnMg 0.400

12 Hours Incubation Time — BnCa 0.025: 92.9, BnCa 0.050, BnCa 0.100, BnCa 0.200: 81.1, BnCa 0.400: 90.2

24 Hours Incubation Time — BnCa 0.025: 97.9, BnCa 0.050, BnCa 0.100, BnCa 0.200: 85.9, BnCa 0.400: 93.9

12 Hours Incubation Time

Cell Viability (%) (y-axis: 0.0–140.0)

BnMg 0.025: 89.4, BnMg 0.050: 90.4, BnMg 0.100, BnMg 0.200, BnMg 0.400

2-HBnMg 0.025: 90.0, 2-HBnMg 0.050: 93.0, 2-HBnMg 0.100, 2-HBnMg 0.200, 2-HBnMg 0.400

2-AcBnMg 0.025: 90.0, 2-AcBnMg 0.050: 88.3, 2-AcBnMg 0.100, 2-AcBnMg 0.200, 2-AcBnMg 0.400: 87.8

Figure 2.7 Concentration- and time-dependent effects of benzoic, 2-hydroxybenzoic and 2-acetylbenzoic acids on viability of HT-1080 cell line grown in 96-well plate for different periods and drug concentrations (Cell seeding density in = 2×10^4 cells/well, 100µl of optimal DMEM medium, under standard growth conditions). Data represent mean ± SE of three replicates. Cell viability measured by MTT assay.

It is interesting to note that most magnesium and calcium 2-hydroxybenzoate analogues exerted their cytotoxic effects at the earlier incubation periods (12, 24 hours), and at lower concentrations (0.025, 0.05mM), similar to the effect of potassium benzoate or 2-

hydroxybenzoate analogues (see Figure 2.5). Results of the effect of other magnesium and calcium treatments generally showed no antiproliferative responses by HT-1080 cells (see Appendix A).

Further investigations were also conducted to see whether the effect of the higher concentrations of calcium 2-hydroxybenzoate analogues on the cell viability of HT-1080 human fibrosarcoma cancer cell line, using MTT assay. Three 2-hydroxybenzoate analogues were used: calcium 2-acetylbenzoate or calcium 2-hydroxybenzoate as well as 2-acetylbenzoic, acid at 0.4, 0.8, 2, 4, 6, and 8mM concentrations and for 24, 48 and 72 hours' incubation time. Figure 2.8 shows that all benzoate compounds induced a concentration and time-dependent reduction in the proliferation of HT-1080 cells.

The proliferation gradually decreased as the 2-hydroxybenzoate analogues' concentration increased. Although the three 2-hydroxybenzoate analogues at 0.4-2mM had no appreciable effects, they were profoundly cytotoxic at 6 and 8mM concentrations. 2-Acetylbenzoic acid (aspirin) increased the antiproliferative activity of HT-1080 cells by approximately 25% and 36% at 6 and 8mM, respectively, after 48' hours incubation, compared to the control. The antiproliferative activity of 2-acetylbenzoic acid was further increased to 47% and 60%, respectively, after 72 hours of incubation (Figure 2.8A). In contrast to the antiproliferation effect of 2-acetylbenzoic acid, calcium 2-acetylbenzoate reduced cell proliferation by approximately 24% and 35% after 48 hours' incubation, which increased to 40% and 63% after 72 hours' incubation at 6mM and 8mM concentration, respectively (Figure 2.8B). For calcium 2-acetylbenzoate, under the same concentrations and incubation times, the increase in the antiproliferation was 34% and 46% after 48 hours, and 52% and 69% after 72' hours incubation (Figure 2.8C).
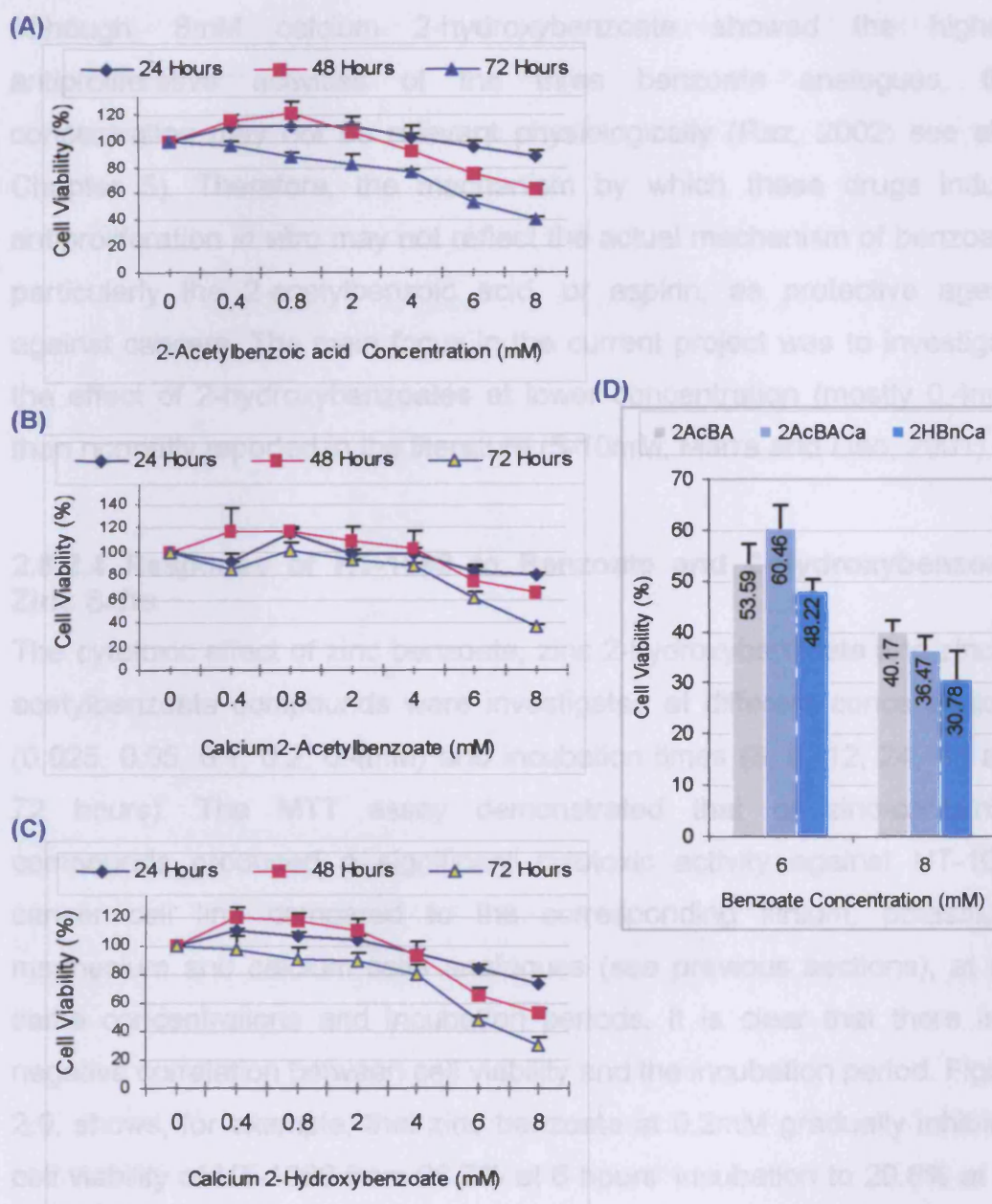
Figure 2.8 Concentration- and time-dependent effects of higher concentration of 2-acetylbenzoic acid (A), Calcium 2-acetylbenzoate (B) Calcium 2-hydroxybenzoate (C) on HT-1080 cell viability, and (D) a comparison between the three compounds at 6mM and 8mM after 72 hours' incubation. Cells seeded at density 15×10^3 cells/well containing 100µl of optimal DMEM medium, in 96-well plate, for different periods and drug concentrations. The MTT assay used to measure cell viability. Data represent mean ±SE of 4 replicates. Cell viability measured by MTT assay. One-Way ANOVA (Fisher's pairwise comparisons, see Appendix A) for (D) showed statistical differences for $p < 0.001$ between the 3 compounds at same concentration and between concentrations with each compound.

Although, 8mM calcium 2-hydroxybenzoate showed the highest antiproliferative activities of the three benzoate analogues, this concentration may not be relevant physiologically (Raz, 2002; see also Chapter 5). Therefore, the mechanism by which these drugs induce antiproliferation *in vitro* may not reflect the actual mechanism of benzoate, particularly the 2-acetylbenzoic acid, or aspirin, as protective agents against cancers. The main focus in the current project was to investigate the effect of 2-hydroxybenzoates at lower concentration (mostly 0.4mM) than normally reported in the literature (5-10mM; Marra and Liao, 2001).

2.5.2.4 Response of HT-1080 to Benzoate and 2-Hydroxybenzoate Zinc Salts

The cytotoxic effect of zinc benzoate, zinc 2-hydroxybenzoate and zinc 2-acetylbenzoate compounds were investigated at different concentrations (0.025, 0.05, 0.1, 0.2, 0.4mM) and incubation times (3, 6, 12, 24, 48 and 72 hours). The MTT assay demonstrated that of zinc-containing compounds produced a significant cytotoxic activity against HT-1080 cancer cell line compared to the corresponding lithium, potassium, magnesium and calcium salts analogues (see previous sections), at the same concentrations and incubation periods. It is clear that there is a negative correlation between cell viability and the incubation period. Figure 2.9, shows, for example, that zinc benzoate at 0.2mM gradually inhibited cell viability of HT-1080 from 98.7% at 6 hours' incubation to 29.8% at 72 hours' incubation or by 70%. A similar cytotoxic effect was also observed when cells were incubated at 0.4mM concentration.

Figure 2.10 shows the cytotoxic effect of the zinc 2-hydroxybenzoate and 2-acetylbenzoate. Both zinc 2-hydroxybenzoate analogues showed cytotoxic effect at 0.2 and 0.4mM concentrations, with a similar pattern to zinc benzoate compound (Figure 2.9). Furthermore, the effect of zinc 2-hydroxybenzoate analogues at the lower concentrations (0.025-0.1mM) showed no cytotoxic or antiproliferative effect on HT-1080 cell line. The cell viabilities under these treatments increased by an average of

approximately 10% in most cases, especially at the earlier incubation periods. Nevertheless, zinc 2-hydroxybenzoate analogues at longer incubation periods induced some cytotoxicity in HT-1080 cells (see Figure 2-10).
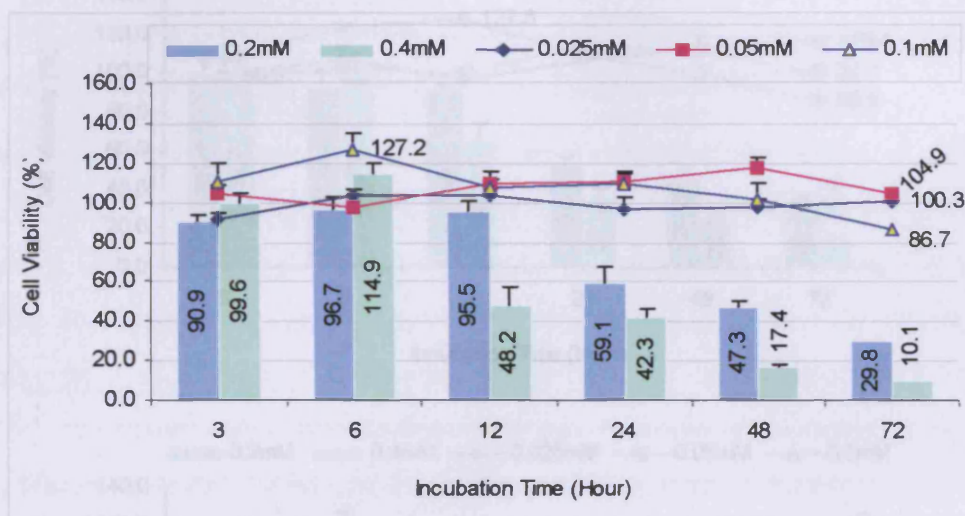
Figure 2.9 Concentration- and time-dependent effects of zinc benzoate on the viability of HT-1080 cell line grown in 96-well plate for different periods and drug concentrations (Cell seeding density in = 2 x10^4 cells/well, 100µl of optimal DMEM medium, under standard growth conditions). Data represent mean ±SE of three replicates. Cell viability measured by MTT assay.

The effects of higher 0.2mM zinc 2-hydrocybenzoate on the HT-1080 cell indicated that viability decreased from 92.1% after 12 hours to 33.9% after 72 hours' incubation, or by 63% over 36 hours of incubation compared to control (Figure 2.10A). At 0.4mM concentration of the same zinc compound and the same incubation period, cell viability was decreased further from 66.2% to 16% compared to the lower concentrations of the same zinc compound (Figure 2.10A).

Figure 2.10B shows the effect of zinc 2-acetylbenzoate on the viability of HT-1080 cells. MTT assay showed that zinc 2-acetylbenzoate was more cytotoxic, especially at higher incubation period. Results in Figure 2.10B indicate that 0.2mM zinc 2-acetylbenzoate decreased the cell viability from

40

94.9% after 12 hours to 25.7% after 72 hours' incubation, while at 0.4mM concentration, the viability decreased from 99.6% to 11.5% over 36 hours' incubation (Figure 2.10B).
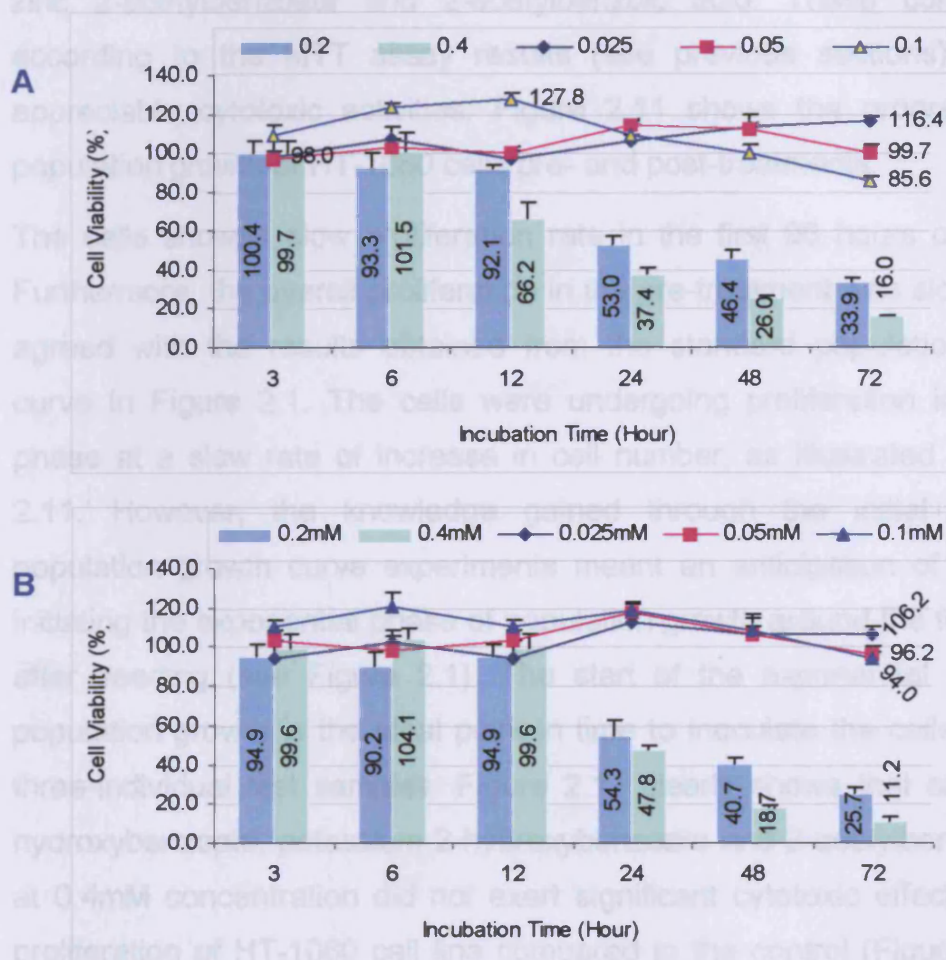
Figure 2.10 Concentration- and time-dependent effects of A- zinc 2-hydroxybenzoate and B- zinc 2-acetylbenzoate on viability of HT-1080 cell line grown in a 96-well plate for different periods and drug concentrations (Cell seeding density in = 2 x10^4 cells/well, 100µl of optimal DMEM medium, under standard growth conditions). Data represent mean ±SE of three replicates. Cell viability measured by MTT assay.

2.5.3 Cell Viability by Haemocytometer Count

Results of the MTT assay in the previous section indicated that the 3 zinc-containing compounds elicited significant cytotoxic effects compared to the other 15 benzoic acid analogues which generally showed a similar pattern of effects on cell viability of HT-1080. The purpose of studying cell viability

by direct count was to double-check the effect of 2-hydroxybenzoate analogues on HT-1080 cell line. Only 5 compounds were used: calcium 2-hydroxybenzoate, potassium 2-hydroxybenzoate, zinc 2-hydroxybenzoate, zinc 2-acetylbenzoate and 2-acetylbenzoic acid. These compounds, according to the MTT assay results (see previous sections) showed appreciable cytotoxic activities. Figure 2.11 shows the progression of population growth of HT-1080 cells pre- and post-treatments.

The cells showed slow proliferation rate in the first 96 hours of culture. Furthermore, the overall proliferation in the pre-treatment was slow, which agreed with the results obtained from the standard population growth curve in Figure 2.1. The cells were undergoing proliferation in the lag phase at a slow rate of increase in cell number, as illustrated in Figure 2.11. However, the knowledge gained through the initial HT-1080 population growth curve experiments meant an anticipation of the cells initiating the exponential phase of population growth around the fourth day after seeding (see Figure 2.1). The start of the exponential phase of population growth is the ideal point in time to inoculate the cells with the three-individual test samples. Figure 2.11 clearly shows that calcium 2-hydroxybenzoate, potassium 2-hydroxybenzoate and 2-acetylbenzoic acid at 0.4mM concentration did not exert significant cytotoxic effects on cell proliferation of HT-1080 cell line compared to the control (Figure 2.11A). Nevertheless, both calcium and potassium 2-hydroxybenzoate elicited some antiproliferative characteristics compared to control during the second day of benzoate treatments (i.e. 168 and 180 hours' culturing, Figure 2.11A).

Both zinc 2-hydroxybenzoate and zinc 2-acetylbenzoate showed an anti-proliferative cytotoxic effect 12 hours after adding the drug at 0.4mM concentration, compared to control and to 2-acetylbenzoic acid (Figure 2.11B). This effect perpetuates with time until no significant viable cells were counted at 72 hours' incubation. Furthermore, both zinc compounds elicited a similar pattern of cytotoxic effect on HT-1080 cells treated for 72 hours (Figure 2.10).

A

B
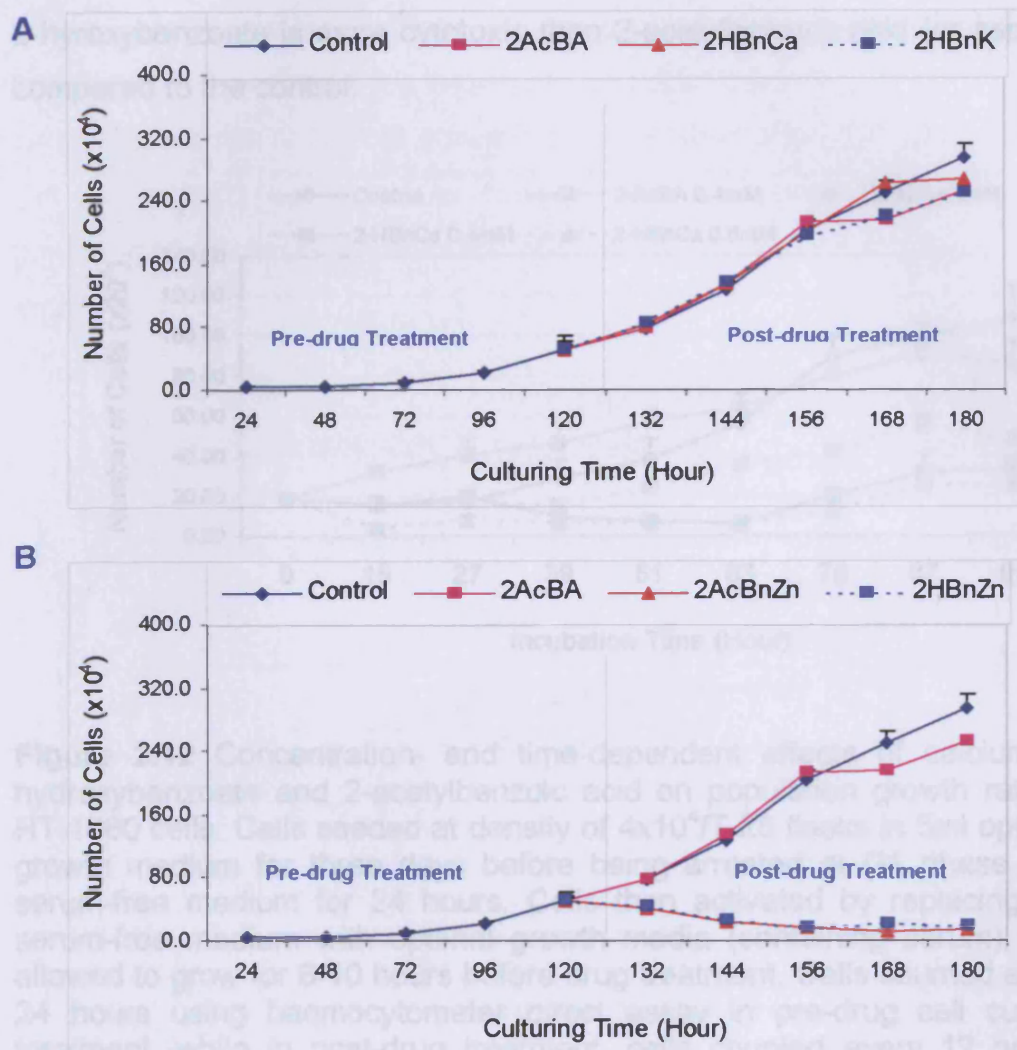
Figure 2.11 Concentration- and time-dependent effects of (A) calcium, potassium 2-hydroxybenzoates, and 2-acetylbenzoic acid, (B) zinc 2-hydroxybenzoate and zinc 2-acetylbenzoate at 0.4mM concentration on HT-1080 cell viability. Cells seeded at density of 4×10^4/T-25 flasks in 5ml optimal growth medium for three days before being arrested at G1 phase with serum-free medium for 24 hours. Cells then activated by replacing serum-free medium with optimal growth medium (containing serum), and cells allowed to grow for 8-10 hours before drug treatment. Cells counted every 24 hours using haemocytometer direct assay in pre-drug cell culture treatment, while in post-drug treatment, cells counted every 12 hours. Data represent mean ±SE of three replicates.

Further investigations were also carried out on the effect of calcium 2-hydroxybenzate but using higher concentrations. Figure (2.12) shows that

43

HT-1080 cell viability was dependent on calcium benzoate concentrations (0.4, 0.8mM) more than incubation time. Results also showed that calcium 2-hyroxybenzoate is more cytotoxic than 2-acetylbenzoic acid (or aspirin) compared to the control.
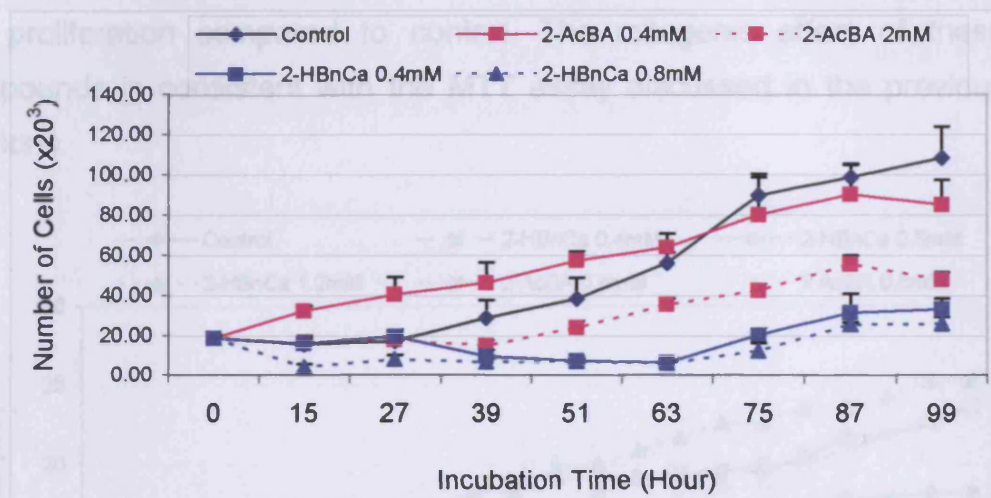
Figure 2.12 Concentration- and time-dependent effects of calcium 2-hydroxybenzoate and 2-acetylbenzoic acid on population growth rate of HT-1080 cells. Cells seeded at density of 4×10^4/T-25 flasks in 5ml optimal growth medium for three days before being arrested at G1 phase with serum-free medium for 24 hours. Cells then activated by replacing the serum-free medium with optimal growth media (containing serum), and allowed to grow for 8-10 hours before drug treatment. Cells counted every 24 hours using haemocytometer direct assay in pre-drug cell culture treatment, while in post-drug treatment, cells counted every 12 hours. Data represent mean and ±SE of four replicates.

2.5.4 Time-lapse Tracking Assay of Cell population Growth Progression

The proliferation of HT-1080 cells was also studied using time-lapse analysis to investigate the effect of both calcium (Figure 2.13) and zinc 2-hydroxybenzoate (Figure 2.14) analogues, but at shorter incubation periods. This experiment aimed to study the effects of these compounds on cell division characteristics, which will be elaborated in Chapter 4. The effect of the 2-hydroxybenzoate compound on the cell proliferation is shown in Figure 2.13. Generally, calcium 2-hydroxybenzoate and 2-

acetylbenzoic acid did not exhibit cytotoxic effects at different concentrations (0.4, 0.8 and 1.2mM) during 22 hours' incubation compared to the control. However, these exhibited a mitogenic effect, where the proliferation increased by a maximum of 28%. Nonetheless, calcium 2-hydroxybenzoate at 0.8mM concentration showed about 6% reduction in the proliferation compared to control. The mitogenic effect of these compounds is consistent with the MTT assay discussed in the previous sections.
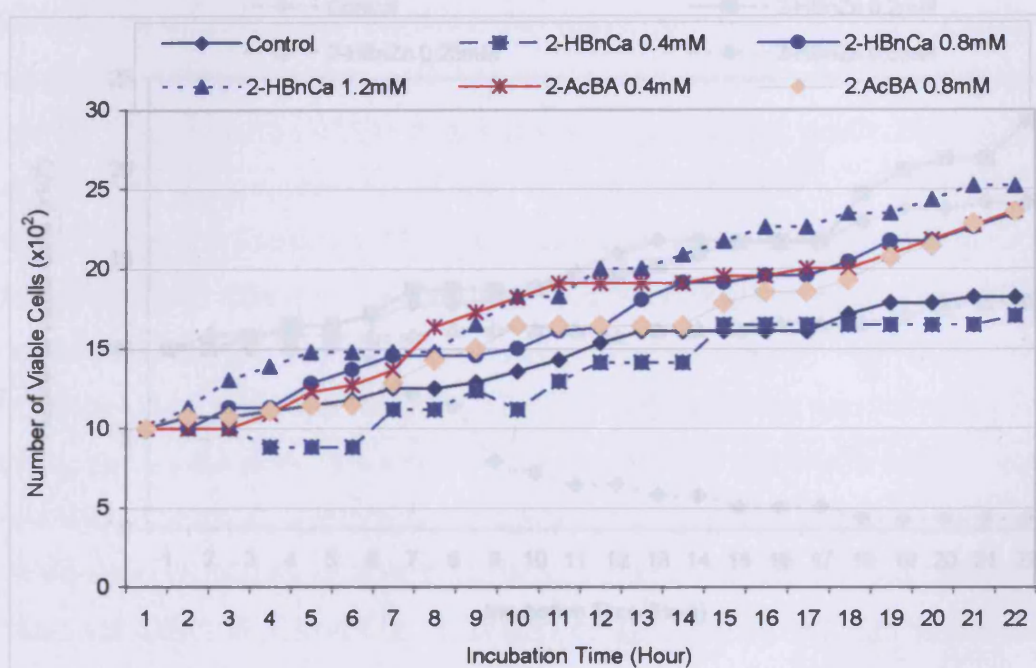
Figure 2.13 Concentration- and time-dependent effects of calcium 2-hydroxybenzoate and 2-acetylbenzoic acid on population growth rate of HT-1080 cells. HT-1080 cells at 1×10^3 cell per well incubated on microscope stage in standard plastic 12-well culture plate. Instrument comprised Zeiss Axiovert 100 microscope fitted with temperature-regulating incubator system and CO_2 supply. Motorised xy microscope stage and phase transmission images (x10 objective lens) set to capture each field every 5 minutes over 22 hours (264 frames per field) using Orca I ER charge-coupled device camera. Camera, stage (xy) and focus (z) PC computer controlled using AQM 2000 software (Kinetic Imaging, Wirral, UK). Tiff-format Images (512 x 512 pixels) played back for analysis as movies using AQM 2000 software.

In comparison with calcium 2-hydroxybenzoate and 2-acetylbenzoic acid, however, zinc 2-hydroxybenzoate showed a concentration- and time-dependent relationship with HT-1080 cell proliferation patterns (Figure 2.14).

The three different methods: MTT, haemocytometer and time lapse image tracking have shown broadly consistent viability measurements that identify the antiproliferative benzoate analogues.
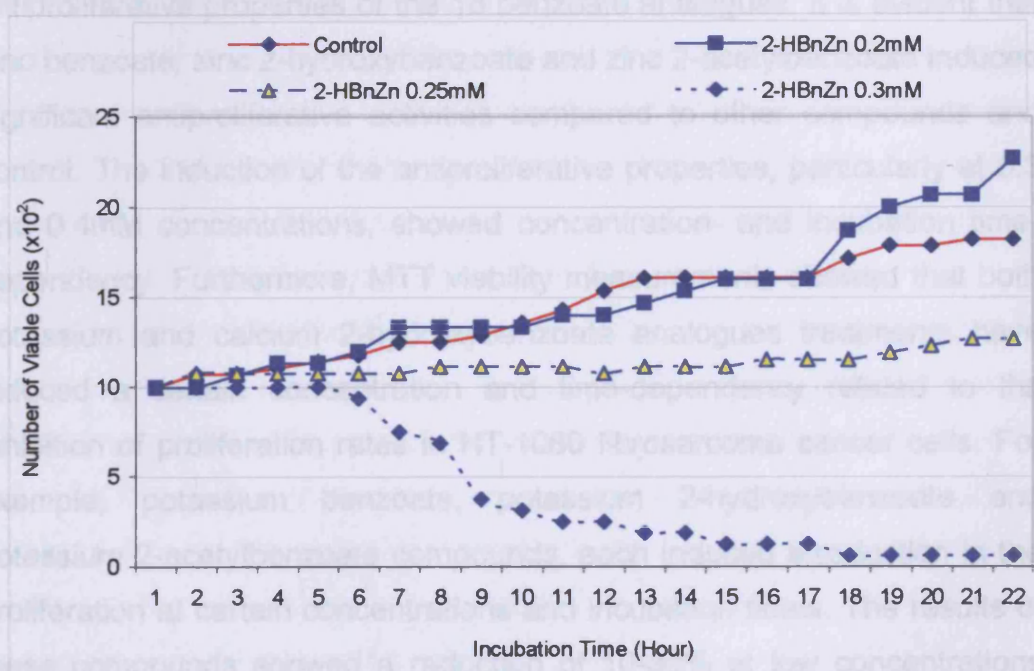
Figure 2.14 Concentration- and time-dependent effects of zinc 2-hydroxybenzoate on the population growth rate of HT-1080 cells. HT-1080 cells at 1×10^3 cell per well incubated on microscope stage in standard plastic 12-well culture plate. Instrument comprised Zeiss Axiovert 100 microscope fitted with temperature-regulating incubator system and CO_2 supply. Motorised xy microscope stage and phase transmission images (x10 objective lens) set to capture each field every 5 minutes over 22 hours (263 frames per field) using Orca I ER charge-coupled device camera. Camera, stage (xy) and focus (z) were PC computer controlled using AQM 2000 software (Kinetic Imaging, Wirral, UK). Tiff-format Images (512 x 512 pixels) were played back for analysis as movies using AQM 2000 software.

46

2.6 Summary and Conclusion

The results of this chapter focus on the antiproliferative activities of 18 2-hydroxybenzoate analogues measured by two methods: MTT and cell count either by haemocytometer or through recorded time-lapse capture microscopy. A range of concentrations (0.025-8mM) and different incubation times (2-180 hour) were used, unless otherwise specified in each experiment. Results demonstrated the differences in the antiproliferative properties of the 18 benzoate analogues. It is evident that zinc benzoate, zinc 2-hydroxybenzoate and zinc 2-acetylbenzoate induced significant antiproliferative activities compared to other compounds and control. The induction of the antiproliferative properties, particularly at 0.3 and 0.4mM concentrations, showed concentration- and incubation time-dependency. Furthermore, MTT viability measurements showed that both potassium and calcium 2-hydroxybenzoate analogues treatments have induced a certain concentration and time-dependency related to the inhibition of proliferation rates in HT-1080 fibrosarcoma cancer cells. For example, potassium benzoate, potassium 2-hydroxybenzoate and potassium 2-acetylbenzoate compounds, each induced a reduction in the proliferation at certain concentrations and incubation times. The results of these compounds showed a reduction of 10-30% at low concentrations (0.025-0.1mM) (see Figure 2.5).

The interest in 2-acetylbenzoate (acetylsalicylates), particularly in respect of cancer research has increased in the last three decades. These studies have demonstrated that 2-acetylbenzoates (particularly, aspirin), at concentrations ranging between 0.5mM to 10mM, inhibit cell population growth, DNA and various proteins synthesis, as well as G1-S phase progression of the cell cycle (Aas *et al.*, 1995; Ricchi *et al.*, 1997; Marra and Liao, 2001; Sharma *et al.*, 2001).

The effects of 2-hydroxybenzoate analogues on cellular function, particularly cell cycle progression may impact on cell population growth at a therapeutic level for cancer. The mechanism of antiproliferative activity

by 2-hydroxybenzoate can be attributed to the modulation of growth-regulatory pathways, *via* genes such as *p53*, *p21*, *Bax*, *Bcl-2*, and others.

The use of high concentrations of these molecules to induce antiproliferative effect *in vitro* may not be physiologically relevant. However, the induction of the significant amount of inhibition supported here might be expected to be translated *in vivo* without further side effect on the normal biological system. The effects of these compounds on the cell viability may result from stimulation of extracellular and/or intracellular signalling pathway(s). Generally, cellular proliferation is governed by complex molecular interactions induced by extracellular and intracellular signalling pathways which determine the accurate reproduction of cells in a way that suits the developmental needs of the organism (Pumin, 1999). Eukaryotic cell division occurs in a series of steps which determine the cell population growth and cell proliferation that occurs in a precisely regulated cell cycle, comprising four distinct phases (G_0/G1, S, and G2) (Zetterberg and Larsson, 1995). Thus several compounds with the potential to restore control of cell division in human cancers have been developed through the understanding of the cell cycle regulation by various regulatory protein families (Charles, 2004). The effect of some of these benzoate compounds will be elaborated further in Chapter 4.

In conclusion some of the antiproliferative 2-hydroxybenzoate analogues used in this study were concentration- and time-dependent in reducing the proliferation rates of HT-1080 cell line. The next chapter will focus on the effect of 2-hydroxybenzoate analogues on the morphology of HT-1080 cell line.

Chapter Three

Effect of 2-Hydroxybenzoate Analogues on the HT-1080 Cell Line: Morphological and Immunocytochemical Evidence of Apoptosis

CHAPTER THREE

Effect of 2-Hydroxybenzoate Analogues on the HT-1080 Cell Line: Morphological and Immunocytochemical Evidence for Apoptosis

3.1 Introduction

This chapter aims to assess the effect of 2-hydroxybenzoate analogues on the morphological characteristics of the HT-1080 fibrosarcoma cell line. Generally, eukaryotic cells undergo either natural or induced morphological changes as a result of, for example, cellular differentiation, proliferation or drug-induced apoptosis. These morphological observations are important to distinguish changes that might occur in the nucleus, cytoplasm, and/or cell surface, in order to understand the normal functions of cells. Acquiring this knowledge is also necessary to understand diseases and their treatments. For example, normal cellular morphology can differ from that of cancer cells, as tumour cell morphology is often characterised by aneuploidy. Furthermore, both types of cell death, programmed cell death (apoptosis) and necrosis, are often distinguishable by their morphological characteristics.

Changes in cellular morphology can be attributed to various biochemical molecular biological processes, and can be observed by light, fluorescence and electron microscopy. These techniques have been used by many researchers as an initial observation strategy during many studies (Zhang *et al.*, 1997; Willingham, 1999; Barrett *et al.*, 2001). Thus, this chapter focuses on the application of a number of morphological and molecular techniques to visualise the changes in the HT-1080 cells induced by various treatments with 2-hydroxybenzoate analogues. Light, fluorescence and electron microscopy are used with or without certain dyes, including haematoxylin and eosin, methyl-green and pyronin, DAPI and Annexin-V. These dyes are mainly aimed at the detection of apoptotic HT-1080 cells. The apoptotic effects of 2-acetylbenzoic acid and calcium, magnesium, potassium and zinc 2-hydroxybenzoate analogues were assessed.

3.2 Morphological Techniques

Several techniques have been developed and systematically used in the literature to investigate morphological changes resulting from the treatment of cancer cells with both synthetic and natural biologically active compounds (Bowen and Ryder, 1976; Stevens, 1977; Wyllie *et al.*, 1980; Kerr *et al.*, 1987; Drachenberg *et al.*, 1997). Light microscopy is the simplest technique that can detect the morphological changes in cancer cells with or without staining. Specific dyes have been used to elucidate certain changes in the cell. Haematoxylin and eosin, for example, stain the cell nuclei blue to black, whilst the eosin stains cell cytoplasm and most connective tissue fibres in varying shades and intensities of pink, orange and red (Stevens, 1977). This technique is routinely used in diagnostic and clinical research for the enhancement of cellular and nuclear structures, together with the recognition of apoptotic bodies. Haematoxylin is an adequate nuclear stain only in the presence of a mordant, such as aluminium, iron, tungsten, and on occasions, lead salts (Stevens, 1977). The mordant in most widespread use is alum haematoxylin in the form of aluminium potassium sulphate. The nuclei are initially stained a red colour, which is then converted to a blue-black colour when washed in tap water, which is a weak alkali.

Eosin is widely used, together with alum haematoxylin, to enhance the general histological structure of a cell or tissue. The eosins are xanthene dyes, of which eosin Y is the most commonly used. As a cytoplasmic stain, it is used as 0.5-1% solution in deionised water with a crystal of thymol to prevent fungal growth (Stevens, 1977). Tap water washing differentiates the eosin stain in the cytoplasm and the subsequent intensity of both the haematoxylin and eosin stain.

Methyl-green and pyronin y are other common dyes that have been used in cytology to stain nuclear morphology, specifically of DNA and RNA, respectively (Elias 1969; Bancroft and Stevens, 1977; Bowen, 1984). The combination of these two dyes was used first by Pappenheim in 1899, and

50

later modified by Unna in 1902 (cited by Moffit, 1994). The technique appears to be specific under certain conditions for DNA, and the pyronin y specific for RNA when used in an acidic environment. Thus methyl-green might emphasise apoptotic cells due to the staining of pyknotic nuclei, while the pyronin y may highlight apoptotic cells due to increases in RNA levels (Bowen et al., 1993). Non-apoptotic (necrotic) cells may also be 'negatively' highlighted due to the loss of RNA and thus lack of pyronin y stain.

Fluorescence dyes like 4',6-diamidino-2-phenylindole (DAPI) have also been used to illustrate the nuclear morphology of cells. DAPI is a fluorescent dye that interacts with the double stranded helix of the DNA at A-T clusters when it is excited at a wavelength of 460nm to give a blue fluorescence colour. The interaction between the DNA helix and DAPI increases the intensity of fluorescence twenty-fold giving enough blue colour to be observed.

In addition to the techniques used for nuclear and cytoplasmic staining, the immunohistochemical analysis of phosphatidylserine offers an earlier detection of changes on the cytoplasmic membrane. The Annexin-V assay is widely used to detect cells undergoing apoptosis and is an excellent indicator of the onset of apoptosis in many cell types. In healthy cells, most of the phosphatidylserine is localised to the interior (cytoplasmic) face of the cytoplasmic membrane, but within one hour after the induction of apoptosis, it rapidly redistributes to the outer leaflet of the lipid bilayer by a mechanism that is unclear, However, Martin et al. (1995) postulated that phosphatidylserine externalisation is an active process (e.g a flippase) needing a threshold presence of energy in the form of ATP. During the process of apoptosis, high levels of ATP are present within the cell to carry out the signal transduction cascades (e.g caspase cascade) of cell death (Fadok et al., 1992; Martin et al., 1995). Thus, during apoptosis ATP is available for the active process of phosphatidylserine translocation. However, during necrosis, a decrease in ATP levels prevents the energy-thirsty phosphatidylserine translocation (Leist et al., 1997). Intracellular

ATP concentration is a switch deciding between apoptosis and necrosis thus the assay is apoptotic-specific. The function of phosphatidylserine externalisation is unclear, but it may serve as a 'tag' to single out apoptotic cells for recognition by macrophages (Fadok et al., 2000). However, once on the cell surface, phosphatidylserine can be easily detected by staining with an FITC conjugate of annexin-V, a protein that has a strong, natural affinity for phosphatidylserine. Other immunohistological techniques have also been developed to study cell death and the changes that occur in cells naturally or induced by drugs. The enzyme-linked immunosorbant assay (ELISA) techniques, for example, use both antihistone and complementary DNA base binding to detect both DNA fragmentation and histone released by nucleosomes (Trauth et al., 1995). The technique has been used successfully at both light and electronic microscope levels to detect histones and DNA localisation (Gregorc and Bowen, 1997; Al-Hazzaa and Bowen, 1998).

In addition to the morphological changes detectable by light and fluoresce microscopy, electron microscopy can reveal more detailed changes to the intracellular membrane compartments, including the endoplasmic reticulum, mitochondria, and Golgi apparatus (Bowen et al., 1996; Leek and Albertsson, 2000). The loss of microvilli observed by electron microscopy, in many cases may be considered as a common feature of cell death (Fernandez-Segura et al., 1990; Nagata, 1996; Kondo et al., 1997). Loss of microvilli has been shown to occur downstream of caspase activation, and along with dephosphorylation of proteins which normally stabilise microvilli to the actin skeleton (Kondo et al., 1997).

3.3 Cell Morphology Changes and Cell Death

Cell death may occur naturally (e.g. apoptosis) as part of cell turnover, during involution of tissue as part of normal embryological development, or pathologically (e.g. apoptosis or necrosis). While apoptosis occurs in both pathological conditions (e.g. Parkinson's and Alzheimer's disease) and

normal conditions (at the end of the natural cellular life-span), necrosis is always pathological (e.g. as a result of an infection), and is usually accompanied by an inflammatory reaction. Both modes of cell death have distinctive morphological characteristics that can be detected by microscopic techniques. Figure 3.1 shows the comparison between the morphological characteristics of both apoptosis and necrosis modes of cell death.

Apoptosis is associated with a distinct set of biochemical and morphological changes involving all components of the cell, including the cytoplasm, nucleus and plasma membrane (Kerr et al., 1972; Wyllie, 1980; Arends and Wyllie, 1991). The early stage of morphological change in cells undergoing apoptosis is characterised by cell rounding-up, losing microvilli, and subsequently the contact with the neighbouring cells. The cells finally shrink and fragment into apoptotic bodies with intact membranes. During apoptosis, the cytoplasm condenses, but the plasma membrane, ribosomes, Golgi apparatus, and mitochondria remain intact. The endoplasmic reticulum dilates, and the cisternae swell to form vesicles and vacuoles that fuse with the surface membrane, giving a characteristic blebbing or bubbling appearance (Figure 3.1). In the nucleus, the chromatin condenses at the nuclear membrane and aggregates into dense compact masses, and is fragmented internucleosomally by endonucleases, which can be analysed by the typical 'DNA ladder' formation of apoptosis, for which DNA is extracted from the cells and separated by gel chromatography (Kerr, 1994; Nagata, 2000; Vaux, 2002). The cells at this stage separate into apoptotic bodies that are surrounded by an intact plasma membrane to prevent any interaction with biological fluids and normal cells. These fragmented cell bodies or apoptotic bodies are easily recognised and are digested by macrophages or epithelial cells, usually without inflammation. This is why apoptosis induction has been considered as one possible strategy in cancer therapy. Indeed, several anticancer molecules have been shown to

restore the missing programmed cell death which proceeds through apoptosis (Vaux, 2002).

It is not clear whether the detectable morphological alterations are subsequently due to a single pathway or multiple interrelated pathways; however, it can be assumed that caspases play a crucial role in the appearance of these alterations. But, *in vitro* the chemical inhibition of caspases only partially inhibits the alterations. An example being when caspase-3 was removed from both mice and human breast cancer cells (Janicke *et al.,* 1998, and Zheng *et al.,* 1998, respectively), only a reduction and not a total elimination of blebbing was observed. Nevertheless this implies that structural events are indeed the consequence of caspase activation, and although blebbing appears to require caspase-3 activity in order to be initiated, once initiated, it can continue even in the presence of caspase inhibitors, implying that caspases activate downstream mechanisms, which mediate the appearance of blebs.
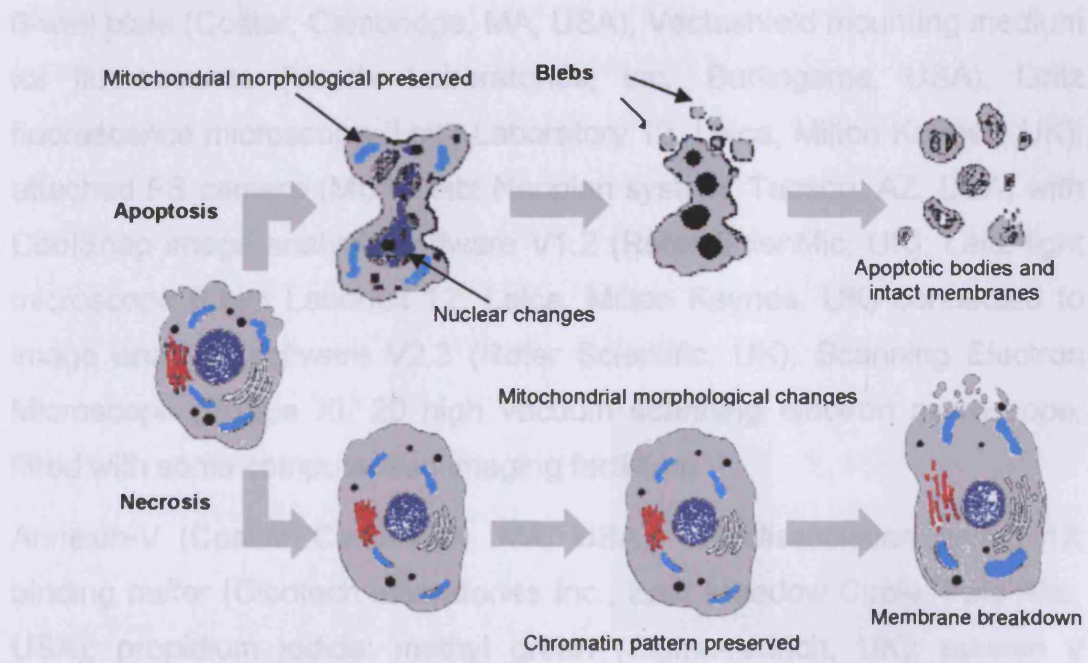
Apoptosis	Normal cell	Condensation	Fragmentation	Secondary necrosis
Necrosis		Reversible swelling	Irreversible swelling	Disintegration

Figure 3.1 Morphological structure of apoptosis and necrosis modes of cell death. Adapted from Duvall and Wyllie (1985) (1986).

This form of physiological cell death is morphologically quite different from the necrotic mode of cell death (Figure 3.1), in which the cell swells and disintegrates in an unordered manner, eventually leading to the destruction of the cellular organelles, and finally rupture of the plasma membrane and leakage of the cell content. During necrosis, the permeability of the plasma membrane increases, the endoplasmic reticulum dilates, the cell alters shape, the mitochondria become denser, the nuclear chromatin flocculates. The disintegration of the plasma membrane and the leakage of cell contents, mainly lysosomal enzymes, often provoke inflammation. A secondary necrosis can also be the final result in situations where there is too much apoptosis occurring for phagocytotic cells to cope with, or in cell culture (Trump *et al.*, 1997) where phagocytotic cells are usually lacking.

3.4 Materials and Methods

3.4.1 Materials and Instruments

6-well plate (Coster, Cambridge, MA, USA), Vectashield mounting medium for fluorescence (Vector Laboratories, Inc., Burlingame, USA), Leitz fluorescence microscope (Leitz Laboratory 12, Leica, Milton Keynes, UK); attached FS camera (MCA Leitz Neoplan system, Tucson, AZ, USA) with CoolSnap image analysis software V1.2 (Rofer Scientific, UK); Leitz light microscope (Leitz Laborlux 12; Leica, Milton Keynes, UK) connected to image analysis software V2.3 (Rofer Scientific, UK); Scanning Electron Microscope (Philips XL 20 high vacuum scanning electron microscope, fitted with some computerised imaging facilities)

Annexin-V (Costar, Cambridge, MA, USA), cell dissociation buffer; 1X binding buffer (Clontech laboratories Inc., East Meadow Circle, Palo Alto, USA); propidium iodide; methyl green (Sigma-Aldrich, UK); pyronin y (Sigma-Aldrich, UK); 4',6-Diamidino-2-phenylindole dihydrochloride Diamidoino-2-Phenylindole (DAPI) (Sigma-Aldrich, UK); haematoxylin (R A Lamb Limited, UK), Eosin (R A Lamb Limited, UK); xylene, ethanol, chloroform, and formaldehyde (Sigma-Aldrich, UK).

Preparation of Methyl green-pyronin y Stain The methyl green component is supplied in an impure form that contains traces of methyl violet which is soluble in chloroform. Methyl green-pyronin y stain was prepared according to Moffit (1994), where 0.75g of methyl green was added to 150ml of acetate buffer at pH 4.9 (4.4g sodium acetate dissolved in 160ml deionised water, pH adjusted to 4.9). The solution was then washed with chloroform (150ml x 4) to remove methyl violet impurities, till the chloroform layer became translucent. 200mg of pyronin y was dissolved in 100ml of purified methyl green, and then the methyl green/pyronin y mixture was filtered. This solution was kept as a stock solution, at 4°C, and used within 5 days.

The haematoxylin and eosin stain was prepared according to Stevens (1977).

3.4.2 Cells and *in vitro* Culture Conditions

HT-1080 cells were grown in 6-well plates containing coverslips at the density described previously, unless otherwise stated, in DMEM optimal growth medium (see Chapter 2, Materials and Methods). After 48 hours, the medium was replaced with fresh medium containing one of the benzoate or 2-hydroxybenzoate analogues under investigation, unless otherwise stated. These compounds were prepared as described in Chapter 2. Two control samples were incorporated in each experiment: no treatment and cell treated with a standard apoptosis-inducing drug (staurosporine) at a final concentration of $1\mu M$. Treated cells were incubated under standard culture conditions for 48 hours, unless otherwise indicated, washed with PBS, and finally stained with one of the dyes outlined above. In each experiment, both apoptotic and non-apoptotic cells were counted in 2 fields of each slide, using a Leitz Laborlux 12 microscope.

3.4.3 Immunoassay- Annexin-V for Apoptosis Detection

HT-1080 cells were seeded into 6-well plates at an initial density of 1.25×10^5 per well and cultured for 48 hours, as described in Section 3.4.2. The optimum DMEM growth medium was then replaced with the same medium containing 2-hydroxybenzoate at different concentration. After treatment for 48 hours, unless otherwise stated, the medium containing non-adherent cells was aspirated into centrifuge tubes, the cells dissociated with 1ml/well of warm (37°C) cell dissociation buffer (previously diluted with 2ml of warm DMEM medium), and incubated for 5-10 minutes. Adherent cells were gently scraped and pooled with the non-adherent cells using a cell scraper. Cells were then pelleted by centrifugation at 200g for 5 minutes, the supernatant removed, and the cells homogenised with 0.5ml of 1X binding buffer (Clontech Laboratories Inc, East Meadow Circle, Palo Alto, USA). The cell suspensions were transferred into Eppendorf pipettes and centrifuged at 200g for 5 mintes, the supernatant was removed, and the homogenised cells resuspended in 50µl of 1X binding buffer. Subsequently, 3µl of Annexin-V -FITC was added to each tube, and these were incubated for 15 minutes at room temperature, in the dark. Immediately after incubation, 2µl of propidium iodide (50µg/ml of 1X binding buffer) was added and incubated for a further 5 minutes at room temperature, in the dark and mounted in vectashield (Vector Laboratories, Inc, Burlingame, USA). Slides were examined using a fluorescence microscope (Leitz Laborlux 12; Leica, Milton Keynes, UK). Five random fields, each of 100 cells, were counted per slide, and the percentage of apoptotic cells was assessed based on nuclear morphology (Rogers et al., 1996). Representative photographic images were taken using a photometrics FS camera (MCA Leitz; Neoplan system, Tucson, AZ, USA) and CoolSnap image analysis software V1.2 (Rofer Scientific, UK).

3.4.4 Diamidoino-2-Phenylindole (DAPI) Staining

HT-1080 cells were seeded into 6-well plates containing coverslips, at an initial density of $2x10^5$ per well, as described in Section 3.4.2. After 48 hours or unless otherwise stated, the cells in each well were washed with 2ml PBS and incubated for 10 minutes at room temperature before fixing with 2ml of 4% formaldehyde in PBS for 10 minutes at room temperature while cells became attached to the coverslips in the wells. After fixation, cells were washed again with PBS, stained for 20 minutes with 2.5mg/ml DAPI solution and each coveslip was mounted in Vectashield mounting medium for fluorescence. The DAPI-stained HT-1080 cells were examined using a fluorescence microscope at 460nm maximum wavelength. Four fields were selected from each sample. Representative photographic images were taken using a photometrics FS camera and CoolSnap image analysis software V1.2.

3.4.5 Haematoxylin and Eosin Staining

HT-1080 cells were seeded into 6-well plates containing coverslips at an initial density of $1.25x10^5$ per well, and grown for 48 hours, as described in Section 3.4.2. The optimum DMEM culture medium was then replaced with the same medium, but containing 2-hydroxybenzoate compounds at concentrations, unless otherwise indicated for each experiment (see legend of each Figure in Results and Discussion Section). Cells were allowed to grow for a further 24 hours. HT-1080 cells were then washed with PBS, fixed with formaldehyde solution, and washed again with PBS for 1 minute at room temperature, as described in the previous section. Cell samples were washed again in 2ml of PBS for 1 minute at room temperature, and stained with Mayer's haematoxylin for 1 minute, followed by three washes in tap water and one in distilled water. The sections were counterstained with 1% eosin for 3-5 minutes, followed by another 3 washes in tap water and one in distilled water. Gently, the converslip containing stained cells was lifted from the well using forceps, and

immersed in the following solvents: deionised water; 70 % alcohol; 95 % alcohol; 100% alcohol twice; xylene twice (xylene vapour is toxic and may be carcinogenic, therefore this step was carried out in a fume cupboard). Excess liquid was removed from the coverslip by gently tapping it on a piece of rolled tissue paper. Finally, the coverslip was air dried and mounted on a labelled slide using a small amount (several drops) of DPX (a synthetic resin). Forceps were used to gently press the coverslip down on the slide. Images of treated and untreated HT-1080 cells were viewed under Leitz light microscope. The significant images were recorded through the use of Analysis Image, Analysis software V2.3.

3.4.6 Methyl-green/pyronin y Staining

HT-1080 cells were seeded into 6-well plates containing coverslips, at initial density of 1.5×10^4 per well, and grown for 48 hours as described in Section 3.4.2. The optimum DMEM culture medium was then replaced with the same medium but containing 2-hydroxybenzoate analogue at different concentrations, (see legend of each Figure in Results and Discussion Section). After 48 hours, the DMEM optimal growth medium was replaced with fresh medium containing 2-hydroxybenzoate analogue unless otherwise stated. After treatment for 48 hours, the old medium was aspirated and the adherent cells were washed in 2ml of PBS and incubated for 10 minutes at room temperature before fixing with 2ml of 4% (v/v) formaldehyde in PBS for 10 minutes at room temperature. The samples were washed again in 2ml of PBS for 1 minute at room temperature, and incubated for 45 minutes in methyl-green/pyronin y staining solution at room temperature. The coverslips were removed from the wells, then washed by dipping for 3-4 seconds in deionised water at 1°C. Coverslips were air dried and mounted with DPX. The coverslips were viewed under a light microscope and images recorded through the use of Analysis Image, Analysis software V2.3.

3.4.7 Scanning Electron Microscopy

HT1080 cells were seeded in a 12-well plate containing microscope coverslips at density of 1.5 x 10^4 cells per well, and incubated for 24 hours under standard growth conditions in the optimal DMEM growth medium, before being treated with salicylates at different concentration and incubation periods (see Section 3.4.2). Cells were then treated with the fixative (0.8% glutaraldehyde, 0.6% osmium tetroxide, 2 mM $CaCl_2$, and 0.2M sucrose in 0.1M sodium cacodylate buffer pH 7.4) for one hour, washed several times in PBS buffer, and dehydrated with different alcohol concentrations (30%, 50%, 70%, 90%, each for 5 minutes, and 100% for 10 minutes, twice). The dehydrated samples were then dried to the critical point in a Blazers CPD 030 using CO_2. Cell samples were then mounted onto 12 mm 'Philips type' aluminium stubs, using silver paint, and then gold sputter-coated in an Edwards S150B sputter coater. Finally, the samples were imaged using a Philips XL20 SEM under various magnifications ranging from x500 up to x5000.

3.5 Statistical Analysis

The immunohistochemical detection of the number of labelled cells with Annexin-V was obtained from 2-3 slides. The resulting average was used to calculate mean ±SE. To determine the effect of drug treatment on the induction of apoptosis, data were calculated as a percentage of control and expressed as means ±SE. One-Way Analysis of Variance was performed using Minitab statistical program. A value of $p < 0.01$ was considered significant.

3.6 Results and Discussion

3.6.1 Morphology of Untreated HT-1080 Cell Line

The fibrosarcoma HT-1080 cells showed an irregular shape with a distinct microvilli as revealed by scanning microscopy. The dimensions of HT-1080 cells ranged between 10-15μm wide and 20-30μm long (Figure 3.2A). Cells also appeared in a flat monolayer structure (Figure 3.2A) and retained their attachment to the surface, as well as their plasma membrane processes. The control cells of HT-1080, stained by DAPI and observed under a phase contrast of fluorescence/light and scanning electron microscope, indicated that these cells were viable, as confirmed by the above-mentioned features and the presence of cell connection fibres (Figure 3.2B). It is possible to identify the nucleus of HT-1080 cells by DAPI staining as a blue colour (Figure 3.2B), or as a dark colour when cells were stained by haematoxylin (Figure 3.2D) or methyl green (Figure 3.2C). Furthermore, the cytoplasm of HT-1080 cells showed responses to pyronin y and eosin to give, respectively, pink or red colours to the RNA of the cells (Figures 3.2C and 3.2D). It appeared that there were a few cells either apoptotic (Figure 3.2C, blue arrows) or mitotic (Figure 3.2D, black arrows).
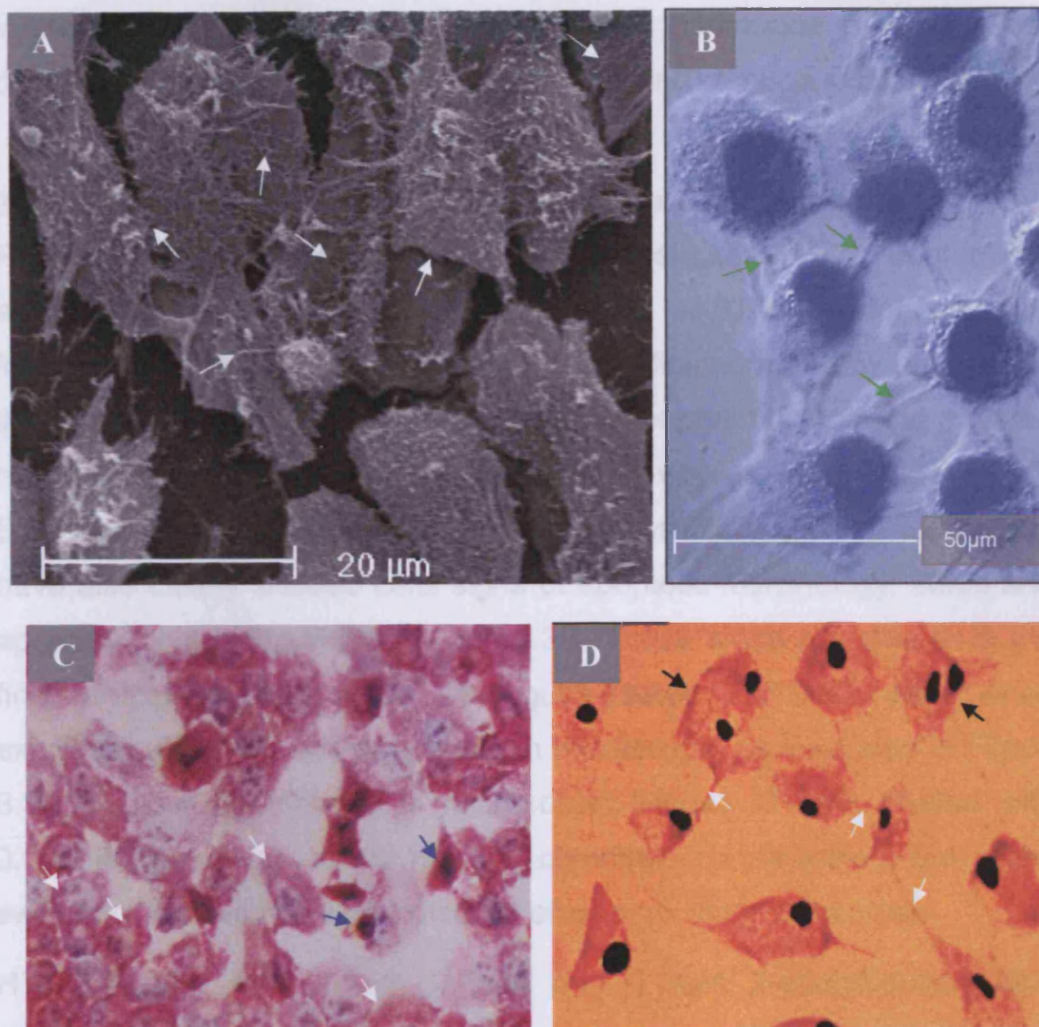
Figure 3.2 HT-1080 fibrosarcoma cell images: **A** SEM revealing distinctive filaments and filopodia (white arrows); **B** Phase contrast image showing cell connections (green arrows) and fluorescent DAPI blue stained nucleus; **C** Methyl green-pyronin y stained HT-1080 cells, blue indicates DNA in the nucleus, while pink colour indicates RNA rich cytoplasm. Apoptotic cells (blue arrows), and normal HT-1080 cells (white arrows) (magnification x200). **D** Haematoxylin-eosin-stained HT-1080 cells, nucleus dark-stained by haematoxylin, and cytoplasm red- stained by eosin, filopodial attachment (white arrows), and mitotic cells (black arrows) (magnification x200).

These cells were treated with both 2-acetylbenzoic acid, and 2-hydroxybenzoate calcium, magnesium, potassium and zinc analogues at different concentrations and incubation periods unless otherwise indicated

in the following sections. The effect of these compounds in inducing cell death was investigated by light, fluorescence and electron microscopy.

3.6.2 Morphological Changes Induced by Standard Drugs

Figure 3.3 shows the morphological characteristic of HT-1080 treated with an apoptotic control agent, the staurosporine at 0.001mM concentration for 24 hours. DAPI staining of treated cells indicated that they progressed through apoptosis as cells showing various apoptotic bodies and pyknotic nuclei. In some treated cells, signs of blebbing were observed Figure 3.3A. Both haematoxylin-eosin and methyl green-pyronin y staining techniques have also clearly showed cells signs of apoptotic morphology, blebs and apoptotic bodies Figures 3.3B and 3.3C. These signs are clearer in the fine structure of benzoate analogues-treated HT-1080 cells when examined under the scanning electron microscope, as illustrated in Figure 3.3D. Further examination of microscopic images of cells treated with 0.001mM staurosporine did not find chromatin condensation, but a few swollen cells which may be indicative of an early stage of necrosis.

HT-1080 cells treated with 0.4mM and 0.8mM 2-acetylbenzoic acid showed signs of apoptosis when stained with DAPI. Cell treated with 0.8mM 2-acetylbenzoic acid showed more cells undergoing blebbing compared to 0.4mM treatment (Figure 3.4A, 3.4B) and control sample (Figure 3.2B). Both apoptotic bodies and blebs as evidence of distinct signs for cells undergoing apoptosis were clearly observed by the microscopic examination when HT-1080 cells treated with 0.4mM 2-acetylbenzoic acid and stained by haematoxylin-eosin (Figure 3.4C) or methyl green-pyronin y (Figure 3.4D). Furthermore, the effect of 2-acetylbenzoic acid on the morphological features of HT-1080 cells was also examined by SEM.
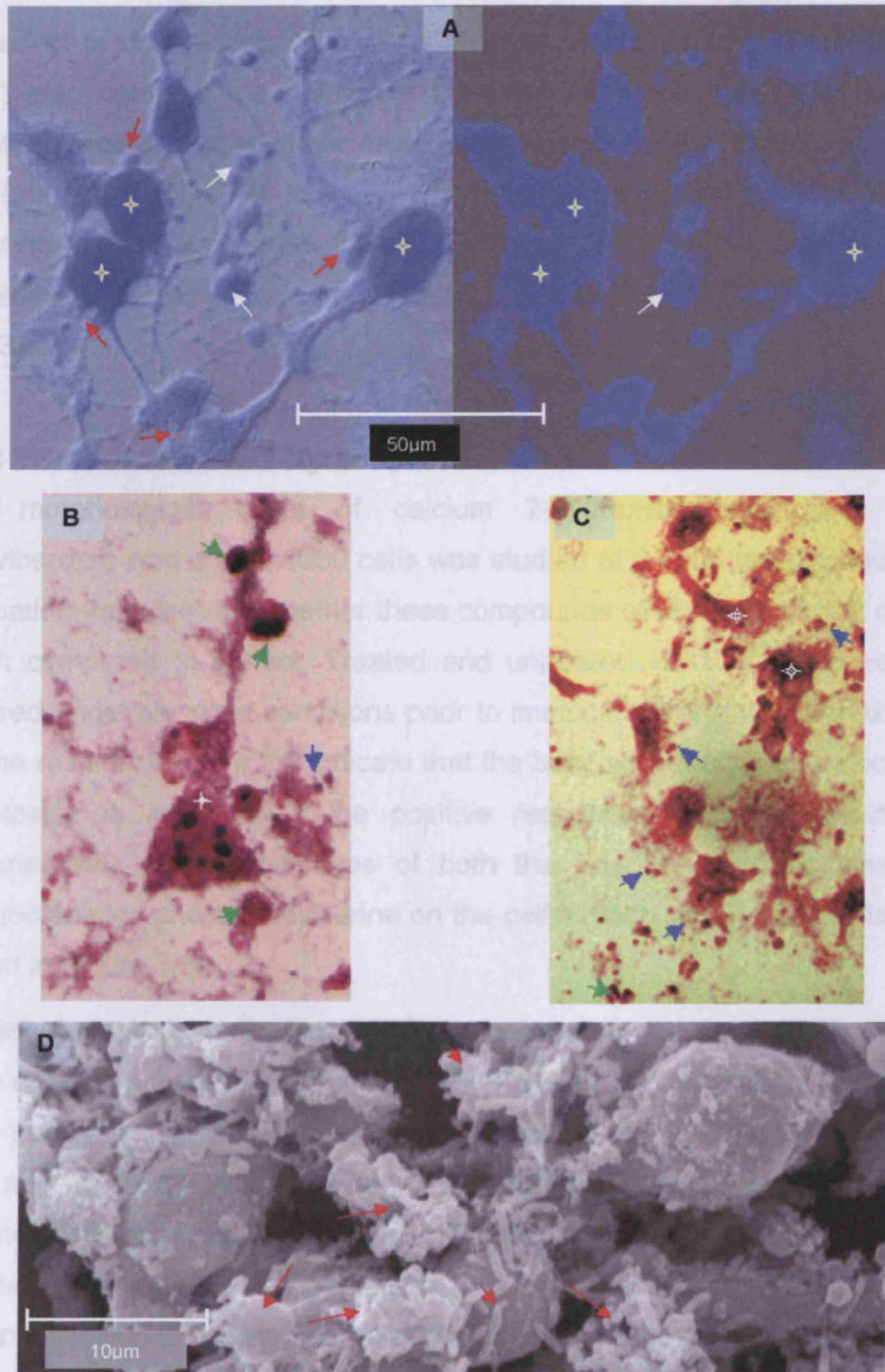
Figure 3.3 Microscopic images of HT-1080 cells treated with 0.001mM staurosporine and examined by (**A**) DAPI staining, white arrows refer to apoptotic bodies, red arrows to blebs and stars to pyknotic nuclei, **B** Haematoxilin-eosin staining, green arrows refer to apoptotic body, blue arrows for blebs, and star for apoptotic cells (magnification x200), **C** Methyl-Green-pyronin y staining, labelling as in B (magnification x200) and (**D**) SEM, red arrows refer to apoptotic bodies.

64

The effect of different concentrations of 2-acetylbenzoic acid (0.4, 2 and 8mM) also confirms the results of the previous cytological techniques about the presence of apoptotic cells, and apoptotic bodies. Examining the morphology of HT-1080 indicates 0.4mM (Figure 3.4E1) caused less cytotoxic effects compared to 2mM (Figure 3.4E2). The number of apoptotic cells increased dramatically at 8mM concentration (Figure 3.4E3).

3.6.3 Effect of Calcium 2-Hydroxybenzoate on HT-1080 Cell Death

The morphological effect of calcium 2-hydroxybenzoate and 2-acetylbenzoic acid on HT-1080 cells was studied at 0.4mM and 24 hours' incubation, to determine whether these compounds elicited significant cell death compared to control. Treated and untreated HT-1080 cells were cultured under standard conditions prior to immunolabelling with Annexin-V. The results in Figure 3.5 indicate that the benzoate analogues induced apoptosis, as indicated in the positive responses to the Annexin-V immunoassay. The percentages of both the positively and negatively immunolabelled phosphatidylserine on the cell surface of HT-1080 cells is shown in Figure 3.5A.

Statistical analysis indicated that both benzoates induced significantly more apoptosis than the control at 0.01% (Figure 3.5A). The percentage of cells positively labelled with Annexin-V were 16.5% by 2-acetylbenzoic acid and 25.3% by calcium 2-hydroxybenzoate. Figure 3.5B1-B3 shows the morphological characteristics of HT-1080 cells undergoing cell death at the early stages, as elucidated by the labelling of the flagged phosphatidylserine (green arrows) and at the later stages (white arrows) of death, as indicated by the cell shrinkage and nuclear condensation during 24 hours and at 0.4mM concentration.

Further investigations of the effect of calcium 2-hydroxybenzoate on the nuclear morphology of HT-1080 cells were also carried out at different concentrations (0.4, 0.8 and 1.2mM) (Figure 3.6). Treated HT-1080 cells

were cultured under optimal conditions for 24 hours before staining with
DAPI.
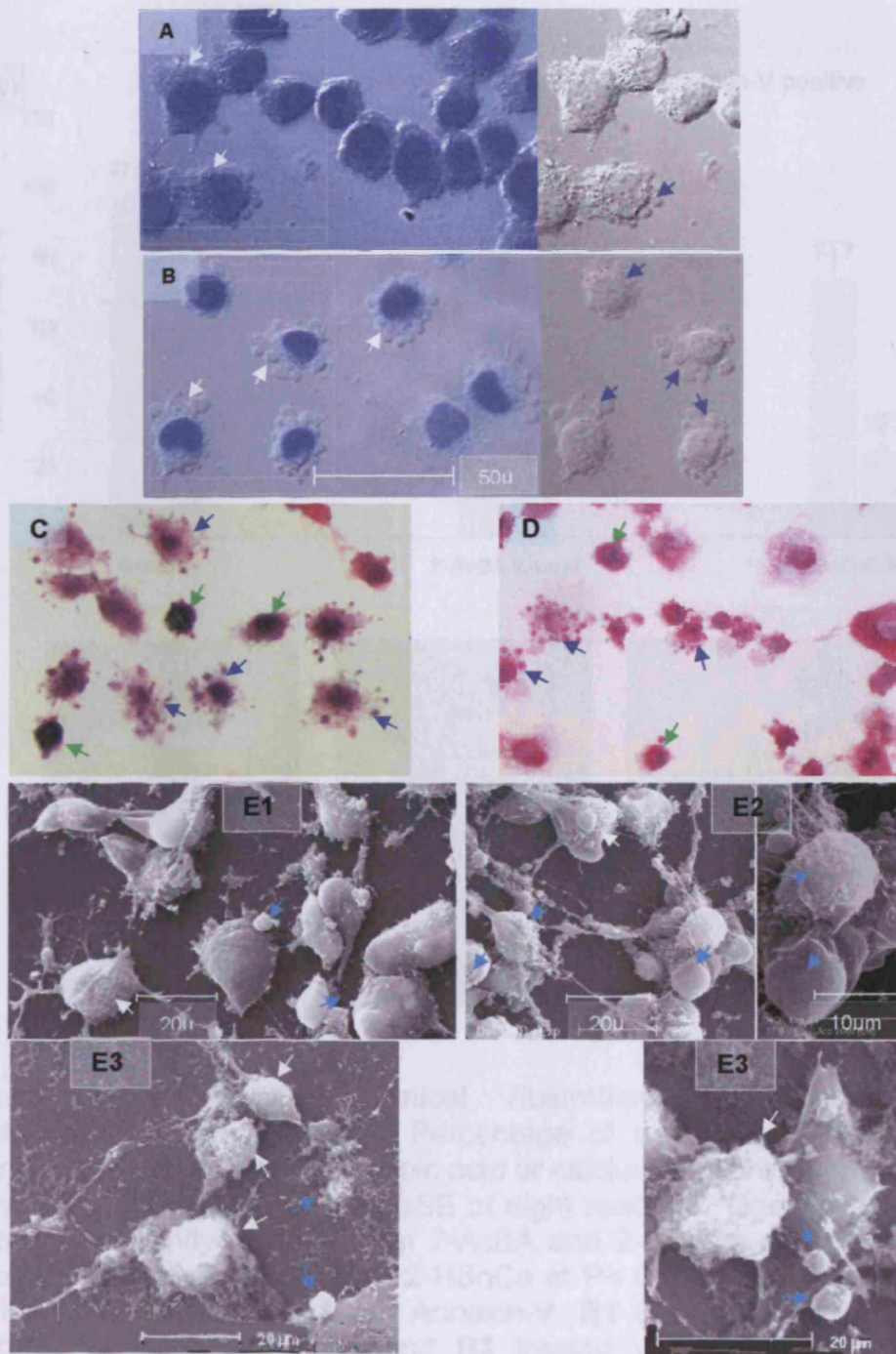
Figure 3.4 Microscopic images of HT-1080 cells treated with (**A**) 0.4 and (**B**) 0.8mM 2-acetylbenzoic acid and examined by DAPI staining, blebs (white and blue arrows). **C** HT-1080 cells treated with 0.4mM 2-acetylbenzoic acid and stained with Haematoxylin-eosin, apoptotic body (green arrows); blebs (blue arrows), (magnification x200). **D** HT-1080 cells treated with 0.4mM 2-acetylbenzoic acid and stained methyl-green-pyronin y staining, labelling as in C, (magnification x200). **E1-E3** SEM of effect of 2-acetylbenzoic acid at (**E1**) 0.4mM, (**E2**) 2.0mM, and (**E3**) 8mM. Apoptotic bodies (blue arrows) and apoptotic cells (white arrows) respectively.
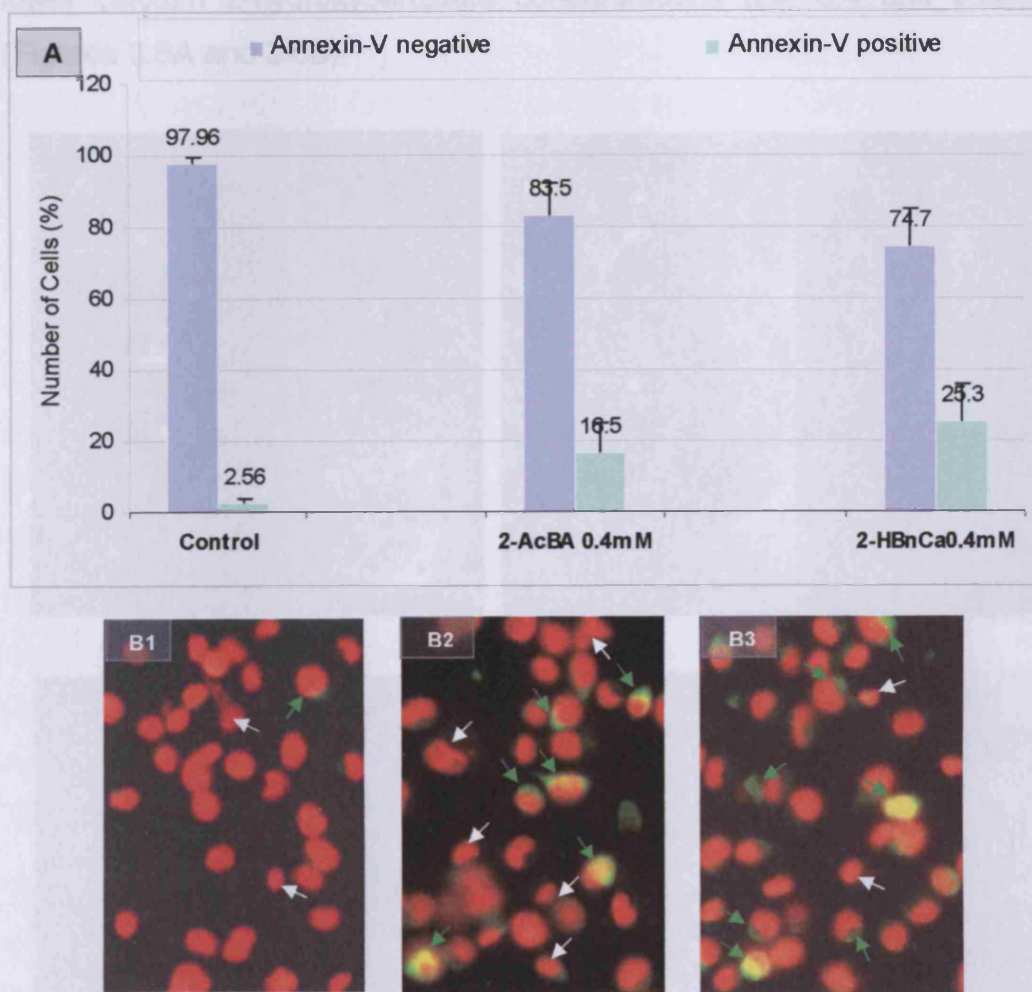
Figure 3.5 Immunohistochemical illustration for effect of 2-hydroxybenzoate analogues. **A** Percentage of apoptotic HT-1080 cells after treatment with 2-acetylbenzoic acid or calcium 2-hydroxybenzoate for 24 hours. Data represent mean ±SE of eight readings. One-way ANOVA; control significantly different from 2-AcBA and 2-HBnCa at $P < 0.000$. 2-AcBA significantly different from 2-HBnCa at $P < 0.003$ (Appendix B). **B1-B3** HT-1080 Cells labelled with Annexin-V. **B1** Control, **B2** treated with 0.4mM 2-acetylbenzoic acid, and **B3** treated with 0.4mM calcium 2-hydroxybenzoate. Early apoptotic cells (green arrows), late apoptotic cells (white arrows). Magnification X40.

The fluorescence/light phase contrast microscopic images of the treated cells clearly showed that the 1.2mM concentration of calcium 2-hydroxybenzoate (Figure 3.6C) induced more apoptotic cells compared to the control HT-1080 cells (Figure 3.2B) and the other treatments of the

lower calcium 2-hydroxybenzoate concentrations (i.e. 0.4 and 0.8mM) (Figures 3.6A and 3.6B).
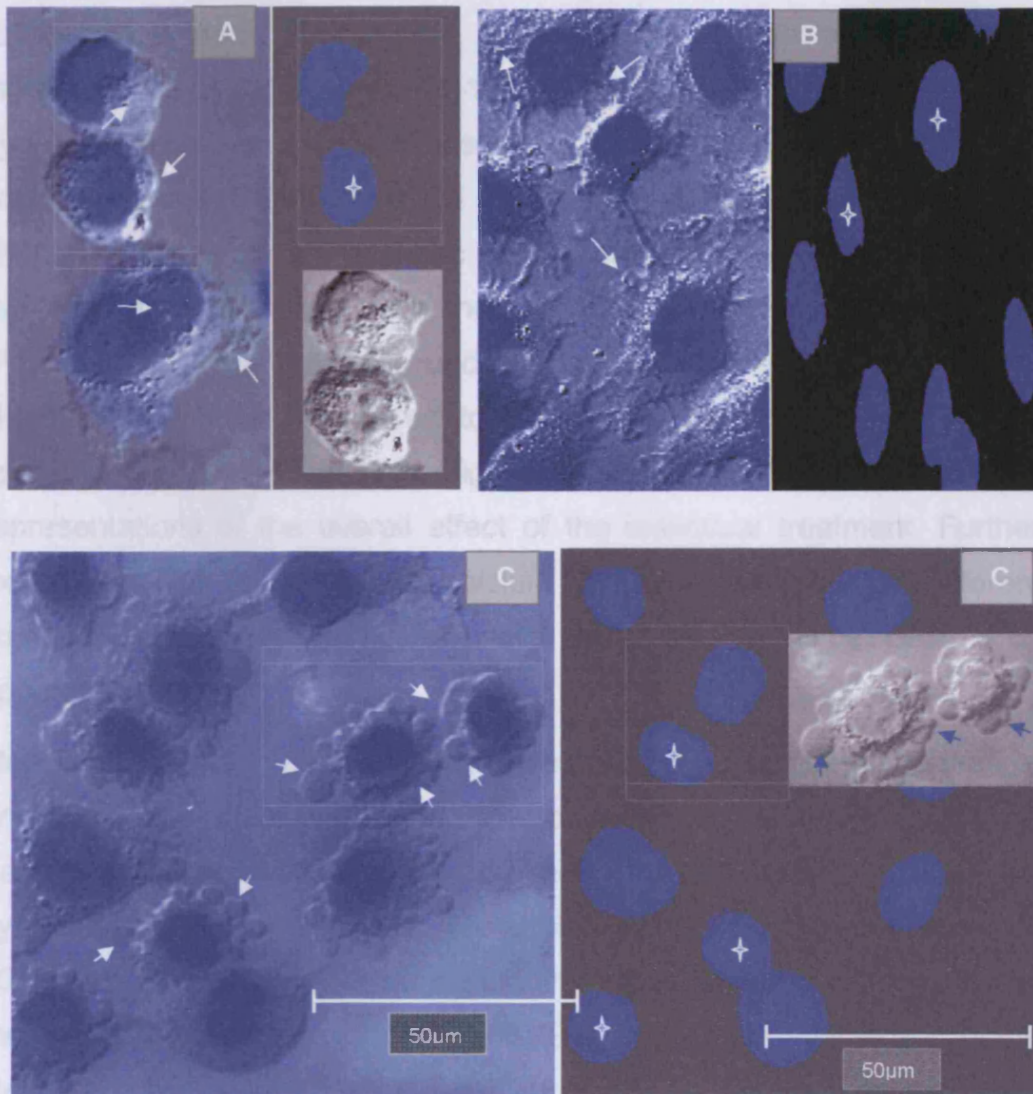
Figure 3.6 Fluorescence/light phase contrast microscopic images of calcium 2-hydroxybenzoate treated HT-1080 cells, and after 24 hours stained with DAPI, **A** at 0.4mM, **B** at 0.8mM, and **C** at 1.2mM concentration. Blebbings of HT-1080 cells (white and blue arrows), and pyknotic nuclei (stars).

Cells undergoing apoptosis showed various blebs coming of the cell surface of HT-1080 cell line (Figure 3.6, note white and blue arrows). The microscopic images of treated cells showed clear morphological changes,

like blebbing and apoptotic bodies, as a result of the incorporation of different concentrations of calcium 2-hydroxybenzoate (0.4, 0.8 and 1.2mM), particularly at the highest concentration (1.2mM) (Figure 3.6C, note white arrows). Furthermore, haematoxylin and eosin also showed morphological changes when HT-1080 cells were treated with calcium 2-hydroxybenzoate at 0.4mM concentration for 24 hours compared to the control (Figure 3.2D). HT-1080 cells showed distinct morphological characteristics such as pyknotic cells (rounded cells) and shrinkage, indicating that cell death was induced through the apoptotic pathway (Figure 3.7A). Note that cells undergoing apoptosis also have lost their filopodial attachment compared to control (Figure 3.2D). The classical apoptotic signs appearing in Figure 3.6 and other figures are true representations of the overall effect of the individual treatment. Further examination of the effect of calcium 2-hydroxybenzoate at different concentrations showed no necrotic cells, indicating that the cell death is by apoptotic pathway.

Methyl green and pyronin y staining was next used in the morphological analysis of the effect of calcium 2-hydroxybenzoate. HT-1080 cells were treated prior to the staining procedure with 0.4mM calcium 2-hydroxybenzoate for 24 hours. Morphologically, the nucleus of the HT-1080 cells is stained dark blue with methyl green, while pyronin y stained the cytoplasm pink or red (Figure 3.7B). This morphological technique clearly showed cellular blebbing and shrinkage as evidence for apoptosis when cells were incubated with calcium 2-hydroxybenzoate. Note that the dark blue colour of some stained nuclei is due to the staining of the chromatin as well.

The fine structure of the treated HT-1080 cells with calcium 2-hydroxybenzoate at different concentrations (0.4 and 0.8mM) also confirms that cells were dying through apoptosis. The scanning electron micrographs showed many apoptotic cells at both benzoate concentrations (Figure 3.7C - 3.7E).
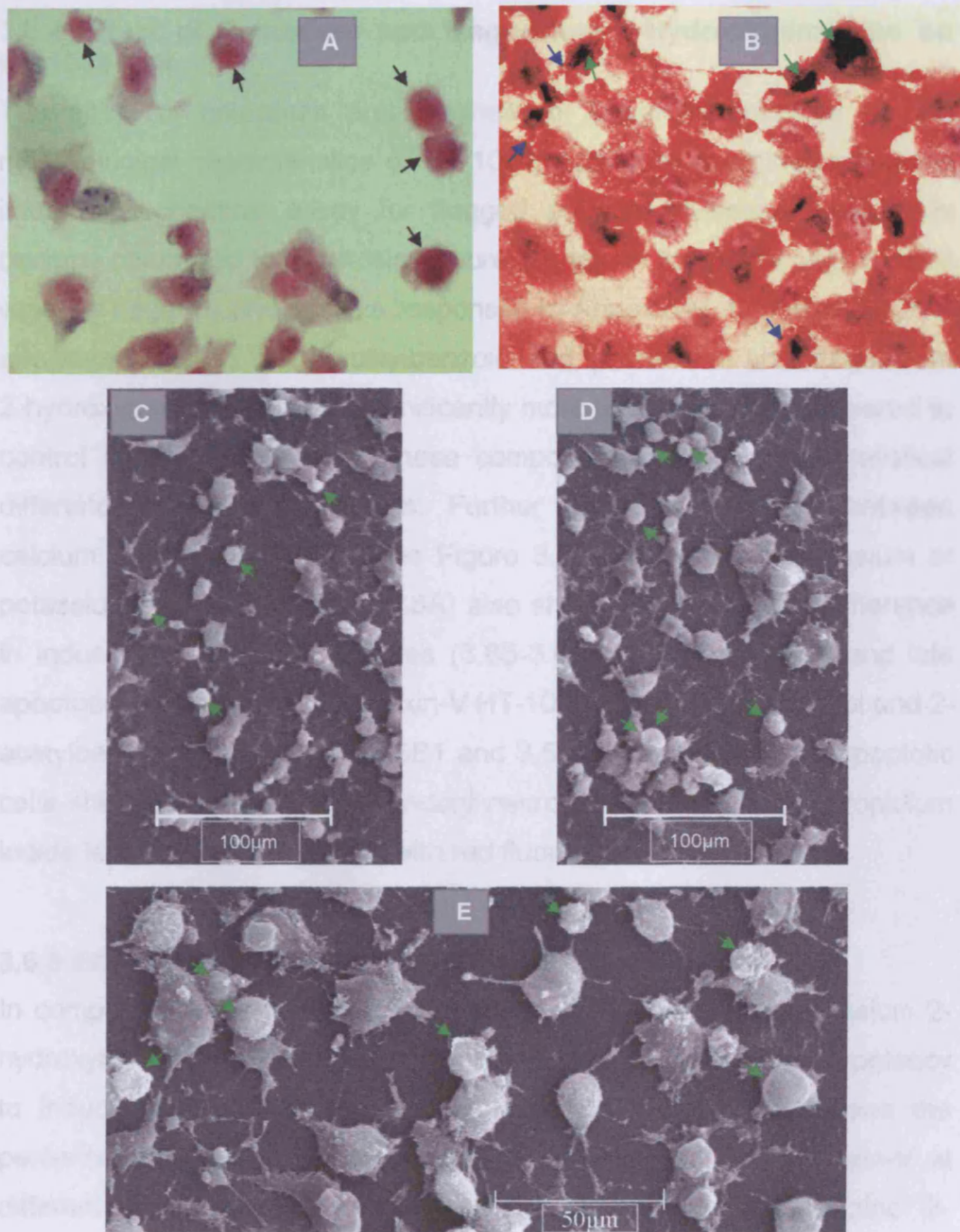
Figure 3.7 HT-1080 cells treated with different concentrations of calcium 2-hydroxybenzoate for 24 for hours. **A** Cell treated with 0.4mM and stained with haematoxylin-eosin, pyknotic cells (black arrows), magnification x200. **B** Cells treated with 0.4mM and stained with methyl-green and pyronin y staining, Chromatin staining (green arrows) and apoptotic cells with blebs (blue arrows), magnification x200. **C-E** SEM image of treated cells, (**C**) at 0.4mM, and **D-E** at 0.8mM, apoptotic cells in **C-E** with green arrows.

3.6.4 Effect of Potassium and Magnesium 2-Hydroxybenzoates on HT-1080 Cell

The effect of potassium and magnesium 2-hydroxybenzoates on the morphological characteristics of HT-1080 cells were examined using the immunocytochemical assay for flagged phosphatidylserine when cells became committed to apoptosis. Figure 3.8 shows the percentage of cells with the negative and positive responses to Annexin-V. One-way ANOVA analyses indicated that 2-acetylbenzoic acid, potassium, and magnesium 2-hydroxybenzoate induced significantly more apoptotic cells compared to control at p< 0.0. However, these compounds did not show statistical differences among themselves. Further statistical analyses between calcium 2-hydroxybenzoate (see Figure 3.5A) and either magnesium or potassium analogues (Figure 3.8A) also showed no significant difference in inducing of apoptosis. Figures (3.8B-3.8C) show both early and late apoptotic cells labelled by Annexin-V HT-1080 cells (see the control and 2-acetylbenzoic acid in Figure 3.5B1 and 3.5B2). Indeed, the late apoptotic cells show some signs of secondary necrosis, and hence, the propidium iodide labels nuclear materials with red fluorescence.

3.6.5 Effect of Zinc 2-Hydroxybenzoate on HT-1080 Cell Death

In comparison with calcium (Figure 3.5A), magnesium and potassium 2-hydroxybenzoate (Figure 3.8A), the zinc analogue showed more potency to induce apoptosis in the HT-1080 cell line. Figure 3.9A shows the percentage of cells positively and negatively labelled with Annexin-V at different concentrations and incubation periods. 0.3mM of zinc 2-hydroxybenzoate induced about 59.03% apoptosis when cells were cultured for 24 hours under the optimal conditions.

The number of apoptotic cells increased to 81.65% by increasing the dose to 0.4mM at the same incubation period, or 24 hours. Furthermore, at 0.4mM zinc 2-hydroxybenzoate and 48 hours' incubation period, all cells appeared to be labelled with Annexin-V. The formal treatment showed a decrease in the total number of cells. The ANOVA statistical analysis

indicated that the zinc benzoate analogue treatments induced significantly more (p<0.001) apoptotic cells than the control sample and the other benzoate analogues examined in this study. Figure 3.9B shows the labelled HT-1080 cells with Annexin-V after the treatment with zinc 2-hydroxybenzoate compound at 0.3 and 0.4mM for 24 and 48 hours.
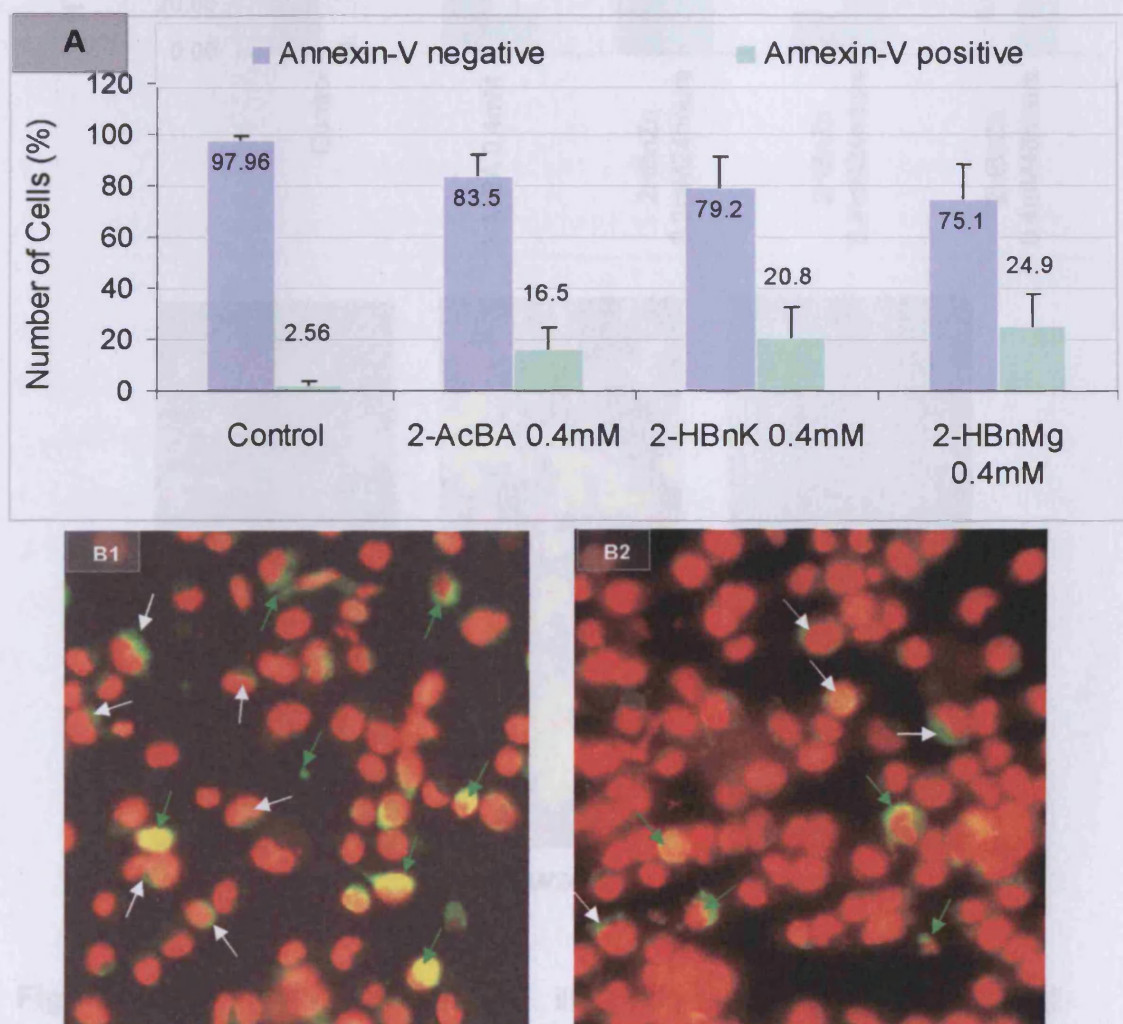
Figure 3.8 Immunohistochemical illustration for effect of 2-hydroxybenzoate analogues. **A** Percentage of apoptotic HT-1080 cells after treatment with 2-acetylbenzoic acid, potassium or magnesium 2-hydroxybenzoate for 24 hours. Data represent mean ±SE of eight readings. One-way ANOVA: control significantly different from AcBA, HBnK, and HBnMg at p< 0.00; No significant differences among AcBA, HBnK, and HBnMg at p < 0.001 (Appendix B). Cells labelled with Annexin-V. **B1** Treated with 0.4mM potassium 2-acetylbenzoate, and **B2** treated with 0.4mM magnesium 2-hydroxybenzoate. Early apoptotic cells (green arrows), and late apoptotic cells (white arrows), which also show red fluorescence due to propidium iodide leakage. Magnification X40.

A (chart)

Legend: ■ Annexin-V negative ■ Annexin-V positive

HT-1080 Cells (%) — y-axis: 0.00, 20.00, 40.00, 60.00, 80.00, 100.00, 120.00

- Control: 97.96 / 2.56
- 2-AcBA 0.4mM: 83.50 / 16.5
- 2HBnZn 0.3mM24hours: 38.92 / 59.03
- 2HBnZn 0.4mM24hours: 18.36 / 81.65
- 2HBnZn 0.4mM48hours: 0.00 / 100

B1 — 0.3mM/24Hours B2 — 0.4mM/24Hours B3 — 0.4mM/48 hours
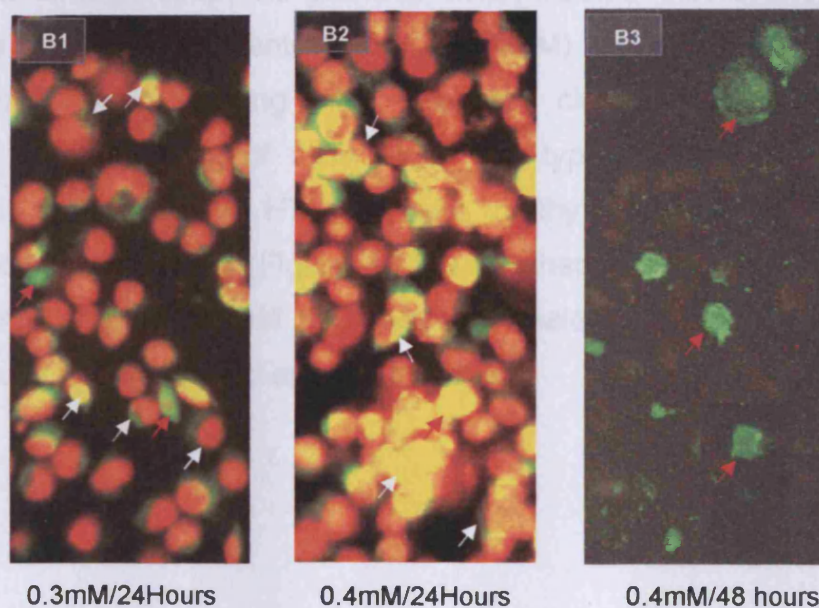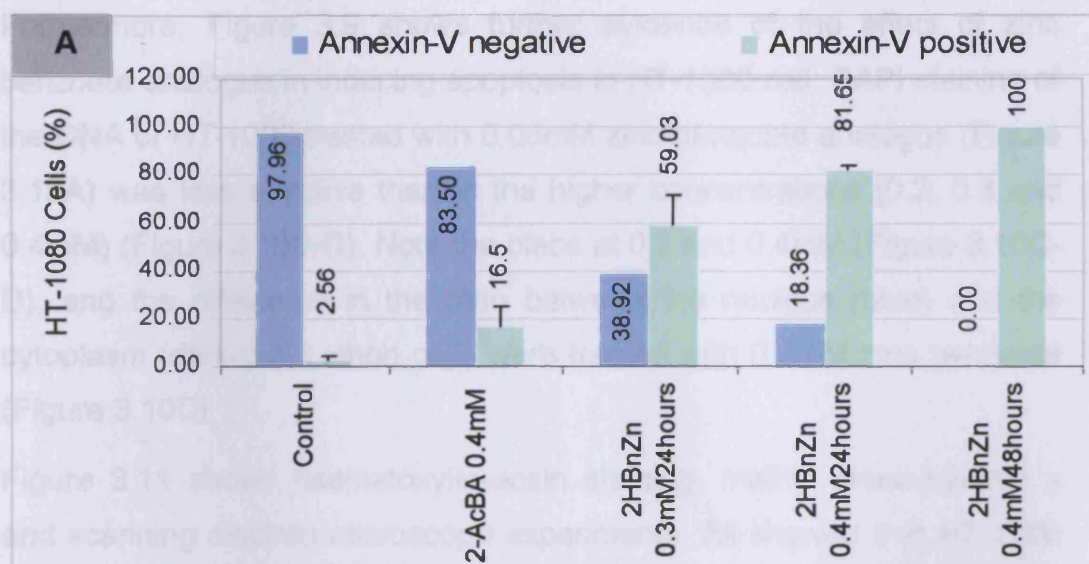
Figure 3.9 Immunohistochemical illustration for effect of zinc 2-hydroxybenzoate. **A** Percentage of apoptotic HT-1080 cells after treatment with 0.3mM and 0.4mM 2-acetylbenzoic acid, zinc 2-hydroxybenzoate for 24 and 48 hours. Data represent mean ± SE of eight readings. One-way ANOVA: control significantly different from AcBA and zinc benzoate analogue at 0.3 and 0.4mM concentrations at p< 0.01. Both concentrations and incubation periods treatments significantly different at p < 0.001 (Appendix B), **B1-B3** cells treated with zinc 2-hydroxybenzoate and labelled with Annexin-V; **B1** treated with 0.3mM for 24 hours, **B2** with 0.4mM for 24 hours and **B3** with 0.4mM for 48 hours. Early apoptotic cells (white arrows), Apoptotic cells (red arrows), also show red fluorescence due to propidium iodide leakage. Magnification x40.

Furthermore, Figure 3.9 shows further evidence of the effect of zinc benzoate analogue in inducing apoptosis in HT-1080 cell. DAPI staining of the DNA of HT-1080 treated with 0.05mM zinc benzoate analogue (Figure 3.10A) was less effective than at the higher concentrations (0.2, 0.3 and 0.4mM) (Figure 3.10B-D). Note the blebs at 0.3 and 0.4mM (Figure 3.10C-D), and the difference in the ratio between the nucleus (blue) and the cytoplasm (dark-grey) when cells were treated with 0.4mM zinc benzoate (Figure 3.10D).

Figure 3.11 shows haematoxylin-eosin staining, methyl green-pyronin y and scanning electron microscope experiments. All showed that HT-1080 cells died through apoptosis pathway when treated with zinc benzoate analogue at different concentrations (0.1-0.4mM) for 24 hours' incubation. Haematoxylin-eosin staining after treatment clearly showed signs of blebbing, and shrinking of cells which are typical signs of apoptosis (Figure 3.11A). Staining HT-1080 with methyl green-pyronin y also showed cellular blebbing (Figure 3.11B). Furthermore, SEM of HT-1080 cells treated with 0.1-0.4mM zinc benzoate analogue (Figure 3.11C1-C3) for 24 hours mainly showed apoptotic bodies.
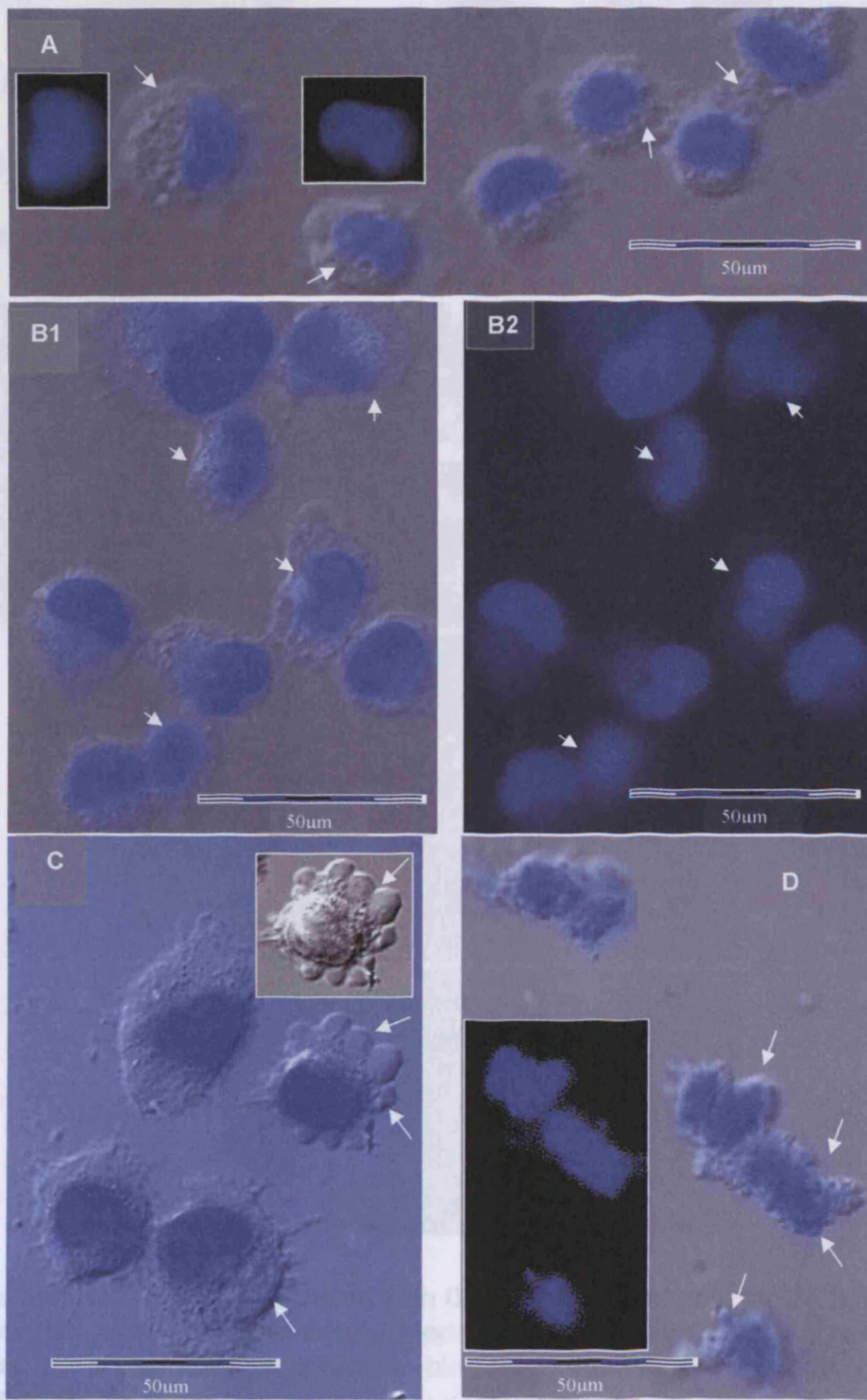
Figure 3.10 DAPI staining of HT-1080 cells treated with zinc benzoate analogue for 24 hours at the following concentrations (**A**) 0.05mM, **B1**-**B2** 0.2mM, **C** 0.3mM and **D** 0.4mM. Apoptotic cells (white arrows).
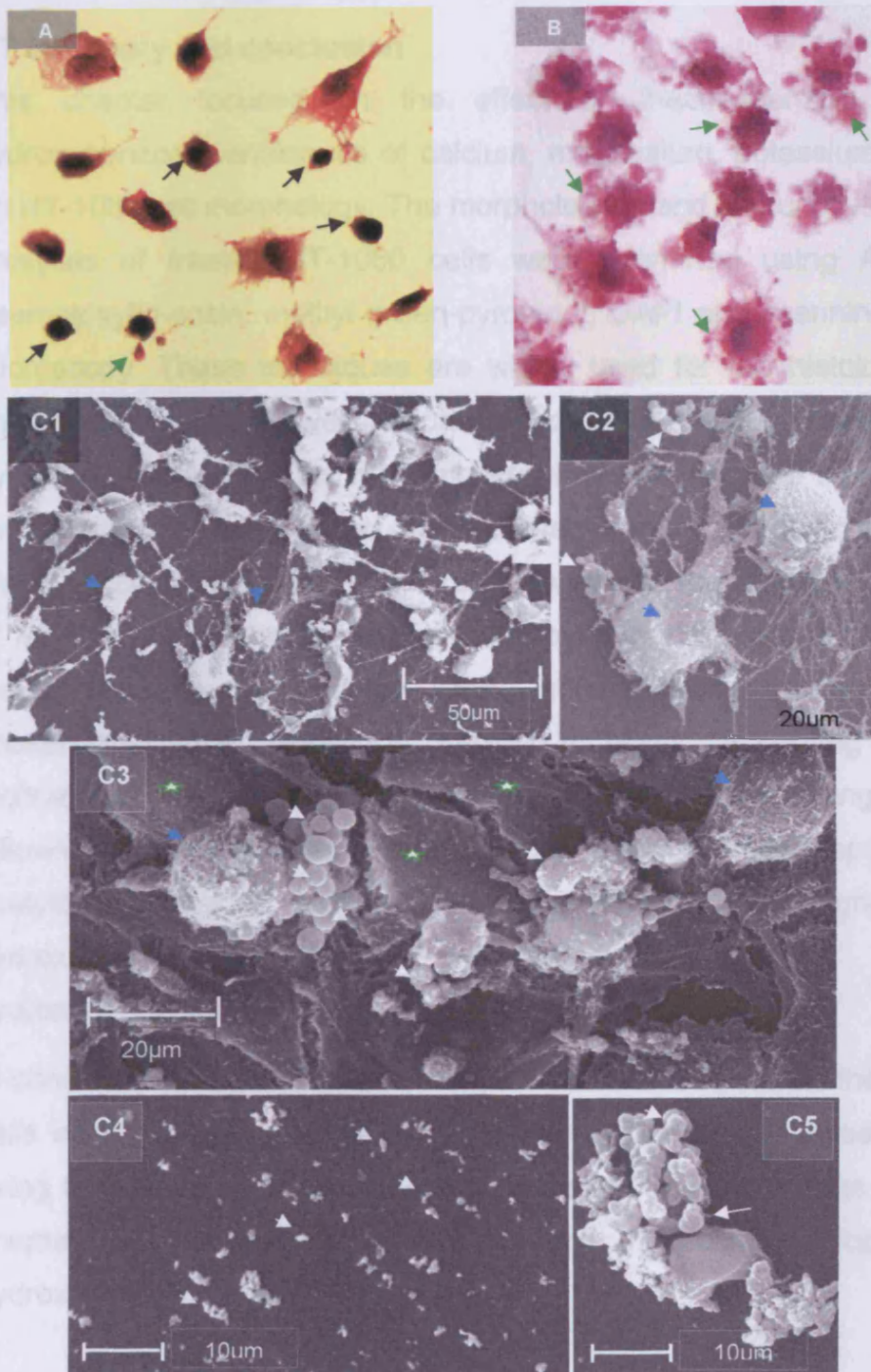
Figure 3.11 HT-1080 cells treated with 0.4mM zinc benzoate for 24 hours and stained with (**A**) Haematoxylin-eosin and (**B**) with Methyl green-pyronin y; green arrows indicate blebbing. Notice pronounced cell shrinkage (black arrows), magnification x200.
C1-C5, SEM of HT-1080 cells treated with zinc benzoate analogue, **C1**-**C2** at 0.1mM for 24 hours; **C3** at 0.2mM for 24 hours; **C4** at 0.4mM for 24 hours and (**C5**) at 0.4mM for 24 hours. Apoptotic cells (blue arrows); apoptotic bodies (white arrows) and pronounced cell shrinkage (green stars).

3.7 Summary and conclusion

This chapter focused on the effect of 2-acetylbenzoic acid, 2-hydroxybenzoate analogues of calcium, magnesium, potassium and zinc on HT-1080 cell morphology. The morphological and immunocytochemical analyses of treated HT-1080 cells were examined using Annexin-V, haematoxylin-eosin, methyl green-pyronin y, DAPI and scanning electron microscopy. These techniques are widely used for the histological and immunocytochemical investigations of both the nucleus (DNA) and the cytoplasm (RNA). Results in this chapter have shown clear morphological evidence for apoptosis based on the presence of the apoptotic bodies, cell blebbing, cell rounding and shrinkage, as well as the increased presence of RNA in the cytoplasm, as shown by pyronin y staining. These results were also supported by the immunochemical labelling of phosphatidylserine, using the Annexin-V assay. According to these techniques, the 2-hydroxybenzoate analogues can be arranged in the following ascending order in terms of their ability to induce apoptosis: 2-acetylbenzoic acid, potassium 2-hydroxynbenzoate, magnesium 2-hydroxynbenzoate, calcium 2-hydroxynbenzoate and zinc 2-hydroxynbenzoate.

In conclusion, the effect of 2-hydroxybenzoate analogues on the HT-1080 cells clearly showed that cells die through apoptosis, as investigated by using both morphological and immunocytochemical techniques. The next chapter will focus on aspects of the molecular biology of 2-hydroxybenzoate-treated HT-1080 cells.

Chapter Four

Effect of 2-Hydroxybenzoate Analogues on the Molecular Biology of HT-1080 Cell Line: Evidence of Apoptosis

CHAPTER FOUR

Effect of 2-Hydroxybenzoate Analogues on Molecular Biology of HT-1080 Cell Line: Evidence of Apoptosis

4.1 Introduction

Results in the previous chapter have clearly demonstrated, by various morphological techniques, the possible role of 2-hydroxybenzoate analogues in the induction of apoptosis in the HT-1080 cells *in vitro*. The significant changes that were observed in these studies included the presence of apoptotic bodies, blebbing, and the labelling of the externalised phosphatidylserine by Annexin V. The focus in this chapter is to (1) confirm the apoptotic effects of 2-hyroxybenzoate analogues on HT-1080 cells, and (2) investigate further cellular and molecular changes. Therefore, both cell cycle analysis and molecular events occurring in treated HT-1080 cells were studied, including cell cycle duration, level of mitosis, and cell cycle phases. Changes in gene expression after treatment with a number of apoptosis-related proteins were also investigated, including p53, p21, Bax, Bcl-2, TNF-α and histones. Western blotting analysis was used in addition to analysis of caspase-3 and Annexin V by flow cytometry.

4.2 Cell Cycle: Regulatory and Function

Many eukaryotic cells often undergo frequent cell cycles distinguished by 4 main phases or gaps: G1, S, G2 and M (Figure 4.1). The fundamental phases of the cell cycle are synthesis (S) where the DNA replicates and mitosis (M) where the cell divides into 2 daughter cells. The central task of the cell cycle is to ensure that the DNA is replicated precisely during S phase, and that identical chromosome copies are distributed equally between the 2 daughter cells during M phase (Heichman and Roberts, 1994; Grana and Reddy, 1995; Wuarin and Nurse, 1996; Nurse, 2000).

79

The ultimate task of the process is to ensure that each mitotic cell is usually genetically identical to the parent cell.

The cell cycle pathway also includes three other phases: G_0, G1 and G2. Generally, cells respond to various regulatory signalling, which either direct cells to divide (proliferate) or to withdraw from the cell cycle into the G_0 state, where cells are quiescent, or resting (see later in this section). Resting cells may remain in this state for an indefinite time, until they either resume proliferation or die.
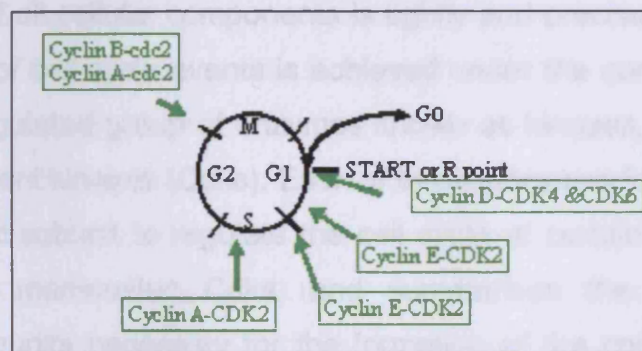
Figure 4.1 Eukaryotic cell division cycle and role of cyclin-CDKs in cell cycle control. Cycle made up of four stages: G1, S, G2 and M. Interphase consists of G1, G2 and S phase. Cell goes through these phases to replicate itself and divide into two daughter cells. G_0 is quiescent stage when the cell faces unfavourable conditions and stops the cycle. R point, restriction point (Diffley and Evan, 2000).

Generally, the period between one M phase and the next is known as interphase, during which preparations for cell division are occurring in a closely ordered sequence. Interphase consists of three sub-phases: G1, S and G2 (Baserga, 1985). During G1, cells are preparing for S phase and the cell 'decides' whether to commit itself to DNA replication and proliferation. DNA replication occurs during the S (synthesis) phase of the cell cycle (Murray and Hunt, 1993).

The progression from the G1 to S-phase is a key regulation point during the cell cycle. Mitogenic and anti-mitogenic signals converge at the restriction point (R-point) in the late G1-phase, and 'make the cell continue the cycle or not. Once the cells pass through the R-point, they no longer

require the extracellular mitogenic signals to complete the cycle (Bartek *et al.*, 1996; Blagosklonny and Pardee, 2002).

Fundamentally, the cell cycle is similar in all eukaryotic cells, hence research in this area has contributed to the overall understanding of how events are controlled and coordinated in humans. It is clearly understood, for example, that perturbations to cell population growth pathways are a basis for tumourigenesis and malignant disease. In healthy cells, the successful division is dependent on ensuring that the duplication and segregation of all cellular components is tightly and precisely coordinated. Coordination of cell cycle events is achieved under the control of a family of a highly regulated group of enzymes known as kinases, or specifically, cyclin-dependent kinases (Cdks). Each of these enzymes forms a complex with a specific subunit to regulate the cell cycle at certain phases. Table 4.1 lists the mammalian Cdks, and summarises the corresponding regulatory subunits necessary for the formation of the complexes, which function at certain phases of the cell cycle (Carnero, 2002).

Table 4.1 Cyclin-dependent kinases (Cdks), regulatory units, substrates and designated functions.

Cdk	Regulatory subunit	Substrate	Function
Cdk1	cyclin A,B	pRb,NF,histone H1	G2/M
Cdk2	cyclin A,E	pRb,p27,histone H1	G1/S,S
Cdk3	cyclin E	E2F1	G1/S
Cdk4	cyclin D1,D2 &D3	pRb	G1/S
Cdk5	cyclin D1 &D3,p35	NF,Tau	Neuronal differentiation
Cdk6	cyclin D1,D2 &D3	pRb	G1/S
Cdk7	cyclin H, MAT1	Cdk1,Cdk2/4/6	Cdk-activating kinase
Cdk8	cyclin C	RNA Pol II	Transcription regulation
Cdk9	cyclin T	pRb,MBP	G1/S

The general principles by which progression through the cell cycle is regulated are: (1) activation of Cdks driven by the sequential expression and association with cyclin subunits which bind to the active site for the activation of cyclin enzymes; (2) the activity of one Cdk-cyclin sets up the

conditions needed for the activation of the next; (3) destruction of cyclins ensures a unidirectional cell cycle; and (4) inhibition of assembled Cdk-cyclin complexes, either through phosphorylation or by the binding of inhibitory protein delays, Cdk activation, and slow cell cycle progression in adverse conditions (for review on cell cycle, see: Pardee, 1989; Sherr, 1993; Grana and Reddy, 1995; Bartek et al., 1996; Nurse, 2000; Blagosklonny and Pardee, 2002).

Cell cycle progressions start with the expression of cyclin D first, when the cell 'decides' to enter the cell cycle, and levels remain high to the end of M phase. Cyclin D complexes with Cdk4 and Cdk6 to induce cell cycle progression. Entry into S phase correlates with the hyperphosphorylation of the retinoblastoma (Rb) tumour suppressor protein, resulting in its inactivation. This allows activation of the E2F family (a group of proteins that associate with phosphorylated Rb) of transcription factors and promotes the transcription of proteins required for G1 and S phases (Sherr, 1993; McGowan, 2003). Cyclin E is also expressed at G1 phase, accumulates at S phase, and complexes with Cdk2 to give the active kinase which leads to the initiation of DNA replication and a number of substrates that are required to carry out the task of duplicating and segregating cellular contents (Sherr, 1993; Hinchdiffe and Gluder, 2001; Hall et al., 2001). The levels of cyclin E mRNA and protein rise significantly in the last quarter of G1 phase when pRb undergoes phosphorylation (Koff et al., 1991; Weinberg, 1995). Mouse model experiments have suggested that cyclin E is a downstream target of cyclin D (Fantl et al., 1995; Sicinski et al., 1995; Geng et al., 1999).

The expression of cyclin A lags behind that of cyclin E which occurs at the G1-S boundary (Norbury and Nurse, 1992). The induction of the activities of cyclin E-Cdk2 and cyclin A-Cdk2 are essential for the initiation and completion of DNA replication, and to ensure that replication occurs once in each cycle (Pagano et al., 1992; Ohtsubo et al., 1995). Furthermore, cyclin A also plays a significant role in the termination of S phase by increasing transcription of histone and other genes needed to

accommodate replication (Obaya and Sedivy, 2002). Finally, cyclin B is expressed late in S phase, and remains high throughout G2 and M phases. Cyclin B complexes with Cdc2 protein to regulate the cell cycle G2-M phases progression (Lee and Nurse, 1988; Dalton, 1992). Three main isoforms have been identified: cyclin B1-3, cyclin-1 and cyclin-2, which are found in the cytoplasm. Cyclin-3 is in the nucleus (Pines and Hunter, 1991; Gallant and Nigg, 1992; 1994; Jackman *et al.*, 1995).

The activity of Cdks at various stages of the cell cycle needs to be tightly regulated if uncontrolled cell proliferation is to be avoided. This is primarily achieved though the expression of specific Cdk inhibitors (CdkIs) which target a specific active Cdk complex (Morgan, 1995). CdkI-4, for example, specifically inhibits the activity of both Cdk-4 and Cdk-6. The less specific cyclin inhibitors are represented by the Cip/Kip family (p21, p27 and p35) of proteins which disrupt the association between cyclin subunit and its corresponding Cdk of Cdk-D, CdK-E and Cdk-A (Lees, 1995). *p53* also inhibits the progression of cell division (Milner, 1984).

Defects in cell cycle regulation and checkpoint controls often result in genomic instability and a pre-disposition to cancer. One of the most frequently mutated genes in human cancers is the *p53* gene. Understanding the molecular mechanisms that regulate these processes is therefore of considerable medical as well as scientific interest.

4.3 Tumour Suppressor Protein p53

p53 plays a vital role in the regulation of the cell cycle to ensure that when genotoxic damage occurs, cells arrest in G1, and DNA gets repaired before replication (Kastan *et al.*, 1991; Dennis, 1998). Mutations that result in cancer usually occur in the DNA binding domain of the p53 protein (Ko and Prives, 1996). In healthy cells, p53 interacts with Mdm-2 (a ubiquitin ligase) whose expression is induced by p53. Mdm-2 neutralises p53 activity by binding to and inhibiting its transactivating domain (Oliner *et al.*, 1992). When DNA damage occurs however, a protein kinase

phosphorylates p53 and reduces binding to Mdm-2, thus activating p53. The loss of *p53* predisposes cells to drug-induced gene amplification and decreases the fidelity of the mitotic chromosome transmission. Duplication of the centrosomes, for example, normally occurs during the G1-S boundary, but in the case of p53 deficiency, multiple centrosomes are generated in a single cell cycle, which results in aberrant chromosomal segregation during mitosis.

When DNA damage is irreparable in multicellular organisms, the individual cell with the damaged DNA commits suicide through a programme of cell death (apoptosis). This mechanism is vital in protecting the organism from genetic damage that may lead to cancer. For example, mutation to a single amino acid in the Ras protein (involved in the initiation of mitosis) can cause it to become permanently overactive, promoting mitosis even in the absence of mitogenic stimuli. Another example is mutation resulting in the over-expression of the Myc protein, which promotes cell cycle entry, causing unwanted cell population growth and proliferation leading to cancer. The actual decision for the cell to enter apoptosis in response to such damage relies on the activation of p53. This apoptotic pathway, however does not require p21^{CIP1}; p53 can directly activate death genes, like *Bax*, or suppress survival genes, like *Bcl-2*. G1 arrest and apoptosis are two alternative p53 induced outcomes. Even though *p53*-induces *p21^{CIP1}*, limiting *Rb* hyperphosphorylation, loss of Rb function can bypass p53-mediated G1 arrest. The incorporation of the Rb and p53 pathways determines whether *p53* will induce apoptosis or cell cycle arrest (Evan and Littlewood, 1998). The loss of *Rb* activity usually causes the p53 pathway to induce apoptosis.

Most identified proto-oncogenes function in signal transduction to reproduce the effects of mitogenic stimulation, which makes the cell insensitive to environmental controls. They function to disrupt the mechanism controlling the passage through the G1 phase by inducing G1 cyclins and overriding Cdk inhibitors, consequently preventing cell cycle exit and disregarding checkpoint control. Despite the vast variety of

oncogenes, it is clear that the most frequently disrupted pathways are those dominated by the two tumour suppressor genes *Rb* and *p53*. Other less direct mechanisms also contribute to *p53* inactivation. The Mdm2 protein and human papillomavirus E6 can be oncogenic, as they oppose p53 function. Even tumours that retain a wild type *p53* accumulate epistatic lesions that have the same effect as loss of p53 function. Preventing p53-dependent apoptosis is the key to tumourogenesis. Loss of a vital death gene or the over-expression of a survival genes may mirror the effects of p53 loss (Sherr, 1996).

4.4 Apoptosis and Cancer Therapy

Apoptosis, the major mechanism of cell death in the body, is under genetic control, and deregulation of the pathways involved can lead to a number of neurodegenerative diseases such as, Huntington's, Parkinson's and Alzheimer's (Ona *et al.*, 1999). Alternatively, inadequate apoptosis can lead to the survival of DNA damage that contributes to cancer (Thompson, 1995; Evan and Littlewood, 1998; Wong *et al.*, 1999). Two main factors induce apoptosis, the first is self-initiation. The activation of Fas (binding to FAS ligand), for example, leads to apoptosis (Nagata, 1997) which subsequently forms *death-induced signalling complex* (DISC) in the cytoplasm. The complex mediates activation of caspase-8 which then activates procaspase-3 (Kischkel *et al.*, 1995). The second factor that contributes to the induction of apoptosis takes the form of protein molecules, such as MutS proteins. These proteins can recognise DNA chemical damage, caused by chemotherapy for example, and then initiate apoptosis through the activation of *p53* or *p53*-related gene, *p73* (Gong *et al.*, 1999; Li, 1999). Therefore, a certain level of p53 is important to determine the cell status. Loss of *p53* is implicated in the production of 50 to 55% of human tumours, such as colorectal carcinoma and human lung (Levine, 1997; Giaccia and Kastan, 1998).

As indicated in Chapters 1 and 3, apoptosis is morphologically distinct from necrosis. Both types of cell death are also different in relation to genetic control. Apoptosis is usually initiated and proceeds through a complex sequence of gene control, while little gene control appears in necrosis which is mainly caused by physical effects such as high temperatures, anoxia, ishaemia excessive force or by infection. Generally, apoptosis includes two phases: an initial commitment to cell death, followed by an execution phase, characterised by synthetic biochemical and morphological changes, respectively (Wong et al., 1999).

Apoptosis is an energy-dependent process and, during the biochemical phase, is initiated in specific cell types by both endogenous tissue-specific agents (e.g. hormones) and exogenous, cell-damaging treatments or triggered by radiation, chemicals, and viruses (Denmeade and Issacs, 1996). These signals act through receptors or ligands on the cell surface, and are transmitted to the cytosol and nucleus by signal transduction pathways (Wong et al., 1999). Activation of the caspase family begins the execution phase and their activity leads to morphological changes, first in the mitochondria and the nucleus, followed later by changes in the cell membrane. Caspases, the critical mediators of the execution phase, are proteases that cleave exclusively after aspartate residues, and have a conserved active site containing the amino acid cysteine. During apoptosis, upstream caspases are activated and subsequently cleave and activate downstream caspases. The caspases act in a cascade and eventually lead to the formation of membrane-enclosed apoptotic bodies, containing the contents of the cell, which are rapidly recognised, phagocytosed, and digested by macrophages or adjacent epithelial cells (Denmeade and Issacs, 1996).

Apoptosis is tightly regulated, and loss of this regulation is critical to the pathogenesis of a number of diseases. In the adult, the relationship between cell proliferation and death is balanced, such that neither regression nor excessive growth of tissue will occur under normal conditions. Any events that shift this equilibrium in favour of an enhanced

survival of damaged cells promote the carcinogenic process by allowing the survival of potentially neoplastic cells (Denmeade and Issacs, 1996). Thus, cancer arises not only from increased and unregulated cell division, but also from a reduction in the rate of apoptosis. An abnormal cell that proliferates uncontrollably (i.e. exceeds the rate of cell death), results in the net accumulation of malignant cells, which have the ability to invade surrounding cells and produce the lethality of cancer (Denmeade and Issacs, 1996).

DNA damage can lead to cell cycle arrest at the checkpoints until the damage is repaired. ATM and ATR, both protein kinases, respond to different stresses, and thus play a role in the detection of damaged DNA. Expression of ATM and ATR proteins leads to phosphorylation of the protein p53, which eventually results in cell cycle arrest. p53 provides another level of regulation in healthy cells, and is active in times of potentially severe DNA damage. p53 comes into action when the checkpoints cannot cope and is able to steer the cells into apoptosis. p53 is involved in the detection of abnormal DNA, and whether detects to arrest the cell cycle and initiate DNA repair or, if the damage is irreparable, initiates apoptosis. Usually a very short-lived protein, p53 is stabilised and accumulates in cells with damaged DNA or in those responding to certain forms of stress (Sherr, 1996). The decision on whether to commit to apoptosis occurs in G2.

Tumours often have a mutant form or are deficient in checkpoint proteins, allowing the cells to behave abnormally. Cancer cells tend to abandon checkpoint controls and remain in cycle, and as cell cycle exit can facilitate maturation and terminal differentiation, these processes are often abandoned too (Sherr, 1996). The *p53* gene, which functions as a transcription factor, is the most commonly mutated gene in human cancers, and cancer-related mutations cluster in its binding domain (Sherr, 1996). Mutations affecting the gene coding for other components of apoptosis, such as *Bcl-2*, *Bax*, *Apaf-1* and *p21*, may also be associated with cancer (Bowen and Saunders, 2004)

A successful therapy for cancer must readjust the relationship between mitosis and apoptosis so that cell death exceeds cancer cell proliferation (Denmeade and Issacs, 1996). Apoptosis has been reported in tumours by Kerr *et al.*, (1987) and by Sarraf and Bowen (1986; 1988), in both untreated cells and in cells exposed to chemotherapeutic agents. "*Apoptosis is arguably the most potent natural defence against cancer, because it eliminates premalignant cells that enter S phase inappropriately after genetic sabotage of restriction point controls*" (Sherr, 1996).

Successful cancer therapy requires drugs that will activate apoptosis in tumours, with minimal side effects to normal cells. Novel apoptotic agents are continuously being sought.

4.5 Materials and Methods

4.5.1 Cells and *in vitro* Culture Conditions

HT-1080 cells were cultured in an optimal DMEM medium and under a humidified atmosphere of 95% air and 5% CO_2 at 37°C using standard suitable culture vessels unless otherwise indicated (see Chapter 2, materials and methods). HT-1080 cells were seeded at specific density unless otherwise stated, and allowed to grow for 3 days, followed by 24 hours' culturing in serum-free DMEM medium before being treated with 2-hydroxybenzoate analogues (for the preparation of the solutions, see Chapter 2), individually, at specific concentration(s) and for certain time(s). Cells were harvested and centrifuged at 1000g for 5 minutes before conducting the test by specific technique.

4.5.2 Time lapse Microscopic Analysis of HT-1080 Cell Cycle

2-Hydroxybenzoate analogues (2HBnCa, 0.4, 0.8mM; 2HBnZn, 0.2, 0.25, 0.3mM; 2AcBA, 0.4, 2mM) treated-HT-1080 cells were seeded in 12-well plate at an initial density of 1×10^3 per well (see Section 2.4.2.6, Chapter 2, for full experimental details). In addition, control experiments were performed parallel to the treatment experiments. The sequences for the cell images, captured digitally by Orca IER charge-coupled device camera (Hammamatsu, Welwyn Garden City, UK) were analysed by Lucida Analyse-6 software (Kinetic Imaging, Wirral, UK). The capture of a series of images for each treatment was carried out manually, and analysed for cell cycle and mitosis durations, as well as the percentage of mitotic cells in each treatment.

4.5.3 Flow Cytometric Analysis of HT-1080 Cell Cycle

HT-1080 cells were seeded in T-25 flask at an initial density of 1×10^4 per flask. Cells were cultured (see Section 2.4.2.1, Chapter 2) for 3 days post-seeding and 1 day in serum-free medium before being treated with 2-hydroxybenzoate analogues (2HBnCa, 0.4, 0.8mM; 2HBnZn, 0.25, 0.3mM) for 2, 6, 12, or 24 hours. In addition, control experiments were performed in which no benzoate was incorporated in the cultures.

At the end of each treatment, HT-1080 cells were harvested by trypsinisation, centrifuged and resuspended in 200μl of PBS. Aliquots (2ml) of ice-cold 70% ethanol were then added and the cells vortexed prior to being cooled to –20°C for 30 min. Subsequently, 100μl of a RNase (Sigma, UK) at a concentration of 1mg/ml and 100μl of propidium iodide (Biovision Incorporate, CA, USA) at a concentration of 400μg/ml were added prior to incubation at 37°C for 30 min. The cells were analysed using a FACSCalibur flow cytometer (Becton Dickinson, UK), and the percentages of cells in the different phases of the cell cycle were quantified using Cylchred version 1.0.2 software (Terry Hoy, University Hospital of Wales, UK).

4.5.4 Flow Cytometric Analysis of Apoptosis Using Annexin V

HT-1080 cells were seeded in T-25 flasks at an initial density of 1×10^5 per flask and cultured for 3 days before being treated with zinc 2-hydroxybenzate (0.1, 0.2 and 0.4mM) for 48 hours. At the end of the treatment, 1×10^6 cells were harvested by centrifugation and then washed with phosphate buffered saline. Cells were resuspended in 100μl of binding buffer and 1μl (final concentration 1mg/ml) of FITC-labelled Annexin V (Dako Cytomation, UK), and then incubated in the dark for 10 minutes at room temperature. 100μl (final concentration 1mg/ml) of propidium iodide solution (Dako Cytomation, UK) was added to each aliquot prior to analysis by flow cytometry using CellQuest software on a FACSCalibur flow cytometer (Becton Dickinson, UK).

4.5.5 Flow Cytometric Analysis of Caspase-3 activation

HT-1080 cells seeded in T-25 flask at 1×10^3 initial density were cultured in optimal DMEM medium and under standard conditions, before being treated with zinc 2-hydroxybenzoate (0.4mM) or 2-acetylbenzoic acid (3.2mM) for 48 hours. In addition, control experiments were performed in which no benzoate was added to the cultures. Cells were subsequently harvested by centrifugation and incubated for a further 1 hour at 37°C, in the presence of the PhiPhiLux™ G1D₂ substrate (Calbiochem, UK). The substrate contains two fluorophores separated by a quenching linker sequence that is specifically cleaved by active caspase-3. Once cleaved, the resulting products fluoresce green, and can be quantified using flow cytometry. For all experiments, 10,000 events were measured and were analysed on a FACSCalibur flow cytometer (Becton Dickinson, UK).

4.5.6 Western Blot Analysis

4.5.6.1 Preparation of HT-1080 Cell Lysate

HT-1080 cells in 6-well plates at 3×10^4 initial cell density were cultured for 3 days to reach approximately 70% confluent in a DMEM medium and under standard conditions (Chapter 2). The HT-1080 cell population growth was continued for further 24 hours but with serum-free DMEM medium, before they were treated with benzoate analogues (2AcBA, 2HBnCa, 2HBnZn at 0.05 and 0.4mM each) for 24 hours. The medium was removed and cells were then washed with PBS to remove the remaining medium. Following this, 200μl of 2X sample buffer (250mM Tris-HCl pH 6.8, 4% SDS, 0.006% bromophenol blue, 2% β-mercaptoethanol (Pharmacia Uppsala, Sweden), 10% glycerol, (Sigma, U.K.) was added to each well, and cells were then harvested using a cell scraper. 2-hydroxybenzoate analogue- treated HT-1080 cells in lysate buffer were then transferred into a 1.5ml Eppendorph pipette, heated at 100°C for 10 minutes, cooled to room temperature, and centrifuged at 120g for 5 minutes. The supernatant was further centrifuged at 16,000g for 5 minutes to get a clear solution of protein mixture, which was used to measure the expression of p21, p53, Bcl-2, Bax, TNF-α, and histones by Western blotting.

4.5.6.2 Total Protein Determination for HT-1080 Cell Lysate

The total protein concentrations of both HT-1080 cell lysate samples and for the standard bovine serum albumin (BSA) curve were determined according to the method of Karlsson et al. (1994).

66.7μl of 60% w/v trichloroacetic acid in distilled water was added to each well of a 96-well plate containing a pre-warmed 100μl of the different concentrations (0, 50, 100, 150, 200, 250 and 300μg/100μl) of BSA solutions, and of HT-1080 cell lysates (diluted 15x), each in 2x sample buffer, and left for 15 minutes at 37°C, after which spectroscopic

absorption was measured at 575nm. Figure 4.2 shows the albumin standard curve used to calculate the total protein in HT-1080 lysate samples (Table 4.2). Lysate samples were diluted to approximately 100µg/100µl with lysate buffer (Table 4.2).
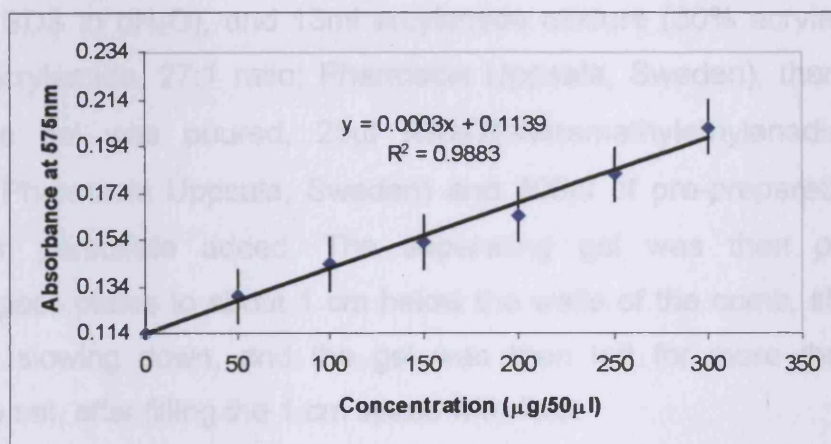
Figure 4.2 Albumin standard curve (Appendix C).

Table 4.2 Total protein in benzoate analogues-treated HT-1080 cells.

Treatment	Average (A575nm)	x = y-0.1139/0.0003[a]	µg/100µl of total protein[b]	µl of original lysate in 100µl lysate buffer containing 100µg protein
Control	0.152	127	1905	5.2[d]
2AcBA 0.05mM	0.210	320	4805	2.1[c]
2AcBA 0.4mM	0.147	110	1655	6.0[d]
2HBnCa 0.05mM	0.178	214	3205	3.1[c]
2HBnCa 0.4mM	0.218	347	5205	1.9[c]
2HBnZn 0.05mM	0.224	367	5505	1.8[c]
2HBnZn 0.4mM	0.183	230	3455	2.9[c]

[a] Value of total protein (µg/100µl) of 15-fold diluted lysate samples.
[b] Value of total protein (µl/100µl) of original lysate samples.
[c] 500µl of 100µg/100µl protein solutions were prepared; [d] 200 µl of 100µg/100µl protein solutions were prepared.

4.5.6.3 Gel Preparation
4.5.6.3.1 Separating Gel

The separating gel was prepared as follows: 0.5g of ammonium persulfate (Pharmacia Uppsala, Sweden) dissolved in 5ml of deionised water (dH_2O). Then, In a 100 ml beaker, 6.7 ml dH_2O, 20ml stock 2 (0.75M Tris-HCl, 0.2% w/v SDS in dH_2O), and 13ml arcylamide mixture (30% acrylamide: 0.8% bisacrylamide, 27:1 ratio; Pharmacia Uppsala, Sweden), then, just before the gel was poured, 25µl NNN'N'-tetramethylethylenediamine (TEMED, Pharmacia Uppsala, Sweden) and 300µl of pre-prepared 10% ammonium persulfate added. The separating gel was then poured between glass plates to about 1 cm below the wells of the comb, starting fast, then slowing down, and the gel was then left for more than 30 minutes to set, after filling the 1 cm space with IMS.

4.5.6.3.2 Stacking Gel

The stacking gel was prepared from 5 ml stock 1 (0.25M Tris, pH 6.8, 0.2% w/v SDS in 500ml dH_2O), 1.3ml of arcylamide mixture (30% acrylamide: 0.8% bisacrylamide, 29:1 ratio), 7.5µl TEMED, and 80µl of pre-prepared 10% ammonium persulfate.

The IMS was removed with dH_2O before adding 5ml the stacking gel which was poured gently to the top of the separating gel and a 10-well comb immediately introduced, ensuring the two spaces in the two far ends were equal, the level of the comb was balanced, and that there were no bubbles. The gel was then left for approximately 20 minutes before assembly of the gel tank. The comb was gently removed, and then the gel with the glasses was removed from the holder and rinsed with tap water.

The gel was placed in a gel rig and then in a special tank containing electrophoresis running buffer (10x stock; 14.11% w/v glycine, 0.5M Tris-HCl, pH 8.3, 1% w/v SDS), the wells were flushed out thoroughly with the buffer prior to running the gel.

Frozen lysate samples were thawed and heated at 100°C for 5 minutes to deactivate proteases, and each was diluted to a final concentration of 100μg total protein/100μl lysate buffer (prepared according to Table 4.2). 20μl (100μg/100μl) of each diluted sample was loaded in each well, and 10μl of a molecular weight marker was added in one well (Table 4.2). The apparatus was connected to a Bio-Rad power pack and run with constant current (40 mA with voltage set at > 300 V) for approximately 1.5 hour.

4.5.6.3.3 Western Transfer

Two nitrocellulose paper sheets were cut in a size slightly bigger than the Western blot gel and put into two square dishes containing blotting buffer (0.05M Tris-HCl, 3% w/v glycine, 3.7% w/v SDS, and 25% alcohol in dH_2O). At the same time, after the electrophoresis run finished (to separate protein bands), the Western blotting gel was gently removed from the cassette with a gel knife (the well side was facing up), and finally, the gel was transfered into a pre-marked square dish containing blotting buffer.

Two 3 mm thick filter papers sheets were soaked in the blotting buffer, and the first was placed on the top of the gel, with the foot of the gel (bottom of the cassette) left uncovered. The second was transferred to the blotting machine, then the nitrocellulose paper underneath the gel was moved to the blotting machine and placed on top of the second filter paper. The transfer membrane was cut with a razor blade to the dimension of the gel and the second soaked filter paper was placed on top of the gel. Air bubbles were removed by gently rolling the sandwich with a 25ml tissue-culture plastic pipette, and the wetted anode cover placed on top. The gel membrane assembly was held securely between the two halves of the blotting module which was held together firmly in order to slide it into the guide rails on the lower buffer chamber. With the power turned off, the red and black leads were plugged into the power supply.

The gels were blotted at 100 mA and 30 V for 1.5 hour to transfer the protein from the gel to the nitrocellulose membrane which was then placed in approximately 20 ml blocking buffer (4% w/v Marvel, Knighton, U.K, 5ml Tween 20, Pharmacia Uppsala, Sweden, 0.87% w/v NaCl, 1% v/v Tris-HCl pH 7.4, Sigma, U.K.) for 1 hour over a rotary shaker, and were then rinsed with 20ml of deionised water prior to immuno-detection.

4.5.6.3.4 Western Immunodetection

The blocking buffer (15ml) in the plastic container containing nitrocellulose membrane was replaced by the same amount of blocking buffer containing a specific primary antibody at pre-determined dilution (Table 4.3). The membrane in the blocking buffer containing the specific primary antibody was placed over a rotary shaker for 3 hours. The nitrocellulose membrane was then washed with 15 ml washing buffer (8.7% w/v NaCl, 1M Tris-HCl, pH 7.4, 0.5% v/v in 1 liter deionised water) three times every 15 minutes, before being treated with the secondary antibody, using also 15 ml of blocking buffer containing a specific secondary antibody (Table 4.3), and the nitrocellulose membrane was incubated with rocking for 1 hour.

The membranes were then washed by 3 quick rinses with washing buffer, followed by 4 x 15 minutes with washing buffer at room temperature. Finally, the membranes were incubated with a fresh 1:1 mixture of Enhanced Chemiluminescent (ECL) reagent (Amersham, UK) for 1 minute, and then covered with cling film and exposed to ECL Hyper film (Amersham, UK) for 1-5 minute. Finally, photographic films were developed.

Table 4.3 Primary and secondary antibodies used and dilution factors.

Primary antibody	Dilution	Secondary antibody	Dilution
Mouse anti-p53 (Cambridge Bioscience, UK)	1:1000	Peroxidase conjugated-Anti-mouse 1gG secondary, (Sigma, UK)	1:1000
Rabbit anti-Bax (Cambridge Bioscience, UK)	1:1500	Peroxidase conjugated-Anti-mouse 1gG secondary, (Sigma, UK)	1:1000
Mouse anti-Human Bcl-2 (Serotec Ltd, UK)	1:1000	Peroxidase conjugated-Anti-mouse 1gG secondary, (Sigma, UK)	1:1000
Mouse anti-P21/WAF1 (Serotec Ltd, UK)	1:1500	Peroxidase conjugated-Anti-mouse 1gG secondary, (Sigma, UK)	1:1000
Anti-histone Pan monoclonal antibody immunoglobulins (Boehringer Mannheim, UK	1:1500	Peroxidase conjugated-Anti-mouse 1gG secondary, (Sigma, UK)	1:1000
Tumour Necrosis Factor Alpha (TNFα). Recombinant [E.coli], Human sequence (System, inc, Minneapolis, MN).	1:500	Peroxidase conjugated-Anti-goat 1gG secondary , (DakoCytomation Ltd, UK)	1:5000
Marker	Prestained SDS-PAGE Standard Solution for Molecular Weights 30,000-120,000 (Sigma, UK).		

4.5.7 Pharmacological Investigations of 2-Hydroxybenzoates Uptake into HT-1080 Cells

Both high-pressure liquid chromatography (HPLC) and atomic absorption were used to investigate whether (1) 2-hydroxybenzoate analogues are up-taken into the HT-1080 cell's cytoplasm, and (2) to find out if 2-hydroxybenzoate or 2-hydroxybenzoic acid and/or metal ion could be detected in HT-1080 lysate samples.

HT-1080 cells in 75-T flask at 1×10^6 initial cell density were cultured for 3 days to reach approximately 70% confluence in DMEM medium and under standard conditions (Chapter 2). The HT-1080 cells' population growth was continued for further 24 hours but with serum-free DMEM medium, before they were treated with benzoate analogues (2AcBA, 2HBnCa, 2HBnZn at 0.4mM each) for 24 hours. HT-1080 cells were harvested by centrifugation 120g for about 10 minutes. Cells were washed with deionised water 0.5ml x 3, before the pellets were digested using 0.5M

nitric acid. Samples were placed in a boiling water bath for 20 minutes. The digested mixture was then extracted with about 30ml x3 chloroform to separate benzoates (for HPLC analysis), while calcium and zinc separately remained in the aqueous solution as nitrate salts after they reacted with nitric acid. The nitrate samples were analysed using atomic absorption.

4.5.7.1 High-Pressure Liquid Chromatography (HPLC)

Analytical HPLC was conducted on a Hewlett Packard (HP) 1090 liquid chromatograph fitted with a C-18 (Latex, Eppelheim, Germany), reverse-phase 25 cm (5μm) column (internal diameter, 4.0 mm). Detection of the benzoates and/or their metabolites was by the UV detector at A 215 nm, at room temperature. The mobile phase was 65% double-distilled water, 35% HPLC grade acetonitrile (Sigma, UK) and 0.1% HPLC grade TFA (trifluroacetic acid, Sigma, UK). 20μl of each sample, including control, was injected into the HPLC. Extracts were dissolved in the mobile phase prior to injection (20μl) into the HPLC. The flow rate of the mobile phase was 1ml/min. Instrument control and data handling were by means of non-Windows-based Prime Reporter software.

4.5.7.2 Atomic Absorption Spectrophotometry (AAS)

Nitric acid digest of 2-hyroxybenzoate-treated HT-1080 cell lysate samples were quantified for zinc and calcium using flame (air-acetylene) AAS, in a Varian AA-100v atomic absorption spectrophotometer with automatic background adjustment. All solutions, including standards, used for calcium or zinc assay contained 1% lanthanum. The standard elements used were at 1000 ppm solution from Fisher.

4.6 Results and Discussion

4.6.1 Cell Cycle Analysis

The effect of 2-acetylbenzoate on the growth of cancer cells *in vitro* has been actively studied. These studies have indicated that 2-acetylbenzoates inhibit cell population expansion, DNA and the synthesis of various proteins, resulting in the inhibition of G1 and S phase progression in a number of cell lines, including mainly human colon adenocarcinoma (Aas *et al.*, 1995; Ricchi *et al.*, 1997). 2-acetylbenzoic acid has been shown to slow down or inhibit cancer cell proliferation by inducing arrest in the G_0/G1 phase of the cell cycle (Elder *et al.*, 1996). These compounds were also found to increase the susceptibility of cells at a late stage of neoplastic progression towards induction of apoptosis (Ruschoff *et al.*, 1998). Most of these studies have used relatively high concentrations of 2-acetylbenzoate, ranging between 5 and 10mM (Santini *et al.*, 1999; Marra and Liao, 2001). Thus, in this study, we have taken the initiative to investigate the effect of 2-acetylsalicylic acid and other analogues at much lower concentrations (mostly 0.05 and 0.4mM).

To evaluate the effects of 2-hydroxybenzoate analogues on the cell cycle of HT-1080 fibrosarcoma cells, the tracking of the capture images of cell population growth progress was used to analyse both cell cycle and mitosis durations. The population growth of treated HT-1080 cells was monitored every 5 minutes over a period of 22 hours. Figure 4.3A shows the mitosis process in HT-1080 cells treated with calcium 2-hydroxybenzoate. The series of micrographs illustrates the continuous process which shows the common stages of mitosis: *prophase*, *metaphase*, *anaphase* and *telophase*. Although the mitotic apparatus (spindle, microtubules) is not shown, due to the low magnification of the microscope lenses used, it is easy to identify the four stages from the sequential frames (Figure 4.3A).
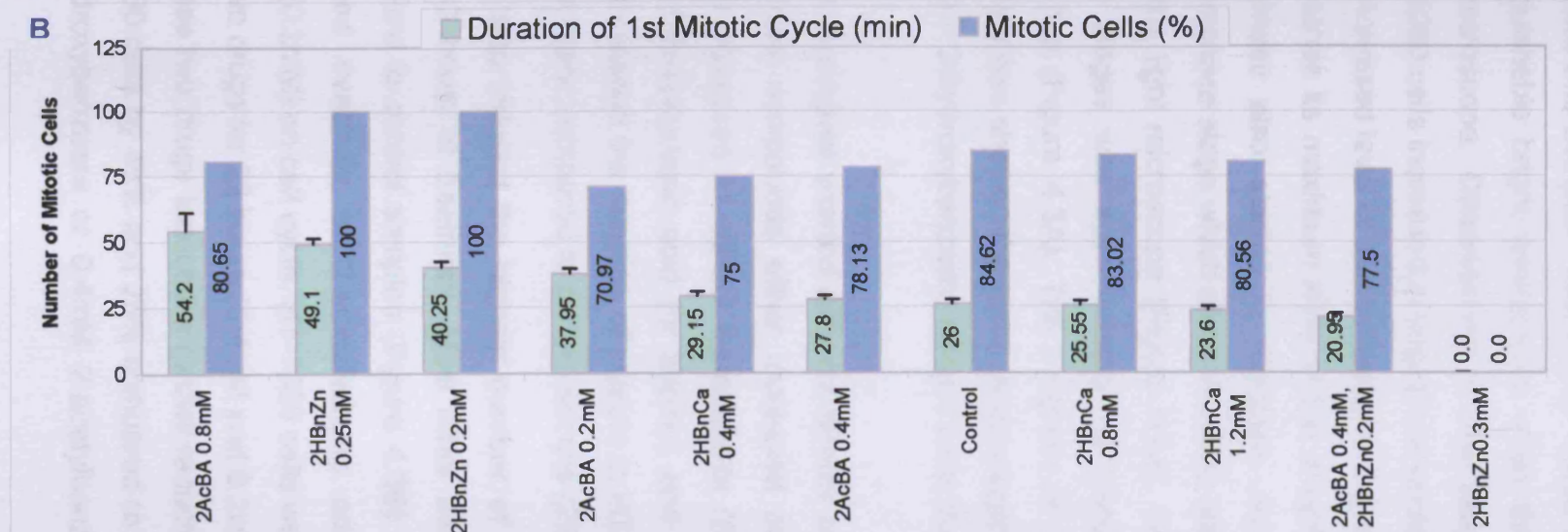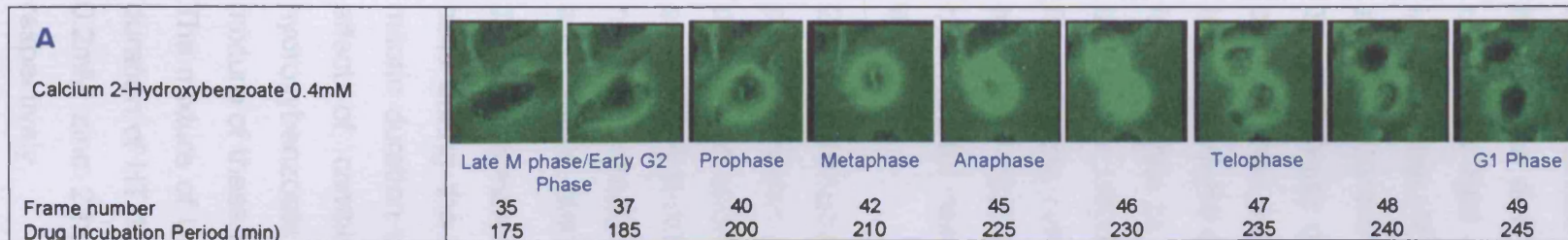
Figure 4.3 HT-1080 mitotic cell durations* and percentage of HT-1080 cells that underwent **first** mitosis** when cells cultured for 22 hours in presence of 2-hydroxybenzoate analogues. **(A)** Series of images illustrate sample of mitotic process with frame number and time events for different stages, **(B)** Representation for percentages of mitotic HT-1080 cells and duration for mitosis when cells cultured in presence of 2-acetylbenzoic acid (0.2, 0.4, 0.8mM), calcium 2-hydroxybenzoate (0.4, 0.8, 1.2mM), zinc 2-hydroxybenzoate (0.2, 0.25mM). Note: 0.3mM concentration did not induce mitosis.

* **First** mitosis duration refers to observed HT-1080 cells that underwent mitosis for first time during 22 hours. In this case, number of HT-1080 cells interring the **first** mitotic cells that were observed during 22 hours' culturing are: 25, 17, 18, 22, 18, 25, 44, 44, 29, 31, 0.0 for treatments in this graph, respectively.

** % of **first** mitotic HT-1080 cells = No. of **first** mitotic cells/Total no. of **first** and **second mitotic** cells during 22 hours.

Morphologically, towards the end of G2, chromosomes condense from extended diffuse form into compact, extensively folded structures, giving the cells a distinguishable bright appearance when they are observed under the light microscope. Observations of the progress of mitosis indicated that HT-1080 cells increased in brightness under the microscope as a result of the increased level of condensation in the *metaphase* stage. The brightness reaches its maximum level in the *anaphase*. Meanwhile, cells in the *anaphase* also started to elongate, but the elongation increased in the *telophase* stage which also showed a distinctive cleavage furrow visible by the light microscope (Figure 4.3A). The time between these two mitotic stages was approximately 15 minutes in HT-1080 fibrosarcoma cell line (Figure 4.3A). The progress of mitosis for other treated-HT-1080 cells also showed the same morphological characteristics observed for calcium 2-hydroxybenzoate-treated cells illustrated in Figure 4.3A.

2-hydroxybenzoate analogues exerted different effects on the first mitotic process, where these compounds either increased or decreased the duration of mitosis compared to control experiments (Figure 4.3B). For example, 0.8mM 2-acetylbenzoic acid (or aspirin) and 0.25mM zinc 2-hydroxybenzoate increased the duration of mitosis in HT-1080 about 2.1- and 1.9-fold, respectively, compared to control sample (26 minutes).

These treatments also induced the highest number of mitotic HT-1080 cells during the 22 hours of treatment. Most other treatments showed mitotic duration close to control samples (Figure 4.3B). To examine the effect of combined treatment of 2-acetylbenzoc acid and zinc 2-hydroxybenzoate (0.2mM) on cell cycle, HT-1080 cells were treated with a mixture of these two drugs for 22 hours (0.4mM and 0.2mM, respectively). The mixture of these two drugs induced a further reduction in the mitotic duration of HT-1080 cells by 48% and 28% compared to cells exposed to 0.2mM zinc 2-hydroxybenzoate or 0.4mM 2-acetylbenzoate treatments respectively.

Figure 4.4 shows that both 0.2 and 0.8mM 2-acetylbenzoic acid increased the duration of the second mitosis about 1.4-fold. All other treatments showed a slightly reduced duration in the second mitotic process compared to the control sample (28.75 min). Generally, the overall second mitotic process ranged between 23 and 41 minutes (control 28.75 min). Although, both 2-acetylbenzoic acid and calcium 2-hydroxybenzoate induced a second mitosis, all the zinc treatments (0.2, 0.25, 0.3mM) inhibited the progression of HT-1080 cells to the second cycle of mitosis during the 22 hours' culture (Figure 4.4).

Further analysis of the time-lapse microscopic results indicated that 2-acetylbenzoic acid (0.2, 0.4, 0.8mM) and calcium 2-hydroxybenzoate (0.4, 0.8, 1.2mM) slightly decreased the cell cycle duration, which ranged from 13.38 to 15.25 hours compared to the cell cycle duration in control, which was approximately 16 hours (Figure 4.5). None of the zinc 2-hydroxybenzoate treatments (0.2, 0.25, 0.3mM) showed a second mitotic cycle, thus it was not possible to measure this cycle duration in treated HT-1080 cells (Figure 4.4).

The above results clearly indicate that 2-hydroxybenzoate analogues induced changes in cell cycle and mitosis durations in HT-1080 cells. In order to determine whether these analogues have any effect on cell cycle phases of HT-1080 cells, they were synchronised in $G_0/G1$ phase by serum starvation for 24 hours before treatment with complete DMEM medium (i.e. with 10% FCS), containing specific 2-hydroxybenzoate analogue at certain concentrations. Results of the flow cytometric determination of cell cycle distribution indicated that the G1 phase reached 49.9% when HT-1080 cells were allowed to grow for 24 hours in serum-free DMEM medium. The control experiment (culture medium contained 10% serum) showed 31.9% for the same phase (Figure 4.6). This indicates that, under stress conditions, HT-1080 cells demonstrated an increase in G1 phase of approximately 36%.
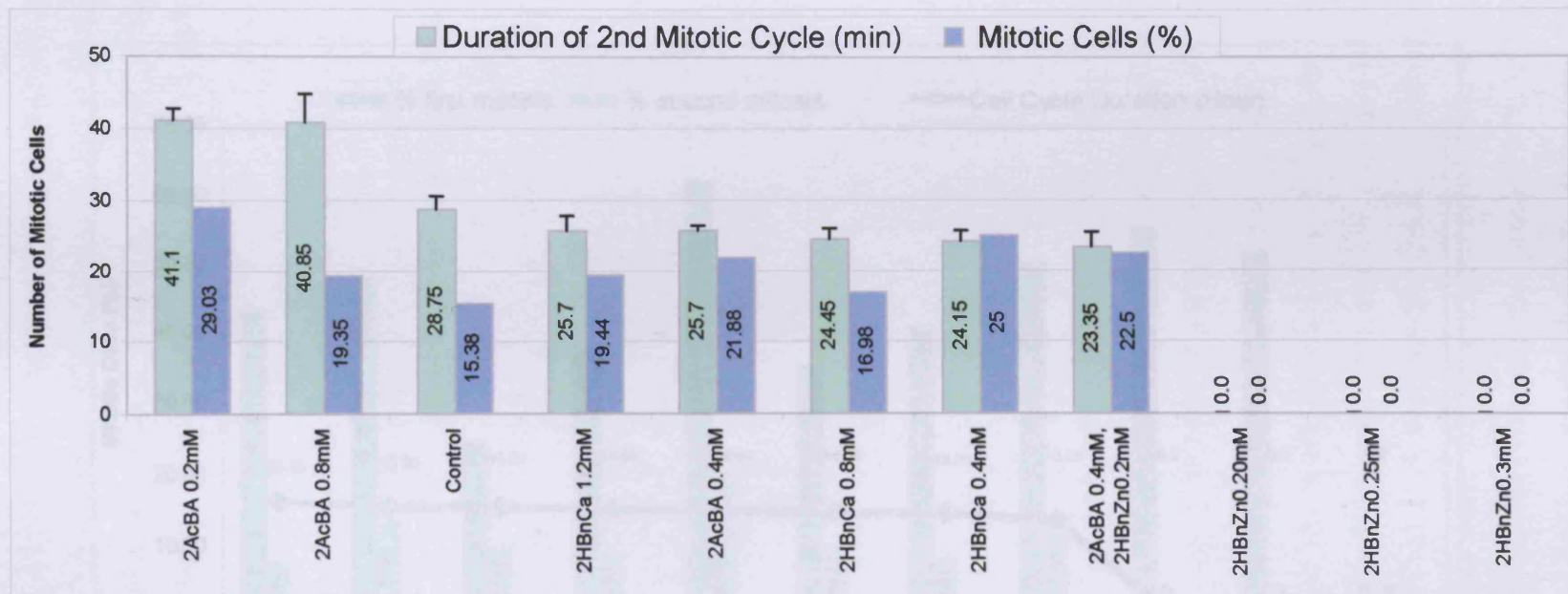
Figure 4.4 HT-1080 mitotic cell durations* and percentage of HT-1080 cells that underwent **second** mitosis** when cells cultured for 22 hours in presence of 2-acetylbenzoic acid (0.2, 0.4, 0.8mM), calcium 2-hydroxybenzoate (0.4, 0.8, 1.2mM), zinc 2-hydroxybenzoate (**Note** 0.2, 0.25 and: 0.3mM concentration did not induce second mitosis).

* **Second** mitosis duration refers to observed HT-1080 cells that underwent mitosis after **first** mitosis during 22 hours' culturing. In this case, number of the **second** mitotic cells observed during 22 hours culturing are 9, 6, 8, 7, 7, 9, 6, 9, 0.0, 0.0, 0.0 for treatment in this graph, respectively.
** % of **second** mitotic HT-1080 cells = No. of 2nd mitotic cells/Total No. of **first** and **second mitotic** cells during 22 hours.
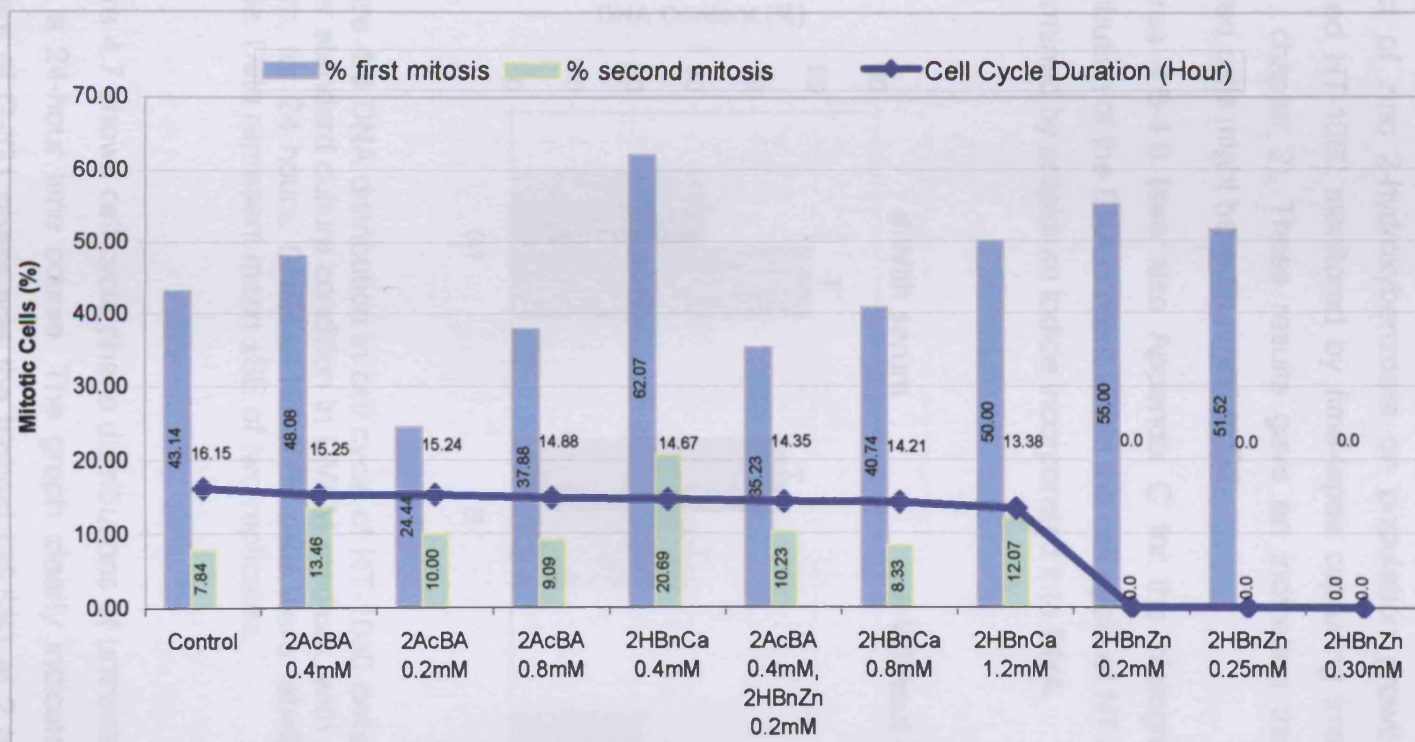
Figure 4.5 HT-1080 cell cycle duration* and percentage of **first**** and **second***** mitotic HT-1080 cells **by** total number of cells cultured for 22 hours in presence of 2-acetylbenzoic acid (0.2, 0.4, 0.8mM), calcium 2-hydroxybenzoate (0.4, 0.8, 1.2mM), zinc 2-hydroxybenzoate (0.2, 0.25, 0.3mM, **Note**: No cell cycle durations obtained when 0.2, 0.25, 0.3mM concentrations used).
*   Cell cycle duration refers to time from end of first mitosis to beginning of second mitosis.
**   % of **first** mitosis = No. of **first** mitotic cells/Total No. of cells at 22 hours' culturing x 100.
*** % of second mitosis = No. of second mitotic cells/Total no. of **cells** at 22 hours' culturing x 100.

To investigate the effect of calcium and zinc analogues on cell cycle, HT-1080 cells were cultured, arrested for 24 hours by serum-free DMEM medium, and treated with the individual benzoate analogue for 2, 6, 12 and 24 hours. The aim of selecting these time points was to explain the effect of zinc 2-hydroxybenzoate on population growth progression of treated HT-1080 monitored by time-lapse capturing images (see Figure 2.11, chapter 2). These results gave an indication that zinc benzoate treated cells might have an arrest at G2.

Figures 4.6-4.8 (see also Appendix C for the histograms) shows the distribution of the DNA content within the cell cycle of HT-1080 cell line, as determined by propidium iodide incorporated into DNA.
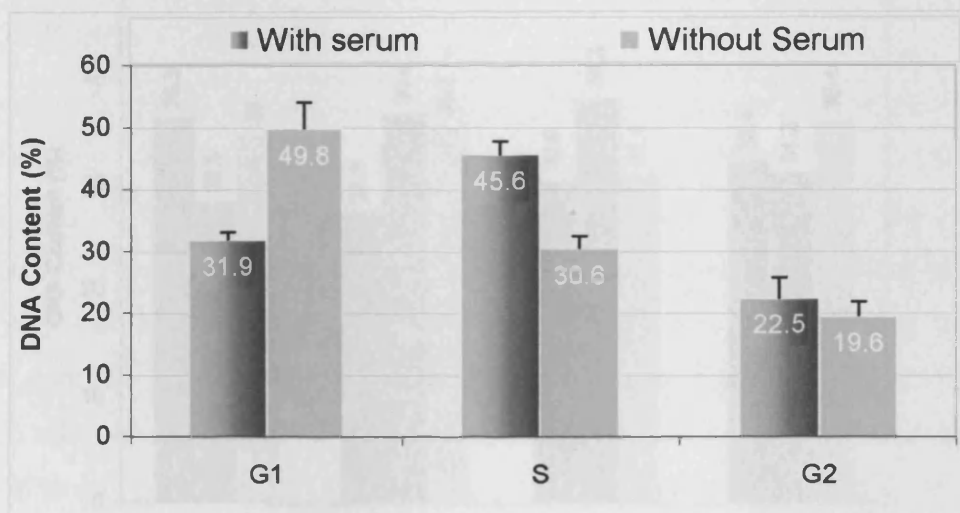
Figure 4.6 DNA distribution in cell cycle of HT-1080 cells allowed to grow under standard culture condition in DMEM medium, with and without 10% serum, for 24 hours. DNAs of HT-1080 cells were labelled by propidium iodide. Data represent mean ±SE of two replicates.

Figure 4.7 shows cell cycle phase distributions of untreated HT-1080 cells over a 24-hour time course. The graph clearly indicates that the DNA content of $G_0/G1$ phase was the highest (36.5%) at 2 hours post-serum cell activation, while the maximal percentage of cells in S phase was after

12 hours. 12 hours later, percentage of cells in both of these phases indicated the start of another cell cycle.

As indicated from time-lapse capturing images of growing HT-1080 cells, the cell cycle duration was approximately 16 hours (Figure 4.5). This result is consistent with the results of cell cycle analysis at the 24 hours' time point, where the percentage of cells in $G_0/G1$ phase increased and dropped in S phase (Figure 4.7). These results will be used as a reference for assessing the effect of 2-hydroxybenzoate analogues on cell cycle phases of HT-1080 cells.
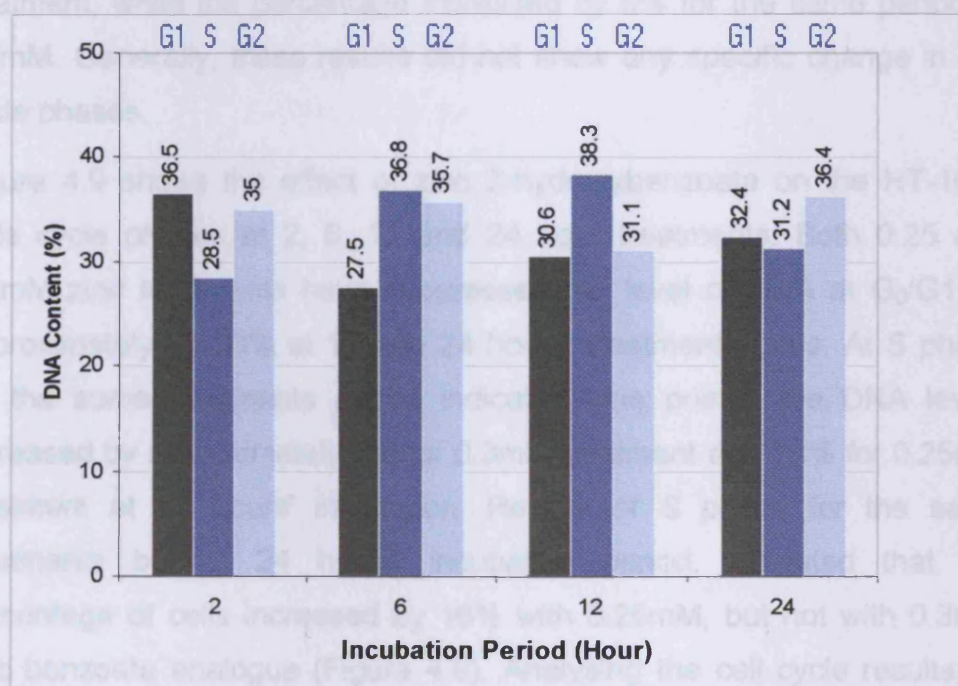
Figure 4.7 FACS results of cell cycle for untreated HT-1080 cells (control). Cells cultured under standard conditions, arrested with serum- free DMEM medium. Cells then harvested at indicated time points and labelled by propidium iodide. Results are average of two independent experiments. Note: see DNA histograms in Appendix C.

The results of cell cycle analysis of calcium 2-hyroxybenzoate-treated HT-1080 cells are shown in Figure 4.8. The calcium compound was found to

affect HT-1080 cell cycle in a concentration-dependent manner at both $G_0/G1$ and S phases, particularly between 6 and 12 hours of treatment. The DNA content of $G_0/G1$ phase, at 6-hour culturing for example, increased by approximately 10% and 24% (control = 27.5%, 0.4mM treatment = 30.3%; 0.8mM treatment = 34.1%) when the treatment concentrations increased respectively from 0.4 to 0.8mM compared to control. The increase in $G_0/G1$ was continued when cells were exposed to calcium compounds for 12 hours compared to control (Figure 4.8). Alternatively, the percentage of cells in S phase for the same period of exposure decreased by between 5% and 16% compared to control and approximately 16% from 6 hours to 12 hours' exposure of 0.4mM treatment, while the percentage increased by 6% for the same period at 0.8mM. Generally, these results did not show any specific change in cell cycle phases.

Figure 4.9 shows the effect of zinc 2-hydroxybenzoate on the HT-1080 cells cycle phases at 2, 6, 12 and 24 hour treatments. Both 0.25 and 0.3mM zinc treatments have suppressed the level of DNA at $G_0/G1$ by approximately 21-23% at 12 and 24 hours' treatment points. At S phase for the same treatments at the indicated time points, the DNA levels increased by approximately 8% for 0.3mM treatment and 23% for 0.25mM treatment at 12 hours' incubation. Results of S phase for the same treatments but at 24 hours' incubation period, indicated that the percentage of cells increased by 16% with 0.25mM, but not with 0.3mM zinc benzoate analogue (Figure 4.9). Analysing the cell cycle results for these treatments indicated that the DNA contents in G2 increased gradually at 6, 12 and 24 hours' time point treatments when cells were treated with 0.3mM zinc 2-hydroxybenzoate. The increase in the G2 phase was approximately 17%, compared to the control sample.

As indicated in Chapter 2, the zinc 2-hydroxybenzoate exerted the highest antiproliferative effects compared to other benzoate analogues, as measured by different techniques (see Chapter 2).

Figure 4.8 FACS results of cell cycle for HT-1080 cells treated with 0.4 and 0.8mM calcium 2-hydroxybenzoate for 2, 6, 12 and 24 hours. Cells cultured under standard conditions, arrested with serum free DMEM medium, treated with calcium benzoate at indicated time points and labelled by propidium iodide. Results average of two independent experiments. Note: see DNA histograms in Appendix C.
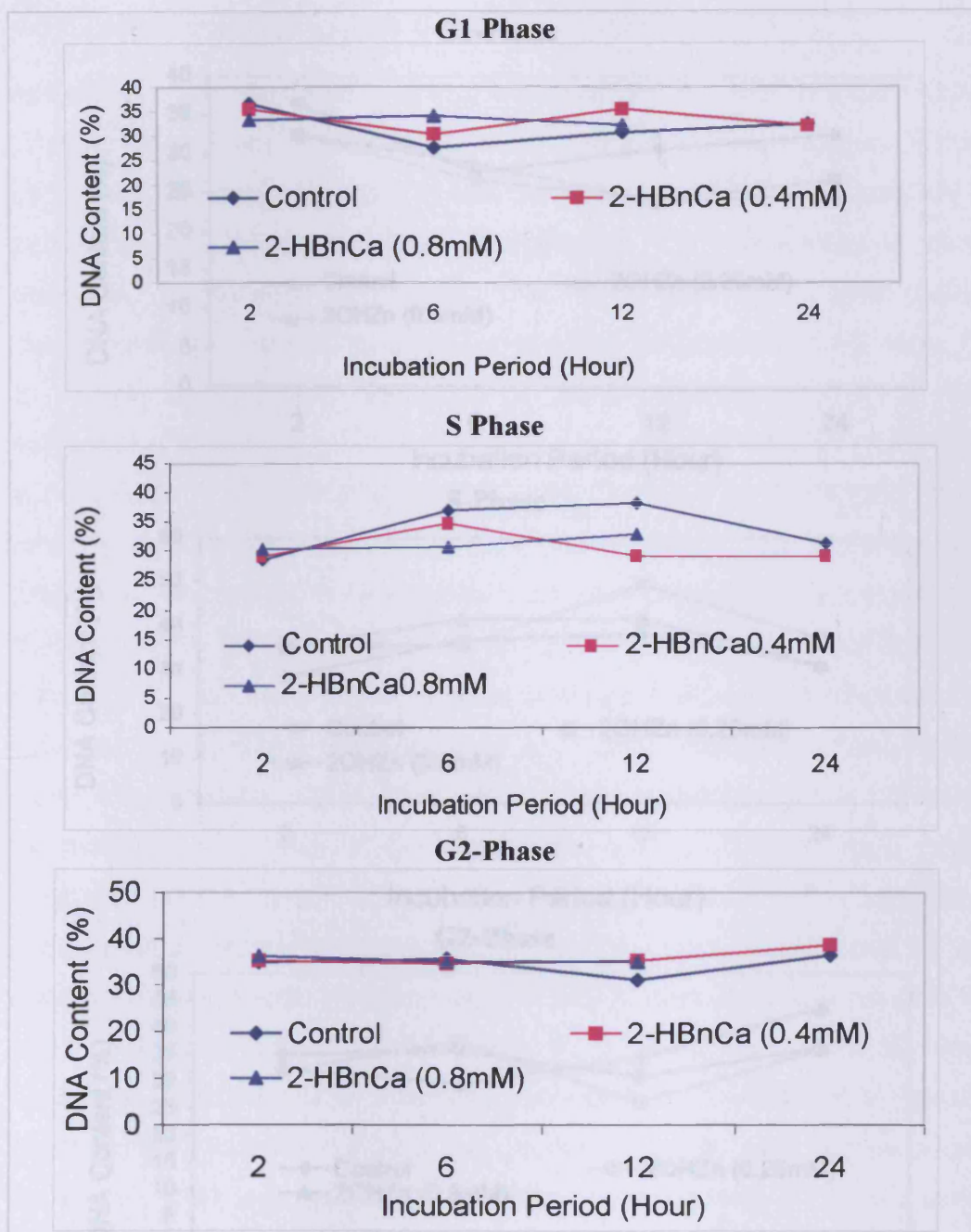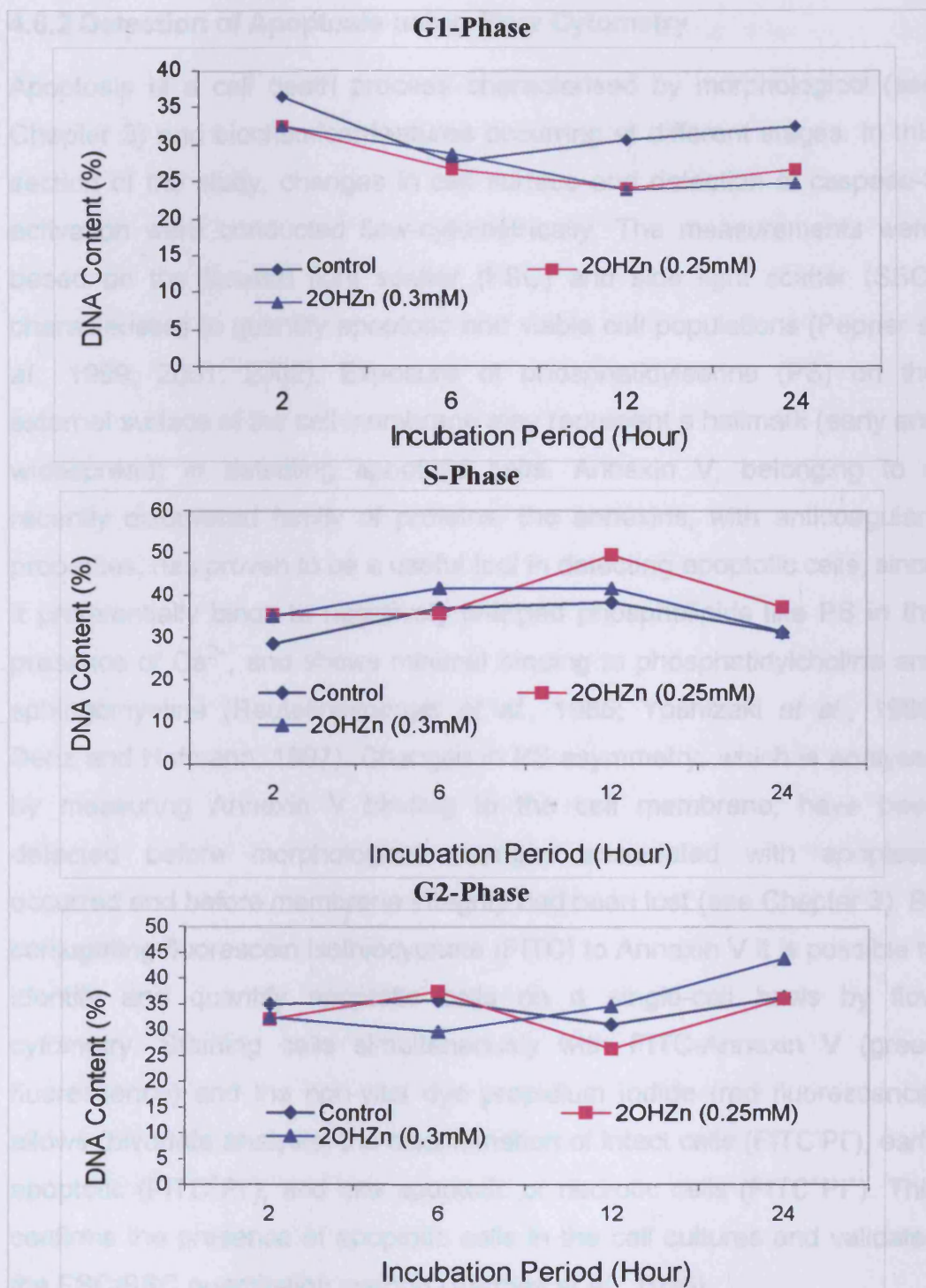
Figure 4.9 FACS results of cell cycle for HT-1080 cells treated with 0.25 and 0.3mM zinc 2-hydroxybenzoate for 2, 6, 12 and 24 hours. Cells cultured under standard conditions, arrested with serum-free DMEM medium, treated with zinc benzoate at the indicated time points, and labelled by propidium iodide. Results average of two independent experiments. Note: see DNA histograms in Appendix C.

4.6.2 Detection of Apoptosis using Flow Cytometry

Apoptosis is a cell death process characterised by morphological (see Chapter 3) and biochemical features occurring at different stages. In this section of the study, changes in cell surface and detection of caspase-3 activation were conducted flow-cytometrically. The measurements were based on the forward light scatter (FSC) and side light scatter (SSC) characteristics to quantify apoptotic and viable cell populations (Pepper *et al.*, 1999; 2001; 2002). Exposure of phosphatidylserine (PS) on the external surface of the cell membrane may represent a hallmark (early and widespread) in detecting apoptotic cells. Annexin V, belonging to a recently discovered family of proteins, the annexins, with anticoagulant properties, has proven to be a useful tool in detecting apoptotic cells, since it preferentially binds to negatively charged phospholipids like PS in the presence of Ca^{2+}, and shows minimal binding to phosphatidylcholine and sphingomyeline (Reutelingsperger *et al.*, 1985; Yoshizaki *et al.*, 1989; Benz and Hofmann, 1997). Changes in PS asymmetry, which is analysed by measuring Annexin V binding to the cell membrane, have been detected before morphological changes associated with apoptosis occurred and before membrane integrity had been lost (see Chapter 3). By conjugating fluorescein isothiocyanate (FITC) to Annexin V it is possible to identify and quantify apoptotic cells on a single-cell basis by flow cytometry. Staining cells simultaneously with FITC-Annexin V (green fluorescence) and the non-vital dye propidium iodide (red fluorescence) allows (bivariate analysis) the discrimination of intact cells (FITC⁻PI⁻), early apoptotic (FITC⁺PI⁻), and late apoptotic or necrotic cells (FITC⁺PI⁺). This confirms the presence of apoptotic cells in the cell cultures and validates the FSC/SSC quantitation method (Vermes *et al.*, 1995)

4.6.2.1 Detection of Apoptosis through Annexin V

In order to quantify the effect of benzoate analogues on the induction of apoptosis in HT-1080 cells, double staining for both FITC-labelled Annexin

V binding and cellular DNA using propidium iodide was used and measured by flow cytometry to substantiate the morphological results that showed the zinc benzoate analogue mostly induced apoptosis compared to others (see Chapter 3). Annexin V was used to measure surface changes through the labelling of the externalised phosphatidylserine (PS) when the cell is committed to the apoptosis pathway of death. Figure 4.10A shows the percentage of late apoptotic (or the secondary necrotic) HT-1080 cells cultured in DMEM optimal population growth medium in the presence of zinc 2-hydroxybenzoate for 24 hours. These results clearly indicate the zinc analogue-induced apoptosis in a concentration-dependent manner, as labelled by propidium iodide (PI) (red fluorescence). The percentages of positively stained cells with PI increased 2.2-fold, 2.5-fold and 3-fold when the HT-1080 cells were exposed to 0.1, 0.2 and 0.4mM zinc 2-hyroxybenzoate, respectively. Furthermore, the FITC-labelled Annexin V and propidium iodide double staining show the viable cells negative (for both AV and PI, shown as dark blue dots), the early apoptotic cells stained (+ AV and − PI, shown as red dots) and the secondary necrotic, or late apoptotic cells stained positive for both AV and PI, (shown as light blue dots) thus labelling both early and late apoptotic HT-1080 cells (Figure 4.10B). As with the PI positively stained cells, the late apoptotic cells also increased by 5.3-fold, 5.7-fold and 7.5-fold when HT-1080 cells were exposed respectively to 0.1, 0.2, and 0.4mM of zinc analogue. These results are in agreement with the corresponding morphological experiment with Annexin V. Other morphological techniques showed no HT-1080 necrotic cells.
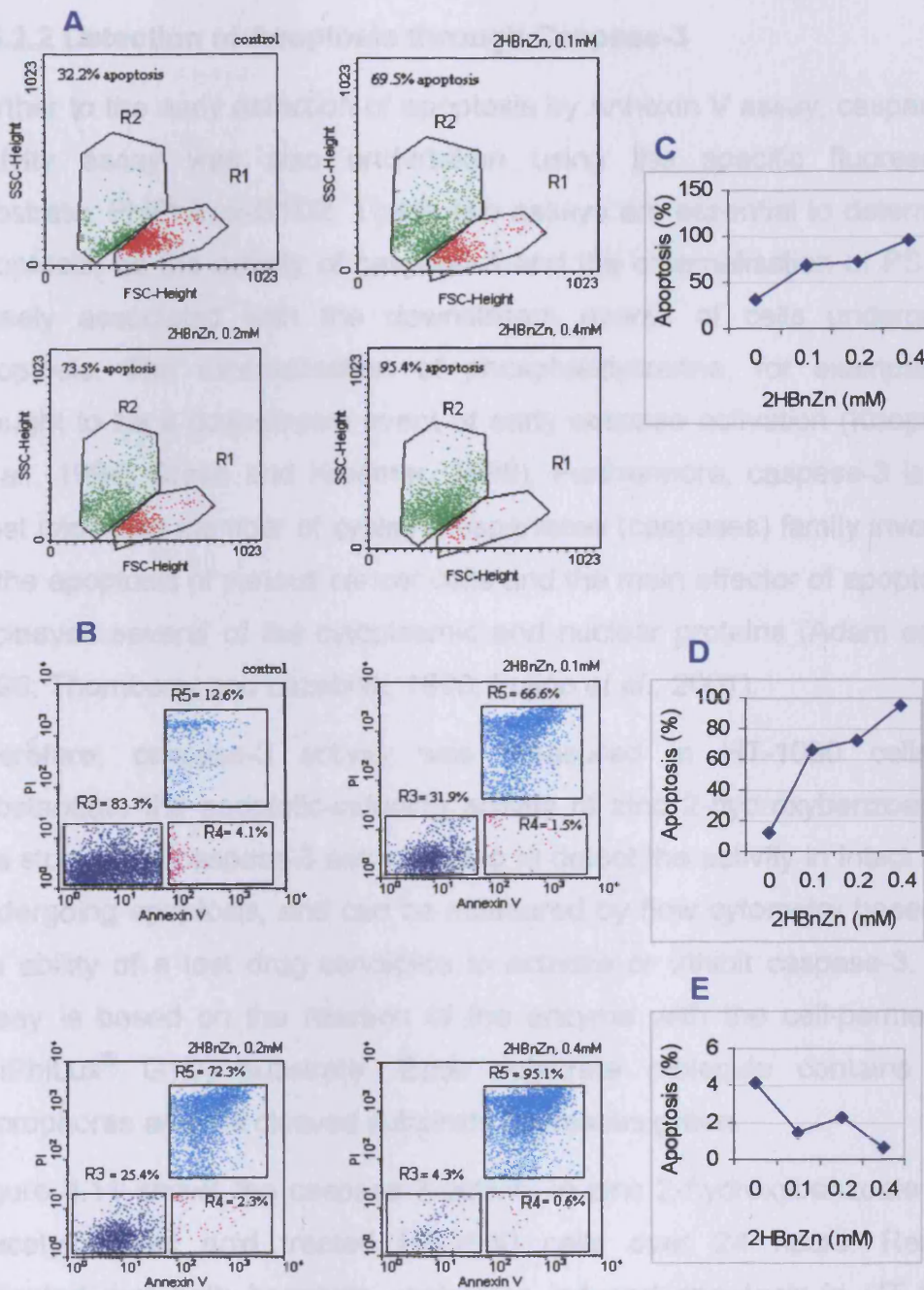
Figure 4.10 FACS results of concentration-dependent increase in (**A**) propidium iodide (PI) and (**B**) Annexin V (An-V)labelling of HT-1080 cells treated with 0.1, 0.2 and 0.4mM zinc 2-hydroxybenzoate for 24 hours. (**C**) % of early and late apoptotic cells labelled by PI (Green), (**D**) % of late apoptotic cells labelled by An-V (blue), and (**E**) % of early apoptotic cells labelled by An-V (red). Cells cultured under standard conditions, arrested with serum-free DMEM medium, treated with zinc benzoate at the indicated concentration points, and labelled by FITC-labelled Annexin V.

4.6.2.2 Detection of Apoptosis through Caspase-3

Further to the early detection of apoptosis by Annexin V assay, caspase-3 activity assay was also undertaken using the specific fluorescent substrate, PhiPhiLux-G1D2. These two assays are essential to determine apoptosis, as the activity of caspase-3 and the externalisation of PS are closely associated with the downstream events of cells undergoing apoptosis. The externalisation of phosphatidylserine, for example, is thought to be a downstream event of early caspase activation (Koopman et al., 1994; Green and Kroemer, 1998). Furthermore, caspase-3 is the most important member of cysteine aspartases (caspases) family involved in the apoptosis of various cancer cells and the main effector of apoptosis. It cleaves several of the cytoplasmic and nuclear proteins (Adam et al., 1998; Thornberry and Lazebnik, 1998; Fujino et al., 2001).

Therefore, caspase-3 activity was measured in HT-1080 cells to substantiate the apoptotic-inducing activity of zinc 2-hydroxybenzoate in this study. The caspase-3 assay is able to detect the activity in intact cells undergoing apoptosis, and can be measured by flow cytometry based on the ability of a test drug candidate to activate or inhibit caspase-3. The assay is based on the reaction of the enzyme with the cell-permeable PhiPhiLux® G1D$_2$ substrate. Each substrate molecule contains two fluorophores and the cleaved substrate fluoresces green.

Figure 4.11 shows the caspase-3 activity in zinc 2-hydroxybenzoate and 2-acetylbenzoic acid treated HT-1080 cells over 24 hours. Results indicated that both benzoate analogues induced apoptosis in HT-1080 cells, which was significantly different from control. Note the 0.4mM of zinc 2-hydroxybenzate induced apoptosis at a 5.9-fold increase over the level of apoptosis in the control sample. The 3.2mM 2-acetylbenzoic acid also induced apoptosis in HT-1080 cells, but at a lower level than zinc 2-hydroxybenzoate.

112

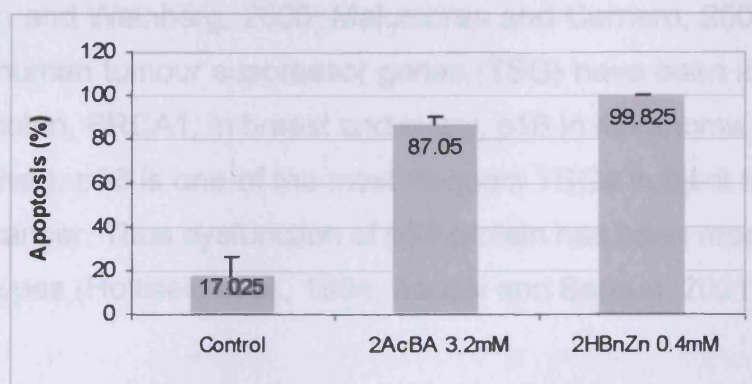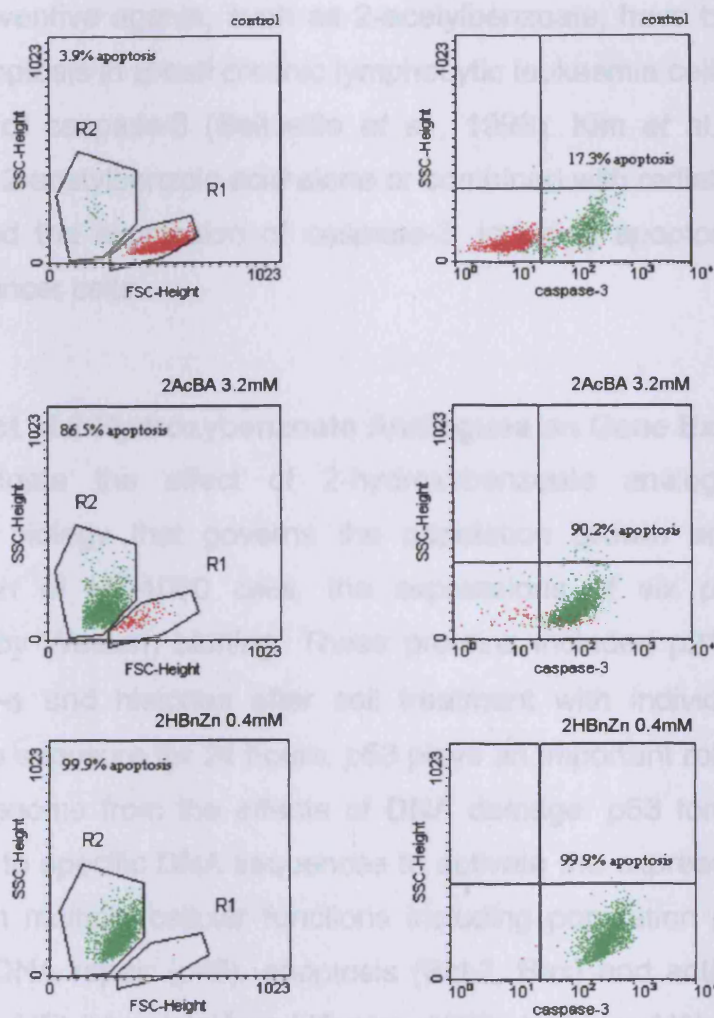**Figure 4.11** FACS results of concentration-dependent increase in caspase-3 activation in HT-1080 cells treated with 3.2mM 2-acetylbenzoic acid or 0.4mM zinc 2-hydroxybenzoate for 24 hours. Cells cultured under standard conditions, arrested with serum-free DMEM medium, treated with zinc benzoate at indicated concentration points, and labelled by fluorescent substrate, PhiPhiLux-G1D$_2$.

Chemopreventive agents, such as 2-acetylbenzoate, have been found to induce apoptosis in B-cell chronic lymphocytic leukaemia cells through the activation of caspase-3 (Bellosillo *et al.*, 1998). Kim *et* al. (2003) also found that 2-acetylbenzoic acid alone or combined with radiation treatment upregulated the expression of caspase-3, inducing apoptosis in human cervical cancer cells.

4.6.3 Effect of 2-Hydroxybenzoate Analogues on Gene Expression

To investigate the effect of 2-hydroxybenzoate analogues on the molecular biology that governs the population growth and cell cycle progression of HT-1080 cells, the expressions of six proteins were analysed by Western blotting. These proteins included p21, p53, Bcl-2, Bax, TNF-α and histones after cell treatment with individual agent in continuous exposure for 24 hours. p53 plays an important role in guarding the cell genome from the effects of DNA damage. p53 forms tetramers and binds to specific DNA sequences to activate the expression of genes involved in multiple cellular functions including population growth arrest (p21^{Cip1}), DNA repair (p48), apoptosis (Bcl-2, Bax) and antiangiogenesis (TSP1/GD-AIF) (Vogelstein and Kinzler, 1992; Jacks and Weinberg, 1996; Hanahan and Weinberg, 2000; Malumbres and Carnero, 2003). Although, several human tumour suppressor genes (TSG) have been identified (e.g. APC in colon, BRCA1, in breast and ovary, p16 in melanoma, Rb Retina in bone, other), p53 is one of the most frequent TSGs subject to mutation in human cancer. Thus dysfunction of p53 protein has been reported in many tumour types (Hollstein et al., 1994; Soussi and Beroud, 2001).

4.6.3.1 Expression of p53 and p21

Both p21 and p53 are closely associated in cell cycle progression. p53, for example, is a transcriptional factor for stimulatation of the synthesis of p21^{Cip1}, a Cdk inhibitor that suppresses the activity of Cdk2-cyclin complex and hence blocks passage through the G1 checkpoint (Xiong *et al.*, 1993;

El Deiry et al., 1993; 1994). It is indicated from animal model studies that p53 can induce apoptosis but not G1 arrest in $p^{21CIP1/WAF1}$-defiicent mice (Brugarolas et al., 1995; Deng et al., 1995; Macleod et al., 1995). Arresting the cell cycle in G1 gives defected cells time to repair DNA damage. Thus, $p21^{Cip1}$-deficient mice are susceptible to spontaneous tumour development (Martin-Caballero et al., 2001).

Detections of p53 protein levels in benzoate analogues-treated-HT-1080 cells were conducted by Western blot after 24 hours' exposure to 0.05mM and 0.4mM of both calcium 2-hydroxybenzoate. Results indicated that the expression of p53 was upregulated at least 0.14-fold more than in the control sample (Figure 4.12). Further increase in the expression of p53 was caused by zinc 2-hydroxybenzoate, where the expression was increased 1-fold compared to control (Figure 4.12). It is very interesting to note that the expression of p53 in both calcium and zinc benzoate treatments was higher at lower drug concentration (0.05mM) than the higher one (0.4mM). A similar result was also obtained when HT-1080 cells were exposed to the 2-acetylbenzoic acid at the same concentrations for 24 hours.

Figure 4.13 shows the effect of calcium 2-hydroxybenzoate, zinc 2-hydroxybenzoate and 2-acetylbenzoic acid on the expression of p21 in treated HT-1080 cells. Calcium benzoate clearly upregulated p21 in HT-1080 cells in a concentration-dependent manner. The induction of p21 expression is higher than 2-acetylbenzoic acid by 2.3-fold, both at 0.4mM concentration and higher than control by approximately 0.79-fold.

The effect of zinc 2-hydroxybenzoate at the same concentration also upregulated the expression of p21 in a parallel experiment being increased by at least 0.4-fold.

Figure 4.12 Effect of 0.05mM and 0.4mM concentration of calcium 2-hydroxybenzoate, zinc 2-hydroxybenzoate and 2-acetylbenzoic acid on expression of p53 in HT-1080 cancer cells. Cells cultured under standard conditions, arrested with serum-free DMEM medium, treated for 24 hours. Western blots data represent mean ±SE of 2 independent gels for 2HBnCa and 4 gels for 2AcBA.
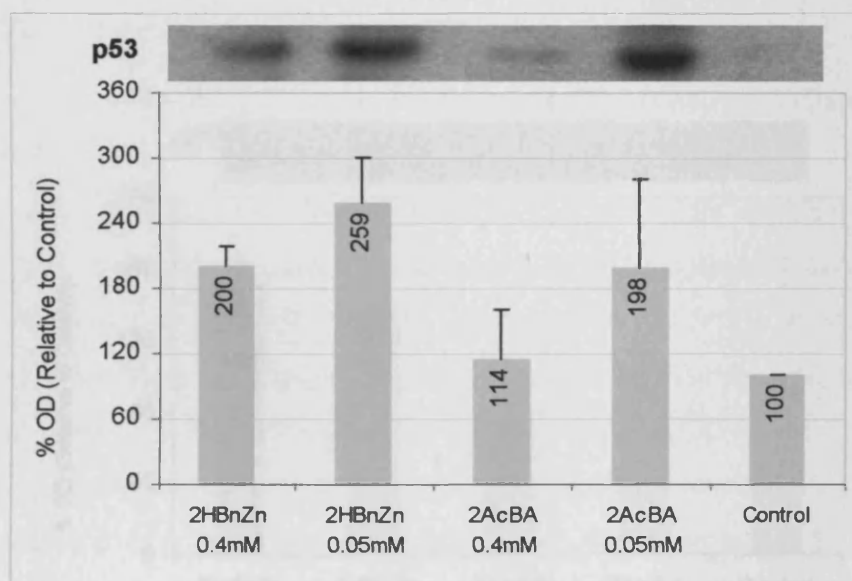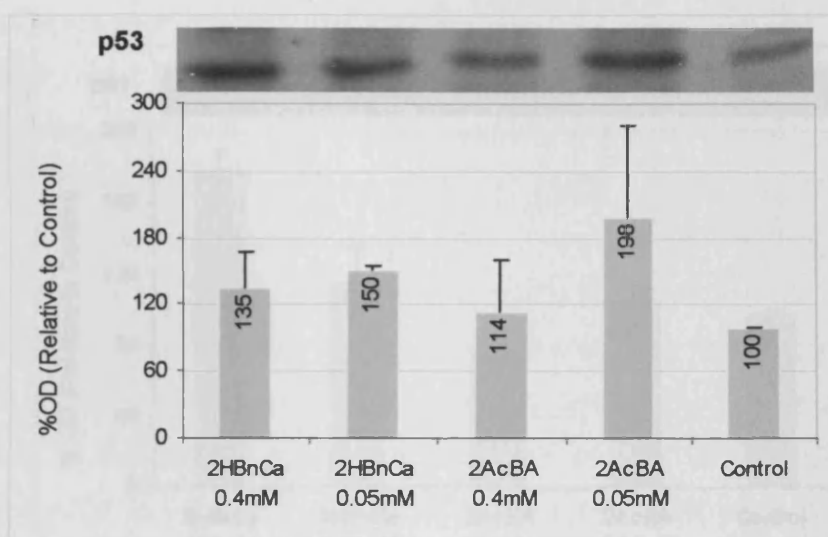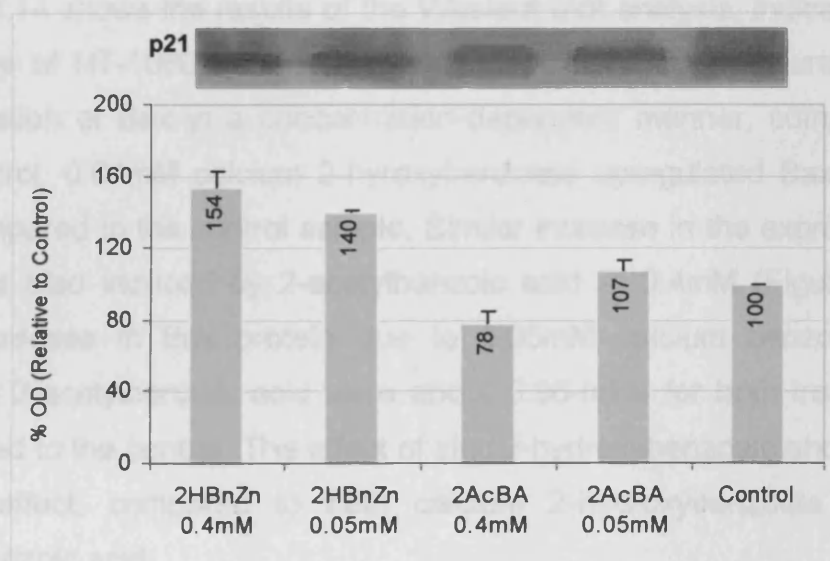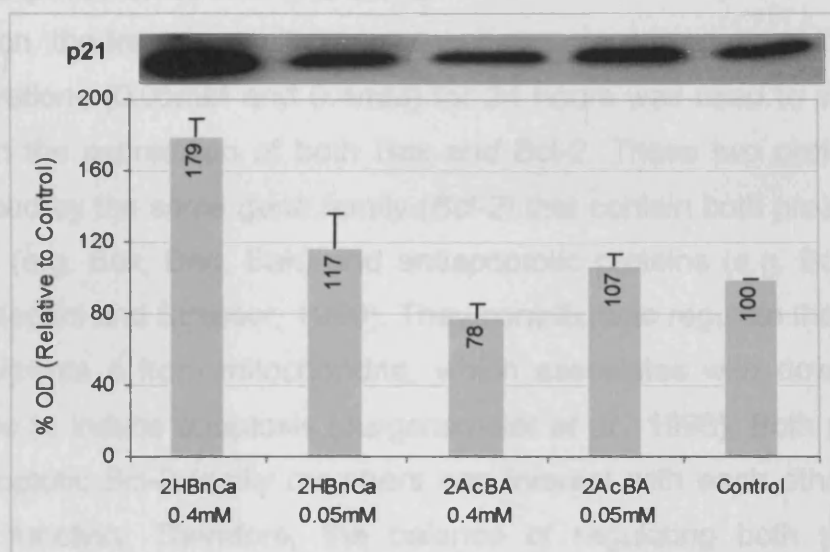
Figure 4.13 Effect of 0.05mM and 0.4mM concentration of calcium 2-hydroxybenzoate, zinc 2-hydroxybenzoate and 2-acetylbenzoic acid on expression of p21 in HT-1080 cancer cells. Cells cultured under standard conditions, arrest with 10% serum-free DMEM medium, treated for 24 hours. Western blots data represent mean ±SE of 2 independent gels for 2HBnCa and 4 gels for 2AcBA.

4.6.3.2 Expression of Bax and Bcl-2

In addition, the treatment with these two benzoate analogues at the same concentrations (0.05mM and 0.4mM) for 24 hours was used to study the effect on the expression of both Bax and Bcl-2. These two proteins are transcribed by the same gene family (Bcl-2) that contain both proapoptotic proteins (e.g. Bax, Bad, Bak) and antiapoptotic proteins (e.g. Bcl-2, Bcl-XL) (Pellegrini and Strasser, 1999). They contribute to regulate the release of cytochrome c from mitochondria, which associates with downstream caspases to induce apoptosis (Jurgensmeier et al., 1998). Both pro- and anti- apoptotic Bcl-2 family members can interact with each other in the loss of function. Therefore, the balance of regulating both pro- and resulting anti-apoptotic proteins is important in regulating cell decisions on life or death (Newton and Strasser, 1998).

Figure 4.14 shows the results of the Western blot analysis, indicating that exposure of HT-1080 cells to benzoate analogues for 24 hours caused upregulation of Bax in a concentration-dependent manner, compared to the control. 0.04mM calcium 2-hyroxybenzoate upregulated Bax by 2.3-fold compared to the control sample. Similar increase in the expression of Bax was also induced by 2-acetylbenzoic acid at 0.4mM (Figure 4.14). The increases in Bax protein due to 0.05mM calcium benzoate and 0.05mM 2-acetylbenzoic acid were about 0.96-folds for both treatments, compared to the control. The effect of zinc 2-hydroxybenzoate showed the lowest effect, compared to both calcium 2-hydroxybenzoate and 2-acetylbenzoic acid.

In contrast, both 0.05mM and 0.4mM calcium 2-hydroxybenzoate downregulated the expression of Bcl-2 compared to the control sample by about 21% at both concentrations (Figure 4.15). The effect of 2-acetylbenzoic acid on the expression of Bcl-2 protein, however, showed an increase of approximately 0.74 and 1.9-fold when HT-1080 cells were exposed to 0.4mM and 0.05mM concentration, respectively, for 24 hours compared to control (Figure 4.15). In contrast, the expression of Bcl-2 in

HT-1080 cells after the exposure to zinc 2-hydroxybenzoate was upregulated 2-fold for both concentration treatments (Figure 4.15).

Figure 4.14 Effect of calcium 2-hydroxybenzoate, zinc 2-hydroxybenzoate and 2-acetylbenzoic acid at 0.05mM and 0.4mM concentrations, on the expression of Bax in HT-1080 cancer cells. Cells were cultured under standard conditions, arrested with serum-free DMEM medium, treated for 24 hours. Western blots data represent means ±SE of 2 independent gels for 2HBnCa and 4 gels for 2AcBA.

Bcl-2

560
490
420
350
280
210
140
70
0

% OD (Relative to Control)

| 2HBnCa-400 | 2HBnCa-50 | 2AcBA-400 | 2AcBA-50 | Control |

79   78   174   290   100

Bcl-2

560
490
420
350
280
210
140
70
0

% OD (Relative to Control)

| 2HBnZn-400 | 2HBnZn-50 | 2AcBA-400 | 2AcBA-50 | Control |

302   308   174   290   100

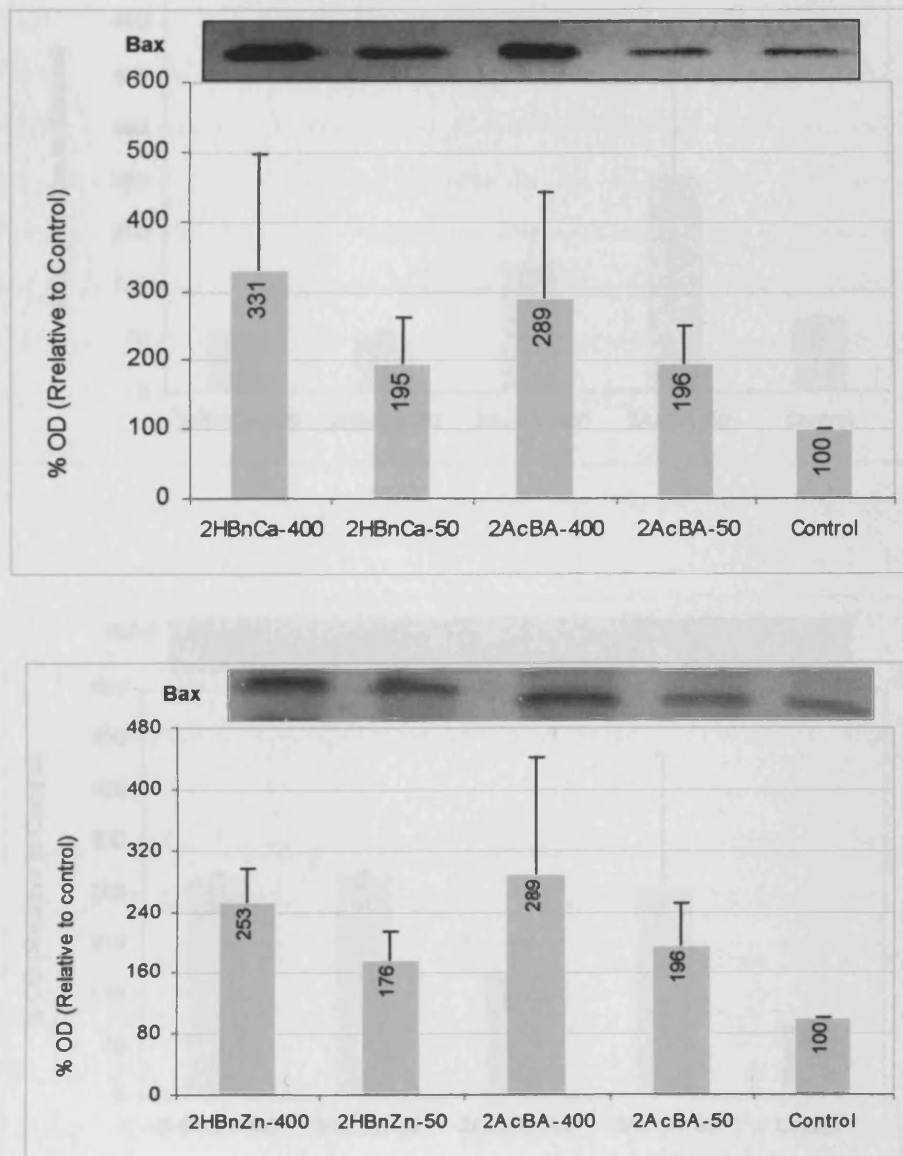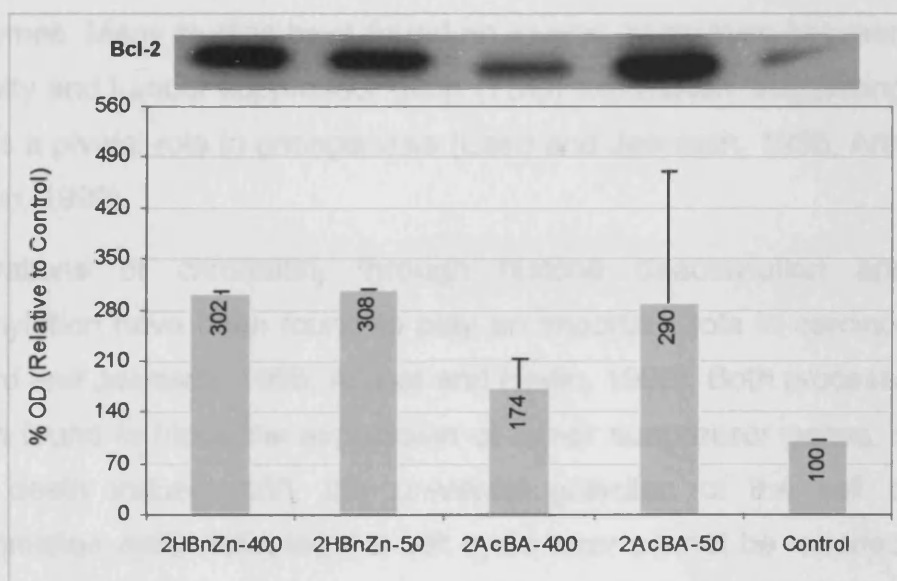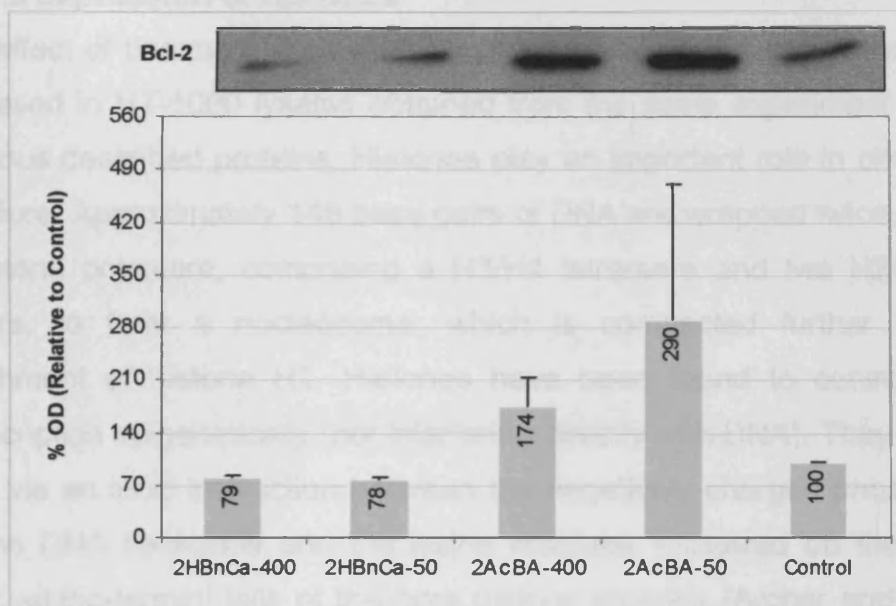**Figure (4.15)** The effect of calcium 2-hydroxybenzoate, zinc 2-hydroxybenzoate and 2-acetylbenzoic acid both at 0.05mM and 0.4mM concentrations on the expression of Bcl-2 in HT-1080 cancer cells. Cells were cultured under standard conditions, arrest with serum free DMEM medium, treated for 24 hours. Western blots data represents the mean ±SE of 2 independent gels for 2HBnCa and 4 gels for 2AcBA.

4.6.3.3 Expression of Histones

The effect of benzoate analogues on the expression of histones was also assessed in HT-1080 lysates obtained from the same experiment for the previous described proteins. Histones play an important role in chromatin structure. Approximately 146 base pairs of DNA are wrapped twice around a histone octamere, comprising a H3/H4 tetramere and two H2A, H2B dimers, to form a nucleosome, which is compacted further by the attachment of histone H1. Histones have been found to control gene transcription epigenetically (not interfering directly with DNA). They bind to DNA via an ionic interaction between the negatively charged phosphates on the DNA backbone and the lysine residues, clustered on the highly basic amino-termini tails of the core histone proteins (Archer and Hodin, 1999). Histone acetylation and deacetylation depend on the activity levels of the histone acetyltransferase (HAT) and histone deacetylase (HDACs) enzymes. Many studies have found an inverse correlation between HDAC activity and tumour suppressor gene (TSG) expression, suggesting HDAC plays a pivotal role in oncogenesis (Laird and Jaenisch, 1996; Archer and Hodin, 1999).

Alterations of chromatin, through histone deacetylation and DNA methylation have been found to play an important role in carcinogenesis (Laird and Jaenisch, 1996; Archer and Hodin, 1999). Both processes have been found to block the expression of tumor suppressor genes, such as cell death inducer p53, the universal guardian of the cell cycle in mammalian cells, activated if a cell cycle error cannot be repaired by the cell repair mechanisms.

Figure 4.16 shows the effect of 0.05mM and 0.4mM calcium 2-hydroxybenzoate, zinc 2-hydroxybenzoate and 2-acetylbenzoic acid on the regulation of histone proteins. These benzoates upregulate histones at least 1.1-fold compared to the control sample. In the case of calcium benzoate, results showed no differences between 0.05mM and 0.4mM concentrations. However, the effect of zinc analogue on the expression of histones showed a concentration-dependent effect, where 0.4mM

concentration expressed histone more than doubled the expression of histone than that induced by 0.05mM of zinc 2-hydroxybenzoate (Figure 4.16).

The figure also shows the effect of 2-acetylhybenzoic acid on the expression of histones at the same concentrations. Results of Western blotting showed that lower concentration (0.05mM) of 2-acetylbenzoic acid was more effective is upregulating histone than 0.4mM.

Figure 4.16 Effect of calcium 2-hydroxybenzoate, zinc 2-hydroxybenzoate and 2-acetylbenzoic acid, both at 0.05mM and 0.4mM concentrations, on the expression of histone in HT-1080 cancer cells. Cells cultured under standard conditions, arrested with 10% serum free DMEM medium, treated for 24 hours. Western blots data represent mean ±SE of 2 independent gels for 2HBnCa and 4 gels for 2AcBA.

4.6.3.4 Expression of Tumour Necrotic Factor (TNF-α)

Two TNF receptors are found on the cell surface: TNF-R1 and TNF-R2. The TNF-R1 is expressed in cells binding to TNF-α, which has important biological functions including induction of apoptosis and antiviral activity (Schulze-Osthoff *et al.*, 1998). 2-acetylbenzoic acid was found to induce apoptosis in colon cancer cells through the activation of nuclear factor-kappa beta (NF-κB) signalling pathway (Stark *et al.*, 2001). This pathway was identified as a target for the antiinflammatory effects of 2-acetylbenzoic acid and other NSAIDs (Kopp and Ghosh, 1994; Yin *et al.*, 1998). TNF-α is able to activate pro-apoptotic proteins including capases, resulting in apoptosis, or to activate NF-kB and initiate proliferation or differentiation. Therefore, the expression of TNF-α was investigated.

Figure 4.17 shows the results of TNF-α expression in HT-1080 cells when exposed to benzoate analogues for 24 hours. Results indicated that both calcium and zinc 2-hydroxybenzate upregulated TNF-α by at least 1.23-fold compared to the control sample. Furthermore, 2-acetylbenzoic acid also increased the expression of TNF-α, but not in a concentration-dependent manner, since 0.05mM induced more expression of TNF-α than 0.4mM concentration.

4.6.4 Investigation of 2-Hydroxybenzoate Analogues Uptake by HT-1080

The aim of this study was also to investigate the uptake of 2-hydroxybenzoates by HT-1080 cells. Therefore, both high pressure liquid chromatography and atomic absorption were used to detect 2-hydroxybenzoic acid and metal ions, respectively. Authentic samples of 2-hydroxybenzoic and 2-acetylbenzoic acids were run first to specify the retention time for each benzoate, and used as a reference for the same molecules that were extracted from treated cells.
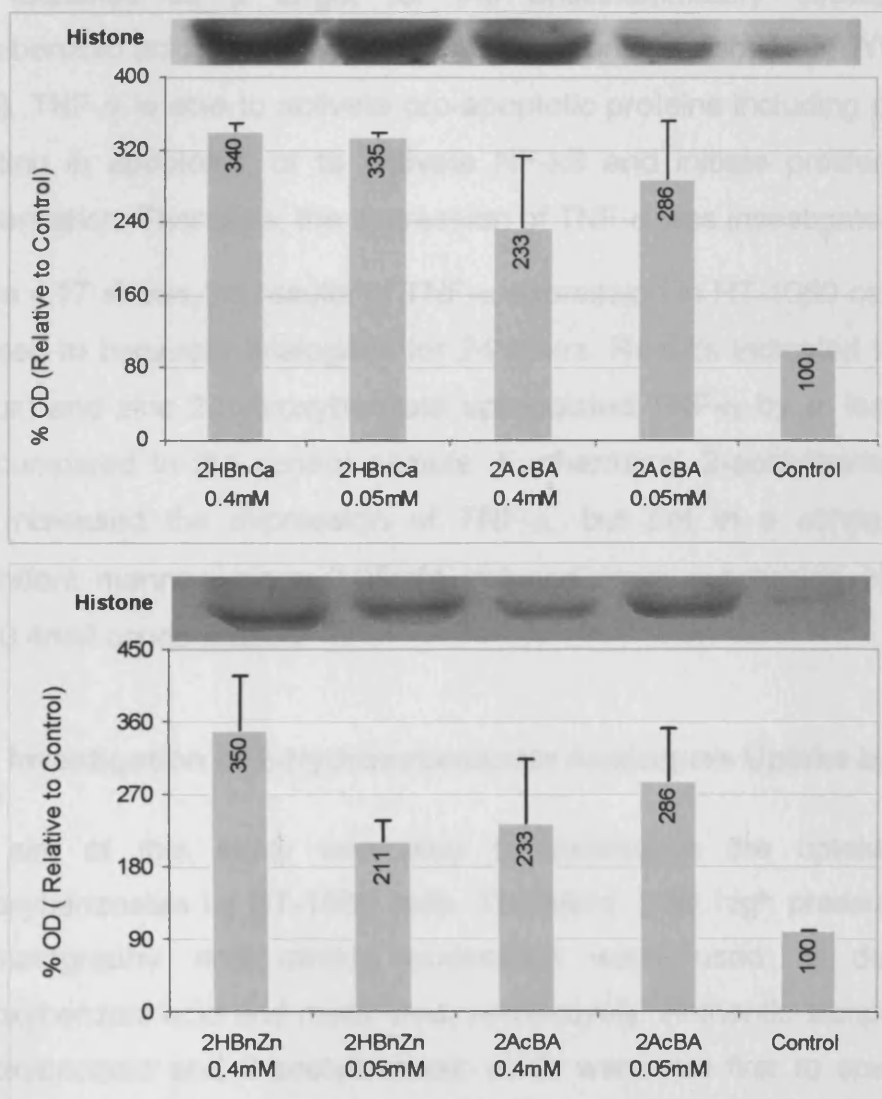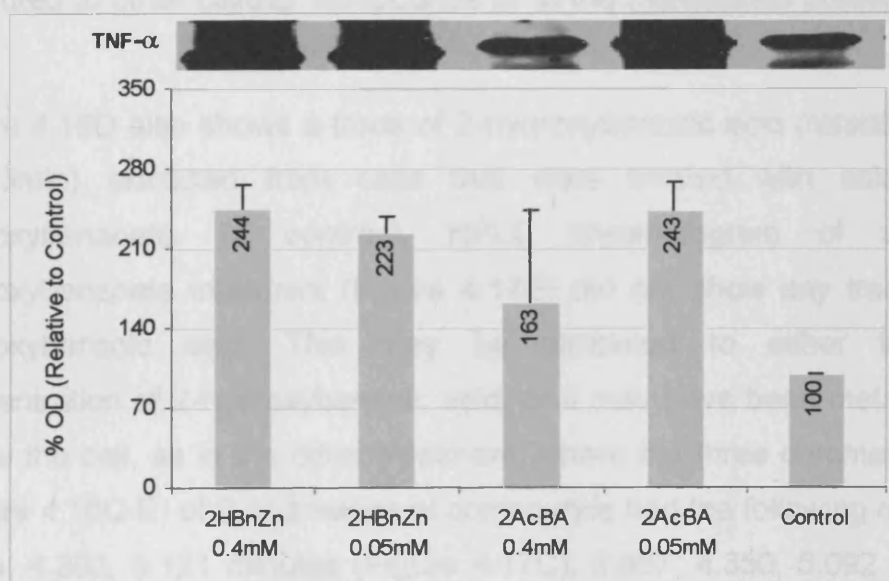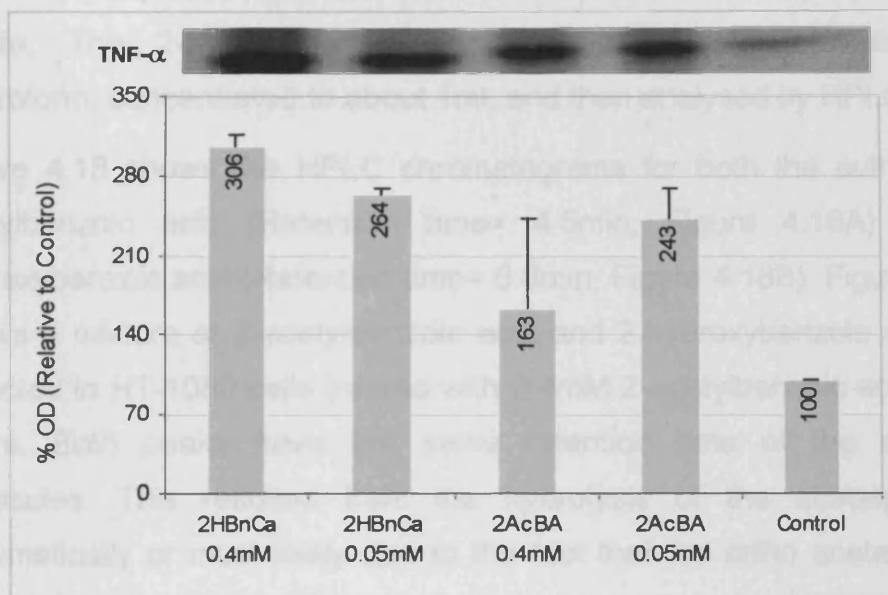
Figure 4.17 Effect of calcium 2-hydroxybenzoate, zinc 2-hydroxybenzoate and 2-acetylbenzoic acid, at both 0.05mM and 0.4mM concentrations, on the expression of TNF-α in HT-1080 cancer cells. Cells cultured under standard conditions, arrested with 10% serum-free DMEM medium, treated for 24 hours. Western blots data represent mean ±SE of 2 independent gels for 2HBnCa and 4 gels for 2AcBA.

HT-1080 cell pellets of 0.4mM calcium 2-hydroxybenzoate and zinc 2-hydroxybenzoate-treated samples were digested with nitric acid to free

both 2-hydroxybenzic acid and the metal ion in the form of calcium or zinc nitrate. The 2-hydroxybenzoic acid samples were extracted with chloroform, concentrated to about 1ml, and then analysed by HPLC.

Figure 4.18 shows the HPLC chromatograms for both the authentic 2-acetylbenzoic acid (Retention time= 4.5min; Figure 4.18A) and 2-hydroxybenzoic acid (Retention time= 6.3min; Figure 4.18B). Figure 4.18C shows a mixture of 2-acetylbenzoic acid and 2-hydroxybenzoic acid was detected in HT-1080 cells treated with 0.4mM 2-acetylbenzoic acid for 24 hours. Both peaks have the same retention time of the authentic molecules. This resulted from the hydrolysis of the acetate, either enzymatically or most likely due to the fact that the ortho acetate group forms intrahydrogen bonding which promotes hydrolysis. Other peaks are attributed to other cellular compounds or to the metabolites present in the cell.

Figure 4.18D also shows a trace of 2-hydroxybenzoic acid (retention time = 6.3min) extracted from cells that were treated with calcium 2-hydroxybenzoate. In contrast, HPLC chromatogram of zinc 2-hydroxybenzoate treatment (Figure 4.17E) did not show any trace of 2-hydroxybenzoic acid. This may be attributed to either the low concentration of 2-hydroxybenzoic acid, or it may have been metabolised inside the cell, as in the other treatment, where the three chromatograms (Figure 4.18C-E) of 2 or 3 traces of compounds had the following retention times: 4.392, 5.121 minutes (Figure 4.17C); 2.867, 4.350, 5.092 minutes (Figure 4.18D), and 2.854, 3.171, 4.333, 5.067 minutes (Figure 4.18E).

In this study, we also examined the presence of both calcium and zinc in HT-1080 cells treated independently with calcium 2-hydroxybenzoate and zinc 2-hydroxybenzoate at 0.4mM concentration for 24 hours. Table 4.4 shows that only zinc could be detected using atomic absorption. Although zinc was detected, the validity of the atomic absorption results remain questionable, due to the insensitivity of this technique to detect traces of zinc and calcium.
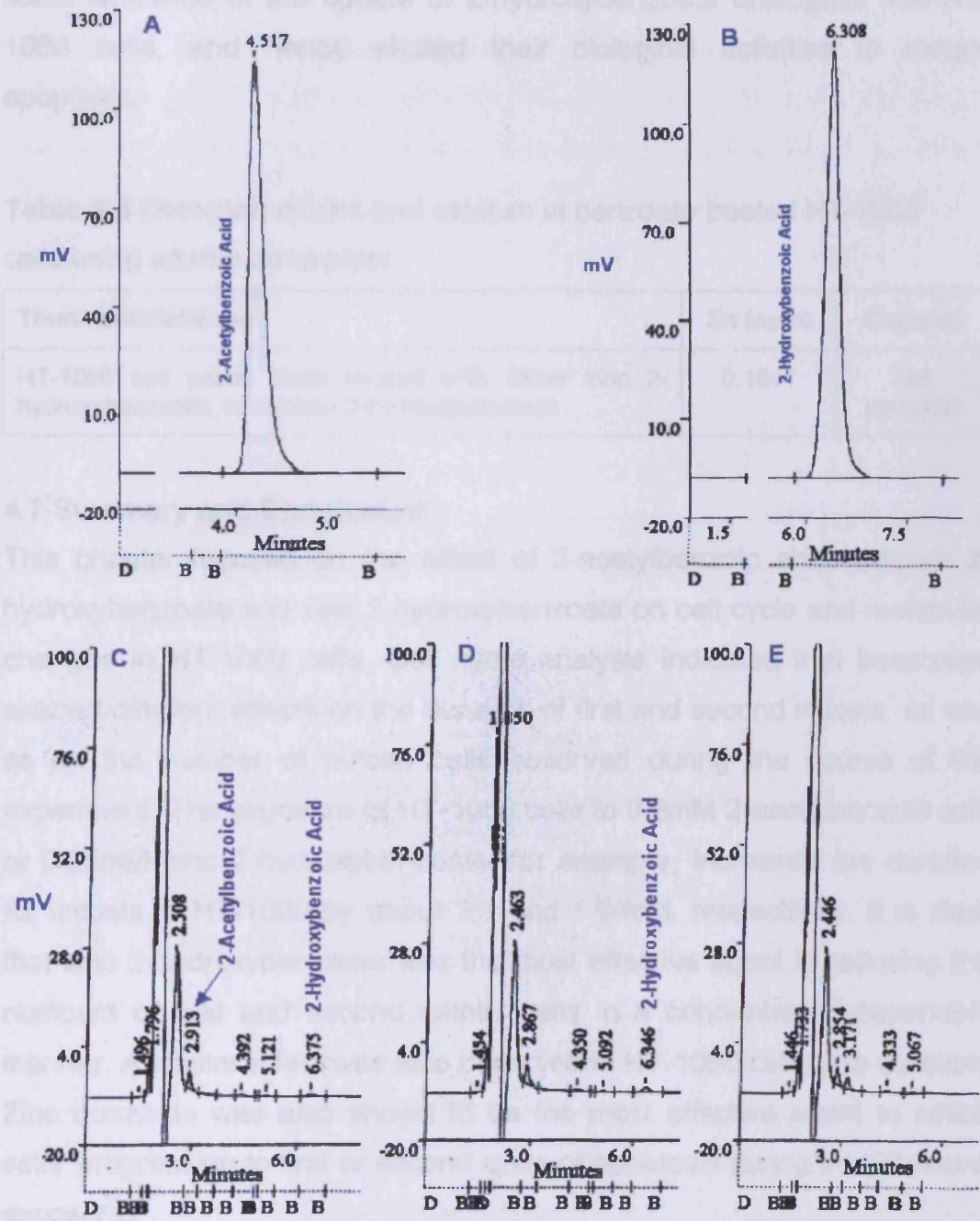
Figure 4.18 HPLC chromatograms of (A) authentic 2-acetylbenzoic acid, (B) authentic 2-hydroxybenzoic acid, (C) HT-1080 cell extract after treatment with 0.4mM 2-acetylbenzoic acid, (D) HT-1080 cell extract after treatment with 0.4mM calcium 2-hydroxybenzoate, (E) HT-1080 cell extract after treatment with 0.4mM zinc 2-hydroxybenzoate.

It seems likely that the overall results obtained in this section have shown some evidence of the uptake of 2-hydroxybenzoate analogues into HT-1080 cells, and hence elicited their biological activities to induce apoptosis.

Table 4.4 Detection of zinc and calcium in benzoate treated HT-1080 cells using atomic absorption.

Treatment/Metal ion	Zn (ppm)	Ca(ppm)
HT-1080 cell pellet. Cells treated with either zinc 2-hydroxybenzoate, or calcium 2-hydroxybenzoate	0.1841	Not detected

4.7 Summary and Conclusion

This chapter focused on the effect of 2-acetylbenzoic acid, calcium 2-hydroxybenzoate and zinc 2-hydroxybenzoate on cell cycle and molecular changes in HT-1080 cells. Cell cycle analysis indicated that benzoates exerted different effects on the duration of first and second mitosis, as well as on the number of mitotic cells observed during the course of the experiment. The exposure of HT-1080 cells to 0.8mM 2-acetylbenzoic acid or 0.25mM zinc 2-hydroxybenzoate, for example, increased the duration for mitosis in HT-1080 by about 2.1 and 1.9-fold, respectively. It is clear that zinc 2-hydroxybenzoate was the most effective agent in reducing the numbers of first and second mitotic cells in a concentration-dependent manner. A similar effect was also observed in HT-1080 cell cycle duration. Zinc benzoate was also shown to be the most effective agent to inhibit cells' progression to first or second cycle of apoptosis during the 22 hours' exposure.

The effect of calcium and zinc benzoate analogues on cell cycle phase distributions indicated that neither of the treatments induced a significant cell cycle arrest. On the other hand, both calcium and zinc benzoate treatments have shown evidence of their apoptotic mode of action. The flow cytometric analysis of both Annexin V and caspase-3, for example, showed evidence of apoptosis. Both cell cycle analysis and the evidence

of apoptosis may indicate that the induction of cell death is by a mechanism that does not involve a specific phase arrest. To better understand the mechanism of action of benzoate analogues on cellular population growth and apoptosis in HT-1080 cells, we investigated the expression of six proteins that are involved in the downstream molecular organisation. These proteins included p53, p21, Bax, Bcl-2, histones and TNF-α using Western blot analysis. Results of the experiments are summarised as follows and in Table 4.5.

1   2-Acetylbenzoic acid treatments: p53, p21, Bax, Bcle-2, histones and TNF-α were upregulated in HT-1080 by both 0.05mM and 0.4mM 2-acetylbenzoic acid treatments by values ranging from 7% to 189% above the control (100%). However, 0.4mM concentration down- regulated **p21** by 28%. Most treatments were **not concentration- dependent**.

2   Calcium 2-hydroxybenzoate treatment: p53, p21, Bax, histones and TNF-α were upregulated in HT-1080 by both 0.05mM and 0.4mM calcium 2-hydroxybenzoate treatments by values ranging from 17% to 240% above the control (100%). However, both 0.05mM and 0.4mM concentrations downregulated **Bcl-2** by 21%. Most treatments were **concentration-dependent**.

3   Zinc 2-hydroxybenzoate treatments: p53, p21, Bax, histones and TNF-α were upregulated in HT-1080 by both 0.05mM and 0.4mM Zinc 2-hydroxybenzoate treatments by values ranging from 40% to 250% above the control (100%). However, 0.4mM concentration regulated p53 to the same extent as the control sample (or 100%). Most treatments were **concentration-dependent**.

4   The ratios between Bax (apoptotic promoter) to Bcl-2 (apoptotic inhibitor) induced by the three agents were **concentration-dependent**. The regulation of Bax was higher than Bcl-2 in HT-1080 cells when they were exposed to 2-acetylbenzoic acid, calcium 2-hydroxybenzoate, or zinc 2-hydroxybenzoate.

5 The ratios between Bcl-2 and p53 showed an increase in 2-acetylbenzoic acid treated HT-1080 while they decreased in presence both calcium and zinc 2-hydroxybenzoate treatments. Furthermore, the Bax/p53 ratios increased in most treatments (Table 4.5).

Table 4.5 Optical densities for protein expressions in benzoate-treated HT-1080 cells exposed for 24 hours.

Protein	2-Acetylbenzoic Acid (%)		Ca 2-hydroxybenzoate (%)		Zn 2-hydroxybenzoate (%)	
	0.4mM	0.05mM	0.4mM	0.05mM	0.4mM	0.05mM
P53	114	198	135	150	200	259
p21	78	107	179	117	154	140
Bax	289	198	331	195	253	176
Bcl-2	174	290	79	78	302	308
Histone	233	286	340	335	350	211
TNF-α	163	243	306	264	244	223
Bcl-2:Bax	1:1.66	1:0.676	1:4.190	1:2.5	1:0.838	1:0.571
Bcl-2:p53	1:0.66	1:0.68	1:1.71	1:1.92	1:1.51	1:1.89
Bax:p53	1:0.29	1:1	1:0.41	1:0.77	1:0.79	1:1.47

The increase in the upregulation of p53, Bax, histones and TNF-α as a result of exposing HT-1080 cells to 2-acetylbenzoic acid induced apoptosis measured by Annexin V and caspase-3. These four proteins are promoter agents in the induction of apoptosis, which suggests that the cell death proceeds through different apoptotic signalling pathways. Another principal observation made in these experiments is that, contrary to the function of Bcl-2 as an apoptotic inhibitor, its level increased at both 2-acetylbenzoic acid concentrations, while p21 decreased in cells undergoing apoptosis.

However, the incorporation of calcium 2-hydroxybenzoate (at both 0.05mM and 0.4mM) induced downregulation of Bcl-2 which participates in initiating apoptosis. The expression of other proteins was also increased,

which substantiates the apoptotic-inducing mechanism of calcium benzoate.

Results for the six protein expressions in zinc 2-hydroxybenzoate are similar to the effect of 2-acetylbenzoic acid, where Bcl-2 (apoptotic inhibitor) increased, while both Annexin V and caspase-3 assays indicated that HT-1080 cells died by apoptosis. Finally, it is important to note that the pharmacological investigations of the 2-hydroxybenzoate analogues showed the presence of these compounds inside HT-1080 cells, as indicated by HPLC and atomic absorption spectroscopy.

Chapter Five

General Discussion
and Conclusions

CHAPTER FIVE

General Discussion and Conclusions

5.1 Introduction

In the previous last three chapters, the biological activities of 2-hydroxybenzoate analogues on HT-1080 fibrosarcoma cells have been demonstrated. The results have identified the cytotoxic effect of zinc 2-hyroxybenzoate and its ability to induce various molecular changes in HT-1080 cells. Both morphological and molecular studies confirm that 2-hydroxybenzoate salts affect HT-1080 fibrosarcoma cells, and indeed inhibit their growth by apoptosis. Apoptosis was confirmed by two immunoassays: Annexin V and caspase-3 assays using flow cytometry. It is important to note that: (1) 2-hydroxybenzoate analogues used in this work have not been previously investigated, and (2) low concentrations (mostly 0.4mM) were used, even for the 2-acetylbenzoic acid (aspirin) compared to the commonly reported concentration of 5-10mM (Santini *et al.*, 1999; Marra and Liao, 2001). This chapter will shed light on the overall effects of 2-hydroxybenzoates on cell cycle components, morphological and the molecular changes in HT-1080 cells.

5.2 Growth *in vitro* of HT-1080 Cells: Research Perspective

The HT-1080 cell line is an epithelial-like adherent cell line, developed from a fibrosarcoma isolated from a 35 year-old Caucasian male (Rasheed *et al.*, 1974). Fibrosarcoma can infect bone and soft tissues including lung, kidney and lymph nodes. This human fibrosarcoma cell line was used in this work where enough cells were subcultured and frozen in batches in liquid nitrogen for subsequent work. Each batch was then subcultured 2-3 times depending on the planned experiments. General microscopic observation of each batch of HT-1080 cells indicated that they were healthy and grew well, and a consistent mode of growth was achieved.

131

Cells reached about 40-50% confluence in about 4 days after the initial seeding. To ensure a consistent benzoate effect on cultured cells, HT-1080 were cultured for 3 days in a full DMEM medium, followed by another day, but in serum-free DMEM, before cells were exposed to the benzoate compounds at certain concentration and time points. The purpose of culturing cells in a serum-free medium is to synchronise most cells at $G_0/G1$ phase at the beginning of the exponential phase of their growth, which was determined by a growth curve (see Figure 2.2). There are various methods for synchronisation such as physical (gentle shaking) and chemical (serum deprivation, chemical agents) methods (Matherly *et al.*, 1989; Chen *et al.*, 1996; Nguyen *et al.*, 1999; Albino *et al.*, 2000). The physical method includes harvesting cells by gentle shaking, where cells in M phase are less attached. In this study, serum deprivation was used, where HT-1080 cells were serum starved for 24 hours. Results of the flow cytometry indicated that the distribution of G1 phase reached 49.9% when HT-1080 cells were grown in serum-free DMEM medium for 24 hours, compared with 31.9% in the control experiment (culture medium containing 10% serum) (see Figure 4.6).

One of the main aims of this research was to investigate the anticancer activities of 2-hydroxybenzoic acid analogues using lower concentrations than those reported in the literature for 2-acetylbenzoic acid and its benzoate analogues (i.e. 5-10mM; Santini *et al.*, 1999; Marra and Liao, 2001). 2-acetylbenzoic acid, or aspirin, is the most common drug that has received a deal of research interest and been actively studied in different medical areas including cancer. Various studies have demonstrated that 2-acetylbenzoic acid and other NSAIDs play significant roles as protective agents against various types of cancer such as of the larynx and of the oral cavity (Funkhouser and Sharp, 1995; Claudia, 2003). However, relatively high concentrations of 2-acetylbenzate analogues (mostly 5-10mM) have been used *in vitro* of culture treatment (Santini *et al.*, 1999; Marra and Liao, 2001). Using the high concentration of 2-acetylbenzoic acid for an *in vitro* treatment is not compatible with the commonly

prescribed 75mg (4.17×10^{-4}M) of aspirin. Xu *et al.*, (1999) indicated that 2-acetylbenzoic acid at 10^{-4} to 10^{-5}M is the therapeutic concentration that is commonly achieved to selectively inhibit Cox-2 transcription in fibroblasts, and endothelial cells at high concentrations. In contrast, the high concentrations used for *in vitro* experiments exhibit nonspecific inhibition of a large number of kinases in cells. Therefore, high concentration of drugs can induce side effects. Indeed, Raz (2002) and others (Frantz and O'Neill, 1995; Yin *et al.*, 1998) questioned the use of high 2-acetylbenzoate concentrations, and concluded that the anti- tumourogenic effect of 2-acetylbenzoate *in vivo* is due to the inhibition of tumour Cox-2. This mechanism, however, may not have substantial relevance to the one that mediates the effects of NSAIDs *in vitro*, due to the high concentration of drug being used in *in vitro* experiments (Raz, 2002). Furthermore, it has been reported recently that high aspirin concentration used in cancer treatment causes complications to heart function (Patrono *et al.*, 2004). Thus, it was decided to use a low concentration (mostly 0.4mM). Indeed, we have noticed in this study that high concentrations (up to 8mM) of benzoate were required to observe explicit cytotoxicity in calcium 2-hydroxybenzoate-treated HT-1080 cells (Figure 2.8), although at lower concentrations of calcium 2-hydroxybenzoate (0.4mM), cytotoxic effects on HT-1080 cells were clearly seen when morphological and molecular investigations were used (see Chapters 3 and 4).

5.3 Appraisal of Cytotoxicity of 2-Hydroxybenzoate Analogues

As indicated in previous chapters, 2-hydroxybenzoates exert chemopreventative and chemotherapeutic potentials by virtue of their antiinflammatory, antipyretic and analgesic properties (Wong *et al.*, 1999; Husain *et al.*, 2001). These compounds also exert antioxidant activities in common with other phenolic compounds (Kikuzaki and Nakatani, 1989; Cuvelier *et al.*, 1996; Chen and Ho, 1997; Rice-Evans, 1997; Owen *et al.*, 2000). Clinical and epidemiological data associated with 2-acetylbenzoic

acid have shown evidence that nonsteroidal antiinflammatory drugs reduced the occurrence and growth of certain tumours such as colon and breast cancers (Harris, 1995; Stellman, 1995; Stark, 2001). In this study, 18 benzoic acid analogues were tested against the HT-1080 fibrosarcoma cell line. These benzoates possess a basic structure of an aromatic acid, with or without hydroxyl or acetyl functional groups (see Section 1.5). These two functional groups (hydroxyl and acetate) give rise to further chemical interactions in biological systems, as both benzoates contain heteroatoms and oxygen atoms. Furthermore, the conjugated system of the aromatic moiety participates to accommodate better conditions for the stability of reaction intermediates. The stabilisation of such intermediates is often accomplished by reactions with free radicals to hydroxylate the aromatic moiety. This gives benzoates the potential for free radical scavenging, and thus benzoates exert antioxidant characteristics. The benzoate analogues used in this study also carry mono or divalent metal ions, such as lithium, sodium, potassium, calcium, magnesium or zinc. In addition to their significant roles in biological systems (Hartwig, 2001; Truong-Tran *et al.*, 2001; Luchinat, 2003; see also Chapter 1), chemically, metal ions bonded to carboxylate, improve the solubility of organic acid molecules. The solubility of 2-acetylbenzoic acid, for example, is poor in water (3g/L), while its metal ion salts are readily soluble in water. Therefore, using different metal ions not only exerts biological effects but also improves physical properties which become available for interaction with cellular molecules. Both sodium and calcium 2-acetylbenzoate have been tested against various cancer cell lines (Santini *et al.*, 1999; Ishihara *et al.*, 2003; Lee *et al.*, 2003); however, other benzoates used in this study have not been tested before to our knowledge. In particular, the use of zinc- containing compounds (which exerted a significant biological potential against HT-1080 cells in this study) appears to be novel.

The anticarcinogenic effects of 2-acetylbenzoic acid have been widely studied in the large bowel, but the relationship between 2-acetylbenzoic acid use and cancer sites outside the large bowel have not been clearly

elucidated. Pagnate-Hill *et al.,* (1989) showed that there was no statistically significant association between 2-acetylbenzoic acid usage and risk of cancers of the lung, bladder, kidney, prostate or breast. Rosenbuurg *et al.,* (1991) also found no association between 2-acetylbenzoic acid usage and risk of cancers of the lung, breast, endometrium, ovary, testis, bladder, lymphomas, leukaemias and melanoma. Thun *et al.,* (1997) showed that there was no consistent association with 2-acetylbenzoic acid usage and cancer of the buccal cavity and pharynx, respiratory system, breast, male or female genital system, urinary system, brain and other nervous system, lymphatic and haematopoietic systems. However, a report from an American Health Foundation Workshop referred to various evidence that 2-acetylbenzoic acid may exhibit anticancer activities, and found data indicating an association between 2-acetylbenzoic acid use and reduced breast cancer risk (Stellman, 1995). In this study, the anti-carcinogenic activities of 18 of the benzoate analogues was studied in detail on HT-1080 cell.

The response of HT-1080 cells to benzoate analogues was studied to elucidate the effect on cell proliferation at different exposure times (12, 24, 48 and 72 hours) and at different benzoate concentrations (0.025, 0.05, 0.1, 0.2, 0.4mM). The results obtained from the MTT assay helped to identify the most promising targets for further studies. It is interesting to note that the effects of 2-hydroxybenzoate analogues except Zinc, were not concentration- or time-dependent (at concentration between 0.025 and 0.4mM). Generally, the biological effects of these analogues were biphasic, ranging between cytotoxic and mitogenic. For example, 0.1mM potassium benzoate, 0.05 and 0.1mM potassium 2-hydroxybenzoate, and 0.05mM potassium 2-acetylbenzoate reduced HT-1080 population number by about 30% when cells were exposed to these compounds for 12 and 24 hours, and compared to the control experiment (see Figure 2.5). However, the incubation of HT-1080 cells for longer periods (48 and 72 hours) induced a mitogenic effect, as measured by MTT assay. Similar results were obtained when HT-1080 cells were exposed for 6, 12, 24, 48 and 72

hours at low concentrations (0.025, 0.5 and 0.1mM) of calcium, magnesium, or zinc benzoates, 2-hydroxybenzoate and 2-acetylbenzoate analogues (see Figures 2.6, 2.7, 2.9, 2.10). However, both 0.2 and 0.4mM concentrations of zinc benzoate, 2-hydroxybenzoate and 2-acetylbenzoate analogues were both concentration- and time-dependent when compared to the control experiment (see Figures 2.9, 2.10). The three zinc benzoate analogues had similar cytotoxicity. In comparison to the reported concentration, 5-10mM, of 2-acetylbenzoic acid. We have found in this study that the minimum effective concentration of zinc 2-hydroxybenzoate is 0.2mM, or 25-50-fold less than previously been reported (5-10mM; Santini et al., 1999; Marra and Liao, 2001); hence, it may have a therapeutic potential. Zinc ion is an essential trace metal for various biological processes. Zinc, for example, functions as a cofactor for various enzymes, nuclear factors and hormones, hence it influences cell viability, proliferation, differentiation and cell death (Keen and Hurley, 1989; Falchuk, 1998; Chimienti et al., 2001). Zinc also acts as an antioxidant, due to protection of protein sulphydryl groups (Powell, 2000). The metabolically active cellular zinc pool is thereby controlled by the mechanism of action of the redox unit of the metallothionein/thionein couple, which works as a two-cluster network (Maret, 2000).

The results obtained from this study showed that zinc benzoate, zinc 2-hydroxybenzoate, and zinc 2-acetylbenzoate inhibited HT-1080 cell proliferation by about 90% at 0.4mM, and by about 70% at 0.2mM concentrations (see Figure 2.9, 2.10). The cytotoxic effect of zinc benzoate analogues on HT-1080 cells was also observed by direct cell count using a haemocytometer (see Figure 2.11), and by time-lapse tracking images (see Figure 2.13). The results of the three methods were consistent, indicating that zinc benzoate analogues have a greater cytotoxic effect on HT-1080 cells compared to other benzoate analogues (see Chapter 2). The cytotoxic effects of zinc-containing compounds have been verified in the literature. Gibson et al., (1985) showed that zinc pyrithione reduced the proliferation of hamster kidney cells (BHK 21)

above 0.1μg/ml. 0.4mM and 0.8mM Zinc sulphate (ZnSO$_4$) was also toxic to epithelial cells of the human intestinal cell line Caco-2 (Scarino *et al.*, 1992; Zödl *et al.*, 2003).

5.4 Appraisal of Apoptotic Potential of 2-Hydroxybenzoate Analogues

Physiological programmed cell death, or apoptosis, has significant virtues over necrotic cell death in therapy, and hence one of the strategies in designing and developing anticancer drugs is concentrated on compounds that can induce apoptosis. Our interest in this project was to investigate whether 2-hydroxybenzoate analogues could trigger apoptosis in HT-1080 fibrosarcoma cells. The MTT and other cell viability assays showed evidence of significant potential of cytotoxicity exerted by a number of 2-hydroxybenzoate analogues in HT-1080 cells (see Chapter 2). These mainly included zinc analogues. However, as indicated in the previous section, viability assays may not be powerful enough to reveal the apoptotic potential. Therefore, various analytical techniques were applied, including microscopic assessment of treated HT-1080 cells. Morphological cell changes induced by chemical agents can easily be detected under the light and fluorescent microscope, and enhanced with dyes and stains. This therefore allows subtle morphological changes to be visualised, and a definitive conclusion on the 2-hydroxybenzoate analogues' effect can be drawn. Although the morphological characteristics of apoptosis are distinctive under the microscope, staurosporine was also used as a positive apoptotic control in this study. Generally, results of the morphology (see Chapter 3) revealed definitive signs that 2-acetylbenzoic acid, calcium and zinc 2-hydroxybenzoates do indeed induce classical apoptosis. The morphological results obtained from DAPI, haematoxylin-eosin, methyl green pyronin, Annexin V and SEM (see Chapter 3) were consistent with the classical apoptotic signs illustrated in the literature, including blebbing of the cell membrane, appearance of apoptotic bodies,

and cell shrinkage (Wyllie, 1981; Smith *et al.*, 1990; Ruschoff *et al.*, 1998; Wong *et al.*, 1999; Stark *et al.*, 2001).

As indicated in Chapters 1-4, apoptosis occurs naturally, and it is part of normal physiological events such as embryogenesis (Schutte and Ramaekers, 2000). Apoptosis is an integral biological process necessary for the development and homeostasis of multicellular organisms (Zou *et al.*, 1997). Both extracellular (like TNF-α) or intracellular (accumulation of calcium for example) signalling induce apoptosis (Azmi *et al.*, 1992; Vaux *et al.*, 1996). Furthermore, several chemical compounds, such as 2-acetylsalicylic acid, induce apoptosis in gastric cancer cells (Wong *et al.*, 1999; Zhou *et al.*, 2001; 1999). Sodium 2-acetylbenzoate, for example, induces apoptosis in human myeloid leukaemia cell lines and vascular smooth muscle cells (Klampfer *et al.*, 1999; Marra *et al.*, 2000). In this study, the apoptotic effect of zinc 2-hydroxybenzoates and 2-acetylbenzoic acid were assessed at final concentrations of 0.1mM and 3.2mM, respectively (see Figures 4.10 and 4.11).

Several pathways for the effect of 2-acetylbenzoic acid and its benzoate analogues have appeared in the literature. These compounds modulate the cellular molecular biology, including mitogen-activated protein kinase (MAPK) signalling. 2-acetylbenzoates, for example, inhibit tumour necrotic factor (TNF)-induced extra cellular signal-regulated kinase (ERK) (Klampfer *et al.*, 1999). Law *et al.*, (2000) provided the first evidence for the effect of 2-acetylbenzoate on the mTOR/p70 pathway. They found that 2-acetylbenzoate inhibits p70^{S6K} activity and phosphorylation in a p38 MAPK-independent manner. The effect of 2-acetylbenzoate on caspase activation has also been studied in the literature. Pique *et al.*, (2000) indicated that 2-acetylbenzoic acid induces apoptosis through mitochondrial cytochrome c release and caspases 9, 3 and 8 in different cell lines (Jurkat, MOLT-4, Raji and HL-60). However, the mechanism leading to caspase activation remains unknown. Our results also showed that 0.4mM zinc 2-hydroxybenzoate and 3.2mM 2-acetylbenzoic acid induced apoptosis through caspase-3 activation (see Figure 4.11). The

apoptotic effects of these compounds were also confirmed flow-cytometrically by Annexin V (see Figure 4.10). Caspase-3 is an important protein involved in apoptosis of various cells, and the main effector of apoptosis (Thornberry and Lazebnik, 1998).

The accumulation of calcium inside the cell subsequently leads to the activation of the calcium/magnesium-dependent endonucleases. These enzymes are responsible for the induction of DNA fragmentation (Wyllie, 1980; Walker and Sikorska, 1997). Our results showed that calcium 2-hydroxybenzoate and other analogue treatments induced apoptosis (see Chapter 3). Generally, cationic metal ions, such as Ca^{2+}, and Zn^{2+}, are capable of forming various ionic bonds with a range of cellular molecules (with anionic counter ions) under a strict stereochemical and conformational set-up. Ionic bonding can occur, for example, with nucleic acids, which posses negative charges on the phosphate groups incorporated in both RNA and DNA. Proteins also posses negative charge capable of bonding with cations. Both aspartate and glutamate, for example, are negatively charged, and hence, cations brought into the cell may create ionic bonds with proteins containing negatively charged amino acid moieties. The elevation of cellular ions by the uptake of calcium or zinc 2-hydroxybenzoate could result in significant biological responses, such as triggering apoptosis, as revealed in the results. As indicated previously, metal ions act as cofactors necessary for protein function. A zinc finger, for example, is a small functionally important, independently folded domain that requires the coordination of a zinc ion to stabilise its structure. Folding of the zinc finger is vital in order for the enzyme to maintain its particular DNA, RNA and protein associations (Qian *et al.*, 1993a; 1993b). A good example of a protein containing zinc finger motifs is the Bcl-6 protein. It is a 706 amino acid nuclear protein containing six zinc fingers at its C-terminus and acts as a sequence-specific transcription repressor. Bcl-6 is expressed in most tissues and in many cell types *in vitro*. Its induction can completely suppress cell growth and triggers both cell-cycle arrest and apoptosis (Albagli, 1999). The mechanism by which it

induces apoptosis has not been elucidated. Elevated concentration of zinc ion may assist in the induction of Bcl-6, and consequently apoptosis (see also Chapter 1).

Our evidence for apoptosis triggered by 2-hydrohydroxybenzoate analogues was based on various techniques, including morphology and molecular measurements. Results were obtained from DAPI, methyl green/pyronin, haematoxylin and eosin, Annexin V immunolabelling, and scanning electron microscopy. The results from these techniques substantiate each other, and confirm the apoptotic signs such as blebbing, cell rounding and shrinking, as well as the increased presence of RNA in the cytoplasm, as shown by pyronin y staining. 0.4mM and 0.8mM 2-acetylbenzoic acid, and 0.4mM calcium 2-hydroxybenzoate, as shown by all five techniques, induced blebbing, apoptotic bodies, and other signs of morphological changes in apoptosis (see Figure 3.4-3.7). The quantitative analysis of early apoptosis activated by these two benzoates using Annexin-V indicated that both 0.4mM 2-acetylbenzoic acid and 0.4mM calcium 2-hydroxybenzoate induced significantly more apoptotic cells (16.5% and 25%, respectively) compared to the control samples (see Figure 3.5). Potassium and magnesium 2-hydroxybenzoates also induced apoptosis at 0.4mM concentration, and were significantly higher than the control by about 20.8 and 24.9%, respectively (see Figure 3.8).

A complex relationship exists between magnesium and cancer. There is a general notion that magnesium possesses anti-carcinogenic properties (Durlach et al., 1990). However, the preventive effects of magnesium exist only at the early stages of the carcinogenic process. A magnesium deficiency tends to increase the incidence of tumours in humans and animals, whilst excessive magnesium promotes the growth of pre-existing tumours due to the profound alterations of magnesium homeostasis in tumour cells (Hartwig, 2001). Magnesium may interfere with carcinogenesis through a variety of biochemical roles in the cell. Increased intracellular magnesium may act either as an anticancer or carcinogenic agent. This may explain the incidence of increased cell proliferation in

cells treated with 2-hydroxybenzoic acid magnesium salts. However, it is not clear whether only magnesium ions and/or 2-hydroxybenzoate play the significant role in promoting these biological activities.

The number of apoptotic cells labelled by Annexin V increased in a concentration- and time-dependent manner after treatment with zinc 2-hydroxybenzoate. At 0.3mM, the percentage of apoptotic cells was 59% compared to the control. This percentage increased to 81.65% when HT-1080 cells were exposed to 0.4mM zinc 2-hydroxybenzoate (see Figure 3.9). At the same concentration (0.4mM), but for a longer exposure time (48 hours), all HT-1080 cells were labelled by Annexin V, indicating that cells died by apoptosis (see Figure 3.9). The results also showed further morphological evidence for apoptosis, specifically through DAPI, methyl green/pyronin, haematoxylin and eosin, and scanning electron microscopy (see Figures 3.10-3.11).

The Annexin V and morphological evidence for apoptosis induced by zinc 2-hydroxybenzoate was also confirmed by flow cytometric measurement of Annexin V binding to phosphatidylserine. The effect of zinc 2-hydroxybenzoate was also concentration-dependent, 0.1mM induced 66.6% apoptosis, which increased to 72.3% and to 95.1%, upon increasing the zinc 2-hydroxybenzoate concentration to 0.2 and 0.4mM respectively. Furthermore, the changes in light scatter due to changes in cell morphology when exposed to cytotoxic agent also were used to quantify the apoptotic cells flow-cytometrically (Ferlini *et al.,* 1996; Pepper, 1999). The changes in the forward (F) and side (S) scattering characteristics (SC) measurements can be used to gate apoptotic cells. The quantification of apoptotic cells by light scattering and cells labelled by Annexin V showed a strong correlation between the two methods (r^2 =0.99), as calculated by linear regression (Pepper *et al.,* 1997; 1999). The results obtained from morphology and flow-cytometric measurement (labelled by PI and Annexin V) have clearly indicated that zinc 2-hydroxybenzoate induces apoptosis in HT-1080 treated for 24 hours. However, it is not clear whether the benzoate salt molecule, benzoate or

141

metal ions are responsible for the biological activities inducing apoptosis. Results obtained from the calcium or zinc benzoates uptake experiments were not enough to demonstrate which part of the 2-hydroxybenzoate is responsible for the biological activity. This could be due to either the insensitivity of the HPLC and atomic absorption used and/or the low concentrations of treated HT-1080 cell samples (see Figure 4.17, and Table 4.4). Although the results presented here have demonstrated the cytotoxic effect of both calcium and zinc 2-hydroxybenzoate, it is possible that the effect may be attributed to the metal ions. Indeed, the simple zinc (II) salts, such as zinc chloride (Berger et al., 2004; our laboratory) and zinc sulphate (Zödl et al., 2003), reduced cell proliferation in a concentration-dependent way. In contrast, the 2-hydroxybenzoic acid was found not to be cytotoxic to HT-1080 cells at 0.4mM or less (see Chapter 2). Apoptosis can be trigged by the elevation of intracellular calcium ion which is necessary to activate the calcium/magnesium-dependent endonuclease responsible for DNA fragmentation (Wyllie, 1980). On the other hand, the increase in intracellular zinc inhibits DNA fragmentation, in part by inhibiting the calcium/magnesium-dependent endonuclease (Cohen and Duke, 1984; Lohmann and Beyersmann, 1993). Other studies have indicated that depletion (by chelating agents) of intracellular zinc in many cell types promote apoptosis (Zalewski et al., 1993; Parat et al., 1997; Ahn et al., 1998) through caspase-3 (Perry et al., 1997) and TNF-α (Vaux and Strasser, 1996) upregulation. However, in this study, zinc 2-hydroxybenzoate was found to induce apoptosis by upregulating caspase-3 at moderate concentrations (0.1-0.4mM; see Figure 4.10; Chapter 4).

5.5 Appraisal of Effect of 2-Hydroxybenzoate Analogues on Molecular Expression

In addition to the apoptotic evidence demonstrated by morphological and immunocytochemical investigations, some molecular investigations were also conducted to establish the mechanism of the apoptotic action for 2-hydroxybenzoate analogues. In this study, the expression of various key

142

proteins responsible for the regulation of physiological cell death by apoptosis was investigated, using Western blot. They included both pro apoptotic proteins, such as p53, p21, Bax, and TNF-α, and the anti apoptotic proteins, Bcl-2, as well as the expression of histones was also investigated. The expression of genes such as caspases, p53, Bcl-2 family proteins, and p21 has been demonstrated to occur in the process of apoptosis (Huang and Strasser, 2000; Mayer *et al.*, 2003). Caspase-3, upon activation, is a significant downstream executioner in apoptosis, responsible for the cleavage of a number of substrates such as poly (ADP-ribose) polymerase (PARP), D4-GDI, and lamin A (Lee *et al.*, 2003). *p21* is a downstream gene regulated by *p53* gene, and both p21-dependent and independent apoptosis have been identified (Tsao *et al.*, 1998; Yoneda *et al.*, 1998; Kuo *et al.*, 2002). Induction of p21 altered the progression of cell cycle and arrested cells at the G1 phase through blocking CDK4 activity, and promoted the occurrence of apoptosis (El-Deiry *et al.*, 1993). Additionally, activation of proapoptotic Bcl-2 family proteins such as Bax and Bad or inactivation of antiapoptotic Bcl-2 family proteins such as Bcl-2 and Mcl-1, have been shown to regulate the intrinsic apoptosis pathway (Green, 2000; Reed *et al.*, 2000). Their expression is variable in normal and neoplastic human tissues, and their biological significance depends on the site of and type of tissue (Soini *et al.*, 1999).

It is evident from the literature that 2-acetylbenzoic acid and other NSAIDs induce apoptosis and inhibit cellular proliferation (Sebolt-Leopold *et al.*, 1999; Wong *et al.*, 1999; Pique *et al.*, 2000; Husain *et al.*, 2001). The mechanism of 2-acetylbenzoic acid action is associated with the inhibition of cylooxygenase responsible for the synthesis of prostaglandin by acetylation of serine-530 in Cox-1 but not Cox-2 (Elder and Paraskeva, 1998; Shiff and Rigas, 1999 Williams *et al.*, 1999). This explains the anti-inflammatory effect of 2-acetylbenzoic acid, but how is this related to its anti-neoplastic properties? Many tumours contain high concentrations of prostaglandins (PGs), which promote angiogenesis, but more importantly, cellular proliferation and tumour growth (Munkarah *et al.*, 2002). Although

the exact mechanisms by which Cox-2 contributes to carcinogenesis, and thus the anti- neoplastic properties of NSAIDs as Cox-2 inhibitors is not known, it is probable that increased Cox-2 expression in tumours increases prostaglandin and cellular proliferation of the cancer cells by default. However, Munkarah (2002) suggested an alternative mechanism, and raises the important point that Cox-2 over-expression in tumour cells is associated with the reduction in apoptosis, probably mediated through an alteration in the balance between Bcl-2 and Bax, resulting in an increase in the ratio of Bcl-2 to Bax in these cells, thus inhibiting apoptosis. According to Jaattela (1999) and others (Oltvai et al., 1993; Sedlak et al., 1995; Reed, 2000), the Bcl-2/Bax ratio reflects cell sensitivity to apoptotic stimuli. A high Bcl-2/Bax ratio is linked to poor prognosis and a high histological tumour grade (Brambilla et al., 1996; Gazzaniga et al., 1996) whereas a low Bcl-2/Bax ratio is associated with a favourable histological grade and a better patient outcome in combination with a lack of relapse and sensitivity to chemotherapy (Aguilar-Santelises et al., 1996; Chresta et al., 1996; Gazzaniga et al., 1996). In this respect, the results here showed that the ratio of Bcl-2 to Bax decreased upon exposing HT-1080 cells to 2-acetylbenzoic acid (1:1.66) or calcium 2-hydroxybenzoate (1:4.19) at 0.2mM and 24 hours incubation. Furthermore, the results in this study indicated that the ratio increased in a concentration dependent manner at 0.05mM and 0.4mM, indicating that apoptosis may be preceded via the Bax promoting effect (see Table 4.5; Chapter 4). A study by Zhou et al., (2001) confirmed that the induction of apoptosis was mediated through Bax over expression without changes in Bcl-2 expression.

In contrast, the ratio of Bcl-2 to Bax increased in the case of zinc 2-hydroxybenzoate treated HT-1080 cells at the same concentrations and incubation times. Results also indicated that the ratio increased in a concentration dependent manner from 1:0.57 at 0.05mM exposure to 1:0.83 at 0.4mM and both concentrations expressed Bcl-2 more than Bax (see Table 4.5; Chapter 4). The effect of zinc 2-hydroxybenzoate on the expression of Bcl-2/Bax proteins suggests that HT-1080 cell's biological

characteristics have to be explained with other mechanisms that could counteract the pro-apoptotic effects of Bax. Fukamachi *et al.,* (1998) reported an increase of the Bcl-2/Bax ratio by 1mM cupper sulphate treated U937 cells at 4 hours incubation but suppressed hydrogen peroxide induced apoptosis. Furthermore, Vaux *et al.,* (1992) reported that Bcl-2 did not prevent apoptosis in targeted cells exposed to cytotoxic T cells. The results above imply that the mechanism underlining the induction of apoptosis exists in multiple pathways. Not all of them necessarily involve genetic control but may well share some signals and/or intermediate steps.

In addition to the association between Bcl-2 and Bax, the balance between Bcl-2 and p53 is important in assessing the apoptotic effect of 2-hydroxybenzoates. 2-acetylbenzoic acid increased the Bcl-2:p53 ratio at both 0.05mM and 0.4mM. However, both calcium and zinc 2-hydroxybenzoates decreased the ratio in treated HT-1080 cells at the same concentrations. The same pattern of Bax and p53 protein regulations we also observed in HT-1080 cells treated at 0.05mM and 0.4mM and incubated for 24 hours (see Table 4.5; Chapter 4). Findley *et al.,* (1997) found that the Bcl-2 expression was p53-dependent in 18 pediatric acute lymphoblastic leukemia cells after exposure to ionizing radiation. Furthermore, earlier studies also found an inverse correlation between the expression of the Bcl-2 and p53 proteins, where Bcl-2 was decreased in several breast cancer cells and non-Hodgkin's lymphoma (Pezzella *et al.,* 1993; Haldar *et al.,* 1994).

The apoptotic action of 2-acetylbenzoic in gastric cancer cell lines AGS (wild-type p53) and MKN-28 (mutant p53) showed the increase of caspases-3, Bax and Bad activity (Zhou *et al.,* 2001). In the current study the expression of caspase-3 was increased dramatically when HT-1080 cells were exposed to 0.4mM zinc 2-hydroxybenzoate for 24 hours. In contrast, a similar increase in the expression of caspase-3 was obtained during the same exposure period by at higher concentration (3.2mM). In this respect, the measured apoptosis through caspase-3 activation was

99.8% for 0.4mM zinc 2-hydroxybenzoate, and 87.05% for 3.2mM 2-acetylbenzoic acid (see Figure 4.11).

Caspases play a central role in the execution of apoptosis. The two most well studied pathways of caspase activation in cells include a surface death receptor and the mitochondrial initiated pathway. There is the potential that aspirin may activate the latter, with little or no evidence suggesting aspirin can trigger caspase activation through the cell surface death receptors. Pique *et al.*, (2000) demonstrated that aspirin is taken up into the cell, where it subsequently induces caspase activation through cytochrome c release from the mitochondria, preceding the loss of mitochondrial membrane potential and the subsequent activation of caspases 9, 3 and 8.

Our results clearly indicated that 2-acetylbenzoic acid, calcium 2-hydroxybenzoate and zinc 2-hydroxybenzoate have increased the expression of p53, p21, Bax, histones and TNF-α in HT-1080 at both 0.05mM and 0.4mM, and for 24 hours' exposure. However, the effects for the expression of these proteins were different in term of concentration. 2-acetylbenzoic acid treatments, for example was not concentration-dependent, while the effect of most calcium 2-hydroxybenzoate and zinc 2-hydroxybenzoate treatments was concentration dependent (see Chapter 4; Figures 4.12-4.16, and Section 4.4).

5.6 Conclusions

The results presented in this thesis indicate that 2-hydroxybenzoates can reduce proliferation of HT-1080 cells, most likely through the induction of apoptosis. The apoptosis was exclusively confirmed by various morphological and biochemical techniques. This thesis also presents definitive evidence to show that cell death was trigged by a lower concentration (0.4mM) of 2-acetylbenzoic acid than has been commonly used in the literature (5-10mM). Also, modification of the 2-acetylbenzoic

acid structure has been successful in introducing a new potential anticancer drug zinc 2-hydroxybenzoate.

Data presented here indicated that 2-acetylbenzoic acid, calcium 2-hydroxybenzoate and zinc 2-hydroxybenzoate at 0.4mM exhibit different effects on the expression of investigated proteins (see summary of Western blot results, Table 4.4). This may indicate that the three 2-hydroxybenzoate analogues exert different mechanisms of action to induce apoptosis, although this will need to be further investigated (see Chapters 3 and 4). The ratio between Bax (apoptotic promoter) and Bcl-2 (apoptotic inhibitor) for both 2-acetylbenzoic acid and calcium 2-hydroxybenzoate at 0.4mM concentration were 1.7:1 and 4.2:1 respectively. The interaction between pro- and anti-apoptotic members set the threshold that determines whether a cell should die or not (Fleischer *et al.*, 2003; Tsujimoto, 2003). Bax and Bcl-2 belong to the Bcl-2 family, which encompasses three subfamilies: the anti-apoptotic Bcl-2 (Bcl-2, Bcl-XL, Bcl-W, Mcl-1), the pro-apoptotic BH3 (Bad, Bik, Bid, Bik), and the pro-apoptotic Bax (Bax, Bak, Bok). These proteins are found in many parts of the cell, but their association with mitochondria has become a centre of various investigations (Green and Reed, 1998). Bcl-2 family members appear to regulate the release of cytochrome c from mitochondria, which acts in concert with specific downstream factors, like caspases, to induce apoptosis. Thus the induction of apoptosis by 2-acetylbenzoic acid and calcium 2-hydroxybenzoate may take place through the downstream activities of Bax and caspase-3. Both 2-acetylbenzoic acid and calcium 2-hydroxybenzoate also increased the expression of histones, p53, p21 (but not in 2-acetylbenzoic acid) and TNF-α proteins at 0.4mM concentration.

In contrast, the apoptotic effect of 0.4mM zinc 2-hydroxybenzoate appears to proceed not *via* the Bcl-2 family pathway, as the ratio of Bax/Bcl-2 expression was 1:1.2, and both proteins were higher than in the control samples. Treatment of HT-1080 cells with zinc 2-hydroxybenzoate also induced p21 and p53, histones and TNF-α, which may explain the

complex cytotoxic effects on the downstream events of apoptotic cell death.

Finally, it is still not clear whether the metal ions, the 2-hydroxybenzoate, or the combination of the two are causing the apoptosis in HT-1080. Unfortunately, attempts to clarify this point by both HPLC and Atomic Absorption spectroscopy did not reveal any answer, owing to both instrumental insensitivity and low concentrations of both the 2-hydroxybenzoates and the metal ions, respectively.

References

References

Aas AT, Tonnessen TI, Brun A and Salford LG (1995). Growth inhibition of rat glioma cells in vitro and in vivo by aspirin. *J Neurooncol*, **24**, 171-180.

Ackerknecht EH (1973). *Therapeutics: from the primitives to the twentieth century*. Hafner Press, New York.

Adam-Klages S, Schwandner R, Luschen S, Ussat S, Kreder D and Kronke M (1998). Caspase-mediated inhibition of human cytosolic phospholipase A2 during apoptosis. *Immunology*, **15**, 5687-5694.

Adams JM and Cory S (1998). The Bcl-2 protein family: Arbiters of cell survival. *Science*, **281**, 1322-1326.

Aguilar-Santelises M, Rottenberg ME, Lewin N, Mellstedt H and Jondal M (1996). Bcl-2 Bax and p53 expression in B-CLL in relation to in vitro survival and clinical progression. *Int J Cancer*, **69**, 114-119.

Ahn YH, Kim YM, Hong SM and Koh JY (1998). Depletion of intracellular zinc induces protein synthesis-dependent neuronal apoptosis in mouse cortical culture. *Exp Neurol*, **154**, 47-56.

Albagli O, Lantoine D, Quief S, Quignon F, Englert C, Kerckaert J-P, Montarras D, Pinset C and Lindon C (1999). Overexpressed Bcl6 (LAZ3) oncoprotein triggers apoptosis, delays S phase progression and associate with replication foci. *Oncogene*, **18**, 5063-5075.

Albino AP, Juan G, Traganos F, Reinhart L, Connolly J, Rose DP and Darzynkiewicz Z (2000). Cell Cycle Arrest and Apoptosis of Melanoma Cells by Docosahexaenoic Acid: Association with Decreased pRb Phosphorylation. *Cancer Research*, **60**, 4139-4145.

Al-Hazzaa AA and Bowen ID (1998). Improved cytochemical methods for demonstrating cell death using LR White as an embedding medium. *Histochem J*, **30**, 897-902.

Amborabé B-E, Fleurat-Lessard P, Chollet J-F and Roblin G (2002). Antifungal effects of salicylic acid and other benzoic acid derivatives towards *Eutypa lata*: structure–activity relationship. *Plant Physiol Biochem*, **40**, 1051-1060.

Archer SY and Hodin RA (1999). Histone Acetylation and Cancer. *Current Opinion in Genetics and Development*, **9**, 171-174.

Arends MJ and Wyllie AH (1991). Apoptosis: mechanisms and roles in pathology. *Inter. Rev. Experim. Pathol*, **32**, 223-254.

Azmi S, Dhawan D and Singh N (1996). Calcium ionophore A 23187 induces apoptotic cell death in rat thymocytes. *Cancer Lett*, **107**, 97-103.

Bancroft JD and Stevens A (Eds.) (1977). *Theory and practice of histological techniques*, Churchill Livingstone, Edinburgh, London, and New York, 85-94.

Barrett KL, Willingham JM, Garvin AJ and Willingham MC (2001). Advances in Cytochemical Methods for Detection of Apoptosis. *J. Histochem and Cytochem*, **49** (7), 821-832.

Bartek J, Bartkova J and Lukas J (1996). The retinoblastoma protein pathway and the restriction point. *Curr Opin Cell Biol*, **8**, 805-814.

Baserga R (1985). *The Biology of Cell Reproduction*. Cambridge, MA:Harvard University Press.

Bellosillo B, Pique M, Barragan M, Castano E, Villamor N, Colomer D, Montserrat E, Pons G and Gil J (1998). Aspirin and salicylate induce apoptosis and activation of caspases in B-cell chronic lymphocytic leukemia cells. *Blood*, **92**, 1406-1414.

Benz J and Hofmann A (1997). Annexins: from structure to function, *Biol Chem*, **378**,177-183.

Berger M, Rubinraut E, Barshack I, Roth A, Keren G and George J (2004). Zinc reduces intimal hyperplasia in the rat carotid injury model. *Atherosclerosis*, **175**, 229-234.

Beyersmann D and Haase H (2001). Functions of zinc in signalling, proliferation and differentiation of mammalian cells. *BioMetals*, **14**, 331-341.

Blagosklonny MV and Pardee AB (2002). The restriction point of the cell cycle. *Cell Cycle*, **1**, 103-110.

Bowen ID and Ryder TA (1976). Use of the p-nitrophenyl phosphate method for the demonstration of acid phosphatase during starvation and cell autolysis in the planarian *Polycelis tenuis Iijima*. *Histochemistry J*, **8**, 319-329.

Bowen ID (1984). Laboratory techniques for demonstrating cell death. In *Cell Ageing and Cell Death*.Vol. 25, Davies I, Sigee D, (Eds): Cambridge University Press, Cambridge, 1-38.

Bowen ID, Morgan SM and Mullarkey K (1993). Cell death in the salivary glands of metamorphosing Calliphora vomitoria. *Cell Biol Int*, **17**, 13-33.

Bowen ID, Morgan SM and Mullarkey K (1996). Programmed cell death in the salivary gland of the blow fly Calliphora vomitoria. *Microsc Res Tech*, **34**, 202-217.

Bowen ID, Bowen SM and Jones A (1997). *Mitosis and Apoptosis - Matters of Life and Death*. Chapman and Hall, London.

Bowen ID (1999). *Methods in Aging Research*. CRC Press, London.

Brambillà E, Negoescu A, Gazzeri S, Lantuejoul S, Moro D, Brambilla C and Coll JL (1996). Apoptosis-related factors p53, Bcl_2 and Bax in neuroendocrine lung tumors. Am J Pathol, **149**, 1941-1952.

150

Brooks G, Yu XM, Wang Y, Crabbe MJ, Shattock MJ and Harper JV (2003). Non-steroidal anti-inflammatory drugs (NSAIDs) inhibit vascular smooth muscle cell proliferation via differential effects on the cell cycle. *J Pharm Pharmacol*, **55** (4), 519-26.

Brown S, *Otorhinolaryngology, Head and Neck Surgery: 7th edition.*

Brugarolas J, Chandrasekaran C, Gordon JI, Beach D, Jacks T and Hannon GJ (1995). Radiation-induced cell cycle arrest compromised by p21 deficiency. *Nature*, **377**, 552-557.

Carmichael J, DeGraff WG, Gazdar AF, Minna JD and Mitchell JB (1987). Evaluation of a tetrazolium-based semiautomated colorimetric assay: assessment of chemosensitivity testing. *Cancer Research*, **47** (4), 936-942.

Carmichael J, Mitchell JB, DeGraff WG, Gamson J, Gazdar AF, Johnson BE, Glatstein E and Minna JD (1988). Chemosensitivity testing of human lung cancer cell lines using the MTT assay. *British J Cancer*, **57** (6), 540-547.

Carnero A (2002).Targeting the cell cycle for cancer therapy. *British J Cancer*, **87**,129-33.

Charles S (2004). Cell-cycle Targeted Therapies. *The Lancet Oncology*, **5**, 27-36.

Chen JH and Ho C-T (1997). Antioxident activities of caffeic acid and its related hydroxycinnamic acid compounds. *J Agric Food Chem*, **45**, 2374-2378.

Chen Y, Knudsen ES and Wang JYJ (1996). Cells Arrested in G1 by the v-Abl Tyrosine Kinase Do Not Express Cyclin A Despite the Hyperphosphorylation of RB. *J Biological Chemistry*, **271**, 19637-19640.

Chimienti M, Richard S, Mathieu J and Favier A (2001). Role of cellular zinc in programmed cell death: temporal relationship between zinc depletion, activation of caspases, and cleavage of Sp family transcription factors. *Biochem Pharmacol*, **62**, 51-62.

Choi DW (1988). Glutamate neurotoxicity and diseases of the nervous system. *Neuron*, **1**, 623-634.

Choi DW (1995). Calcium still center-stage in hypoxic-ischemic neuronal death. *Trends Neurosci*, **18**, 58-60.

Chresta CM, Masters JRW and Hickman JA (1996). Hypersensitivity of testicular tumors to etoposide-induced apoptosis is associated with functional p53 and high bax/bcl-2 ratio. *Cancer Res*, **56**, 1834-1841.

Chung W, Jung Y, Surh Y, Lee S and Park K (2001). Antioxidative and antitumour promoting effects of [6]-paradol and its homologs. *Mutation Research*, **496**, 199-206.

Claudia O (2003). Aspirin protects against cancer of the upper aerodigestive tract. *The Lancet Oncology*, **4**, 200-200.

Cohen JJ and Duke RC (1984). Glucocorticoid activation of a calcium-dependent endonuclease in thymocyte nuclei leads to cell death. *J Immunol*, **132**, 38–42.

Cole SPC (1986). Rapid chemosensitivity testing of human lung tumor cells using the MTT assay. *Cancer Chemotherapy and Pharmacology*, **17**, 259-263.

Cory AH, Owen TC, Barltrop JA and Cory JG (1991). Use of an aqueous soluble tetrazolium/formazan assay for cell growth assays in culture. *Cancer Commun*, **3**, 207-12.

Cuvelier ME, Berset C and Richard H (1996). Antioxidative activity and phenolic composition of pilot-plant and commercial extracts of sage and rosemary. *J Am Oil Chem Soc*, **73**, 645-652.

Dalton S (1992). Cell cycle regulation of the human cdc2 gene. *EMBO J*, **11**, 1797-1804.

Daniel WN (2002). Transcription factors and cancer: an overview. *Toxicology*, **181-182**, 131-141.

Dawson TM and Snyder SH (1994). Gases as biological messengers: nitric oxide and carbon monoxide in the brain. *J Neurosci*, **14**, 5147–5159.

Deng C, Zhang P, Harper JW, Elledge SJ and Leder P (1995). Mice lacking p21CIP1/WAF1 undergo normal development, but are defective in G1 checkpoint control. *Cell*, **82**, 675-84.

Denmeade SR and Issacs JT (1996). Programmed Cell Death (Apoptosis) and Cancer Chemotherapy. *Cancer Control*, **3**, 306-309, www.moffitt.usf.edu/cancjrnl/v3n4/article1. html.

Dennis WR (1998). *Introduction to Oncogenes and Molecular Cancer Medicine*. Springer-Verlag, New York.

Dewick PM (2002). *Medicinal Natural Products: A Biosynthetic Approach*. 2nd edition. John Wiley and Sons, London.

Diffley and Evan. (2000). Oncogenes and cell proliferation. Cell cycle, genome integrity and cancer - a millenial view. *Curr Opinion in Genetics & Development*, **10**, 13-16.

Dizdaroglu M, Jaruga P, Birincioglu M and Rodriguez H (2002). Free radical-induced damage to DNA: mechanisms and measurement. *Free Radical Biology and Medicine*, **32**, 1102-1115.

Drachenberg CB, Ioffe OB and Papadimitriou JC (1997). Progressive increase of apoptosis in prostatic intraepithelial neoplasia and carcinoma: comparison between *in situ* end-labeling of fragmented DNA and detection by routine hematoxylin-eosin staining. *Arch Pathol Lab Med*, **121**, 54-58.

Durlach J, Bara M and Guiet-Bara A (1990). Magnesium and its relationship to oncology, in Sigel, H and Sigel, A (Eds), *Metal Ions in Biological Systems*. Marcel Dekker, New York, 549-578.

Durner J, Shah J and Klessig DF (1997). Salicylic acid and disease resistance in plants. *Trends Plant Sci*, **2**, 266-274.

Duvall E, Wyllie AH and Morris RG (1985). Macrophage recognition of ells undergoing programmed cell death (apoptosis). *Immunology*, **56**, 351-358.

Duvall E and Wyllie AH (1986). Death and the cell. *Immun Today*, **7**, 115-119.

El Deiry WS, Tokino T, Velculescu VE, Levy DB, Parsons R, Trent JM, Lin D, Mercer WE, Kinzler KW and Vogelstein B (1993). WAF1, a potential mediator of p53 tumor suppression. *Cell*, **75**, 817-825.

El Deiry WS, Harper JW, O'Connor PM, Velculescu VE, Canman CE, Jackman J, Pietenpol JA, Burrell M, Hill DE and Wang Y (1994). WAF1/CIP1 is induced in p53-mediated G1 arrest and apoptosis. *Cancer Res*, **54**,1169-1174.

Elder DJ, Hague A, Hicks DJ and Paraskeva C (1996). Differential growth inhibition by the aspirin metabolite salicylate in human colorectal tumor cell lines: enhanced apoptosis in carcenoma and in vitro-transformal adenoma relative to adenoma cell lines. *Cancer Res*, **56**, 2273-2276.

Elder DJ and Paraskeva C (1998). COX-2 inhibitors for colorectal cancer. *Nat Med*, **4**, 393-393.

Elias JM (1969). Effects of temperature poststaining rinses and ethanol-butanol dehydrating mixtures on methyl green pyronin y staining. *Stain Technology*, **44**, 201-204.

Evan G and Littlewood T (1998). A matter of life and death, *Science*, **281**, 1317-1322.

Fadok VA, Voelker DR, Cambell PA, Cohen JJ, Bratton DL and Henson PM (1992). Exposure of phosphatidylserine on the surface of apoptotic lymphocytes triggers specific recognition and removal by macrophages. *J Immun*, **148**, 2207-2216.

Falchuk KH (1998). The molecular basis for the role of zinc in developmental biology. *Mol Cell Biochem*, **188**, 41-48.

Fantl V, Stamp G, Andrews A, Rosewell I and Dickson C (1995). Mice lacking cyclin D1 are small and show defects in eye and mammary gland development, *Genes Dev*, **9**, 2364-2372.

FDA (Food and Drug Administration) (1973). *Evaluation of the Health Aspects of Benzoic Acid and Sodium Benzoate as Food Ingredients.* DHEW, Washington, DC. Report No. SCOGS-7. NTIS PB-223 837/6.

Feeney GP, Errington RJ, Wiltshire M, Marquez N, Chappell SC and Smith PJ (2003). Tracking the cell cycle origins for escape from topotecan action by breast cancer cells. *British Journal of Cancer*, **88**, 1310-1317.

Ferlini C, Cesare SD, Rainaldi G, Malorni W, Samoggia P, Bisseli R and Fatorossi A (1996). Flow cytometry analysis of the early phases of apoptosis by cellular and nuclear techniques. *Cytometry*, **24**, 106-115.

Fernandez-Segura E, Garcia JM and Campos A (1990). Scanning electron microscopic study of natural killer cell-mediated cytotoxicity. *Histol Histopathol*, **5**, 305-310.

Findley HW, Gu L, Yeager AM and Zhou M (1997). Expression and regulation of Bcl-2, Bcl-xl, and Bax correlate with p53 status and sensitivity to apoptosis in childhood acute lymphoblastic leukemia. *Blood*, **89**, 2986-93.

Fleischer A, Rebollo A and Ayllon V (2003). BH3-only proteins: the Lords of death. *Archivum Immunolog. Therapiae Experiment*, **51**, 9-17.

Frantz B and O'Neill EA (1995). The effect of sodium salicylate and aspirin on NF-κB. *Science*, **270**, 2017-2018.

Fukamachi Y, Karasaki Y, Sugiura T, Itoh H, Abe T, Yamamura K and Higashi K (1998). Zinc Suppresses Apoptosis of U937 Cells Induced by Hydrogen Peroxide through an Increase of the Bcl-2/Bax Ratio. *Biochemical and Biophysical Research Communications*, **246**, 364-369.

Fujino M, Li XK, Guo L, Amano T and Suzuki S (2001). Activation of caspases and mitochondria in FTY720-mediated apoptosis in human T cell line Jurkat, *International Immunopharmacology*, **1**, 2011-2021.

Funkhouser EM, and Sharp GB (1995). Aspirin and reduced risk of esophageal carcinoma. *Cancer*, **76**, 1116-1119.

Gallant P and Nigg EA (1992). Cyclin B2 undergoes cell cycle-dependent nuclear translocation and, when expressed as a non-destructible mutant, causes mitotic arrest in HeLa cells. *J Cell Biol*, **117**, 213-224.

Gallant P and Nigg EA (1994). Identification of a novel vertebrate cyclin: cyclin-B3 shares properties with both A- and B-type cyclins. *EMBO J*, **13**, 595-605.

Gazzaniga P, Gradilone A., Vercillo R, Gandini P, Silvestri I, Napolitano M, Vincenzoni A, Gallucci M and Agliano AM (1996). Bcl-2/bax mRNA expression ratio as prognostic factor in low-grade urinary bladder cancer. *Int J Cancer* **69**, 100-104.

Geng Y, Whoriskey W, Park MY, Bronson RT, Medema RH, Li T, Weinberg RA and Sicinski P (1999). Rescue of cyclin D1 deficiency by knocking cyclin E. *Cell*, **97**, 767-777.

Giaccia AJ and Kastan MB (1998). The complexity of p53 modulation: emerging patterns from divergent signals. *Genes Dev*, **12**, 2973-2983.

Gibson WT, Hardy WS and Groom MH (1985). The effect and mode of action of zinc pyrithione on cell growth. II. In vivo studies. *Food Chem Toxicol*, **23**, 103-110.

Goel A, Chang DK, Ricciardiello L, Gasche C and Boland CR (2003). A novel mechanism for aspirin-mediated growth inhibition of human colon cancer cells. *Clin Cancer Res*, **9**, 383-390.

Gong JG, Costanzo A, Yang HQ, Melino G, Kaelin WG Jr, Levrero M and Wang JY (1999). The tyrosine kinase c-Abl regulates p73 in apoptotic response to cisplatin-induced DNA damage. *Nature*, **399**, 806-809.

Gougeon ML and Montagnier L (1993). Apoptosis in AIDS. *Science*, **260**, 1269-1270.

Grana X and Reddy EP (1995). Cell cycle control in mammalian cells: role of cyclins, cyclin dependent kinases (CDKs), growth suppressor genes and cyclin-dependent kinase inhibitors (CKIs). *Oncogene*, **11**, 211-219.

Green DR (2000). Apoptotic pathways: paper wraps stone blunts scissors. *Cell*, **102**, 1-4.

Green DR and Reed JC (1998). Mitochondria and apoptosis. *Science*, **281**, 1309-1312.

Gregorc A and Bowen ID (1997). Programmed cell death in the honey-bee (Apis Mellifera L.) larvae midgut. *Cell Biol Int*, **21**, 151-158.

Haldar S, Negrini M, Monne M, Sabbioni S and Croce CM (1994). Down-regulation of Bcl-2 by p53 in breast cancer cells. *Cancer Research*, **54**, 2095-2097.

Halliwell B and Gutteridge JMC (1990). Role of free radicals and catalytic metal ions in human disease: an overview. *Methods Enzymol*, **186**, 1-85.

Hall C, Nelson DM, Ye X, Baker K, DeCaprio JA, Seeholzer S, Lipinski M and Adams PD (2001). HIRA, the human homologue of yeast Hir1p and Hir2p, is a novel cyclin-cdk2 substrate whose expression blocks S-phase progression. *Mol Cell Biol*, **21**, 1854-1865.

Hamatake M, Iguchi K, Hirano K and Ishida R (2000). Zinc induces mixed types of cell death, necrosis, and apoptosis, in molt-4 cells. *J Biochem (Tokyo)*, **128**, 933-939.

Hammond-Kosack KE and Jones JDG (1996). Resistance gene–dependent plant defence responses. *Plant Cell*, **8**, 1773-1791.

Hanahan D and Weinberg RA (2000). The hallmarks of cancer. *Cell*, **100**, 57-70.

Harrington EA, Fanidi A and Evan GI (1994). *Oncogenes and cell death. Curr Opin Genet Dev*, **4**, 120-129.

Harris RE, Namboodiri KK, Stellman SD and Wynder EL (1995). Breast cancer and NSAID uses: Heterogeneity of effect in a case-control study. *Prev Med*, **24**, 119-120.

Hartwig A (2001). Role of Magnesium in genomic stability. *Mutation Resarch*, **475**, 113-121.

Hector AA, Suzane I, Williams SR, Denis C and Jeanne LB (2001). Aspirin effects on endometrial Cancer Cell Growth. *Obstetrics and Gynecology*, **97**, 423- 427.

Heichman KA and Roberts JM (1994). Rules to replicate by cell. *Cell*, **79**, 557-561

Hinchdiffe EH and Gluder G (2001). "It Takes Two to Tango": understanding how centrosome duplication is regulated throughout the cell cycle. *Genes Dev*, **15**, 1167-1181.

Hollstein M, Rice K, Greenblatt MS, Soussi T, Fuchs R, Sorlie T, Hovig E, Smith-Sorensen B, Montesano R and Harris CC (1994). Database of p53 gene mutations in human tumors and cell lines. *Nucleic Acids Res*, **22**, 3551-3555.

Huang DC and Strasser A, (2000). BH3-Only proteins-essential initiators of apoptotic cell death. *Cell*, **103**, 839-842.

Husain SS, Szabo IL, Pai R, Soreghan B, Jones MK and Tarnawski AS (2001). MAPK (ERK2) kinase- a key target for NSAIDs-induced inhibition of gastric cancer cell proliferation and growth. *Life Sciences*, **69**, 3045-3054.

Huveneers-Oorsprong MBM, Hoogenboom LAP and Kuiper HA (1997). The Use of the MTT Test for Determining the Cytotoxicity of Veterinary Drugs in Pig Hepatocytes. *Toxicology in Vitro*, **11**, 385-392.

Hyrc K, Handran SD, Rothman SM and Goldberg MP (1997). Ionized intracellular calcium concentration predicts excitotoxic neuronal death: observations with low-affinity fluorescent calcium indicators. *J Neurosci*, **17**, 6669-6677.

Ishihara K, Horiguchi K, Yamagishi N and Hatayama T (2003). Identification of sodium salicylate as an hsp inducer using a simple screening system for stress response modulators in mammalian cells. *Eur J Biochem*, **270**, 3461-3468.

Jaattela M (1999). Escaping cell death: survival proteins in cancer. *Exp Cell Res*, **248**, 30–43.

Jackman M, Firth M and Pines J (1995). Human cyclins B1 and B2 are localized to strikingly different structures: B1 to microtubules, B2 primarily to the Golgi apparatus. *EMBO J*, **14**, 1646-1654.

Jacks T and Weinberg RA (1996). Cell-cycle control and its watchman. *Nature*, **381**, 643-644.

Janicke RU, Sprengart ML, Wati MR and Porter AG (1998). Caspase-3 is required for DNA fragmentation and morphological changes associated with apoptosis. *J Biol Chem*, **273**, 9357-9360.

Jiang X and Wang X (2000). Cytochrome c promotes caspase-9 activation by inducing nucleotide binding to Apaf-1. *J Biol Chem*, **275**, 31199-31203.

Jurgensmeier JM, Xie ZH, Deveraux Q, Ellerby L, Bredesen D and Reed JC (1998). Bax directly induces release of cytochrome c from isolated mitochondria. *Pro Natl Acad Sci, USA*, **95**, 4997-5002.

Karlsson JO, Ostwald K, Kabjorn C and Andersson M (1994). A method for protein assay in Laemmli buffer. *Anal Biochem*, **219**, 144-146.

Kastan MB, Onyekwere O, Sidransky D, Vogelstein B and Craig RW (1991). Participation of p53 protein in the cellular response to DNA damage. *Cancer Research*, **51**, 6304-6311.

Keen CL and Hurley LS (1989). Zinc and reproduction: *effects of deficiency on fetal and postnatal development. In:* Mills C F (Ed.), *Zinc in Human Biology*. Springer-Verlag, London, 183-200.

Kerr JFR, Searle J, Harmon BV and Bishop CJ (1987). Apoptosis. In: Potten CS (Ed.), *Perspectives on mammalian cell death*, Oxford University Press, Oxford, 93-128.

Kerr JFR, Winterford CM and Harmon BV (1994). Apoptosis. Its significance in cancer and cancer therapy. *Cancer*, **73**, 2013-2026.

Kerr JFR, Wyllie AH and Currie AR (1972). Apoptosis: a basic biological phenomenon with wide ranging implications in tissue kinetics. *British J Cancer*, **26**, 239-257.

Kikuzaki H and Nakatani N (1989). Structure of a new antioxidative phenolic acid from oregano (*Origanum vulgare* L). *J Agric Biol Chem*, **53**, 519-524.

Kim Y (2001). COX-2 and apoptosis regulation in breast cancer. www.ucop.edu/srphome/bcrp/progressreport/absracts/patho/SF6-0170html Accessed/ 3/2003

Kim KY, Seol JY, Jeon GJ and Nam MJ (2003). The combined treatment of aspirin and induces apoptosis by the regulation of bcl-2 and caspase-3 in human cervical cancer cell. *Cancer Letters*, **189**, 157-166.

Kirchoff S, Krueger A and Krammer PH (2003). *Apoptosis: A brief introduction.* Oncogene Research Products, Catalogue and Technical Guide.

Kischkel FC, Hellbardt S, Behrmann I, Germer M, Pawlita M, Krammer PH and Peter ME (1995). Cytotoxicity-dependent APO-1 (Fas/CD95)-associated proteins form a death-inducing signaling complex (DISC) with the receptor. *EMBO J*, **14**, 5579-5588.

Klampfer L, Cammenga L, Wisniewski H and Nimer SD (1999). Sodium salicylate activates caspases and induces apoptosis of myeloid leukaemia cell lines. *Blood*, **93**, 2386-2394.

Ko LJ and Prives C (1996). P53: puzzle and paradigm. *Genes Dev*, **10**, 1054-1072.

Koff A, Cross F, Fisher A, Schumacher J, Leguellec K, Philippe M and Roberts JM (1991). Human cyclin E, a new cyclin that interacts with two members of the CDC2 gene family. *Cell*, **66**, 1217-28.

Kondo T, Takeuchi K, Doi Y, Yonemura S, Nagata S and Tsukita S (1997). ERM (ezrin/radixin/moesin)- based molecular mechanism of microvillar breakdown at an early stage of apoptosis. *J Cell Biol*, **139**, 749-758.

Koopman G, Reutlingsperger CPM and Kuijten GAM (1994). Annexin V for flow cytometric detection of phosphatidylserine expression on B cells undergoing apoptosis. *Blood*, **84**, 1415-1420.

Kopp E and Ghosh S (1994). Inhibition of NF-kappa B by sodium salicylate and aspirin. *Science*, **265**, 956-959.

Kudo C, Kori M, Matsuzaki K, Yamai K, Nakajima A, Shibuya A, Niwa H, Kamisaki Y and Wada K (2003). Diclofenac inhibits proliferation and differentiation of neural stem cells. *Biochemical Pharmacology*, **66**, 289-295.

Kuo P-L, Lin T-C and Lin C-C (2002). The antiproliferative activity of aloe-emodin is through p53-dependent and p21-dependent apoptotic pathway in human hepatoma cell lines. *Life Sciences*, **71**, 1879-1892.

Laird PW and Jaenisch R (1996). The Role of DNA Methylation in Cancer Genetics and Epigenetics. *Annual Review of Genetics*, **30**, 441-464.

La Monica V, Kyung Song S, Andrew, YH and Danielpour D (2003). Regulation of trespin expression by modulators of cell growth, differentiation and apoptosis in prostatic epithelial cells. *Experimental Cell Research*, **284**, 301-313.

Law BK, Waltner-Law ME, Entingh AJ, Chytil A, Aakre ME, Norgaard P and Moses HL (2000). Salicylate-induced growth arrest is associated with inhibition of p70s6K and down-regulation of c-Myc, cyclin D1, cyclin A and proliferating cell nuclear antigen. *J Biol Chem*, **275**, 38561-38267.

Lee M and Nurse P (1988). Cell cycle control genes in fission yeast and mammalian cells. *Trends Genet*, **4**, 287-290.

Lee EJ, Park HG and Kang HS (2003). Sodium salicylate induces apoptosis in HCT116 colorectal cancer cells through activation of p38MAPK. *Int J Oncol*, **23**, 503-508.

Leek H and Albertsson M (2000). Electron microscopy of squamous cell carcinoma of the head and neck. *Scanning*, **22**, 326-331.

Lees TH (1995). Cyclin dependent kinase regulation. *Curr Opin Cell Biol*, **7**, 773-780.

Leist M, Single B, Castoldi AF, Kuhnle S and Nicotera P (1997). Intercellular adenosine triphosphate (ATP) concentration: a switch in the decision between apoptosis and necrosis. *J Exp Med*, **185**, 1481-1486.

Lévesque H and Lafont O (2000). Aspirin throughout the ages: an historical review: L'aspirine à travers les siècles: rappel historique. *La Revue de Médecine Interne*, **21**(1), 8s-17s.

Levine AJ (1997). p53, the cellular gatekeeper for growth and division. *Cell*, **88**, 323-331.

Li GM (1999). The role of mismatch repair in DNA damage-induced apoptosis, *Oncol, Res*, **11**, 393-400.

Liu JY, Hafner J, Dragieva G and Burg G (2004). Bioreactor Microcarrier Cell Culture System (Bio-MCCS) for Large-Scale Production of Autologous Melanocytes. *Cell Transformation*, **13**, 809-816.

Lohmann RD and Beyersmann D (1993). Cadmium and zinc mediated changes of the Ca^{2+}-dependent endonuclease in apoptosis. *Biochem Biophys Res Commun*, **190**, 1097-1103.

Luchinat C (2003). Metal cofactors in Biology. http://eurobic6.kc.lu.se/abs/luchinat_c_428.pdf. Accessed/ 4/2003.

Macleod KF, Sherry N, Hannon G, Beach D, Tokino T, Kinzler K, Vogelstein B and Jacks T (1995). p53-dependent and independent expression of p21 during cell growth, differentiation, and DNA damage. *Genes Dev*, **9**, 935-944.

Mahdi JG, Mahdi AJ, Mahdi AJ, Bowen ID (2004). Historical Analysis of Aspirin Discovery and its Alliance with Medicinal Willow. *Swiss J History of Medicine and Sciences*, submitted October, 2004.

Malumbres M and Carnero A (2003). Cell cycle deregulation: a common motif in cancer. *Prog Cell Cycle Res*, **5**, 5-18.

Marchetti P, Zamzami N, Susin SA, Patrice PX and Kroemer G (1996). Mitochondrial permeability transition is a central coordinating event in apoptosis. *J Exp Med*, **184**, 1155-1160.

Maret W (2000). The function of zinc metallothionein: A Link between Cellular Zinc and Redox State. *J Nutr*, **130**, 1455S-1458S.

Marra DE, Simoncini T and Liao JK (2000). Inhibition of vascular smooth muscle cell proliferation by sodium salicylate mediated by upregulation of p21[Waf1] and p27[KiP1]. *Circulation*, **102**, 2124-2130.

Matthews REF (1991). *Plant Virology*. San Diego, CA: Academic Press.

Marra DE and Liao JK (2001). Salicylates and vascular smooth muscle cells proliferation: Molecular mechanism for cell cycle arrest. *Trend in Cardiovascular Medicine*, **11**, 339-344.

Martin-Caballero J, Flores JM, Garcia-Palencia P and Serrano M (2001). Tumor susceptibility of p21(Waf1/Cip1)-deficient mice. *Cancer Res*, **61**, 6234-6238.

Martin SJ and Green DR (1995). Protease activation during apoptosis: death by a thousand cuts? *Cell*, **82**, 349-352.

Matherly LH, Schuetz JD, Westion E and Goldman ID (1989). A method for the synchronisation of cultured cells with aphidicolin: application to the large scale synchronisation of L12210 cells and the study of the cell cycle regulation of thymidylate synthase and dihydrofolate reductase. *Anal Biochem*, **182**, 338-345.

Mayer F, Stoop H, Scheffer GL, Scheper R, Oosterhuis JW, Looijenga LH and Bokemeyer C (2003). Molecular determinants of treatment response in human germ cell tumors. *Clin Cancer Res*, **9**, 767-773.

McGowan C (2003). Regulation of eukaryotic cell cycle. *Progress in Cell Cycle Research*, **5**, 1-5.

Mertens JJW, Towndrow KM, Jeong JK, Weber TJ, Monks TJ and Lau SS (2000). Stress and Growth-related Gene Expression are Independent of Chemical Induced Prostaglandin E2 Synthesis in Renal Epithelial Cells. *Chemical Research in Toxicology*, **13**, 111-117.

Milner J (1984). Different forms of p53 detected by monoclonal antibodies in non-dividing and dividing cells, *Nature*, **310**,143-145.

Mitton K (2000). What are the causes of necrosis? *Cell Biology*, **12**, 32-33.

Moffit P (1994). A methyl green-pyronin y technique for demonstrating cell death in the murine tumour S180. *Cell Biol Int*, **18**, 677-679.

Moorghen M, Ince P, Finney KJ, Sunter JP, Appleton DR and Watson AJ (1988). A protective effect of sulindac against chemically-induced primary colonic tumours in mice. *J Pathol Dec*, **156**, 341-347.

Morgan DO (1995). Principles of CDK regulation, *Nature*, **374**, 131-134.

Mosmann T (1983). Rapid colorimetric assay for cellular growth and survival: application to proliferation and cytotoxicity assays. *J Immunol Methods*, **65**, 55–63.

MSDS (Material Safety Data Sheet) (2003). Benzoic acid. http://www.jtbaker.com/msds/englishhtml/b1356.htm, Accessed 1/06/2004.

Munkarah AR, Morris R, Baumann P, Deppe G, Malone J, Diamond MP and Saed GM (2002). Effects of prostaglandin E_2 on proliferation and apoptosis of epithelial ovarian cancer cells. *Journal Soc Gynecol Investig*, **9**, 168-173.

Murray A and Hunt T (1993). *The Cell Cycle: An Introduction*. New York: W.H. Freeman.

Nagata S (1996). Fas-mediated apoptosis. *Adv Exp Med Biol*, **406**, 119-124.

Nagata S (1997). Apoptosis by death factor. *Cell*, **88**, 355-365.

Nagata S (2000). Apoptotic DNA fragmentation. *Exp Cell Res*, **256**, 12-18.

Newton K and Strasser A (1998). The Bcl-2 family and cell death regulation. *Curr Open Genet Dev*, **8**, 68-75.

Nguyen P, Broussas M, Cornillet-Lefebvre P and Potron G (1999). Coexpression of tissue factor and tissue factor pathway inhibitor by human monocytes purifies by leukpheresis and elutriation. Response of nonadherent cells to lipopolysaccharide. *Transfusion*, **39**, 975-982.

Nicholson DW and Thornberry NA (2003). Life and death decisions. *Science*, **299**, 214-215.

Nicotera P and Orrenius S (1998). The role of calcium in apoptosis. *Cell Calcium*, **23**, 173-180.

Norbury C and Nurse P (1992). Animal cell cycles and their control. *Annu Rev Biochem*, **61**, 441-470.

Nurse P (2000). A long twentieth century of the cell cycle and beyond. *Cell*, **7**, 71-78.

Obaya AJ and Sedivy JM (2002). Regulation of cyclin-Cdk activity in mammalian cells. *Cell Mol Life Sci*, **59**, 126-142.

Ohtsubo M, Theodoras AM, Schumacher J, Roberts JM and Pagano (1995). Human cyclin E, a nuclear protein essential for the G1-to-S phase transition. *Mol Cell Biol*, **15**, 2612-2624.

Oliner JD, Kinzler KW, Meltzer PS, George DL and Vogelstein B (1992). Amplification of a gene encoding a p53-associated protein in human sarcomas. *Nature*, **358**, 80-83.

Oltvai ZN, Milliman CL and Korsmeyer SJ (1993). Bcl-2 heterodimerizes in vivo with a conserved homolog, bax, that accelerates cell apoptosis, *Cell*, **74**, 609-619.

Ona VO, Li M, Vonsattel JPG, Andrews LJ, Khan SQ, Chung WM, Frey AS, Menon AS, Li X-J, Stieg PE, Yuan J, Penney JB, Young AB, Cha J-HJ and Friedlander RM (1999). Inhibition of caspase-1 slows disease progression in mouse model of Huntington's disease. *Nature*, **399**, 263-267.

Owen RW, Mier W, Giacosa A, Hull WE, Spiegelhalder B and Bartsch H (2000). Phenolic compounds and squalene in olive oils: the concentration and antoxidant potential of total phenols, simple phenols, secoiridoids, lignans and squalene. *Food and Chemical Toxicology*, **38**, 647-659.

Pagano M, Pepperkok R, Verde F, Ansorge W and Draetta G (1992). Cyclin A is required at two points in the human cell cycle. *EMBO J*, **11**, 961-971.

Pagnate-Hill A, Chao A, Roses RK, Henderson BE (1989). Aspirin use and chronic diseases: a cohort study of the elderly. *BMJ*, **299**, 1247-1250.

Parat MO, Richard MJ, Pollet S, Hadjur C, Favier A and Beani JC (1997). Zinc and DNA fragmentation in keratinocyte apoptosis: its inhibitory effect in UVB irradiated cells. *J Photochem Photobiol B*, **37**, 101–106.

Pardee AB (1989). G1 events and regulation of cell proliferation. *Science*, **246**, 603-608.

Patrono C, Coller B, FitzGerald GA, Hirsh J, Roth G (2004). Platelet-active drugs: the relationships among dose, effectiveness, and side effects: the Seventh ACCP Conference on Antithrombotic and Thrombolytic Therapy. *Chest*, **126**, 234S-264S.

Pellegrini M and Strasser A (1999). A portrait of the Bcl-2 protein family: life, death and the whole picture. *J Clin Immunol*, **19**, 365-377.

Pennisi E (2001). Behind the scenes of gene expression. *Science*, **293**, 1064-1067.

Pepper C, Hoy T and Bentley DP (1997). Bcl-2/Bax ratios in chronic lymphocytic leukaemia and their correlation with in vitro apoptosis and clinical resistance. *British Journal of Cancer*, **76** (7), 935-938.

Pepper C, Thomas A, Hoy T and Bentley P (1999). Chlorambucil resistance in B-cell chronic lymphocytic leukaemia is mediated through failed Bax induction and selection of high Bcl-2-expressing subclones. *British Journal of Haematology*, **104**, 581-588.

Pepper C, Thomas A, Hoy T and Bentley P (2002). Antisense oligonucleotides complementary to Bax transcripts reduce the susceptibility of B-cell chronic lymphocytic leukaemia cells to apoptosis in a Bcl-2 independent manner. *Leukemia and Lymphoma*, **43**, 2003-2009.

Pepper C, Hooper K, Thomas A, Hoy T and Bentley P (2001). Bcl-2 antisense oligonucleotides enhance the cytotoxicity of Chlorambucil in B-cell chronic lymphocytic leukaemia cells. *Leukemia and Lymphoma*, **42**, 491-498.

Perry DK, Smyth MJ, Stennicke HR, Salvesen GS, Duriez P, Poirier GG and Hannun YA (1997). Zinc is a potent inhibitor of the apoptotic protease, caspase-3. A novel target for zinc in the inhibition of apoptosis. *J Biol Chem*, **272**, 18530-18533.

Perugini RA, McDade TB, Vittimberga FJ, Duffy AJ and Callery MP (2000). Sodium salicylate inhibits proliferation and induces G1 cell cycle arrest in human pancreatic cancer cell lines. *J Gastrointestinal Surgery*, **4**, 24-33.

Pezzella F, Morrison H, Jones M, Gatter KC, Lane D, Harris AL and Mason DY (1993). Immunohistochemical detection of p53 and bcl-2 proteins in non-Hodgkin's lymphoma. *Histopathology*, **22**, 39-44.

Pieters R, Huishmans DR, Leyva A and Veerman AJP (1989). Comparison of the rapid automated MTT-assay with a dye exclusion assay for chemosensi-tivity testing in childhood leukaemia. *British Journal of Cancer*, **59**, 217-220.

Pines J and Hunter T (1991). Human cyclins A and B1 are differentially located in the cell and undergo cell cycle-dependent nuclear transport. *J Cell Biol*, **115**, 1-17.

Pique M, Barragan M, Dalmau M, Bellosillo B, Pons G and Gil J (2000). Aspirin induces apoptosis through mitochondrial cytochrome c release. *FEBS Letters*, **480**, 193-196.

Powell SR (2000). The antioxidant properties of zinc. *J Nutr*, **130**, 1447S-1454S.

Pumin Z (1999). The cell cycle and development: redundant roles of cell cycle regulators. *Current Opinion in Cell Biology*, **11**, 655-662.

Qian X, Gozani SN, Yoon H, Jeon CJ, Agarwal K and Weiss MA (1993a). Novel zinc finger motif in the basal transcriptional machinery: three-dimensional NMR studies of the nucleic acid binding domain of transcriptional elongation factor TFIIS. *Biochemistry*, **32**, 9944-9959.

Qiao L, Hanif R, Sphicas E, Shiff SJ and Rifas B (1998). Effect of aspirin on induction of apoptosis in HT-29 human colon adenocarcinoma cells. *Biochemical Pharmacol*, **55** (1), 53-64.

Qian X, Jeon C, Yoon H, Agarwal K and Weiss MA (1993b). Structure of a new nucleic-acid-binding motif in eukaryotic transcriptional elongation factor TFIIS. *Nature*, **365**, 277-279.

Raff MC, Barres BA, Burne JF, Coles HS, Ishizaki Y and Jacobson MD (1993). Programmed cell death and the control of cell survival: lessons from the nervous system. *Science*, **262**, 695-700.

Raffray M and Cohen GM (1993). Thymocyte apoptosis as a mechanism for tributyltininduced thymic atrophy *in vivo*. *Arch Toxicol*, **76**, 231-236.

Rasheed S, Nelson-Rees WA, Toth EM, Arnstein P and Gardner MB (1974). Characterization of a newly derived human sarcoma cell line (HT-1080). *Cancer*, **33**, 1027-1033.

Raskin I (1992). Role of salicylic acid in plants. *Annu Rev Plant Physiol, Plant Mol Biol*, **43**, 439-463.

Raz A (2002). Is inhibition of cyclooxygenase required for the anti-tumorigenic effects of nonsterolidal, anti-inflammatory drugs (NSAIDs)? In vitro versus in vivo results and the relevance for the prevention and treatment of cancer. *Bioch Pharmacol*, **63**, 343-347.

Reed JC (2000). Mechanisms of apoptosis. *Am J Pathol*, **157**, 1415-1430.

Reutelingsperger CP, Hornstra G and Hemker HC (1985). Isolation and partial purification of a novel anticoagulant from arteries of human umbilical cord. *Eur J Biochem*, **151**, 625-629.

Ricchi P, Pignata S, Di Popolo A, Memoli A, Apicella A, Zarrilli R and Acquaviva AM (1997). Effect of aspirin on cell proliferation and differentiation of colon adenocarcinoma Caco-2 cells. *Int J Cancer*, **73**, 880-884.

Rice-Evans CA, Miller NJ and Paganga G (1997). Antioxidant properties of phenolic compounds. *Trends in Plant Science*, **2**, 152-159.

Roehm NW, Rodgers GH, Hatfield SM and Glasebrook AL (1991). An improved colorimetric assay for cell proliferation and viability utilizing the tetrazolium salt XTT. *J Immunol Methods*, **142**, 257-265.

Roger JBK (2000) . *Cancer Biology,* Second Edition. Pearson Education Limited, Prentice Hall.

Rogers HW, Callery MP, Deck B and Unanue ER (1996). *Listeria monocytogenes* induces apoptosis of infected hepatocytes, *J Immunol*, **156**, 679-684.

Rosenbuurg L, Palmer JR, Zauber AQ, Warshauer ME, Stolley PD and Shapiro S (1991). A hypothesis: nonesteroidal antiinflammatory drugs reduce the incidence of large bowel cancer. *J Natl Cancer Inst*, **83**, 355-358.

Ruschoff J, Wallinger S, Dietmaie W, Bocker T, Brockhoff G, Hofstadte RF and Fishel R (1998). Aspirin suppresses the mutator phenotype associated with hereditary nonpolyposis colorectal cancer by genetic selection. *Proc Natl Acad Sci*, **95**, 11301-11306.

Ryals JA, Neuenschwander UH, Willits MG, Molina A, Steiner H-Y and Hunt MD (1996). Systemic acquired resistance. *Plant Cell*, **8**, 1809-1819.

Salvi A, Carrupt P-A, Tillement J-P and Testa B (2001). Structural damage to proteins caused by free radicals: assessment, protection by antioxidants, and influence of protein binding. *Biochemical Pharmacology*, **61**, 1237-1242.

Santini G, Sciulli MG, Marinacci R, Fusco O, Spoletini L, Pace A, Ricciardulli A, Natoli C, Procopio A, Maclouf J and Patrignani P (1999). Cyclooxygenase-independent induction of p21WAF-1/cip1, apoptosis and differentiation by L-745,337, a selective PGH synthase-2 inhibitor, and salicylate in HT-29 cells. *Apoptosis*, **4**, 151-162.

Sarraf CE and Bowen ID (1986). Kinetic studies in a murine sarcoma and an analysis of apoptosis. *British Journal of Cancer*, **54**, 989-998.

Sarraf CE and Bowen ID (1988). Proportions of mitotic and apoptotic cells in a range of untreated experimental tumours. *Cell Tissue Kinet*, **21**, 45-49.

Saunders MW and Bowen ID (2003). Apoptosis and Cell Death, in *Scott-Browns Otorhinolaryngology: Head and Neck Surgery (Seventh Edition)*.

Scarino ML, Poverini R, Di Lullo G and Bises G (1992). Inhibition of protein synthesis after exposure of caco2 cells to heavy metals. *ATLA*, **20**, 325-333.

Schanne FAX, Kane AB, Young EE and Farber JL (1979). Calcium dependence of toxic cell death: a final common pathway. *Science*, **206**, 700-702.

Schulze-Osthoff C, Ferrari D, Los M, Wesselborg S and Peter ME (1998). Apoptsis signalling by death receptors. *Eur J Biochem*, **254**, 439-459.

Schutte B and Ramaekers FC (2000). Molecular switches that govern the balance between proliferation and apoptosis. *Prog Cell Cycle Res*, **4**, 207-217.

Scudiero DA, Shoemaker RH, Paull KD, Monks A, Tierney S, Nofziger TH, Currens MJ, Seniff D and Boyd MR (1988). Evaluation of a soluble tetrazolium/formazan assay for cell growth and drug sensitivity in culture using human and other tumor cell lines. *Cancer Res*, **48**, 4827-4833.

Sebolt-Leopold J S, Dudley D T, Herrera R, Van Becelaere K, Wiland A, Gowan R C, Tecle H, Barrett S D, Bridges A, Przybranowski S, Leopold W R and Saltiel A R (1999). Blockade of the MAP kinase pathway suppresses growth of colon tumors *in vivo*. *Nat Med*, 5, 810-816

Sedlak TW, Oltvai ZN, Yang E, Wang K, Boise LH, Thompson CB and Korsmeyer SJ (1995). Multiple Bcl-2 family members demonstrate selective dimerizations with Bax. *Proc Natl Acad Sci*, USA, 92, 7834-7838.

Shabir GA (2004). Determination of combined p-hydroxy benzoic acid preservatives in a liquid pharmaceutical formulation by HPLC. *J Pharmaceutical and Biomedical Analysis*, 34, 207-213.

Sharma RA, Manson MM, Gescher A and Steward WP (2001). Colorectal cancer chemoprevention: biochemical targets and clinical development of promising agents. *European Journal of Cancer*, 37, 12-22.

Sherbet GV and Lakshmi MS (1997). *The Genetics of Cancer. Genes Associated with cancer Invasion, Metastasis and Cell Proliferation*. Academic Press.

Sherr CJ (1993). Mammalian G1 cyclins. *Cell*, 73, 1059-1065.

Sherr CJ (1996). Cancer cell cycles. *Science*, 274, 1672-1677.

Shiff SJ, Koutsos MI, Qiao L and Rigas B (1996). Nonsteroidal antiinflammatory drugs inhibit the proliferation of colon adenocarcinoma cells: effects on cell cycle and apoptosis. *Exp Cell Res*, 222, 179-188.

Shiff SJ and Rigas B (1999). The role of cycloxygenase inhibition in the antineoplastic effects of nonsteroidal anti-inflammatory drugs (NSAID's). *J Exp Med*, 190, 445-450.

Shirano Y, Kachroo P, Shah J and Klessig DF (2002). A gain-of-function mutation in an arabidopsis toll interleukin1 receptor-nucleotide binding site-Leucine-rich repeat type R gene triggers defense responses and results in enhanced disease resistance. *Plant Cell*, 14, 3149 - 3162.

Shtivelband MI, Juneja HS, Lee S and Wu KK (2003). Aspirin and salicylate inhibit colon cancer medium- and VEGF-induced endothelial tube formation: correlation with suppression of cyclooxygenase-2 expression. *J Thromb Haemost*, 1, 2225-2233.

Sicinski P, Donaher JL, Parker SB, Li T, Fazeli A, Gardner H, Haslam SZ, Bronson RT, Elledge SJ and Weinberg RA (1995). Cyclin D1 provides a link between development and oncogenesis in the retina and breast. *Cell*, 82, 621-630.

Slater TF, Sawyer B and Strauli UD (1963). Studies on succinate-tetrazolium reductase systems. *Biochem Biophys Acta*, 77, 383–393.

Smith WL, DeWitt DL, Shimokawa T, Kraemer SA and Meade EA (1990). Molecular basis for the inhibition of prostanoid biosynthesis by nonsteroidal anti-inflammatory agents. *Stroke*, 21, IV24-28.

Smith ML, Hawcroft G and Hull MA (2000). The effect of non-steroidal anti-inflammatory drugs on human colorectal cancer cells: Evidence of different mechanisms of action. *Eur J Cancer*, **36**, 664-674.

Soini Y, Kinnula V, Kaarteenaho-Wiik R, Kurttila E, Linnainmaa K and Paakko P (1999). Apoptosis and expression of apoptosis regulating proteins bcl-2, mcl-1, bcl-X, and bax in malignant mesothelioma. *Clin Cancer Res*, **5**, 3508-3515.

Soussi T and Beroud C (2001). Assessing TP53 status in human tumours to evaluate clinical outcome. *Nat Rev Cancer*, **1**, 233-240.

Spence RAJ and Johnston PG (2001). *Oncology*. Oxford University Press, Oxford.

Stark LA, Din FVN, Zwacka RM and Dunlop MG (2001). Aspirin induced activation of the NF-kB signalling pathway: a novel mechanism for aspirin mediated apoptosis in colon cancer cells. *FASEB J*, **15**, 1273-1275.

Stellman SD (1995). Aspirin and cancer: Report on an American Health Foundation Workshop. *Preventive Medicine*, **24**, 101-102.

Stevens A (1977). The haematoxylins. In Bancroft J and Stevens A (Eds.). *Theory and Practice of Histological Techniques*. Churchill Livingstone, 85-94. Edinburgh, London, and New York: Churchill Livingstone.

Steven DS (1995). Aspirin and Cancer: Report on an American Health Foundation Workshop. *Preventive Medicine*, **24**,101-102.

Sumner J (2000). *The natural history of medicinal plants*. Portland, Oregon: Timber Press.

Sun Y (1990). Free radicals, antioxidant enzymes, and carcinogenesis. *Free Radical Biology and Medicine*, **8**, 583-599.

Sun Y, Oberley LW, Elwell JH and Sierra Rivera E (1989). Antioxidant enzyme activities in normal and transformed mice liver cells. *Int J Cancer*, **44**, 1028-33.

Thompson CB (1995). Apoptosis in the pathogenesis and treatment of disease. *Science*, **267**, 1456-1462.

Thornberry NA and Lazebnik Y (1998). Caspases: Enemies Within. *Science*, **281**, 1312-1316.

Thun MJ, Namboodiri MM, Calle EE, Flanders WD and Heath CW (1997). Aspirin use and risk of fatal cancer. *Cancer Res*, **53**, 1322-1327.

Trauth BC, Wittor H and Rubmann E (1995). Two non-radioactive immunoassays for the measurement of apoptotic cell death. *Boehringer Mannheim Biochemica Technical Information.*

Trump BF, Berezesky IK, Chang SH and Phelps PC (1997). The pathways of cell death: Oncosis, apoptosis, and necrosis. *Toxicol Pathol*, **25**, 82-88.

Truong-Tran AQ, Carter J, Ruffin RE and Zalewski S (2001). The role of zinc in caspase activation and apoptotic cell death. *BioMetals*, **14**, 315-330.

Tsao Y-P, Li S-F, Liu J-C and Chen S-L (1998). Apoptosis is induced in aging SV40 T antigen-transformed human fibroblasts through p53- and p21$^{CIP1/WAF1}$-independent pathways. *Cancer Letters*, **133**, 77-82.

Tsujimoto Y (2003). Cell death regulation by the Bcl-2 protein family in the mitochondria. *J Cell Physiol*, **195**, 158-167.

Twentyman PR, Fox NE and Rees JKH (1989). Chemosensitivity testing of fresh leukaemia cells using the MTT colorimetric assay. *British Journal of Haematology*, **71**, 19-24.

Twentyman PR and Luscombe M (1987). A study of some variables on a tetrazolium dye (MTT) based assay for cell growth and chemosensitivity. *British Journal of Cancer*, **56**, 279-285.

Vaux DL (2002). Apoptosis timeline. *Cell Death Differ*, **9**, 349-354.

Vaux DL, Aguila HL and Weissman IL (1992). Bcl-2 prevents death of factor-deprived cells but fails to prevent apoptosis in targets of cell-mediated killing. *International Immunology*, **4**, 821-824.

Vaux DL and Strasser A (1996). The molecular biology of apoptosis. *Proc Natl Acad Sci USA*, **93**, 2239–2244.

Vermes IC, Haanen H, Steffens-Nakken C and Reutelingsperger H (1995). A novel assay for apoptosis. Flow cytometric detection of hosphatidylserine expression on early apoptotic cells using fluorescein labelled Annexin V. *J Immunol Meth*, **184**, 39-51.

Vogelstein B and Kinzler KW (1992). p53 function and dysfunction. *Cell*, **70**, 523-526.

Wajant H (2002). The Fas signalling pathway: More than a paradigm. *Science*, **296**, 1635-1636.

Walker PR and Sikorska M (1997). New aspects of the mechanism of DNA fragmentation in apoptosis. *Biochem Cell Biol*, **75**, 287-299.

Wedge DE and Camper ND (2000). Connection between agrochemicals and pharmaceuticals. In: Cutler SJ and Cutler HG (Eds). *Biological active natural products: Pharmaceuticals*. CRC, London, 1-15.

Wei MC, Song W-X, Cheng EH-Y, Lindsten T, Panoutsakopoulou V, Ross AJ, Roth KA, MacGregor GR, Thompson CB and Korsmever SJ (2001). Proapoptotic BAX and BAK: A requisite gateway to mitochondrial dysfunction and death. *Science*, **292**, 727-730.

Weinberg RA (1995). The retinoblastoma protein and cell cycle control. *Cell*, **81**, 323-330.

Wildermuth MC, Dewdney J, Wu G and Ausubel FM (2001). Isochorismate synthase is required to synthesize salicylic acid for plant defence. *Nature*, **414**, 562–565.

Williams CS, Mann M and DuBois RN (1999). The role of cylooxygenases in inflammation, cancer and development. *Oncogene*, **18**, 7908-7916.

Willingham MC (1999). Cytochemical methods for the detection of apoptosis. *J Histochem Cytochem*, **47**, 1101-1109.

Wong BCY, Zhu GH and Lam SK (1999). Aspirin induced apoptosis in gastric cancer cells. *Biomed & Pharmacother*, **53**, 315-318.

Wu C-T and Morris JR (2001). Genes, genetics, and epigenetics: a correspondence. *Science*, **293**,1103-1105.

Wuarin J and Nurse P (1996). Regulating S phase: CDKs, licensing and proteolysis. *Cell*, **85**, 785-787.

Wyllie AH (1980). Glucocorticoid-induced thymocyte apoptosis is associated with endogenous endonuclease activation. *Nature*, **284**, 555-556.

' Wyllie AH, Beattie GJ and Hargreaves AD (1981). Chromatin changes in apoptosis. *Histochem J*, **13**, 681-692.

Xiong Y, Hannon GJ, Zhang H, Casso D, Kobayashi R and Beach D (1993).p21 is a universal inhibitor of cyclin kinases. *Nature*, **366**, 701-704.

Xu X-M, Sansores-Garcia L, Chen X-M, Matijevic-Aleksic N, Du M and Wu KK (1999). Suppression of inducible cyclooxygenase-2 gene transcription by aspirin and salicylate. *Proc Natl Acad Sci USA*, **96**, 5292-5297.

Yin MJ, Yamamoto Y and Gaynor RB (1998). The antiinflammatory agents aspirin and salicylate inhibit the activity of I(kappa)B kinase-beta. *Nature*, **396**, 77-80.

Yoneda K, Yamamoto T and Osaki T (1998). p53- and p21-independent apoptosis of squamous cell carcinoma cells induced by 5-fluorouracil and radiation. *Oral Oncology*, **34**, 529-537.

Yoshizaki H, Arai K, Mizoguchi T, Shiratsuchi M, Hattori Y, Nagoya T, Shidara and Maki YM (1989). Isolation and characterization of an anticoagulant protein from human placenta. *J Biochem*, **105**, 178-183.

Yu SP, Canzoniero LMT and Choi DW (2001). Ion homeostasis and apoptosis. *Current Openion in Cell Biology*, **13**, 405-411.

Zalewski PD, Forbes IJ and Betts WH (1993). Correlation of apoptosis with change in intracellular labile Zn(II) using zinquin [(2-methyl-8-*p*-toluenesulphonamido-6-quinolyloxy)acetic acid], a new specific fluorescent probe for Zn(II). *Biochem J*, **296**, 403–408.

Zetterberg A and Larsson O (1995). Cell cycle progression and cell growth in mammalian cells. In: Hutchinson C and Glover DM (Eds.) Frontiers in molecular biology: cell cycle control. Oxford University Press, Oxford, 206-227.

Zhang G, Gurtu V, Kain SR and Yan G (1997). Early detection of apoptosis using a fluorescent conjugate of Annexin V. *Biotechniques*, **23**, 525-531.

Zheng TS, Schlosser SF, Dao T, Hingorani R, Crispe IN, Boyer JL and Flavell RA (1998). Caspase-3 controls both cytoplasmic and nuclear events associated with FAS-mediated apoptosis *in vivo*. *Proc Natl Acad Sci USA*, **95**, 13618-13623.

Zhou XM, Chun B, Wong Y, Fan XM, Zhang HB, Kung MCM, Fan DM and Lam SK (2001). Non-steroidal anit-inflammatory drugs induce apoptosis in gastric cancer cells through up-regulation of bax and bak. *Carcinogenesis*, **22**, 1393-1397.

Zhu GH, Wong BCY, Eggo MC, Ching CK, Yuen ST, Chan EYT, Lai KC and Lam SK (1999). Non-steroidal anti-inflammatory drug-induced apoptosis in gastric cancer cells is blocked by protein kinase C activation through inhibition of c-myc. *Br J Cancer*, **79**, 393-400.

Zödl B, Zeiner M, Sargazi M, Roberts NB, Marktl W, Steffan I and Ekmekcioglu C (2003). Toxic and biochemical effects of zinc in Caco-2 cells. *J Inorg Biochem*, **97**, 324-330.

Zou H, Henzel WJ and Liu XA (1997). Lutschg and X. Wang, Apaf-1, a human protein homologous to *C. elegans* CED-4, participates in cytochrome *c*-dependent activation of caspase-3. *Cell*, **90**, 405-413.

Appendices

APPENDIX A

A1 - A3 HT-1080 Cells' Response to Monoaromatic Acids: Cell Growth and Cell Viability

Data in the following histograms represent the mean ±SE of means of three replicates. Cell viability measured by MTT assay.

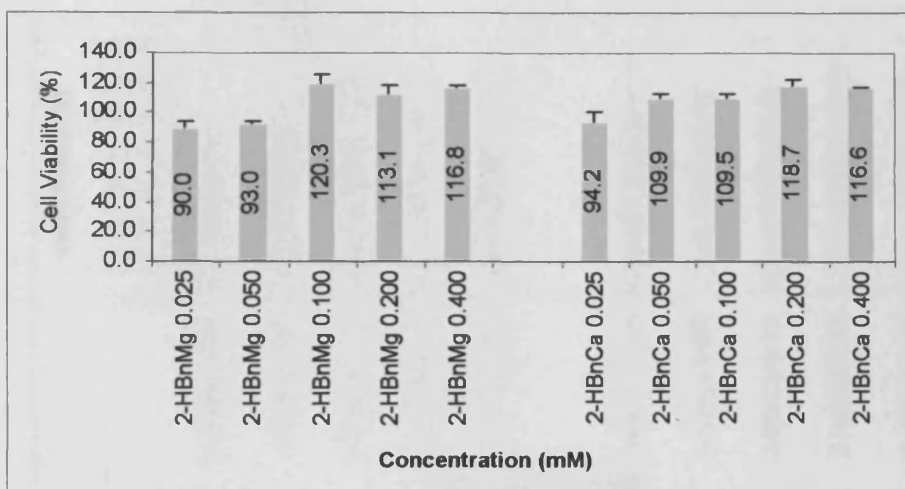**A1.1** Cell viability (%) by benzoic acid and benzoate analogues after **12 hours' incubation**
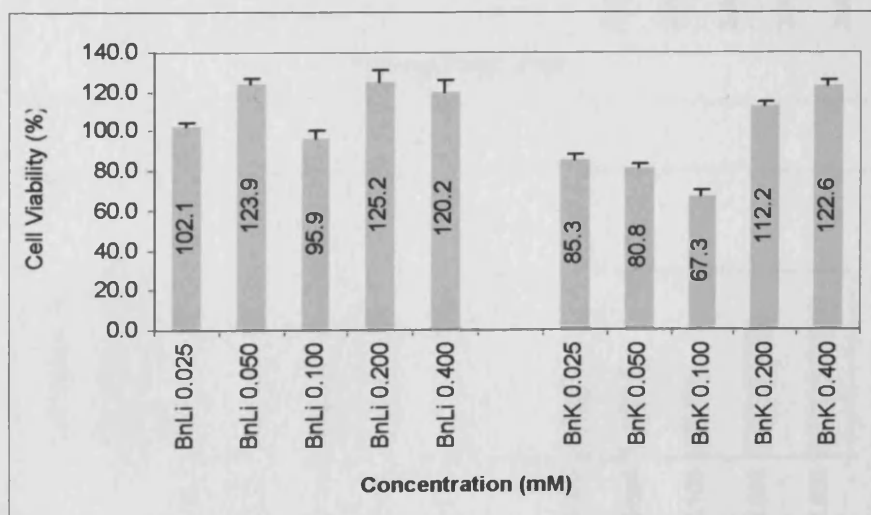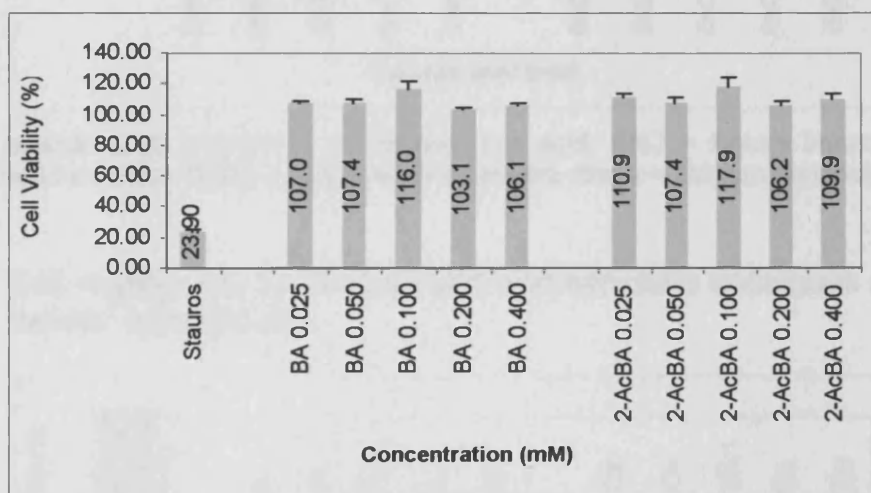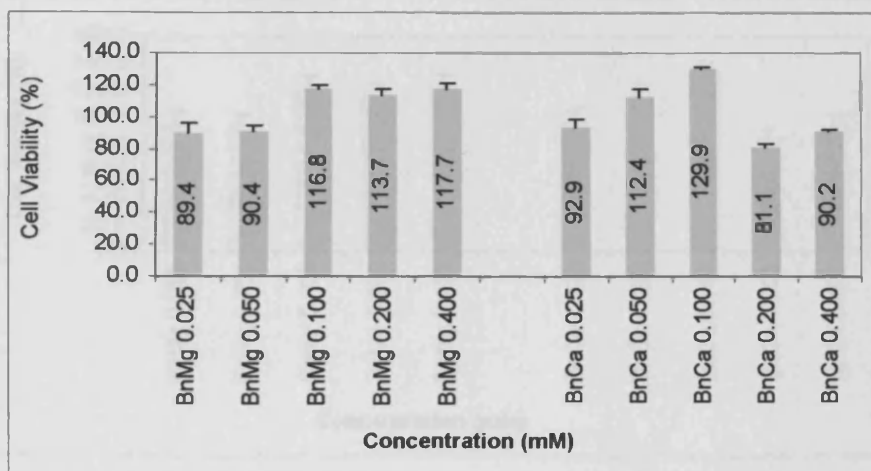
BA = benzoic acid, 2-AcBA = 2-acetylbenzoic acid; BnLi = lithium benzoate, BnK = potassium benzoate; BnMg = magnesium benzoate, BnCa = calcium benzoate.
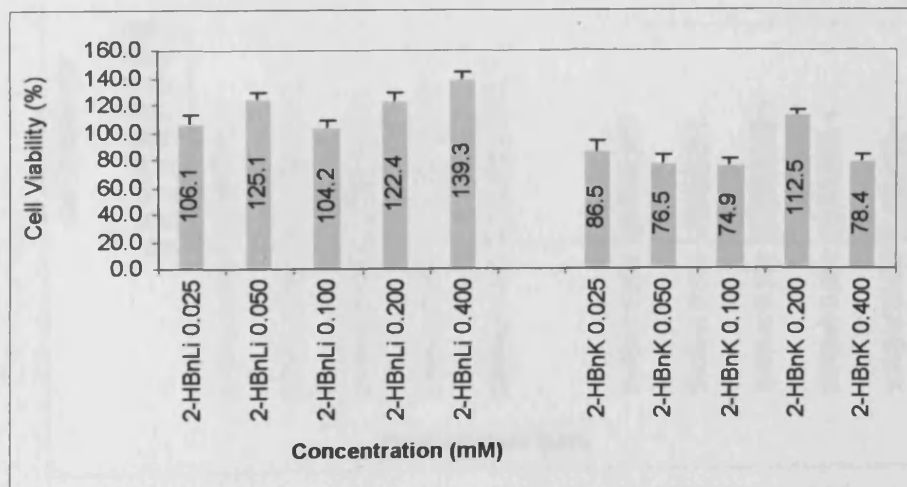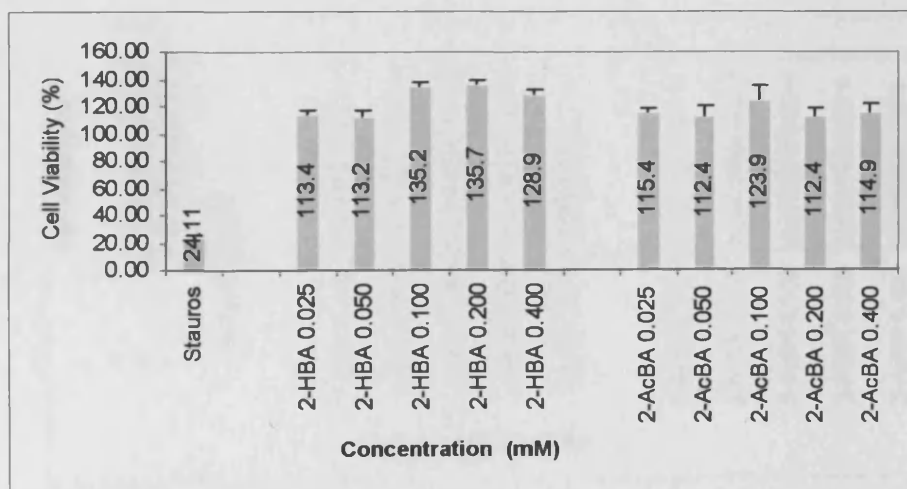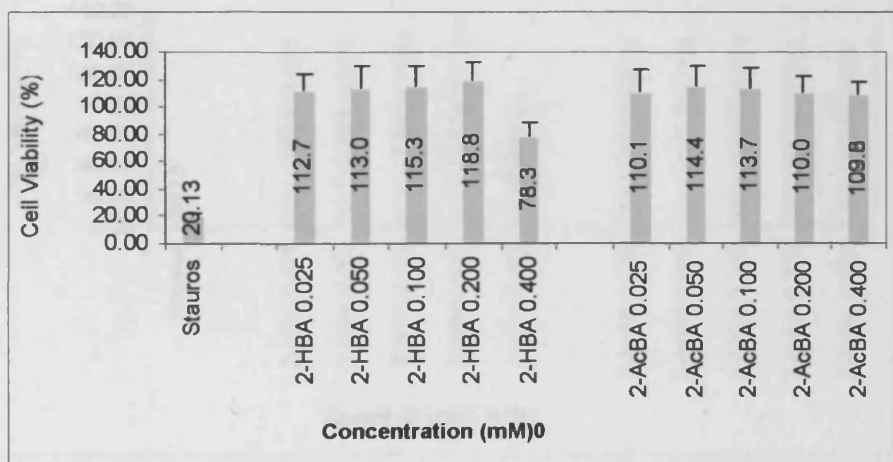
A1.2 Cell viability (%) by benzoic acid and benzoate analogues after 24 hours' incubation.
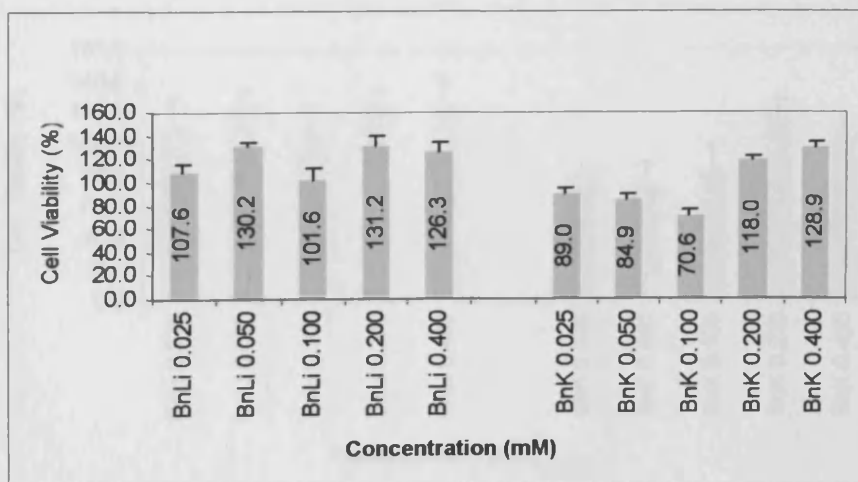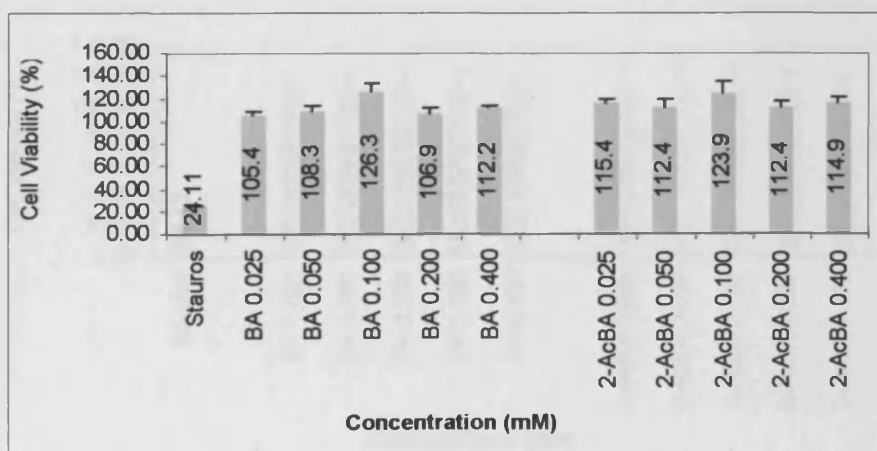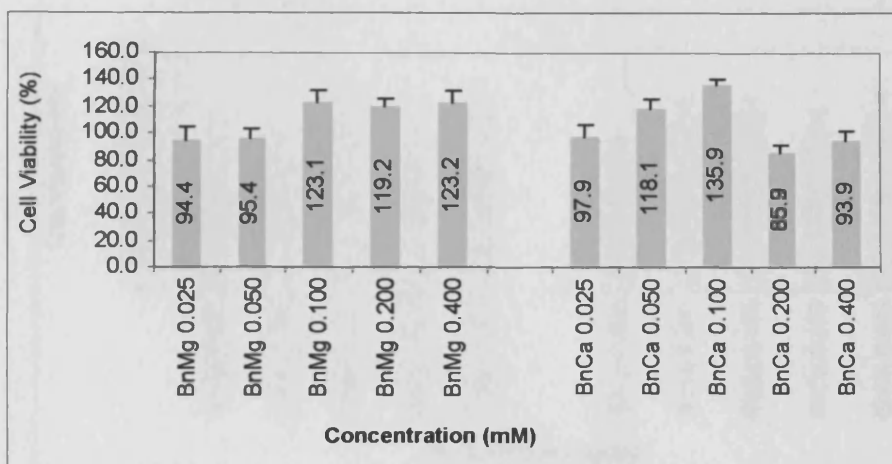
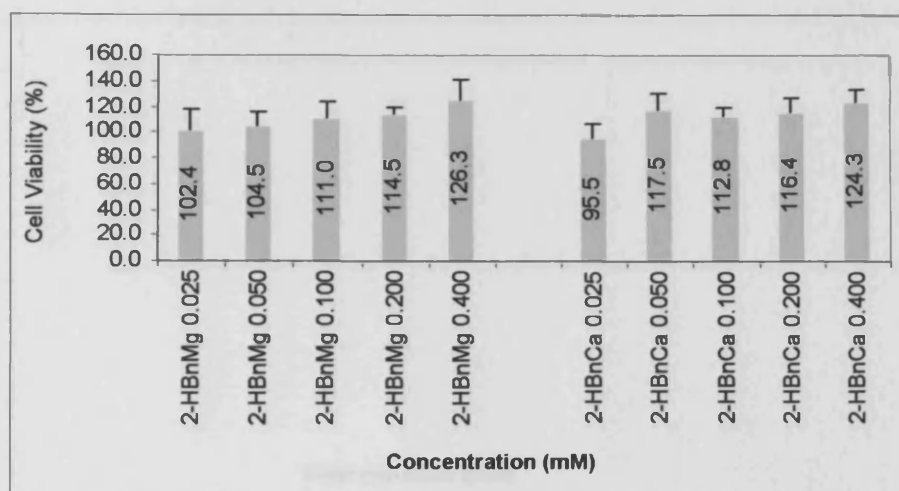BA = benzoic acid, 2-AcBA = 2-acetylbenzoic acid; BnLi = lithium benzoate, BnK = potassium benzoate; BnMg = magnesium benzoate, BnCa = calcium benzoate.

A1.3 Cell viability (%) by benzoic acid and benzoate analogues after 48 hours' incubation.
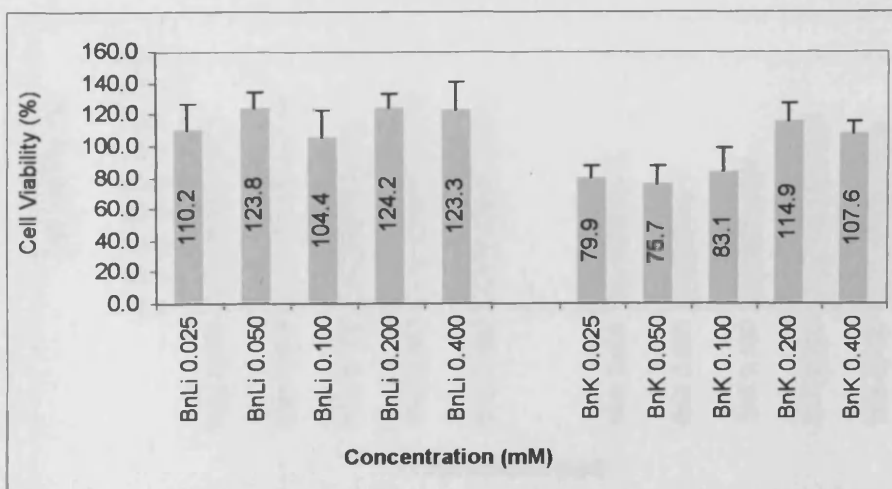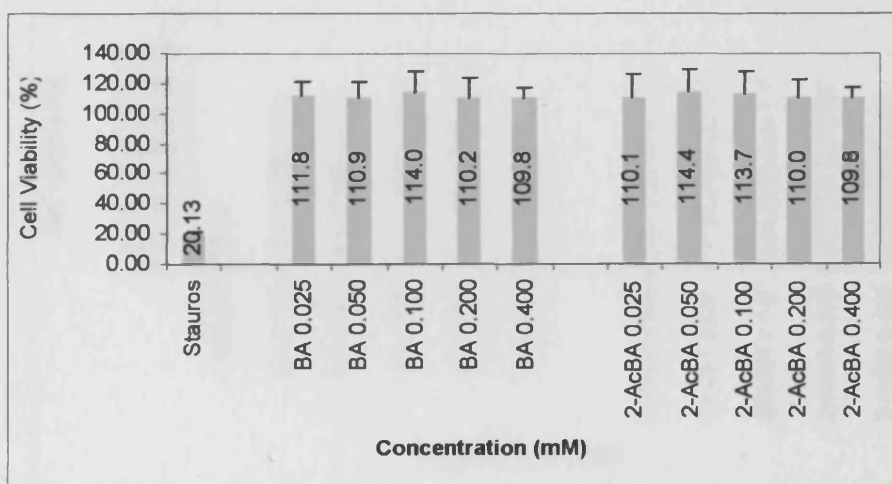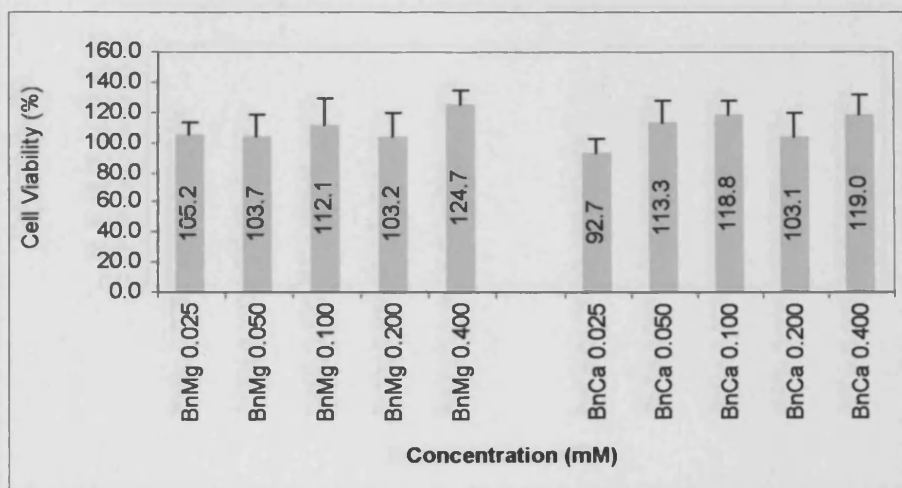
BA = benzoic acid, 2-AcBA = 2-acetylbenzoic acid; BnLi = lithium benzoate, BnK = potassium benzoate; BnMg = magnesium benzoate; BnCa = calcium benzoate.

A1.4 Cell viability (%) by benzoic acid and benzoate analogues after 72 hours' incubation
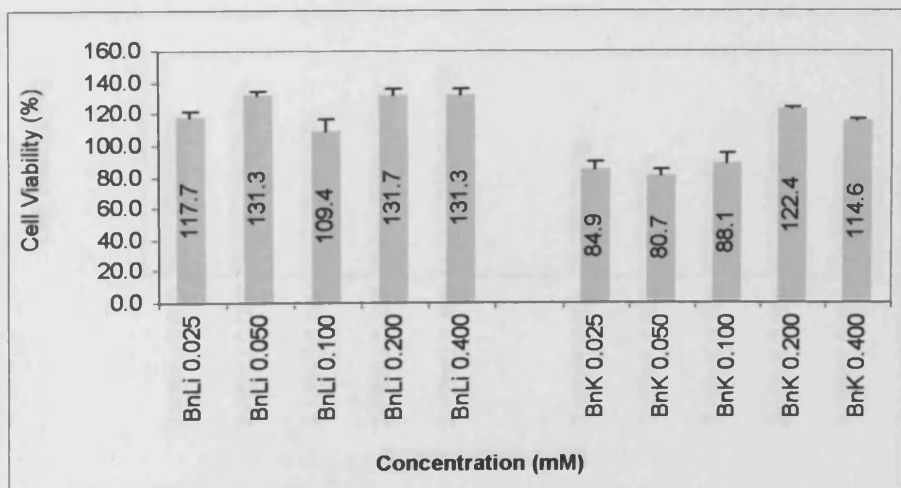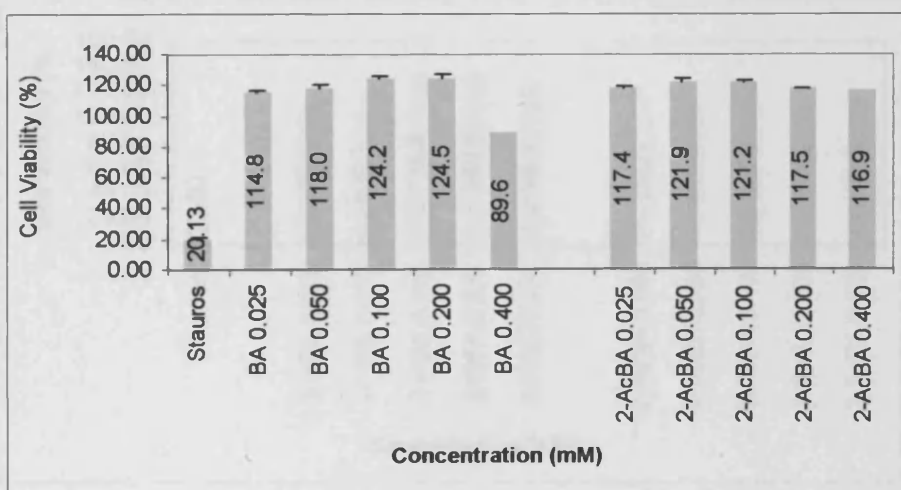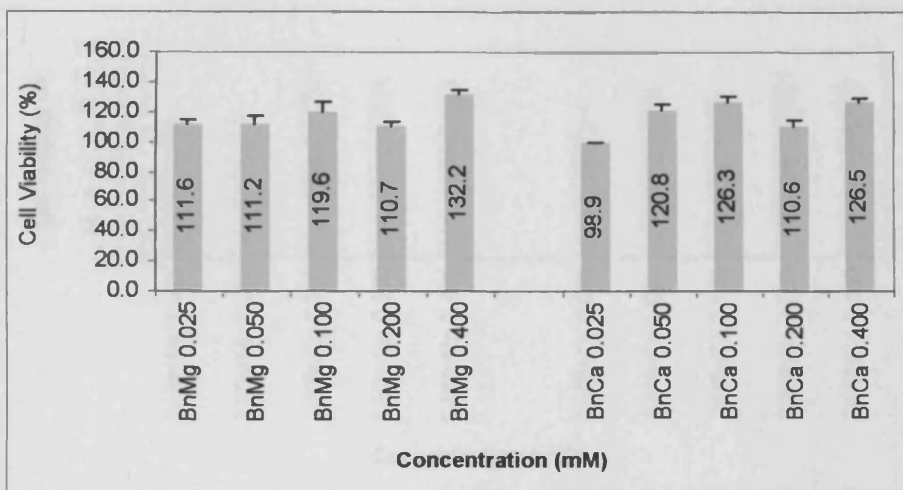
BA = benzoic acid, 2-AcBA = 2-acetylbenzoic acid; BnLi = lithium benzoate, BnK = potassium benzoate; BnMg = magnesium benzoate; BnCa = calcium benzoate.

A2.1 Cell viability (%) by 2-hydroxybenzoic acid and 2-hydroxybenzoate analogues after **12 hours' incubation**
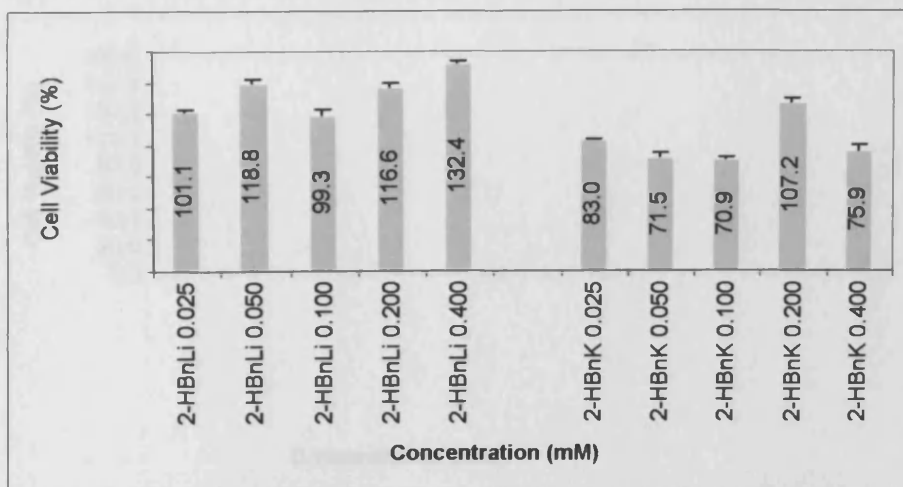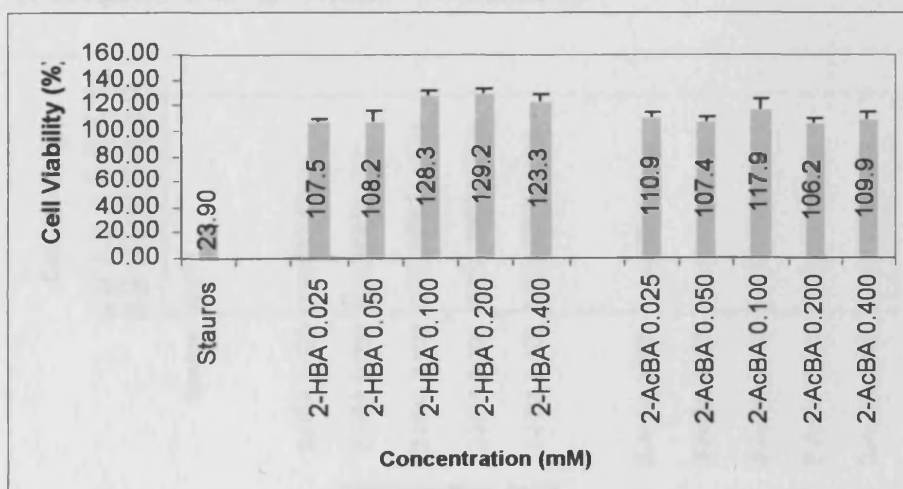
2-AcBA = 2-acetylbenzoic acid; 2-AcBnLi = 2-acetylbenzoate lithium; 2-AcBnK = potassium 2-acetyl benzoate; 2-AcBnMg = magnesium 2-acetylbenzoate; 2-AcBnCa = calcium 2-acetylbenzoate.
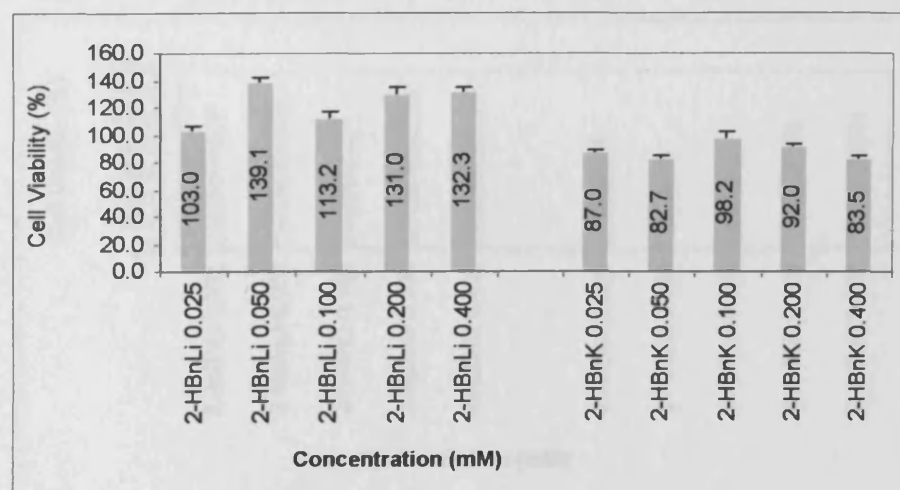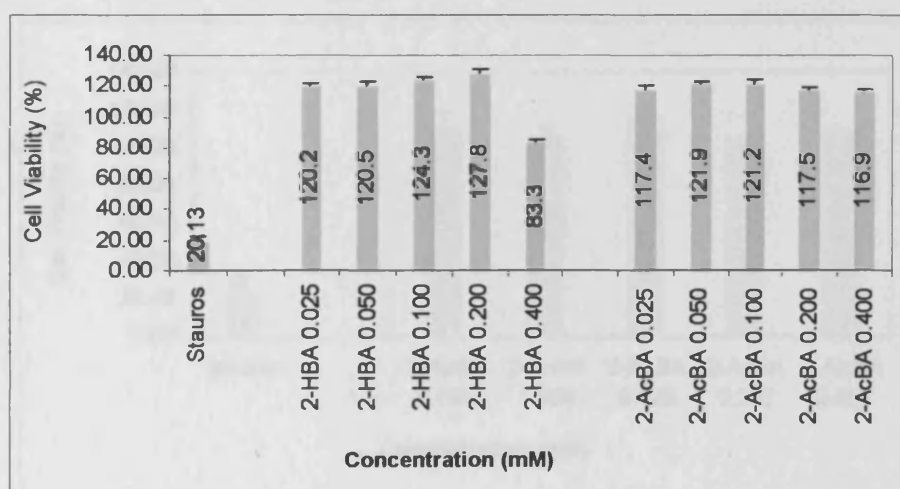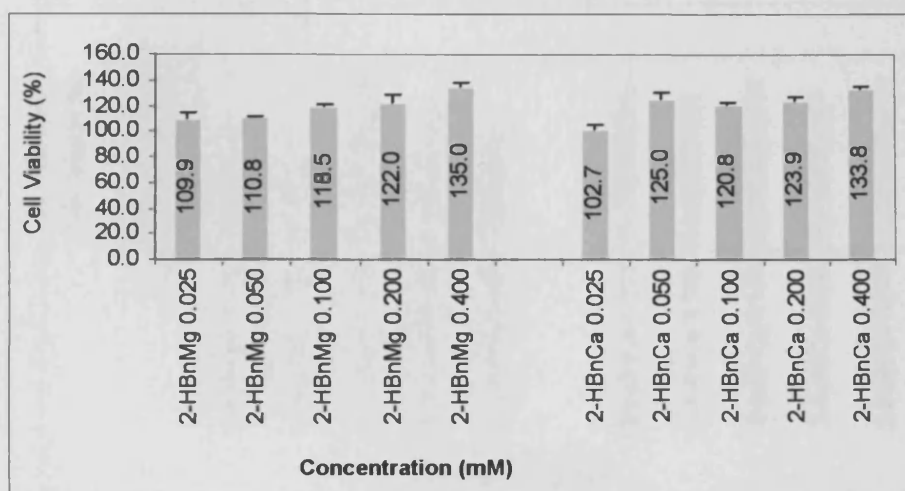
A2.2 Cell viability (%) by 2-hydroxybenzoic acid and 2-hydroxybenzoate analogues after **24 hours' incubation**

Chart 1 (top)

Cell Viability (%)

140.0
120.0
100.0
80.0
60.0
40.0
20.0
0.0

Concentration (mM)	Value
2-HBnMg 0.025	93.8
2-HBnMg 0.050	98.0
2-HBnMg 0.100	125.8
2-HBnMg 0.200	118.6
2-HBnMg 0.400	121.9
2-HBnCa 0.025	101.7
2-HBnCa 0.050	114.8
2-HBnCa 0.100	114.5
2-HBnCa 0.200	124.9
2-HBnCa 0.400	122.9

Concentration (mM)
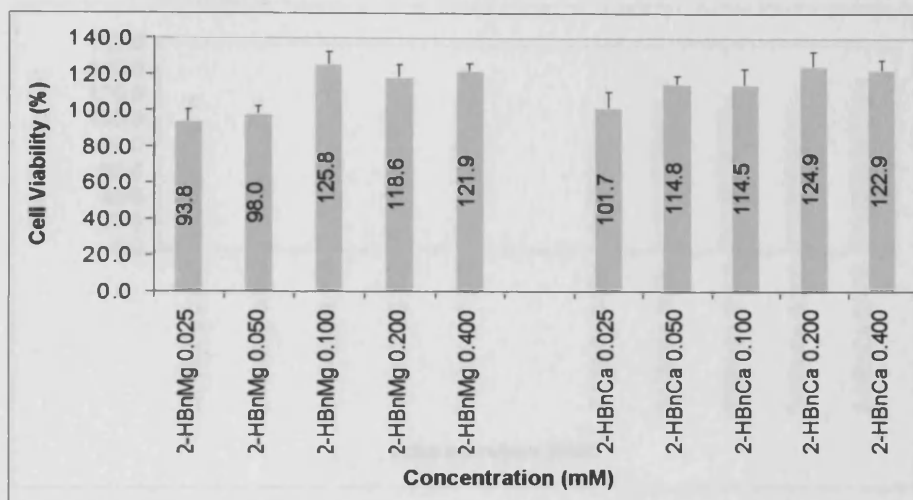
2-AcBA = 2-acetylbenzoic acid; 2-AcBnLi = 2-acetylbenzoate lithium; 2-AcBnK = potassium 2-acetyl benzoate; 2-AcBnMg = magnesium 2-acetylbenzoate; 2-AcBnCa = calcium 2-acetylbenzoate.
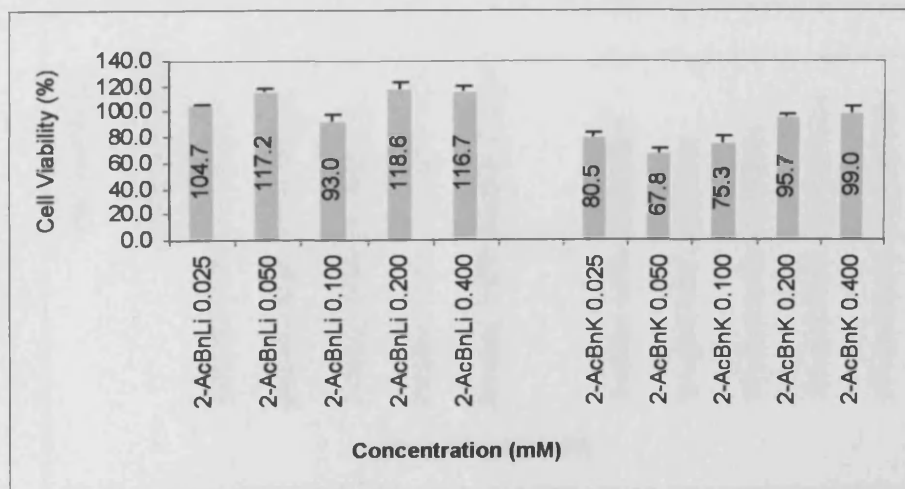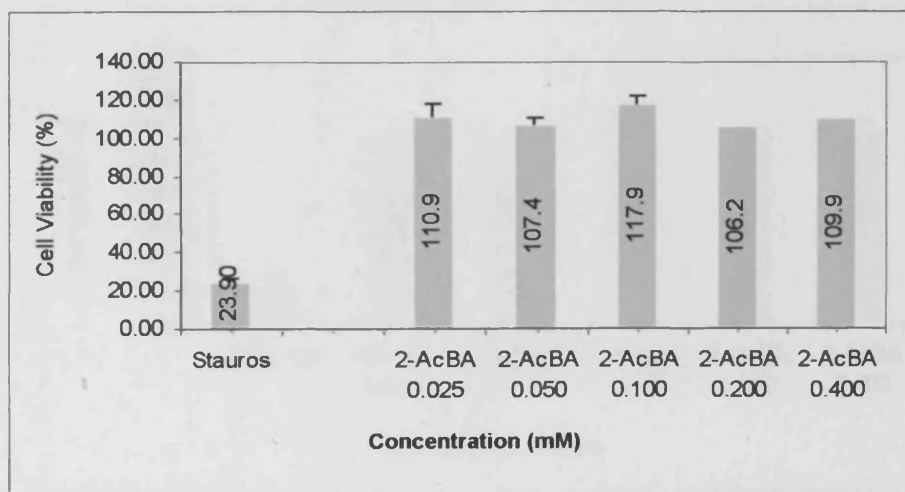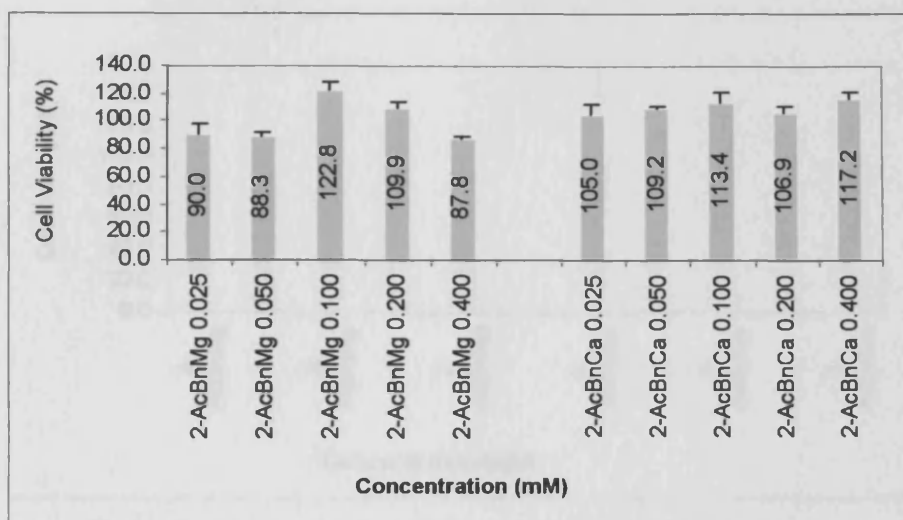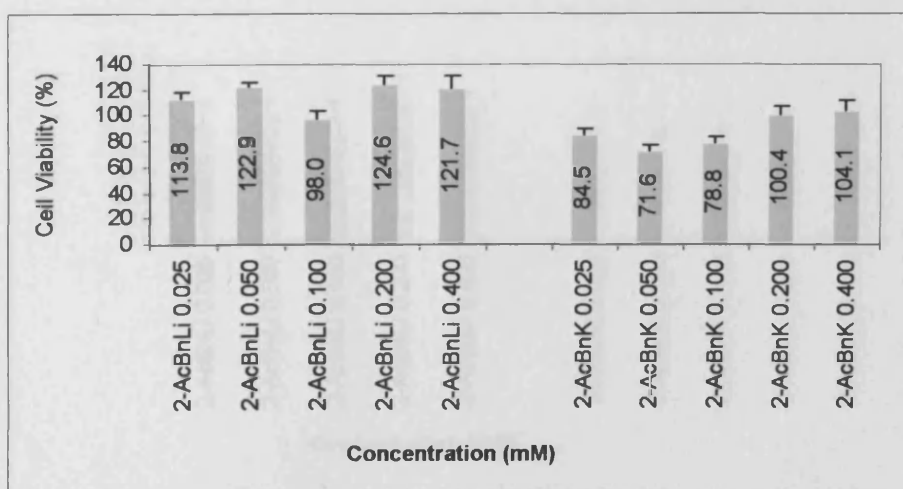
A2.3 Cell viability (%) by 2-hydroxybenzoic acid and 2-hydroxybenzoate analogues after 48 hours' incubation

Chart 2 (middle)

Cell Viability (%)

140.00
120.00
100.00
80.00
60.00
40.00
20.00
0.00

Concentration (mM)	Value
Stauros	20.13
2-HBA 0.025	112.7
2-HBA 0.050	113.0
2-HBA 0.100	115.3
2-HBA 0.200	118.8
2-HBA 0.400	78.3
2-AcBA 0.025	110.1
2-AcBA 0.050	114.4
2-AcBA 0.100	113.7
2-AcBA 0.200	110.0
2-AcBA 0.400	109.8

Concentration (mM)0

Chart 3 (bottom)

Cell Viability (%)

160.0
140.0
120.0
100.0
80.0
60.0
40.0
20.0
0.0

Concentration (mM)	Value
2-HBnLi 0.025	95.5
2-HBnLi 0.050	129.1
2-HBnLi 0.100	105.5
2-HBnLi 0.200	122.0
2-HBnLi 0.400	124.7
2-HBnK 0.025	81.5
2-HBnK 0.050	78.5
2-HBnK 0.100	90.7
2-HBnK 0.200	84.5
2-HBnK 0.400	78.5

Concentration (mM)
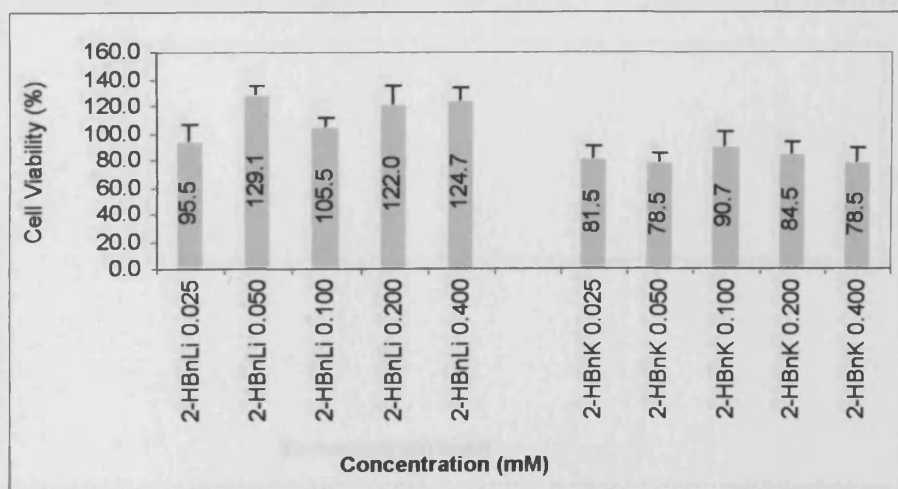
2-AcBA = 2-acetylbenzoic acid; 2-AcBnLi = 2-acetylbenzoate lithium; 2-AcBnK = potassium 2-acetyl benzoate; 2-AcBnMg = magnesium 2-acetylbenzoate; 2-AcBnCa = calcium 2-acetylbenzoate.
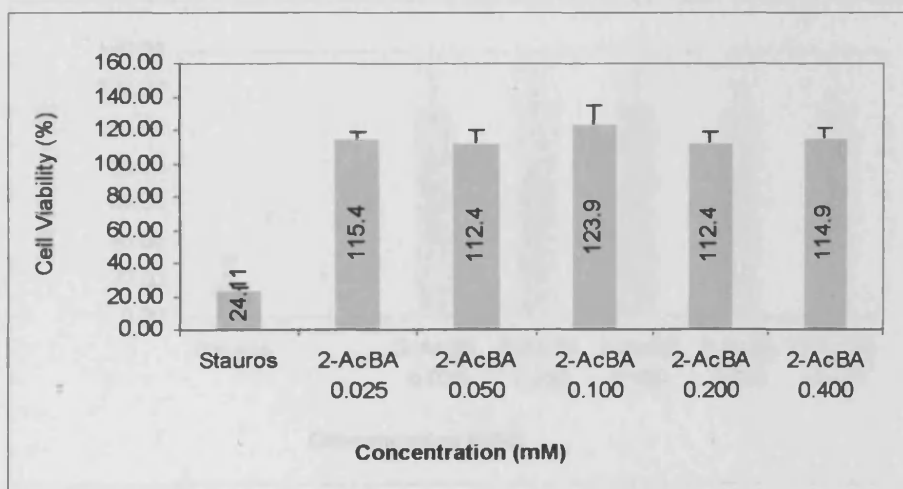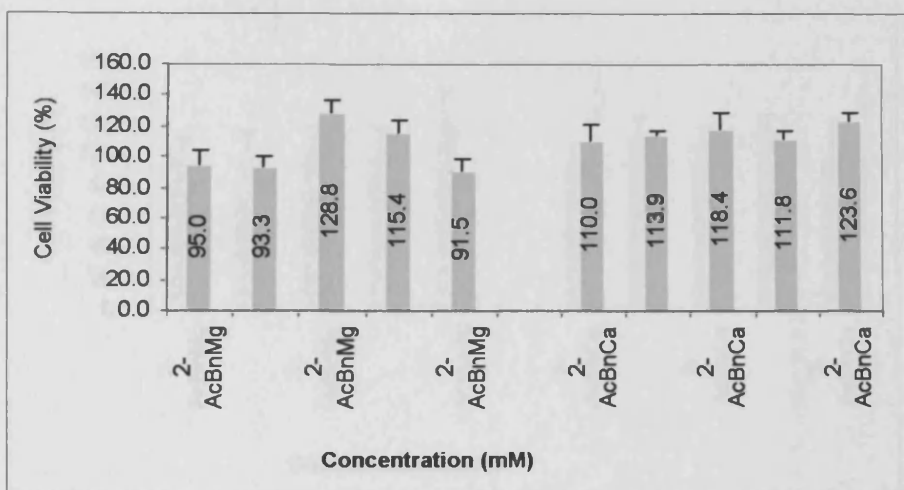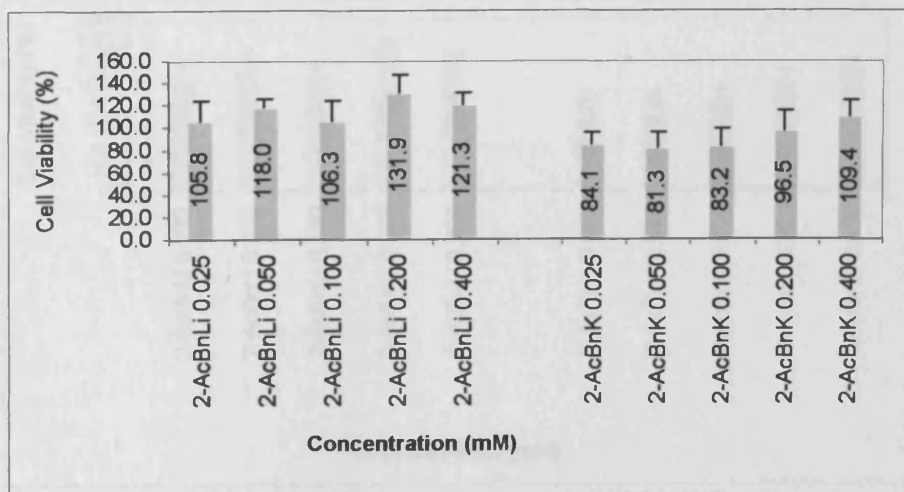
A2.4 Cell viability (%) by 2-hydroxybenzoic acid and 2-hydroxybenzoate analogues after **72 hours' incubation**

2-AcBA = 2-acetylbenzoic acid; 2-AcBnLi = 2-acetylbenzoate lithium; 2-AcBnK = potassium 2-acetyl benzoate; 2-AcBnMg = magnesium 2-acetylbenzoate; 2-AcBnCa = calcium 2-acetylbenzoate.
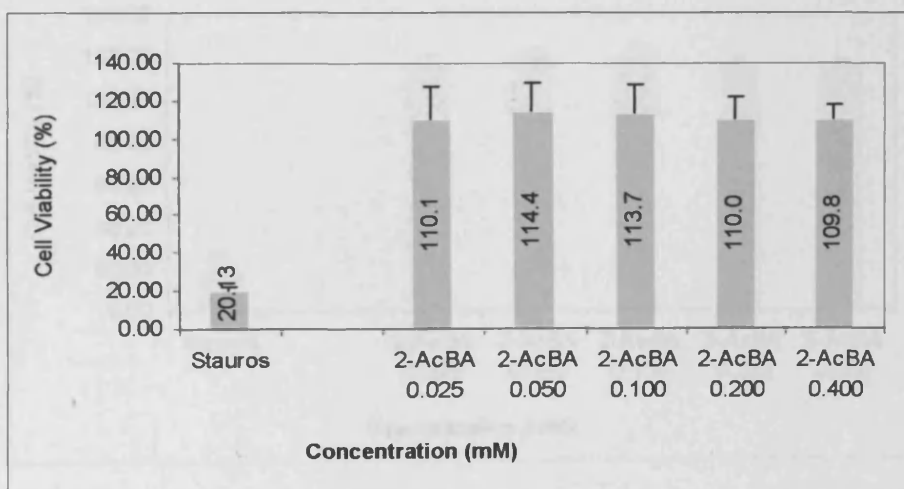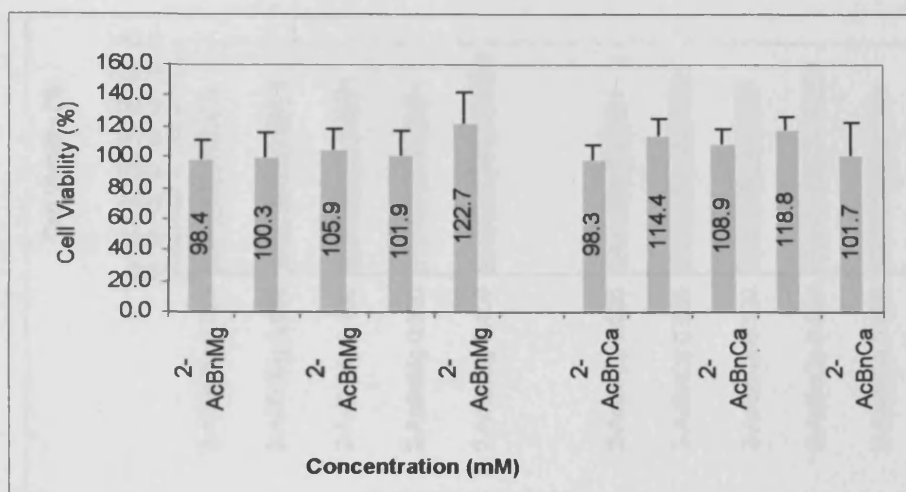
A3.1 Cell viability (%) by 2-acetylbenzoic acid and 2-acetylbenzoate analogues after **12 hours' incubation**

Cell Viability (%) — y-axis (0.0 to 140.0)

Concentration (mM)

Bars: 2-AcBnMg 0.025 = 90.0; 2-AcBnMg 0.050 = 88.3; 2-AcBnMg 0.100 = 122.8; 2-AcBnMg 0.200 = 109.9; 2-AcBnMg 0.400 = 87.8; 2-AcBnCa 0.025 = 105.0; 2-AcBnCa 0.050 = 109.2; 2-AcBnCa 0.100 = 113.4; 2-AcBnCa 0.200 = 106.9; 2-AcBnCa 0.400 = 117.2

2-AcBA = 2-acetylbenzoic acid; 2-AcBnLi = 2-acetylbenzoate lithium; 2-AcBnK = potassium 2-acetyl benzoate; 2-AcBnMg = magnesium 2-acetylbenzoate; 2-AcBnCa = calcium 2-acetylbenzoate.

A3.2 Cell viability (%) by 2-acetylbenzoic acid and 2-acetylbenzoate analogues after **24 hours' incubation**

Cell Viability (%) — y-axis (0.00 to 160.00)

Concentration (mM)

Bars: Stauros = 24.11; 2-AcBA 0.025 = 115.4; 2-AcBA 0.050 = 112.4; 2-AcBA 0.100 = 123.9; 2-AcBA 0.200 = 112.4; 2-AcBA 0.400 = 114.9

Cell Viability (%) — y-axis (0 to 140)

Concentration (mM)

Bars: 2-AcBnLi 0.025 = 113.8; 2-AcBnLi 0.050 = 122.9; 2-AcBnLi 0.100 = 98.0; 2-AcBnLi 0.200 = 124.6; 2-AcBnLi 0.400 = 121.7; 2-AcBnK 0.025 = 84.5; 2-AcBnK 0.050 = 71.6; 2-AcBnK 0.100 = 78.8; 2-AcBnK 0.200 = 100.4; 2-AcBnK 0.400 = 104.1
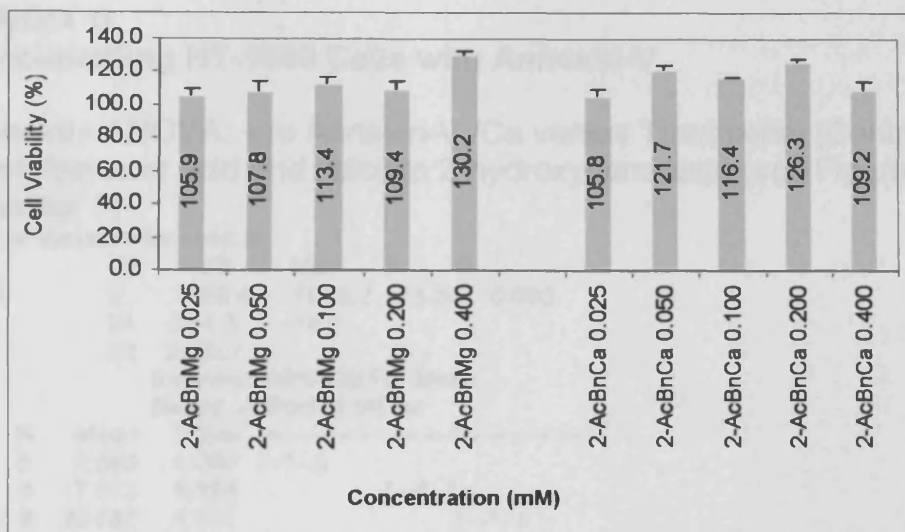
2-AcBA = 2-acetylbenzoic acid; 2-AcBnLi = 2-acetylbenzoate lithium; 2-AcBnK = potassium 2-acetyl benzoate; 2-AcBnMg = magnesium 2-acetylbenzoate; 2-AcBnCa = calcium 2-acetylbenzoate.

A3.3 Cell viability (%) by 2-acetylbenzoic acid and 2-acetylbenzoate analogues after **48 hours' incubation**

2-AcBA = 2-acetylbenzoic acid; 2-AcBnLi = 2-acetylbenzoate lithium; 2-AcBnK = potassium 2-acetyl benzoate; 2-AcBnMg = magnesium 2-acetylbenzoate; 2-AcBnCa = calcium 2-acetylbenzoate.

A3.4 Cell viability (%) by 2-acetylbenzoic acid and 2-acetylbenzoate analogues after **72 hours' incubation**
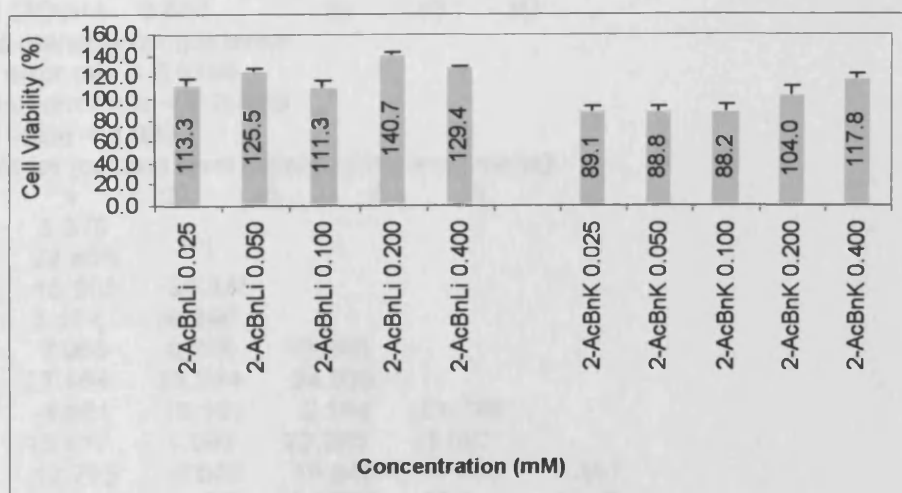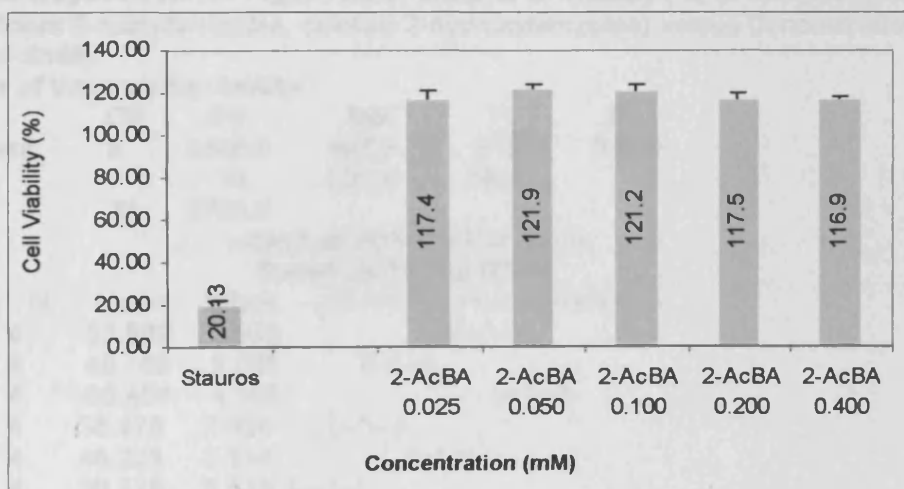
2-AcBA = 2-acetylbenzoic acid; 2-AcBnLi = 2-acetylbenzoate lithium; 2-AcBnK = potassium 2-acetyl benzoate; 2-AcBnMg = magnesium 2-acetylbenzoate; 2-AcBnCa = calcium 2-acetylbenzoate.

A4. **One-way ANOVA for Figure 2.8D, Chapter 2**: Viability (%) (2-acetylbenzoic acid, calcium 2-acetylbenzoate, calcium 2-hydroxybenzoate) versus Concentration (6mM and 8mM).

Analysis of Variance for viability

Source	DF	SS	MS	F	P
Treatment	5	2486.6	497.3	37.87	0.000
Error	18	236.4	13.1		
Total	23	2722.9			

```
                                  Individual 95% CIs For Mean
                                      Based on Pooled StDev
Level   N    Mean    StDev  --------+---------+---------+---------
1       4   53.589   3.660                     (---*--)
2       4   40.169   2.088          (--*---)
3       4   60.464   4.395                         (--*---)
4       4   36.475   2.624       (--*---)
5       4   48.221   2.114                 (--*--)
6       4   30.775   5.510   (---*--)
                             --------+---------+---------+--------
Pooled StDev =   3.624            36        48        60
```

Fisher's pairwise comparisons

Family error rate = 0.0109

Individual error rate = 0.00100

Critical value = 3.922

Intervals for (column level mean) - (row level mean)

```
              1         2         3         4         5
     2     3.370
          23.469
     3   -16.925   -30.345
           3.174   -10.246
     4     7.065    -6.355    13.940
          27.164    13.744    34.039
     5    -4.681   -18.101     2.194   -21.796
          15.417     1.998    22.293    -1.697
     6    12.765    -0.655    19.640    -4.350     7.397
          32.863    19.444    39.739    15.749    27.495
```

182

APPENDIX B
Immunolabelling HT-1080 Cells with Annexin-V

B1 One-way ANOVA: +ve Annexin-V /Ca versus Treatments (Control, 2-acetylbenzoic acid and calcium 2-hydroxybenzoate) (see Figure 3.5, Chapter 3)

```
Analysis of Variance for +ve/Ca
Source          DF      SS       MS       F      P
Tretment        2     2126.4   1063.2   75.86  0.000
Error           21     294.3    14.0
Total           23    2420.7
                          Individual 95% CIs For Mean
                          Based on Pooled StDev
Level   N    Mean    StDev  -+————+————+————+——
1       8    2.560   1.289  (—*—)
2       8   17.313   4.864              (—*—)
3       8   25.281   4.089                       (—*—)
                                 -+————+————+————+——
Pooled StDev =   3.744         0.0     8.0    16.0    24.0
```

Fisher's pairwise comparisons
Family error rate = 0.221
Individual error rate = 0.100

Critical value = 1.721
Intervals for (column level mean) - (row level mean)
```
            1         2
   2    -17.974
        -11.531
   3    -25.943   -11.190
        -19.500    -4.747
```

B2 One-way ANOVA: +ve Annexin-V /K versus Treatments (Control, 2-acetylbenzoic acid, and potassium 2-hydroxybenzoate) (see Figure 3.8, Chapter 3)

```
Analysis of Variance for +ve/K
Source          DF      SS       MS       F      P
Tretment        2     1502.9   751.4    46.93  0.000
Error           21     336.3    16.0
Total           23    1839.2
                          Individual 95% CIs For Mean
                          Based on Pooled StDev
Level   N    Mean    StDev  -+————+————+————+——
1       8    2.560   1.289  (—*—)
2       8   17.313   4.864              (—*—)
3       8   20.825   4.766                  (—*—)
                                 -+————+————+————+——
Pooled StDev =   4.002         0.0     7.0    14.0    21.0
```

Fisher's pairwise comparisons
Family error rate = 0.221
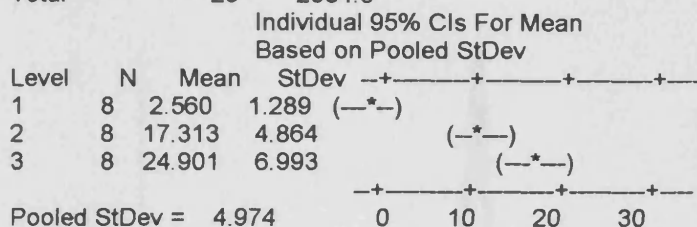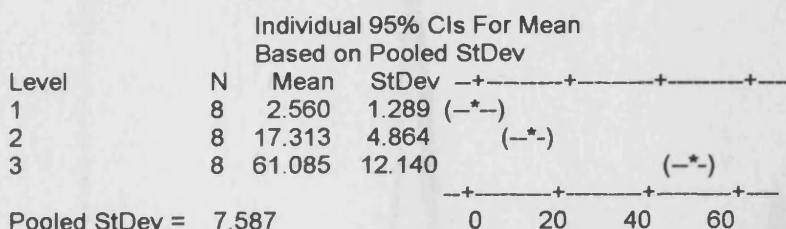Individual error rate = 0.100
Critical value = 1.721

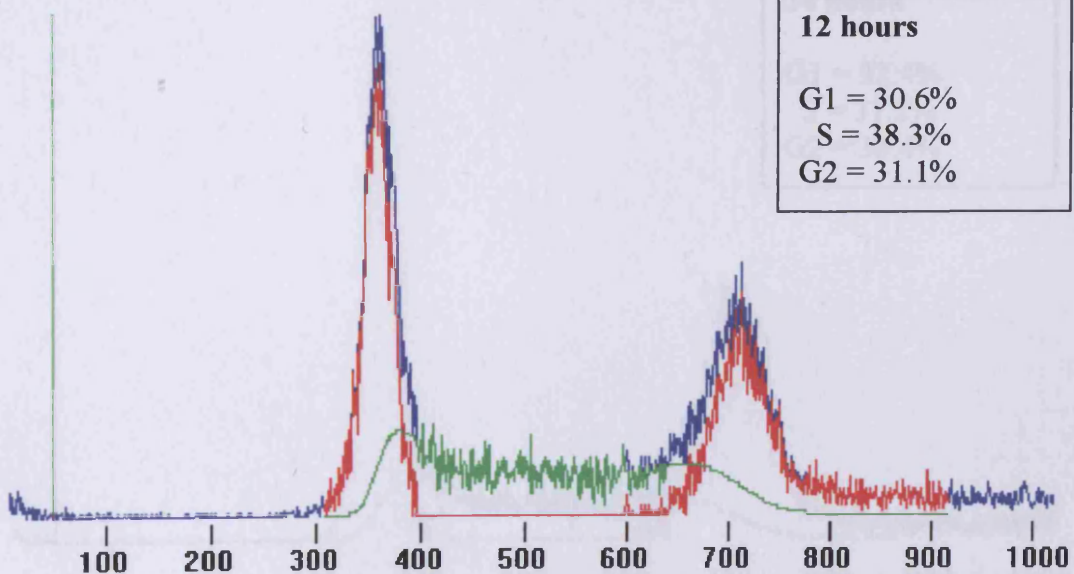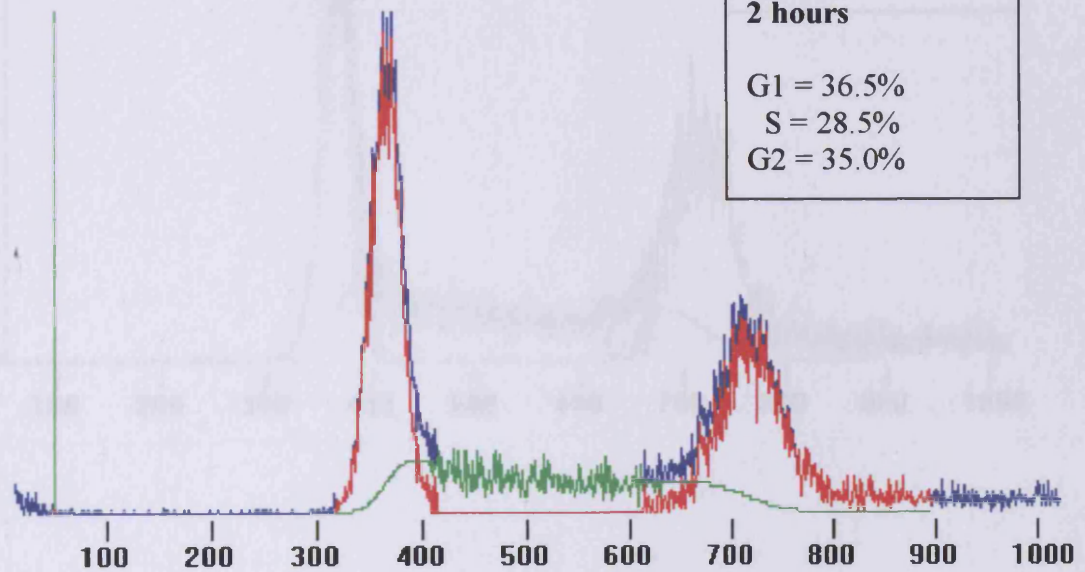Intervals for (column level mean) - (row level mean)
```
            1          2
   2    -18.196
        -11.309
   3    -21.708    -6.956
        -14.822    -0.069
```

B3 One-way ANOVA: +ve Annexin-V /Mg versus Treatments (Control, 2-acetylbenzoic acid, and magnesium 2-hydroxybenzoate) (see Figure 3.8, Chapter 3).

```
Analysis of Variance for +ve/Mg
Source        DF      SS       MS       F       P
Tretment       2    2065.0   1032.5   41.73   0.000
Error         21     519.6     24.7
Total         23    2584.6
                         Individual 95% CIs For Mean
                         Based on Pooled StDev
Level    N    Mean    StDev  --+--------+--------+--------+----
1        8    2.560   1.289  (—*—)
2        8   17.313   4.864            (—*—)
3        8   24.901   6.993                   (—*—)
                             --+--------+--------+--------+----
Pooled StDev =   4.974       0       10       20       30
```

Fisher's pairwise comparisons
Family error rate = 0.221
Individual error rate = 0.100
Critical value = 1.721
Intervals for (column level mean) - (row level mean)

```
            1          2
    2    -19.033
         -10.472
    3    -26.622    -11.869
         -18.061     -3.308
```

B4 One-way ANOVA: +ve Annexin-V /Zn versus Treatments Control, 2-acetylbenzoic acid, and zinc 2-hydroxybenzoate) (see Figure 3.9, Chapter 3)

```
Analysis of Variance for +Ve/Zn
Source        DF      SS       MS       F       P
Tretment       2   14823.6   7411.8  128.75   0.000
Error         21    1208.9     57.6
Total         23   16032.5
```

```
                         Individual 95% CIs For Mean
                         Based on Pooled StDev
Level        N    Mean    StDev  --+--------+--------+--------+----
1            8    2.560   1.289  (—*—)
2            8   17.313   4.864        (—*-)
3            8   61.085  12.140                        (—*-)
                                 --+--------+--------+--------+----
Pooled StDev =   7.587          0       20       40       60
```

Fisher's pairwise comparisons
Family error rate = 0.221
Individual error rate = 0.100
Critical value = 1.721
Intervals for (column level mean)-(row level mean)

```
            1          2
    2    -21.28
          -8.22
    3    -65.05     -50.30
         -52.00     -37.24
```

APPENDIX C

Supporting Data for Chapter 4

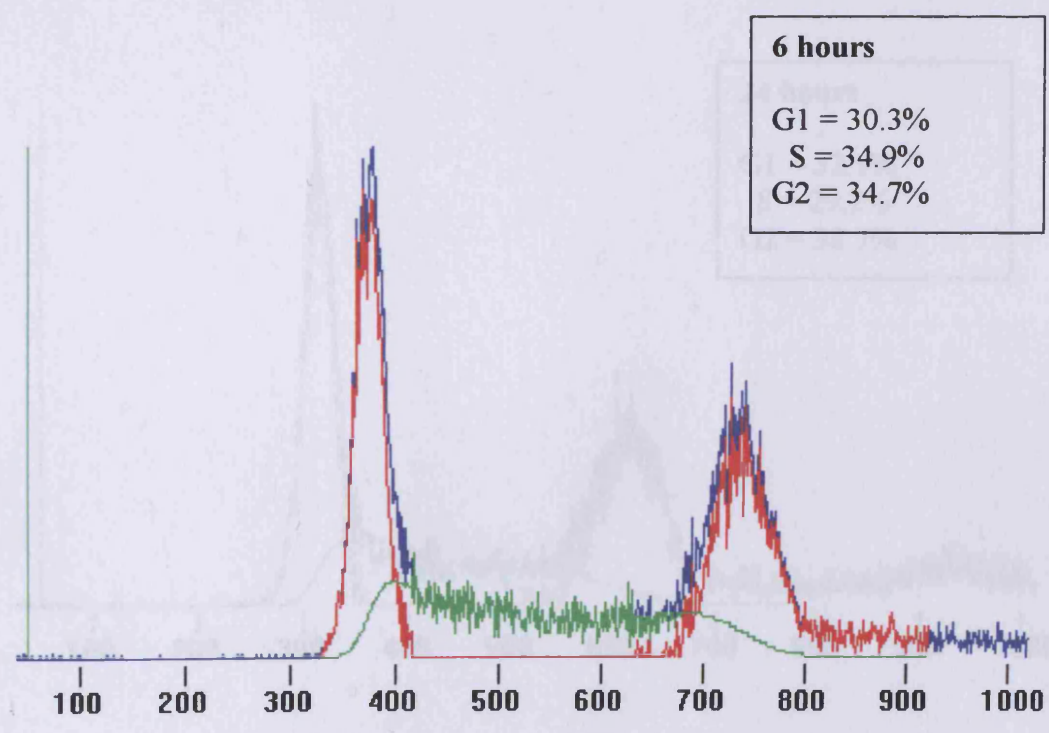**C1 – C3 Flow Cytometric Analysis of Cell Cycle for HT-1080 Cells at 2, 6, 12 and 24 hours.**

C1 Control

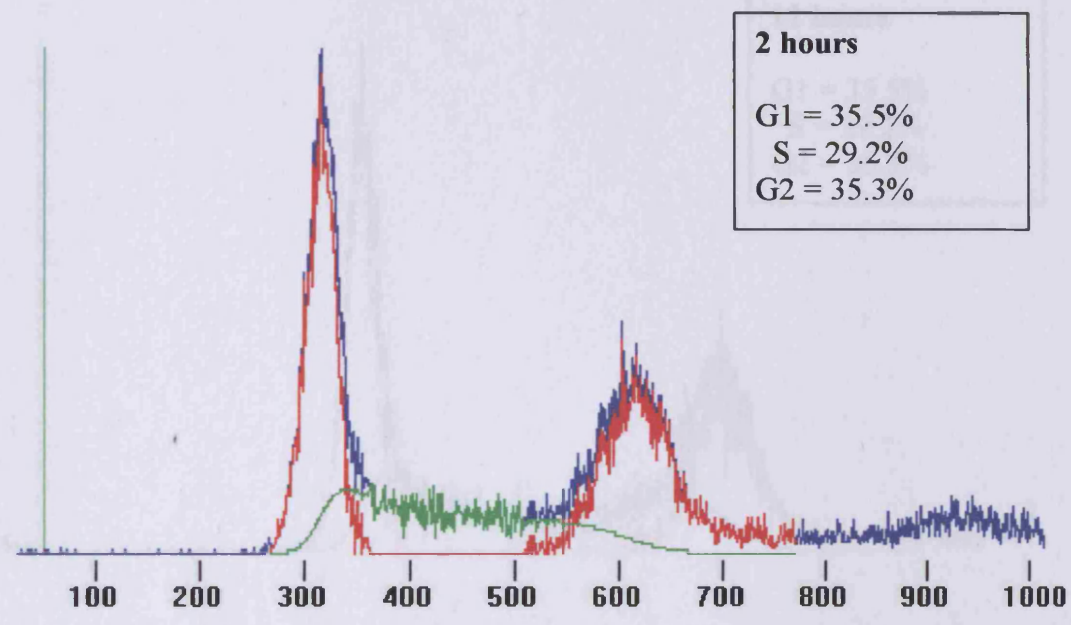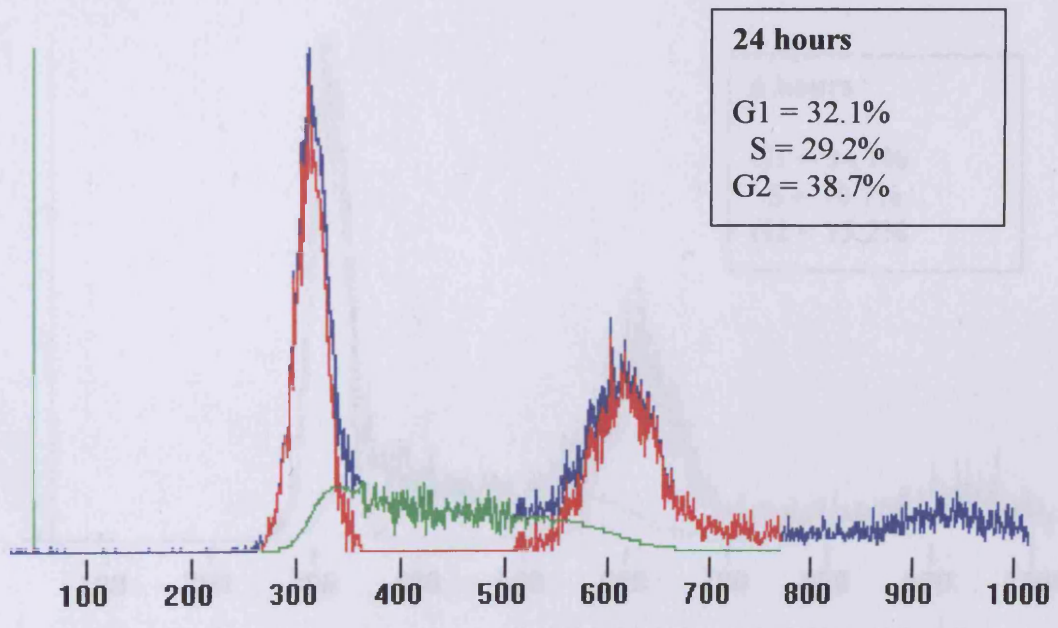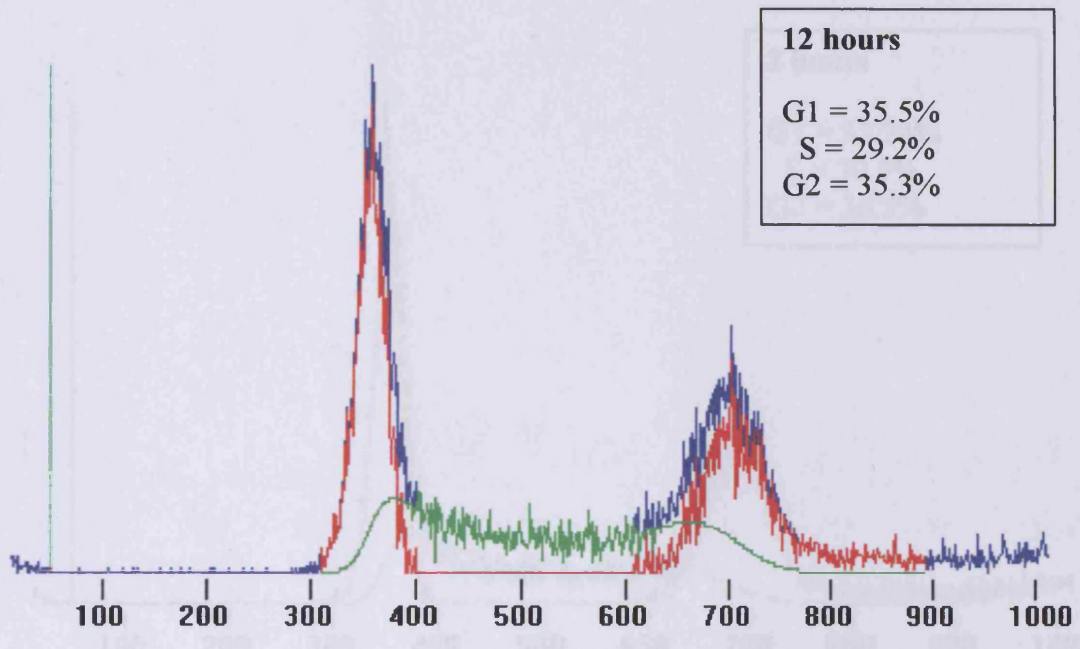2 hours

G1 = 36.5%
S = 28.5%
G2 = 35.0%

12 hours

G1 = 30.6%
S = 38.3%
G2 = 31.1%

6 hours

G1 = 27.5%
S = 36.8%
G2 = 35.7%

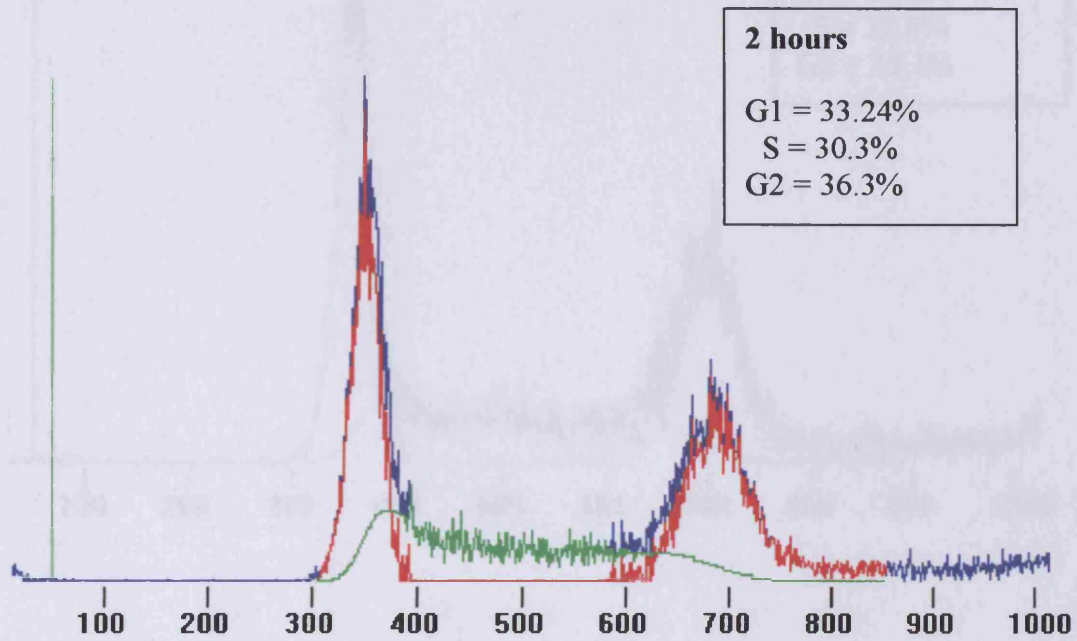**24 hours**

G1 = 32.4%
S = 31.2%
G2 = 36.4%

C2.1 Calcium 2-Hydroxybenzoate (0.4mM)

2 hours

G1 = 35.5%
 S = 29.2%
G2 = 35.3%

6 hours

G1 = 30.3%
 S = 34.9%
G2 = 34.7%

12 hours

G1 = 35.5%
S = 29.2%
G2 = 35.3%

24 hours

G1 = 32.1%
S = 29.2%
G2 = 38.7%
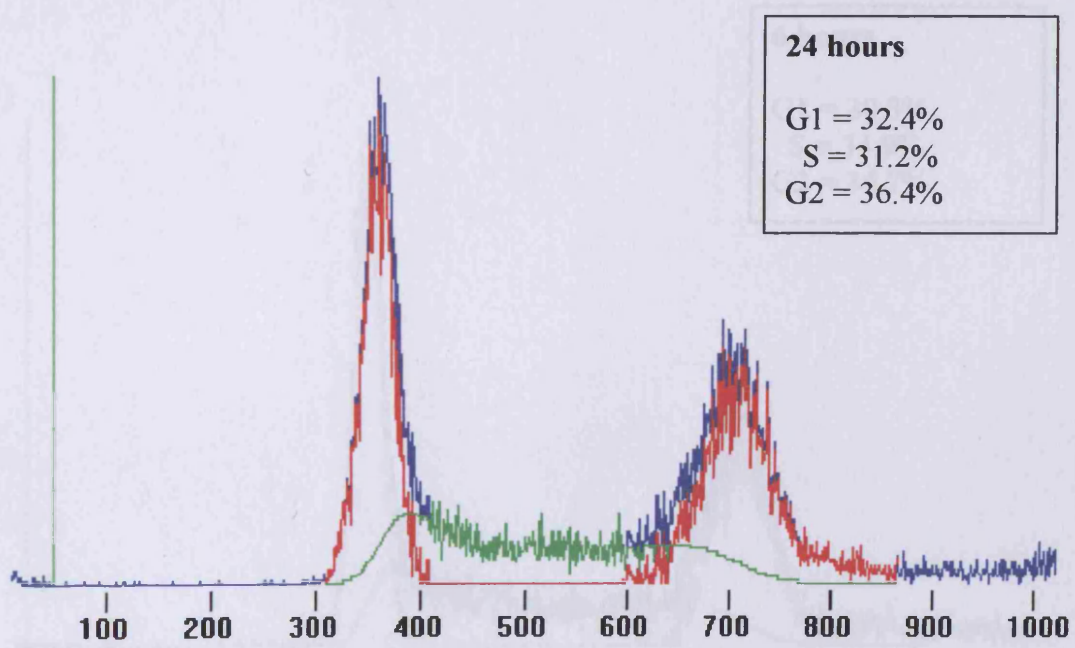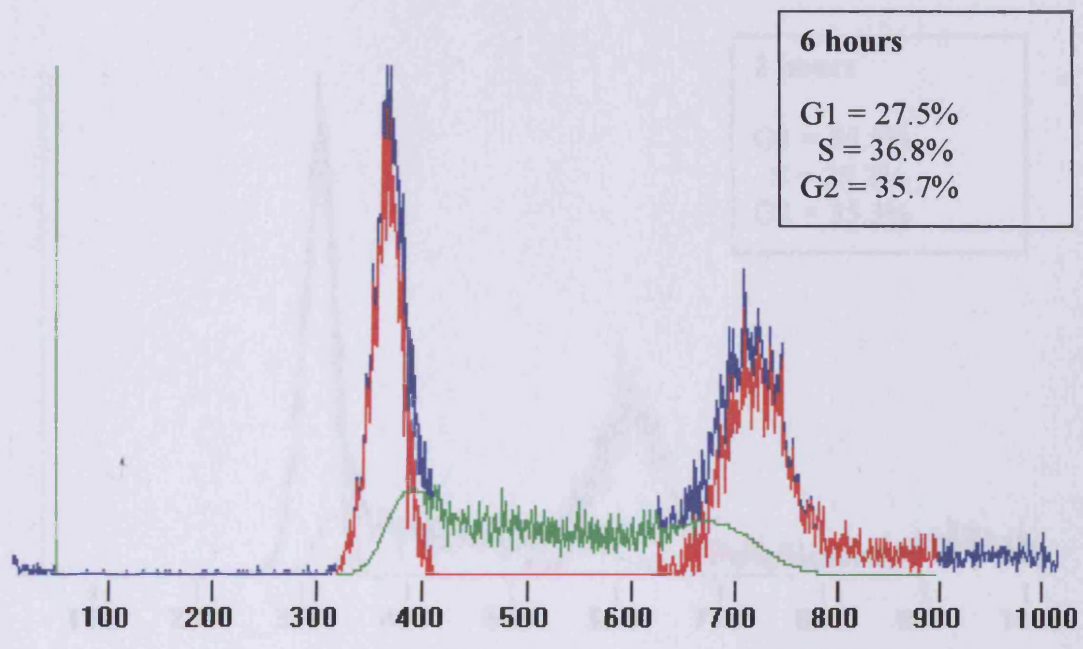
C2.2 Calcium 2-Hydroxybenzoate (0.8mM)

2 hours

G1 = 33.24%
 S = 30.3%
G2 = 36.3%

6 hours

G1 = 34.1%
 S = 30.7%
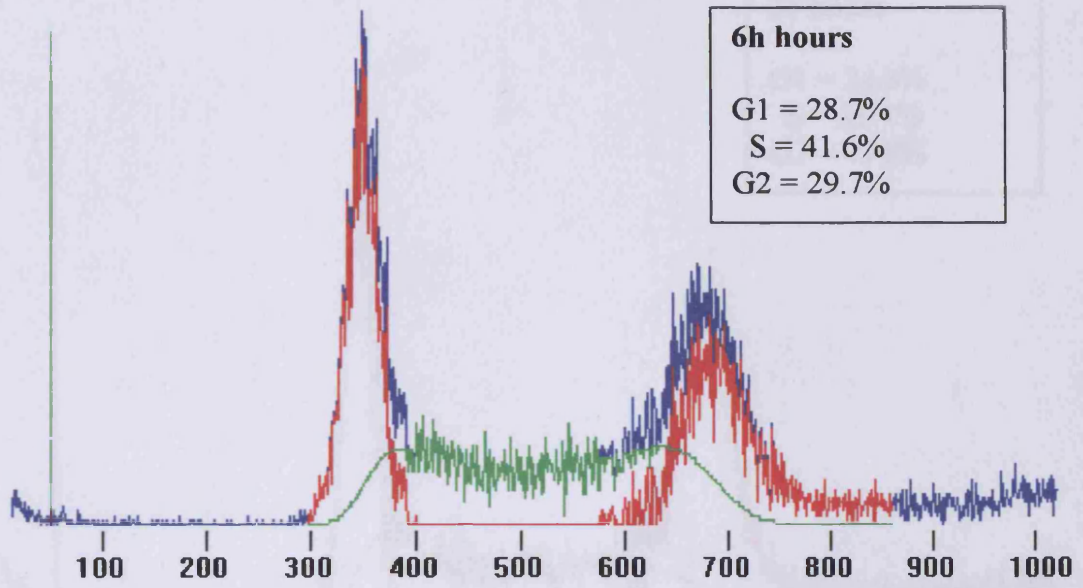G2 = 35.2%

12 hours

G1 = 32.2%
S = 32.8%
G2 = 35.1%

C3.1 Zinc 2-Hydroxybenzoate (0.25mM)

2 hours

G1 = 32.5%
S = 35.4%
G2 = 32.1%

6 hours

G1 = 26.6%
S = 35.9%
G2 = 37.5%

12 hours

G1 = 24.1%
S = 49.5%
G2 = 26.4%

24 hours

G1 = 26.7%
S = 37.2%
G2 = 36.1%
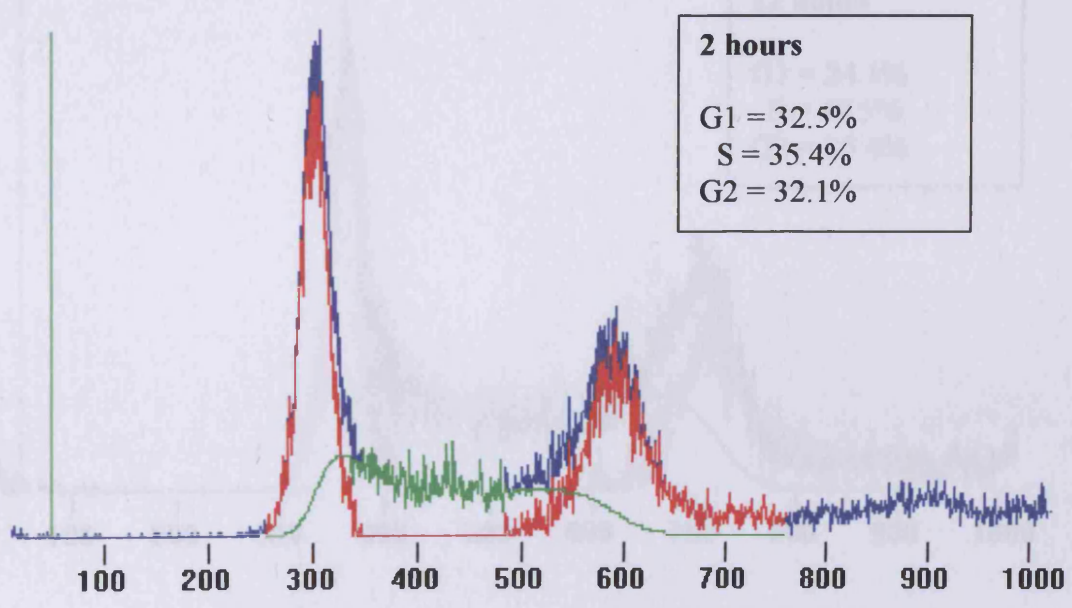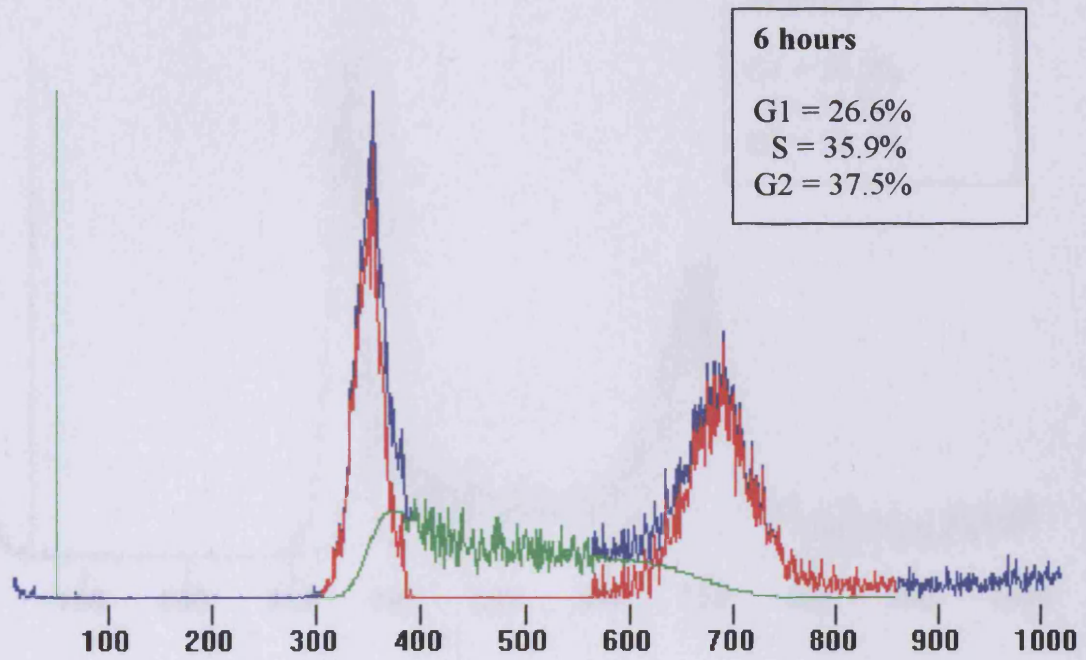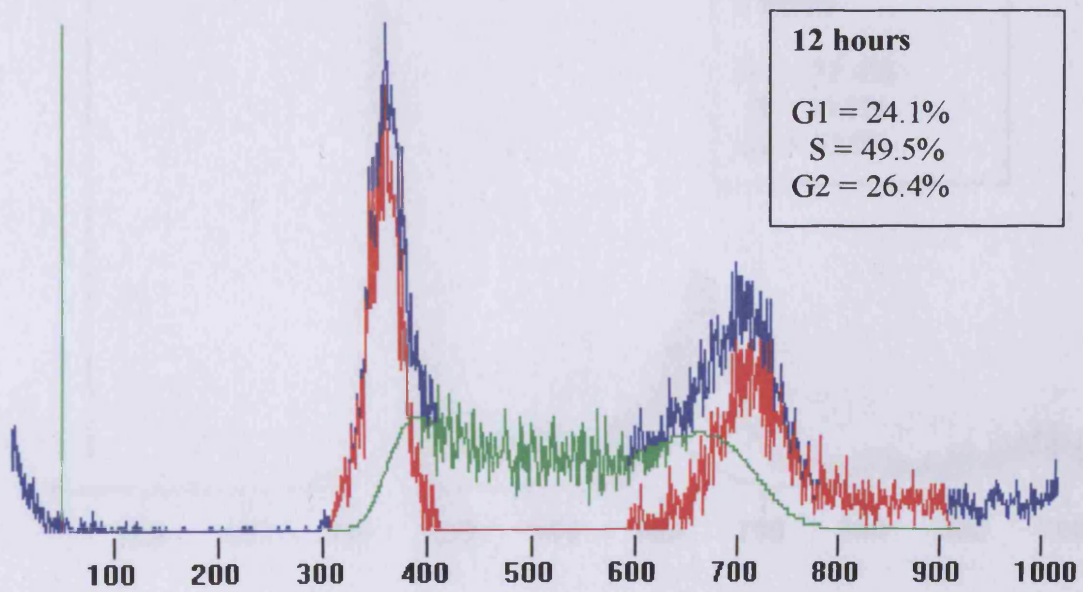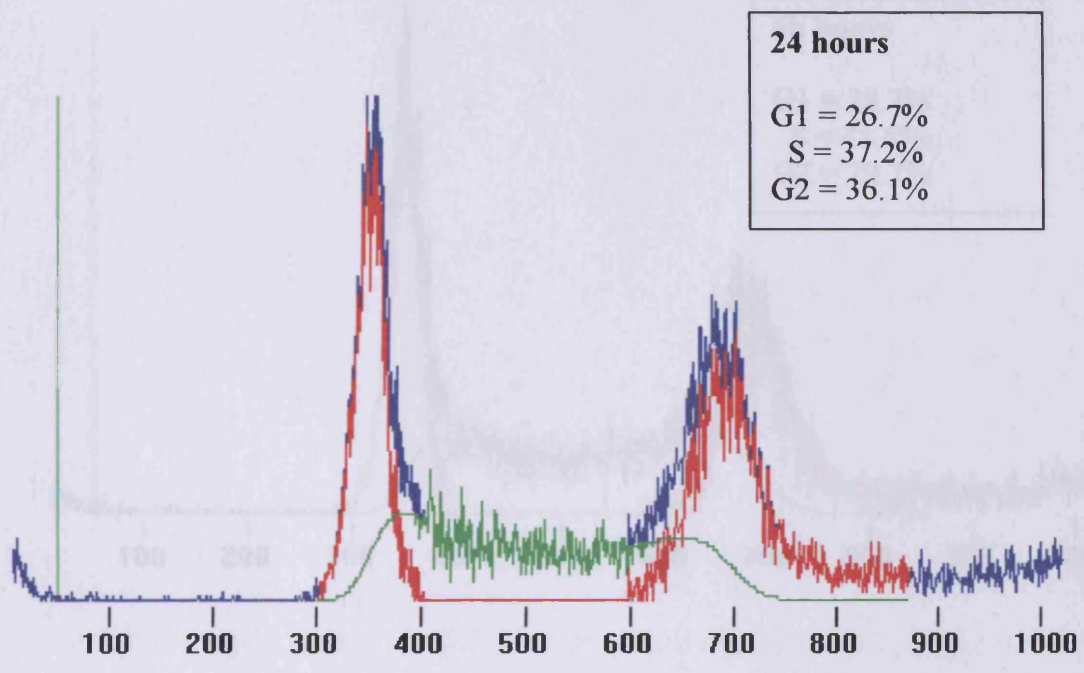
C3.2 Zinc 2-Hydroxybenzoate (0.3mM)

2 hours

G1 = 32.4%
S = 35.1%
G2 = 32.5%

6h hours

G1 = 28.7%
S = 41.6%
G2 = 29.7%

12 hours

G1 = 23.8%
S = 41.6%
G2 = 34.6%

24 hours

G1 = 24.8%
S = 31.4%
G2 = 43.8%

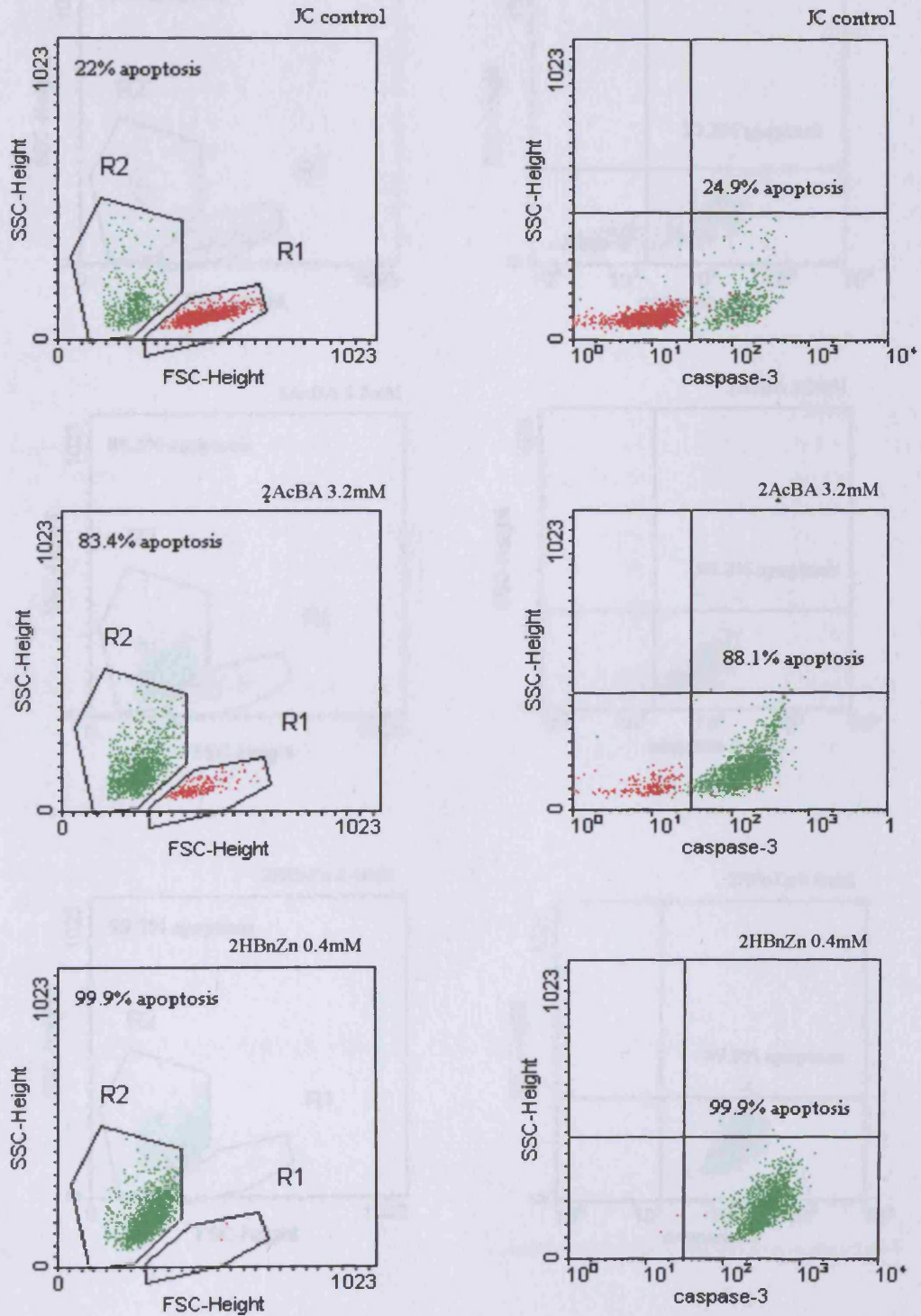100   200   300   400   500   600   700   800   900   1000
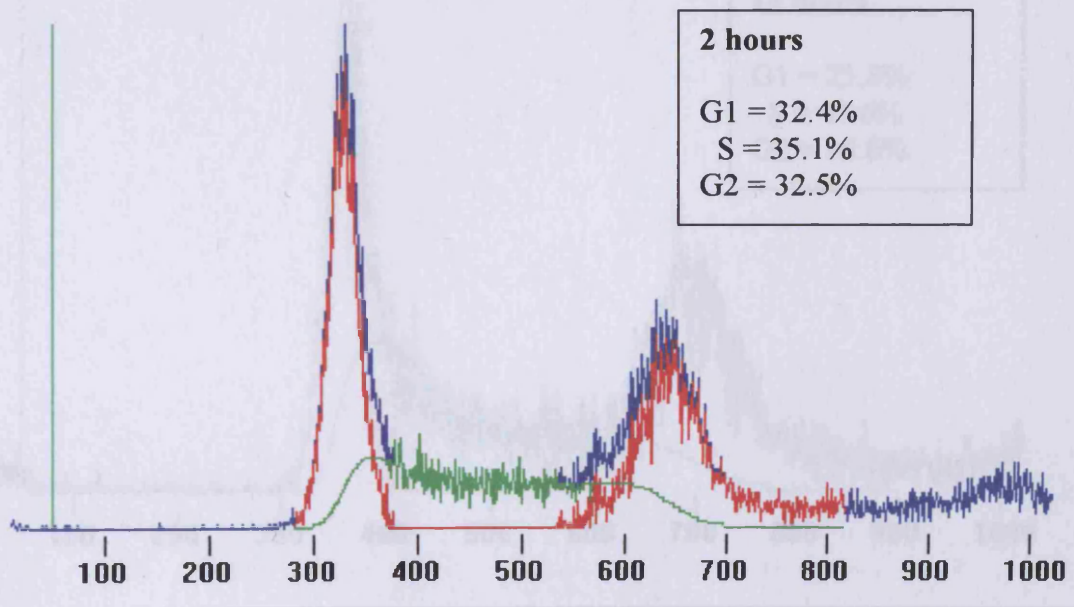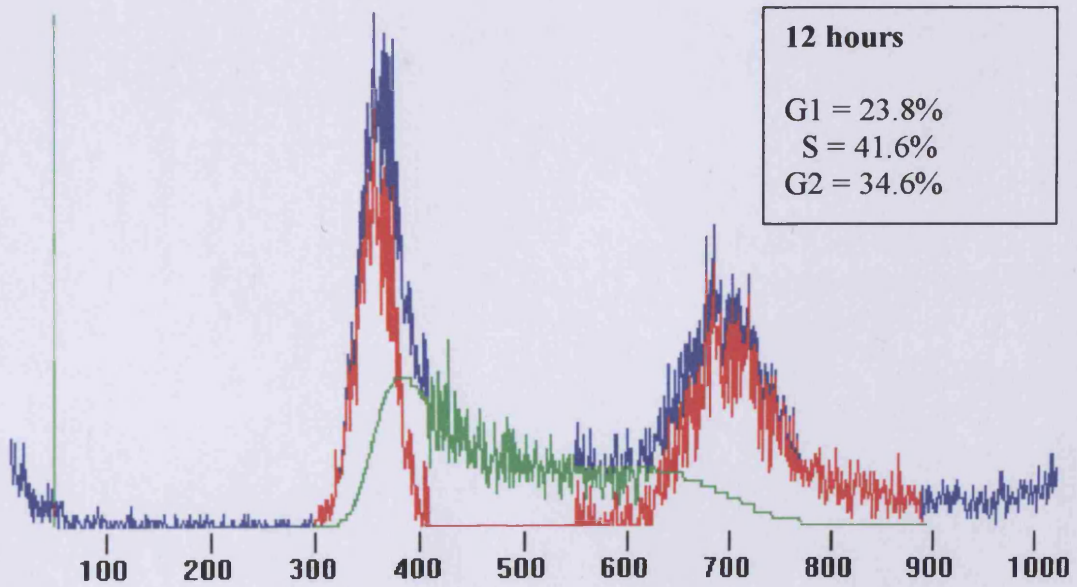
C4.1 Apoptosis measurement using Annexin-V labelling of zinc 2-hydroxybenzoate-treated HT-1080 cells
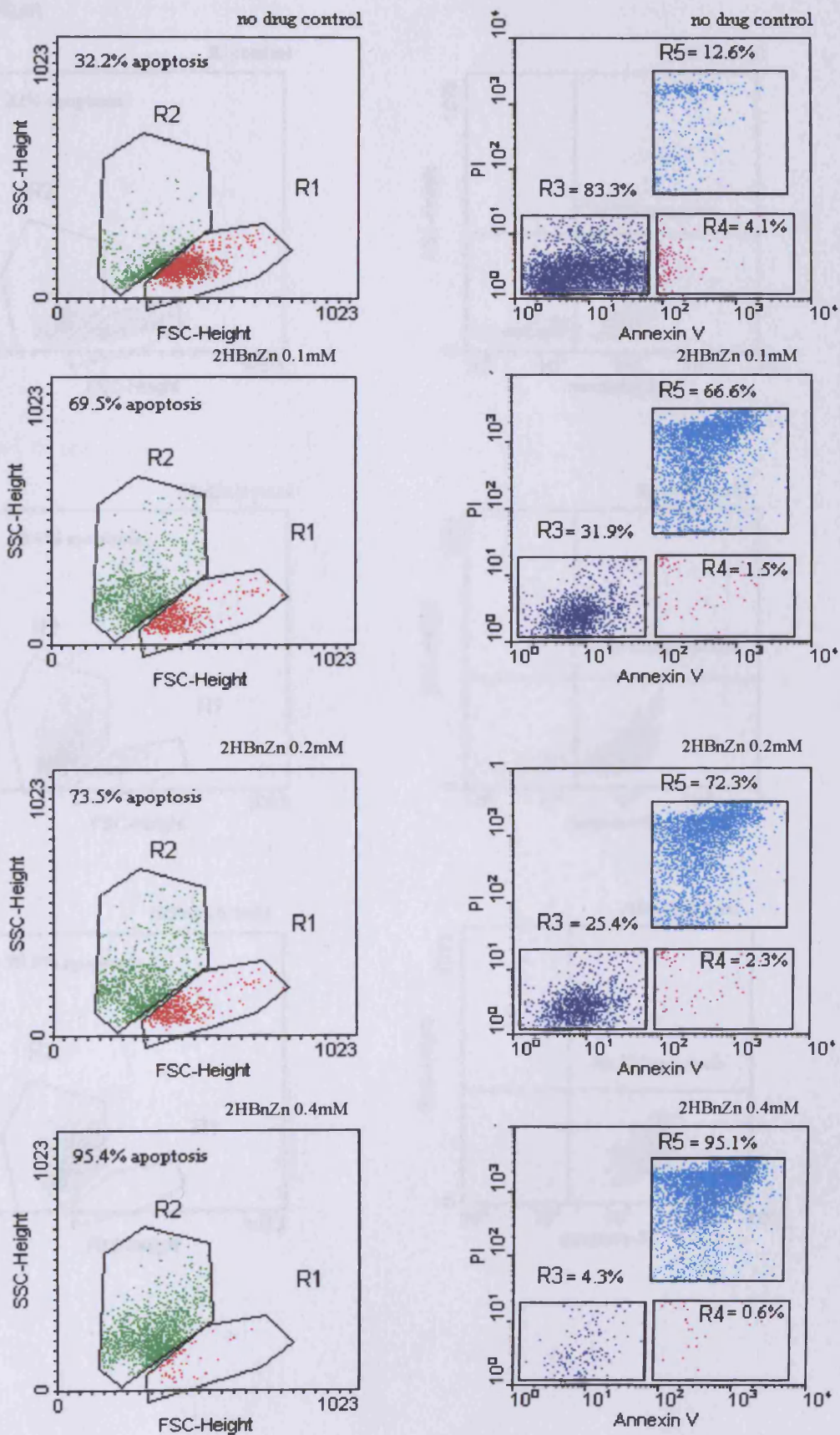
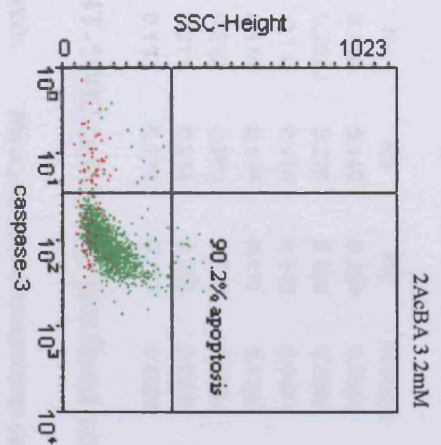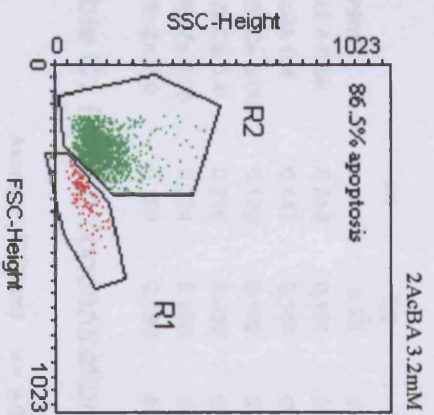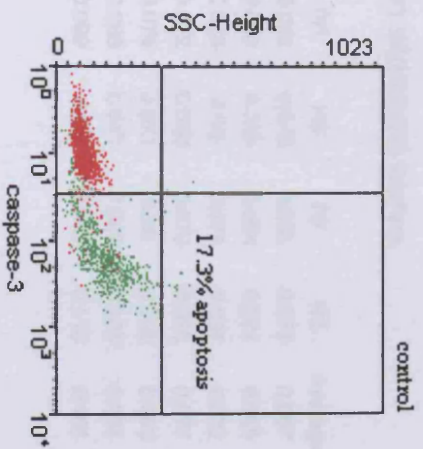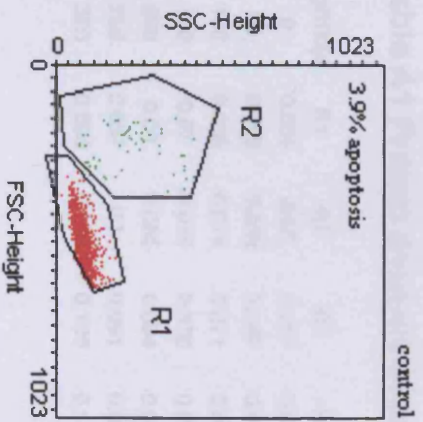## C4.2 Apoptosis measurement using Caspase-3 activity assay of zinc 2-hydroxybenzoate-treated HT-1080 cells

First Run

3.9% apoptosis — control

86.5% apoptosis — 2AcBA 3.2mM

99.7% apoptosis — 2HBnZn 0.4mM

17.3% apoptosis — control

90.2% apoptosis — 2AcBA 3.2mM

99.8% apoptosis — 2HBnZn 0.4mM
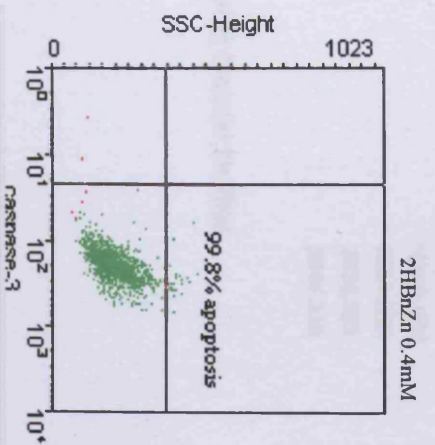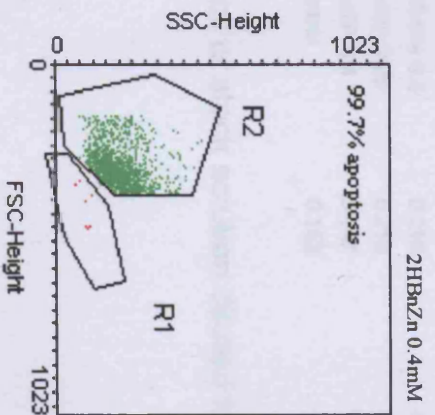
C5 Western Blot: Protein concentrations and antibodies dilutions.

Table A1 Protein analysis of albumin standard curve.

μg/100μl	R1	R2	R3	R4	R5	R6	R7	R8	Average	SE
0	0.051	0.06	0.057	0.059	0.052	0.048	0.055	0.073	0.057	0.0077
50	0.059	0.068	0.067	0.067	0.058	0.056	0.064	0.081	0.065	0.0079
100	0.065	0.074	0.071	0.071	0.065	0.06	0.071	0.097	0.072	0.011
150	0.07	0.079	0.078	0.077	0.072	0.066	0.075	0.095	0.077	0.0087
200	0.08	0.085	0.084	0.085	0.075	0.071	0.08	0.098	0.082	0.0081
250	0.087	0.1	0.091	0.094	0.086	0.077	0.088	0.105	0.091	0.0087
300	0.095	0.106	0.105	0.101	0.099	0.09	0.099	0.113	0.101	0.0071

Table B1 Protein analysis of proteins in HT-1080 cell lysate.

	R1	R2	R3	R4	R5	R6	Average	STDER
Control	–	0.15	0.156	0.149	0.149	0.154	0.1516	0.003
2AcBA 0.05	0.210	0.191	0.214	0.221	0.228	0.194	0.2096	0.015
2AcBA 0.4	0.147	0.155	0.143	0.14	0.156	0.143	0.1474	0.007
2HBnCa 0.05	0.178	0.165	0.203	0.173	0.178	0.171	0.1780	0.013
2HBnCa 0.4	0.218	0.232	0.227	0.212	0.208	0.213	0.2184	0.009
2HBnZn 0.05	0.224	0.208	0.231	0.211	0.233	0.235	0.2236	0.012
2HBnZn 0.4	0.183	0.184	0.181	0.193	0.178	0.177	0.1826	0.006

Table C1 Protein concentrations of HT-1080 cell lysate per fixed volume.

	Average (A575nm)	x = y-0.0569/0.0001	Mass (mg/10ml of concentrated sample)
2HBnZn 0.05	0.224	365.67	10604.333
2HBnZn 0.4	0.183	229.00	6641.000
2HBnCa 0.05	0.178	213.67	6196.333
2HBnCa 0.4	0.218	348.33	10101.667
2AcBA 0.05	0.210	319.00	9251.000
2AcBA 0.4	0.147	111.67	3238.333
Control	0.152	125.67	3644.333

10 ml of stock solution diluted to 100 with lysate buffer.